Insight into the Influence of Chemical Pretreatment and Alkali and Alkaline Earth Metals (AAEM) in Biomass Pyrolysis

A Thesis
Submitted in
Partial Fulfillment of the
Requirements for the Degree of

DOCTOR OF PHILOSOPHY

Philip Bernstein Saynik

School of Energy Science and Engineering
Indian Institute of Technology Guwahati
Guwahati – 781 039, Assam, India
April 2021

INDIAN INSTITUTE OF TECHNOLOGY GUWAHATI
SCHOOL OF ENERGY SCIENCE AND ENGINEERING

STATEMENT

I do hereby declare that the content embodied in this thesis entitled "*Insight into the influence of chemical pretreatment and alkali and alkaline earth metals (AAEM) in biomass pyrolysis*" is the result of investigations carried out by me at the School of Energy Science and Engineering, Indian Institute of Technology Guwahati, Assam, India under the guidance of Prof. Vijayanand S. Moholkar.

In keeping with the general practice of reporting scientific observations, due acknowledgments have been made wherever the work described is based on the findings of other investigators.

April 2021

Philip Bernstein Saynik
(Roll No.: 156151004)

INDIAN INSTITUTE OF TECHNOLOGY GUWAHATI
SCHOOL OF ENERGY SCIENCE AND ENGINEERING

CERTIFICATE

This is to certify that the work described in this thesis entitled "*Insight into the influence of chemical pretreatment and alkali and alkaline earth metals (AAEM) in biomass pyrolysis*" by Mr. Philip Bernstein Saynik (Roll No.: 156151004) for the award of degree of Doctor of Philosophy is an authentic record of the results obtained from the research work carried out under my supervision in the School of Energy Science and Engineering, Indian Institute of Technology Guwahati, Assam, India and this work has not been submitted elsewhere for a degree.

April 2021

Prof. Vijayanand S. Moholkar
(CEng, FIChemE, FRSC, MAIChE(Sr))
Professor
Department of Chemical Engineering and School of Energy Science and Engineering
Indian Institute of Technology Guwahati
Guwahati – 781 039
Assam, India

ACKNOWLEDGMENTS

It gives me great delight to acknowledge the support and assistance I have received from a significant number of people over the entire span of my doctoral research at IITG. At the outset, I thank my Lord for enabling me to pursue my postgraduate studies and sustaining me by his grace throughout my academic journey at IITG.

I would like to express my sincere gratitude to my supervisor, Professor Vijayanand S. Moholkar, for his professional supervision, encouragement and continuous support. His suggestions and constructive feedback at every stage of my research work have helped in the production of this thesis. I would also thank my doctoral committee members: Prof. T. Punniyamurthy, Dr. Nageswara Rao Peela and Dr. Pankaj Kalita, for their valuable suggestions and advice.

I owe my sincere thanks to the School of Energy Science and Engineering, Department of Chemical Engineering and Central Instrument Facility of IIT Guwahati for providing the required analytical facilities for my research. I am grateful to their staff members: Dr. Lepakshi Barbora, Mr. Dhiren Huzuri, Mr. Debarshi Baruah and Mr. Harsaraj Biswanath, for their support.

I take this opportunity to thank my close friends Arunkumar Chandrasekaran, Venu Babu Borugadda, Sumitha Banu, Dharmalingam, Suresh Rajamanickam, Sounak Bera, Mriganka Saha, Pradeep Kumar,

Vignesh Babu, Sanjeev Mishra and Rishiraj Purkayastha for long technical and insightful discussions at the School of Energy Science and Engineering and Core 3 cafeteria.

My research work would not have been possible without the assistance of our research group and members of Energy Efficiency lab – Arup, Ritesh, Bhaskar, Kajal, Udangshree, Karan, Amit, Neha, Niharika, Pushpita, Aradhana, Kuldeep, Madonna, Barasa and Pranab. My sincere thanks to you for your support.

My heartfelt gratitude to Mr. T.T Haokip, Dr. Lyngdoh, Dr. Prakash, Dr. Senthilkumar, Dr. Nelson Muthu and their families, who took special care of me during my stay at IITG and for their prayer support.

My special thanks to the IITG EU family: Bongliba, Deep Anand, Atso, John Nasaba, Biki Teron, Shehzad, Vivian, Sheeba, Archana, Them, Rajsekhar, Rakesh, Varaprasad, Ravi and others members for memorable fellowships. I am also highly thankful to EGF members who were like family to me at Guwahati: Dr. John and family, Santosh Soren and family, Kornelius Basumatari and family, Amjad, John Sangma, Dr. Ano and Dr. Atula.

Lastly, but by no means least, I thank my parents and brother for their continuous support, prayer and encouragement, which has helped me immensely for the successful completion of this endeavor.

Philip Bernstein Saynik
April 2021

CONTENTS

List of Tables **xiii**

List of Figures **xv**

Abbreviations **xviii**

Chapter 1. General Introduction and Literature Review **1-64**

1.1 Global energy scenario 1
1.2 Indian energy scenario 2
1.3 Structure of biomass 5
1.3.1 Cellulose 7
1.3.2 Hemicellulose 8
1.3.3 Lignin 9
1.3.4 Extractives 10
1.3.5 Ash 10
1.4 Biomass to energy conversion techniques 11
1.4.1 Combustion 11
1.4.2 Gasification 12
1.4.3 Pyrolysis/liquefaction 12
1.4.4 Anaerobic digestion 12
1.4.5 Fermentation 13
1.5 Pyrolysis 13
1.5.1 Bio-oil 14
1.5.2 Biochar 15
1.5.3 Non-condensable gases 16
1.6 Literature Review 17
1.6.1 Chemical pretreatment techniques 17
1.6.2 Effect of chemical pretreatment techniques on pyrolysis products 25
1.6.3 Effect of alkali and alkaline earth metals (AAEM) 40
1.7 Aim and Scope of the present study 50
References 54

Chapter 2. Chemical pretreatment of low lignin content *A. donax* biomass to improve critical properties for pyrolysis **65-90**

2.1 Introduction 65
2.2 Materials and methods 66
2.2.1 Biomass gathering and processing 66
2.2.2 Chemical pretreatment experiments 67

2.2.3 Proximate and ultimate (elemental) analysis of untreated biomass 67
2.2.4 Metal concentration by ICP-MS analysis 68
2.2.5 Surface metallic composition by FESEM-EDX 68
2.2.6 Equilibrium moisture content of treated and untreated biomass 68
2.2.7 Gross calorific value 69
2.2.8 Biochemical compositional analysis 69
2.2.9 X-ray diffraction analysis 70
2.2.10 Fourier transform infrared spectroscopy analysis 70
2.2.11 Thermogravimetric analysis 70
2.3 Results and Discussion 71
2.3.1 Characterization of *A. donax* biomass 71
2.3.2 Residual weight and biochemical composition of pretreated biomass 71
2.3.3 Equilibrium moisture content and calorific value 73
2.3.4 Elemental analysis 75
2.3.5 Thermogravimetic analysis 77
2.3.6 XRD analysis 80
2.3.7 FTIR analysis 82
2.4 Conclusion 84
References 86

Chapter 3. Chemical pretreatment of high lignin content *P. juliflora* biomass to improve critical properties for pyrolysis 91-110
3.1 Introduction 91
3.2 Materials and Methods 92
3.2.1 Biomass gathering and processing 92
3.2.2 Chemical pretreatment experiments 93
3.2.3 Proximate, ultimate (elemental) and ash analysis of untreated biomass 93
3.2.4 Equilibrium moisture content, gross calorific value and biochemical compositional analysis of treated and untreated biomass 94
3.2.5 X-ray diffraction analysis 94
3.2.6 Thermogravimetric analysis 94
3.3 Results and Discussion 95
3.3.1 Characterization of *P. juliflora* biomass 95
3.3.2 Residual weight and biochemical composition of pretreated biomass 96
3.3.3 Equilibrium moisture content and calorific value 98
3.3.4 Elemental analysis 100

3.3.5 Thermogravimetric analysis 101
3.3.6 XRD analysis 104
3.4 Conclusion 105
References 107

Chapter 4. Impact of chemical pretreatment on the pyrolytic products of *A. donax* biomass 111-138
4.1 Introduction 111
4.2 Materials and Methods 113
4.2.1 Fixed bed pyrolysis reactor 113
4.2.2 Pyrolysis of treated and raw untreated biomass samples 115
4.2.3 Analysis of bio-oil using GC-MS 115
4.3 Results and Discussion 116
4.3.1 Effect of pretreatment on the overall yield of pyrolysis products 118
4.3.2 Effect of pretreatment on carbohydrate degradation bio-oil products 126
4.3.3 Effect of pretreatment on lignin degradation bio-oil products 130
4.3.4 Effect of pretreatment on biochar and non-condensable gas yield 134
4.4 Conclusion 135
References 136

Chapter 5. Impact of chemical pretreatment on the pyrolytic products of *P. juliflora* biomass 139-156
5.1 Introduction 139
5.2 Materials and Methods 140
5.2.1 Pyrolysis of treated and raw untreated biomass samples 140
5.2.2 Analysis of bio-oil using GC-MS 140
5.3 Results and Discussion 140
5.3.1 Effect of pretreatment on the overall yield of pyrolysis products 142
5.3.2 Effect of pretreatment on carbohydrate degradation bio-oil products 147
5.3.3 Effect of pretreatment on lignin degradation bio-oil products 149
5.3.4 Effect of pretreatment on biochar and non-condensable gas yield 153
5.4 Conclusion 154
References 155

Chapter 6. Investigating the role of AAEM in the pyrolysis of lignocellulosic biomass **157-186**
6.1 Introduction 157
6.2 Materials and Methods 158
6.2.1 Impregnation of AAEM salts into biomass matrix 158
6.2.2 Pyrolysis of salt impregnated biomass 159
6.2.3 Analysis of bio-oil using GCMS 159
6.3 Results and Discussion 159
6.3.1 Effect of AAEM salts on bio-oil composition 163
6.3.1.1 Effect of K and Mg salts on pyrolytic degradation of carbohydrate 165
6.3.1.2 Effect of K and Mg salts on pyrolytic degradation of lignin 172
6.3.2 Effect of K and Mg salts on char and non-condensable gas yield 182
6.4 Conclusion 183
References 184

Chapter 7. Overview and scope for future work **187-192**
7.1 Overview 187
7.2 Scope for future work 190

Annexures **193-216**
Annexure A 193
Annexure B 198
Annexure C 199
Annexure D 210

Research Outputs **217**

LIST OF TABLES

Chapter 1

Table 1.1	Estimated renewable energy potential in India as on 31.03.2019	3
Table 1.2	Biochemical composition of common lignocellulosic biomass	6
Table 1.3	Operating conditions and product streams of different types of pyrolysis	14
Table 1.4	Summary of literature on chemical pretreatment techniques and effects on biomass	23
Table 1.5	Summary of literature on the impact of chemical pretreatment techniques on pyrolysis products	35
Table 1.6	Summary of literature on the effect of alkali and alkaline earth metals on pyrolysis of biomass	47

Chapter 2

Table 2.1	Metal concentration in *A. donax* identified using ICP-MS	71
Table 2.2	Biochemical compositional analysis of untreated and treated *A. donax* biomass	72
Table 2.3	Thermogravimetric parameters of untreated and treated *A. donax* biomass	78
Table 2.4	Crystalline properties of untreated and treated *A. donax* biomass	80
Table 2.5	Characterization of signal labels in FTIR spectra	82

Chapter 3

Table 3.1	Metal concentration in *P. juliflora* identified using ICP-MS	95
Table 3.2	Biochemical compositional analysis of untreated and treated *P. juliflora* biomass	97
Table 3.3	Thermogravimetric parameters of untreated and treated *P. juliflora* biomass	102
Table 3.4	Crystalline properties of untreated and treated *P. juliflora* biomass	104

Chapter 4

Table 4.1	Properties of product streams of pyrolysis of untreated and treated *A. donax* biomass	117
Table 4.2	Pyrolytic liquid compounds identified through GC-MS analysis with their retention time, classification and source	121
Table 4.3	Identified chemicals from pyrolysis of raw untreated *A. donax*	124
Table 4.4	Bio-oil product distribution from pyrolysis of untreated and treated *A. donax*	124

Chapter 5

Table 5.1	Properties of product streams of pyrolysis of untreated and treated *P. juliflora* biomass	141
Table 5.2	Identified chemicals from pyrolysis of raw untreated *P. juliflora*	145
Table 5.3	Bio-oil product distribution from pyrolysis of untreated and treated *P. juliflora*	146

Annexures

Table C.1	Identified chemicals from pyrolysis of *A. donax* and *P. juliflora* biomass	199
Table D.1	Identified chemicals from pyrolysis of treated *A. donax*	210
Table D.2	Identified chemicals from pyrolysis of treated *P. juliflora*	212
Table D.3	Identified chemicals from pyrolysis of AAEM infused *P. juliflora* and *A. donax* biomass samples	214

LIST OF FIGURES

Chapter 1

Figure 1.1	Structure of Cellulose	7
Figure 1.2	Principle C_5 and C_6 monosaccharides of hemicellulose	8
Figure 1.3	Basic structural units in lignin	9
Figure 1.4	Biomass conversion process	11
Figure 1.5	Bio-oil formation through pyrolysis of biomass	15

Chapter 2

Figure 2.1	Combined plot of moisture content and calorific value of untreated and treated *A. donax* sample	74
Figure 2.2	Van Krevelen diagram of untreated and treated *A. donax* samples	76
Figure 2.3	(a) TGA plot of untreated and treated *A. donax* samples (b) DTG plot of untreated and treated *A. donax* samples	77
Figure 2.4	FTIR Spectra of untreated and treated *A. donax* biomass	82

Chapter 3

Figure 3.1	Combined plot of moisture content and calorific value of untreated and treated *P. juliflora* samples	98
Figure 3.2	Van Krevelen diagram of untreated and treated *P. juliflora* samples	100
Figure 3.3	(a) TGA plot of untreated and treated *P. juliflora* samples (b) DTG plot of untreated and treated *P. juliflora* samples	102

Chapter 4

Figure 4.1	Semi-batch pyrolysis reactor setup	114
Figure 4.2	Schematic of the Semi-batch pyrolysis reactor	115
Figure 4.3	Chromatogram of bio-oil from pyrolysis of raw untreated *A. donax* by GC-MS analysis	123

Figure 4.4	Comparison of the chemical composition of bio-oils obtained from (a) H_2SO_4 treated biomass, (b) H_3PO_4 treated biomass, (c) NaOH treated biomass and (d) SDS & Triton X-100 treated biomass.	129

Chapter 5

Figure 5.1	Chromatogram of bio-oil from pyrolysis of raw untreated *P.juliflora* by GC-MS analysis	145
Figure 5.2	Comparison of the lignin-derived chemical composition of bio-oils obtained from (a) H_2SO_4 treated biomass, (b) H_3PO_4 treated biomass and (c) NaOH treated biomass.	150

Chapter 6

Figure 6.1	Concentration of K and Mg in control and AAEM infused biomass samples	161
Figure 6.2	Bio-oil, biochar and gas yields form pyrolysis of K and Mg doped *P. juliflora* and *A. donax* samples	163
Figure 6.3	Classification of bio-oil peak areas on the basis of precursor materials	165
Figure 6.4	Carbohydrate derived pyrolytic bio-oil components: Effect of AAEM salts on the (a), (b) acetic acid yield; (c), (d) overall furan yield; (e), (f) individual furan compounds; (g), (h) overall ketone yield; and (i), (j) individual ketone compounds.	169
Figure 6.5	Lignin derived pyrolytic bio-oil components: Effect of AAEM salts on the (a), (b) overall guaiacol yield; (c), (d) individual guaiacol compounds; (e), (f) overall syringol yield; and (g), (h) individual syringol compounds.	176
Figure 6.6	Lignin derived pyrolytic bio-oil components: Effect of AAEM salts on the (a), (b) overall hydroxyphenol yield; (c), (d) individual hydroxyphenol compounds; (e), (f) overall other aromatics yield; and (g), (h) individual other aromatics compounds.	181

Annexures

Figure B.1	EDX spectra of raw untreated *A. donax* biomass	198
Figure B.2	EDX spectra of raw untreated *P. juliflora* biomass	198
Figure C.1	GC Spectra of bio-oil from pyrolysis of *A. donax* treated with (a) 1% H_2SO_4, (b) 3% H_2SO_4 and (c) 5% H_2SO_4	200
Figure C.2	GC Spectra of bio-oil from pyrolysis of *A. donax* treated with (a) 1% H_3PO_4, (b) 3% H_3PO_4 and (c) 5% H_3PO_4	201

Figure C.3	GC Spectra of bio-oil from pyrolysis of *A. donax* treated with (a) 1% NaOH, (b) 3% NaOH and (c) 5% NaOH	202
Figure C.4	GC Spectra of bio-oil from pyrolysis of *A. donax* treated with (a) 0.5% Triton X-100 and (b) 0.5% SDS	203
Figure C.5	GC Spectra of bio-oil from pyrolysis of *P. juliflora* treated with (a) 1% H_2SO_4, (b) 3% H_2SO_4 and (c) 5% H_2SO_4	204
Figure C.6	GC Spectra of bio-oil from pyrolysis of *P. juliflora* treated with (a) 1% H_3PO_4, (b) 3% H_3PO_4 and (c) 5% H_3PO_4	205
Figure C.7	GC Spectra of bio-oil from pyrolysis of *P. juliflora* treated with (a) 1% NaOH and (b) 3% NaOH	206
Figure C.8	GC Spectra of bio-oil from pyrolysis of *A. donax* doped with (a) 2% CH_3COOK, (b) 2% KCl (c) 2% MgO and (d) 2% $MgCl_2$	208
Figure C.9	GC Spectra of bio-oil from pyrolysis of *P. juliflora* doped with (a) 2% CH_3COOK, (b) 2% KCl (c) 2% MgO and (d) 2% $MgCl_2$	209

ABBREVIATIONS

AAEM	Alkali and alkaline earth metals
A. donax	*Arundo donax*
DTG	Difference thermo gravimetry
FTIR	Fourier transform infrared spectroscopy
GCMS	Gas chromatography mass spectroscopy
HHV	Higher heating value
ICP-MS	Inductively coupled plasma mass spectroscopy
INDC	Intended nationally determined contribution
MNRE	Ministry of new and renewable energy
MOSPI	Ministry of statistics and programme implementation
MW	Molecular weight
P. juliflora	*Prosopis juliflora*
SDS	Sodium dodecyl sulfate
SHP	Small hydropower
TAPPI	Technical association of pulp and paper industry
TGA	Thermo gravimetric analysis
UNFCCC	United Nations framework convention on climate change
XRD	X-ray powder diffraction

Chapter 1

General Introduction and Literature Review

1.1 Global energy scenario

Energy and fuels have been an indispensable part of human existence since time immemorial. Until the mid- to late-1800s, wood was used as the primary energy source. With the subsequent discoveries of higher energy density products: coal and crude oil for power generation and later for transportation, their usage substantially grew and continues to grow. In the last 50 years, from 1965 to 2015, global oil production recorded a three-fold increase from 1.5 to 4.3 million tons/year, coal from 58.1 to 157.8 exajoule/year. British Petroleum, in its 2019 annual report, has reported global crude oil reserves-to-production (R/P) ratio to be 50 with the current oil production rate of 94,718 barrels/day and total proven oil reserves at 2,44,100 million barrels (Dudley, 2019). Coal, with proven reserves of 10,54,782 million tons, has an R/P ratio of 132. Based on the available coal reserves, coal-based energy production can sustain for at least another century. On the flip side, multiple health disorders have proven links to

the air-based toxins and pollutants produced by burning coal. In the long term, the most severe impact of coal is carbon dioxide, which has been claimed to have a significant impact on climate change.

Hence, since the beginning of this century, the energy policies and investment plans of governments around the world started shifting to exploring other renewable energy sources (solar, wind, biomass and hydro) due to the fast dwindling fossil fuels and its adverse effects on the environment and health. China, the largest consumer of coal, has affirmed to achieve 20% power generation from renewable, non-fossil sources (Yang et al., 2016). A few countries plan to go well and over the targets set by the United Nations to hold global warming to below 2 ℃ increase against preindustrial levels. Sweden, for instance, in 2015, announced its goal to eliminate power generation from conventional sources by 2040. Denmark plans to achieve the same by 2050.

1.2 Indian energy scenario

India, being the second most populated country in the world, is the third-largest energy consumer. At the end of India's 10^{th} 5-year plan (2002-2007), the per capita energy consumption, which was at 672 kWh, increased drastically to 1122 kWh by the end of the 12^{th} 5-year plan (2012-2017) (Mhaske and Sharma, 2019). This is indicative of the growing energy needs of India. The statistical review of world energy report published by British Petroleum reported an average annual increase in consumption of primary energy by 5.2% between the years 2007 and 2017 against the global average of 1.5% (Dudley, 2019). As of Mar 2018, India has a cumulative installed energy generating capacity of 344 GW. Despite having significantly high generating capacities and peak loads of 164 and 177 GW during the periods 2017-18 and 2018-19,

respectively, some parts of the country faced power shortages. Surprisingly, India's coal-based power production at 223 GW alone is capable of handling the peak demands. However, due to crucial issues such as local coal shortages, unregulated high prices of imported coal and high transmission cum distribution losses, the power generation is inadequate. To address these issues of power shortfalls and the continually increasing energy needs of a growing country, the focus of the Government of India started shifting towards the development of alternate energy sources. Additionally, with the increasing awareness towards increasing greenhouse gas emissions and climate change, there's a pressing need for developing sustainable, efficient and environmentally friendly technologies for energy generation. Studies from the last decade have revealed huge potentials for energy production from renewable sources such as wind, solar, biomass and hydropower. The energy statistics, undertaken by the Ministry of Statistics and Programme Implementation (MOSPI), has estimated the total potential for renewable energy generation to 10,97,465 MW (Sanyal, 2020). The potential and distribution of each of the renewable energy sources are listed in Table 1.1.

Table 1.1: Estimated renewable energy potential in India as on 31.03.2019 (Source: Sanyal, 2020)

Renewable Energy Source	Potential (in MW)	Distribution (%)
Solar power	7,48,990	68.25
Wind power	3,02,251	27.54
Small hydropower (SHP)	21,134	1.93
Biomass power	17,536	1.60
Biomass based cogeneration	5,000	0.46
Waste to Energy	2,554	0.23
Total	10,97,465	100

As part of India's commitment to combating climate change, the Government of India signed the Paris climate agreement in 2015. In its Intended Nationally Determined Contribution (INDC) to the United Nations Framework Convention on Climate Change (UNFCCC), India has pledged to increase its share of electricity generation from non-fossil based sources to 40% by 2030. In its INDC, India has initially planned to aggressively improve its power scenario by developing its renewable power-generating infrastructure to 175 GW by 2022 from its position of 38.8 GW in 2015 (Khullar, 2015; Kaur, 2016). The breakup of this 175 GW is as follows: 100 GW solar, 60 GW wind, 10 GW biomass and 5 GW SHP. As of December 2019, the Ministry of New and Renewable Energy (MNRE) reported 85.90 GW power generating capacity from non-conventional renewable energy sources has already been installed, accounting for 23% of the total installed capacity (MNRE, 2020). Already established biomass-based power generation is currently contributing 9778 MW against the established potential of 17536 MW.

As per a recent report by MNRE in Dec 2019 the capability of biomass power generation has been upgraded to 26000 MW. This indicates the possibility of biomass-based power contributing significantly towards achieving the 2022 and, eventually, the 2030 targets.

In subsequent sections, the structure of biomass, its basic components and the techniques to convert it to useful energy are discussed.

1.3 Structure of biomass

Biomass, in general, is the renewable organic matter derived from living organisms (plants and animals). The formation of biomass, directly or indirectly, is closely linked to photosynthesis wherein the sun's solar energy is converted into chemical energy. This chemical energy stored in biomass can be utilized as a source of energy. In the context of this present thesis, biomass specifically refers to lignocellulosic biomass (woody biomass).

Lignocellulosic biomass encapsulates all kinds of plant dry matter such as wood, wood processing wastes, agricultural crop residues, grasses and energy crops. Industrial residues products such as bagasse and oil cakes obtained after recovery of products such as oil and sugar juice are also categorized under lignocellulosic biomass. Consequently, a major share of biomasses found on the surface of the earth are categorized under lignocellulosic biomass.

Woody biomass is broadly classified into two types: softwood and hardwood. The term soft or hardwood, as the names suggest, does not refer to the physical property hardness of the wood. Rather, it refers to this origination from an angiosperm (hardwood) or a gymnosperm (softwood) (Hague, 1998).

The presence of three core components: cellulose, hemicellulose and lignin in addition to other components (extractives, ash) are the defining nature of lignocellulosic biomasses. Each biomass type has its own unique composition mixture of each of the components. The component distribution of a specific biomass type also varies with changes in factors such as the age of the biomass, soil type and location. Table 1.2 lists the component proportions of some of the commonly utilized lignocellulosic biomass.

Table 1.2: Biochemical composition of common lignocellulosic biomass

Biomass	Cellulose (%)	Hemicellulose (%)	Lignin (%)	Extractives (%)	Ash (%)	Reference
Hardwood						
Beech	47.7	21.4	25.5	-	0.3	(Bodirlau et al. 2008)
Oak	43.2	21.9	35.4	1.6	0.2	(Yu et al. 2017)
Eucalyptus	48.1	12.7	26.9	-	-	(Sannigrahi et al. 2010)
Eucalyptus loxophleba	42.4	23.8	24.7	9.1	0.5	(Mourant et al. 2011)
Poplar	42.2	16.6	25.6	1.4	-	(Sannigrahi et al. 2010)
Softwood						
Spruce	47.1	22.3	29.2	1.1	0.4	(Yu et al. 2017)
Pine	45.6	24.0	26.8	5.7	1.1	(Yu et al. 2017)
Eastern Red Cedar	40.3	17.9	35.9	-	0.3	(Pasangulapati et al. 2012)
Cypress	46.1	18.4	34.4	0.7	0.3	(Bhaskar et al. 2008)
Grasses						
Bamboo	46.5	18.8	25.7	-	2.3	(Chen et al. 2017)
Elephant grass	22	24	23.9	-	6	(Abbasi and Abbasi 2010)
Switch grass	45	31.4	12	-	-	(Abbasi and Abbasi 2010)
Miscanthus	48.5	20.1	22.4	4.3	2.3	(Selah et al. 2013)
Others						
Sugarcane bagasse	43.2	24.9	23.4	-	3.8	(Kim et al. 2010)
Wheat straw	42.7	25.4	17.3	3.2	5.6	(Selah et al. 2013)
Rice husk	31.3	24.3	14.3	8.4	23.5	(Raveendran et al. 1995)
Corn cob	40.4	35.3	19	2.8	1.2	(Azeez et al. 2010)
Coconut shell	36.3	25.1	28.7	8.3	0.7	(Raveendran et al. 1995)

Strong physico-chemical bonds hold together the various components of lignocellulosic biomass thereby giving the structure to biomass. Each of these components are described below.

1.3.1 Cellulose

Cellulose constitutes the main component of cell wall and amounts to 40-45% of the dry material in wood (Table 1.2). Cellulose consists of three major elements: 44.2% carbon, 6.3% hydrogen and 49.5% oxygen, and thereby it is commonly chemically expressed as $C_6H_{10}O_5$ (Wang and Luo, 2016). Fig. 1.1 shows the structure of cellulose. It is made up of repeating cellobiose units, each of which constitutes of two β-D-glucopyranose units linked by a β-1,4 glucosidic bond. In structure, cellulose being a linear macro-molecular homopolysaccharide is indicated as $(C_6H_{10}O_5)_n$ where *n* refers to the degree of polymerization. With woody biomass, *n* varies between 1000 and 5000, and with cotton having close to 90% pure cellulose, the value of *n* is ~10000 (Hallac and Ragauskas, 2011). The long linear chain structure makes it resistant to chemicals, solvents, hydrolysis and temperature.

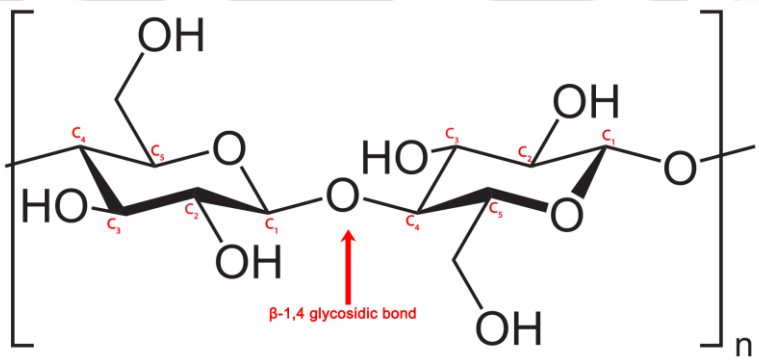

Figure 1.1: Structure of cellulose

1.3.2 Hemicellulose

Hemicellulose is the second abundant polymer present in the plant biomass. Their content varies with different biomass species and locations. Softwoods, in general, have lower hemicellulose than hardwoods. The hemicellulose content in grasses is 20-25%, which is higher than the content in softwood and hardwood, which have 10-15% and 18-23%, respectively (Wang and Luo, 2016). Unlike cellulose, which is a monosaccharide, hemicellulose is a heterocyclic biopolymer consisting of different C_5 and C_6 monosaccharides (sugars). The fundamental sugars, which include glucose, mannose, galactose, xylose and arabinose, shown in Fig. 1.2, form the basic structural units of hemicellulose. Structurally, hemicellulose chains are predominantly branched but are relatively short compared to cellulose with a degree of polymerization, on average, less than 200. The short chains make them vulnerable to chemical agents and easily degradable by weak acids (Fivga, 2012). The thermal degradation temperature lies in the range 220-315 ℃, which is much lower than that of cellulose whose degradation occurs between 315 ℃ and 400 ℃ (Kim et al., 2017).

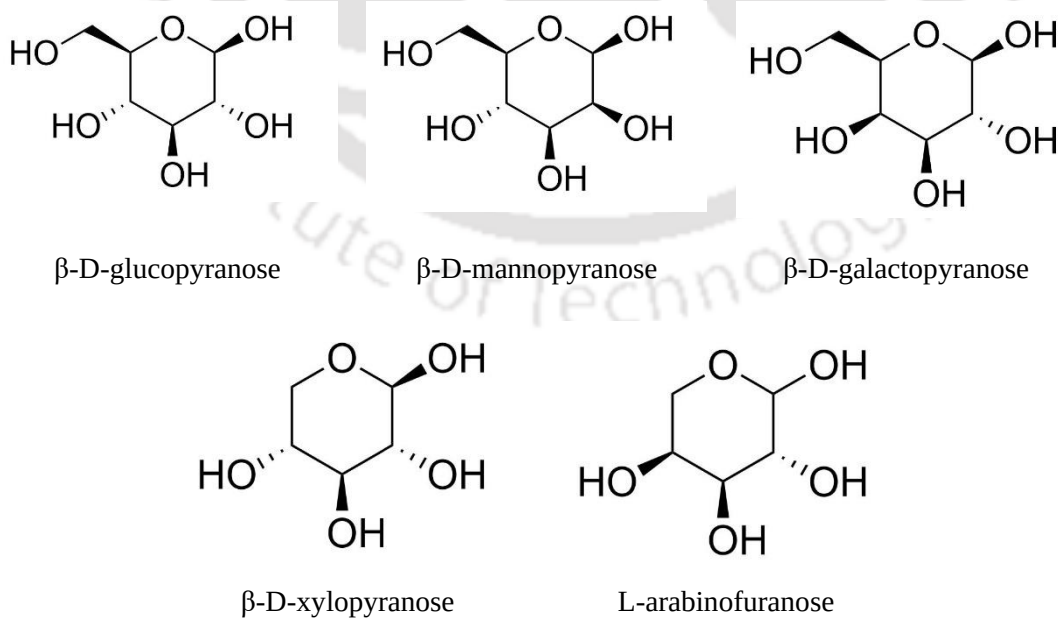

Figure 1.2: Principle C_5 and C_6 monosaccharides of hemicellulose

1.3.3 Lignin

Lignin has a very complex chemical structure, and unlike cellulose and hemicellulose, it is a three-dimensional, high molecular weight cross-linked polymer. This polymer is composed primarily of phenyl propane units in a random and nonlinear form. The three basic phenyl propane units, shown in Fig. 1.3, are hydroxyl, guaiacyl and syringyl, which are obtained from the three basic units observed in lignin: p-hydroxylphenyl (H-lignin) units from p-coumaryl alcohol, guaiacyl (G-lignin) units from coniferyl alcohol and syringyl (S-lignin) units from sinapyl alcohol (Ghalia and Dahman, 2017).

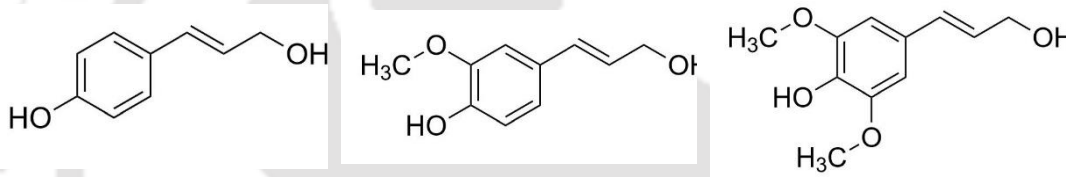

p-coumaryl alcohol Coniferyl alcohol Sinapyl alcohol

Figure 1.3: Basic structural units in lignin

Variations in the lignin of different types of lignocellulosic biomass are observed based on the proportion of H-, G- and S-lignin. Lignin in softwood is wholly composed of guaiacyl units. A combination of both guaiacyl and syringyl units form the lignin framework in hardwoods. H-lignin units form a significant constituent in grasses and a few softwood species (Hague, 1998). Lignin degradation occurs over a wide range of temperatures between 160-190 °C due to the presence of different types of lignin units and its linkages (Kim et al., 2017).

1.3.4 Extractives

Extractives are a group of low molecular compounds constituting a small fraction in biomass besides the three major components (cellulose, hemicellulose and lignin). Extractives, essentially non-structural components, include fats, waxes, tannins, resins, pigments, starches, lignans, etc. (Wang and Luo, 2016). They contribute to the color of the wood, resistance and durability to insect and fungal attacks. Their composition and content varies in different species and even in different sections of the same biomass. Woody biomass contains relatively lower extractive content than herbaceous biomass (Sluiter et al., 2010). The removal of extractives in wood is possible using hot water or organic solvents.

1.3.5 Ash

The inorganic component of plant biomass is called ash. It primarily consists of alkali and alkaline earth metals: sodium (Na), potassium (K), magnesium (Mg), calcium (Ca) and other inorganic elements such as phosphorus (P), chlorine (Cl) and silicon (Si). Trace content of other elements such as titanium, aluminum, manganese, cobalt, vanadium, nickel, molybdenum, barium, zinc, copper and lead are also present. Biomass ash is alkaline by nature. Generally, ash constitutes only a small fraction in woody biomass but can account for up to 20% in certain biomass species (Caillat and Vakkilainen, 2013). Washing with water reduces ash content to a certain extent, but ash removal higher than 90% is possible with chemical agents such as acids (Carrillo et al., 2014; Jiang et al., 2013). Ash does not directly translate into energy during conversion processes but indirectly affects the process viz. by behaving as catalysts during thermochemical process.

1.4 Biomass to energy conversion techniques

Chemical energy trapped in biomass needs to be transformed into other useful forms of energy for its utilization in various fields such as the power sector, fuels, chemicals, etc. The conversion techniques, shown in Fig. 1.4, are broadly classified into three categories viz. direct combustion, thermochemical processes and biochemical processes. Each of these thermochemical processes (gasification, pyrolysis/liquefaction), biochemical processes (fermentation, anaerobic digestion) and combustion are briefly described in the sections

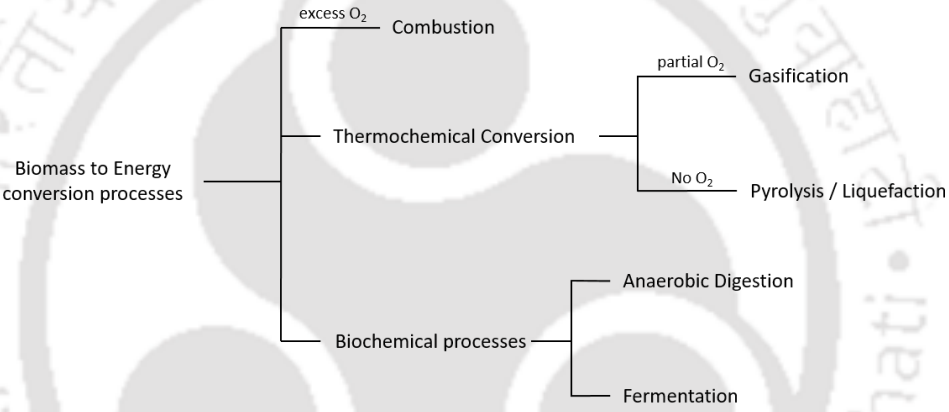

Figure 1.4: Biomass conversion process (Adapted from Agreal et al., 2019)

1.4.1 Combustion

Combustion is the direct burning of biomass in the presence of excess oxygen. It was the oldest approach to convert biomass to heat energy. Combustion of woody biomass was primarily used in earlier times for cooking and to keep warm in cold regions. It is still widely prevalent in rural areas of developing countries due to the easy accessibility and affordability of firewood (Tabuti et al., 2003). The World Bank in 2016 reported that 3 billion people, which is ~ 40% of the global population, do not have access to clean energy for their daily needs and rely on combustion of biomass (World Bank, n.d.). Industrially, biomass is co-fired with coal to produce heat and

power through' co-generation processes simultaneously. Some of the gaseous products of biomass combustion are carbon monoxide (CO), nitrogen dioxide (NO_2), nitrogenated compounds (NO_x), sulfur dioxide (SO_2), carbon dioxide (CO_2) and particulate matter ($PM_{2.5}$, PM_{10}).

1.4.2 Gasification

Gasification is the process of production of carbon monoxide and hydrogen-rich syngas through a controlled oxidation of carbon containing biomass at high temperatures of 500 – 1300 °C (Basu and Basu, 2013). Air, subcritical steam, oxygen, or a mixture of these are used as the gaseous medium for the process to occur. This syngas, which also contains methane, finds application in the production of electrical energy and other value-added products such as chemicals, fertilizers and fuels.

1.4.3 Pyrolysis / Liquefaction

Pyrolysis involved the thermal break down of organic matter at high temperatures of 380 – 530 °C either in the absence of oxygen or in a limited oxygen environment, which does not support gasification (Basu and Basu, 2013; Bridgwater and Bridge, 1991). The temperature of operation is much lower when compared to gasification. Hydrothermal liquefaction which can process both wet and dry biomass is operated at high pressures of around 10 – 25 MPa (Zhang and Chen., 2018). Pyrolysis process and the products generated are discussed at length in section 1.5.

1.4.4 Anaerobic digestion

Anaerobic digestion is the process in which a consortium of microorganisms transforms organic matter in the absence of oxygen. Biogas, being the main product consisting of methane and carbon dioxide, can be used to produce heat and electricity (Rajendran et al., 2019). Food wastes from food processing units, farms, commercial

and retail outlets are the primary sources of feedstock for biogas plants (Labatut et al., 2018). One of the down side is the relatively lengthy digestion time of 20 to 40 days. Sugars generally get digested quickly, followed by polysaccharides such as cellulose and hemicellulose, which take longer duration. Anaerobic microbes do not generally break down the structural frame of lignocellulosic biomass composed of lignin.

1.4.5 Fermentation

Fermentation functions by the action of enzymes, produced by different microorganisms, on sugars to produce biohydrogen or bioethanol. Certain feedstocks (such as carbohydrates) require pretreatment or saccharification to convert polysaccharides into sugars. Bacterial species, such as *Enterobacter* and *Clostridium* are commonly employed to produce biohydrogen from sugars (Rajendran et al., 2019). Bioethanol, produced through the fermentation of glucose to ethanol by microbial species such as *Saccharomyces cerevisiae* and *Zymomonas mobilis* is extensively used as fuel in the transportation sector. The general optimal temperature for fermentation of 30 – 40 °C and high conversion yields of 90 – 97% has been reported (Zabed et al., 2014).

1.5 Pyrolysis

The three main pyrolysis processes are fast, intermediate and slow pyrolysis. Slow pyrolysis is primarily used for char production, while the other two techniques are used for oil production. They are differentiated by the operating conditions and the range of products we receive from them which are tabulated in Table 1.3.

Table 1.3: Operating conditions and product streams of different types of pyrolysis (Adapted from Yang, 2014; Dhyani and Bhaskar, 2017)

Mode of pyrolysis	Operation conditions	Pyrolysis products
Fast Pyrolysis	450 – 600 ℃. Low solid and vapor residence time of < 2s. Heating rate > 1000 ℃/s. Rapid freezing and condensation of pyrolysis vapors	Liquid: 70% Solid: 15% Gas: 15%
Intermediate Pyrolysis	300 – 500 ℃. Longer residence time up to a few minutes.	Liquid: 50% Solid: 20% Gas: 30%
Slow Pyrolysis	200 – 400 ℃. Long residence time up to a few hours. Very low heating rates of around 2 ℃/min	Liquid: 0% Solid: 80% Gas: 20%

Fast pyrolysis, characterized by very high heating rates and rapid condensation of the resulting vapors, gives high liquid bio-oil yield of around 70%. Slow pyrolysis is carried out at low temperatures (200 – 400 ℃) with much longer residence time. This technique, predominantly employed for biochar production, yields close to 80% solid production. Intermediate pyrolysis occurs with conditions in the range between slow and fast pyrolysis. Although it operates in temperature regimes similar to that of fast pyrolysis, the vapour residence time is much higher. The liquid bio-oil yield is thus lower than that produced in fast pyrolysis. Yield of biochar, a valuable by-product, is higher with intermediate pyrolysis due to higher solid residence time of 2 to 30 min (Yang, 2014).

The characteristics and uses of each of the three main properties of pyrolysis are now described.

1.5.1 Bio-oil

The condensation (freezing) of the vapours produced by the thermal treatment of biomass results in the production bio-oil which is generally dark brown in colour with a distinctive smoky odour.

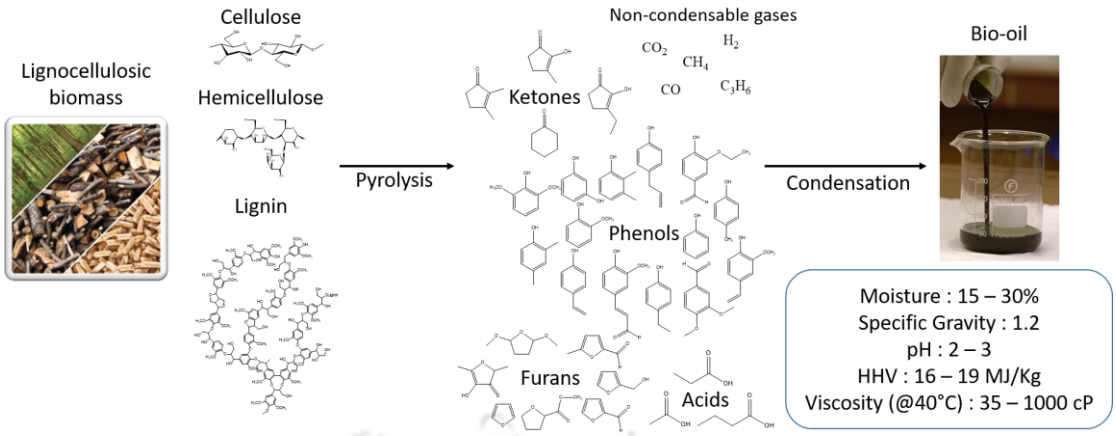

Figure 1.5: Bio-oil formation through pyrolysis of biomass

Bio-oil consists of 300+ compounds with carbon numbers ranging between C_4 and C_{15} and is essentially a mixture of compounds that include furans, alcohols, carboxylic acids, phenols, ketones and aldehydes. Fig. 1.5 shows the main precursor complex bio-polymer substrates which undergo random thermal cracking to form bio-oil. Bio-oils are generally highly acidic (pH of 2 – 3) and viscous (35-1000 cP), which tends to increase with time. Water, which is formed as a by-product of dehydration reactions during pyrolysis, contributes to around 15 – 30% in bio-oil (Czernik and Bridgwater, 2004). The typical calorific value of bio-oil is 16-19 MJ/kg (Pattiya, 2018). Bio-oil is highly unstable due to the nature of the components, which always tend to move towards chemical equilibrium. Hence, bio-oils are stored at low temperature to limit secondary reactions. Various factors such as high viscosity, high oxygen content, high moisture content and low pH limit its direct application.

1.5.2 Biochar

Biochar is the carbon-rich solid residue after pyrolysis of lignocellulosic biomass. Biochar consists predominantly of carbon of up to 80% (Izaurralde et al., 2012). Mineral content in biomass, especially AAEMs, which do not volatilize in the

temperature regimes employed for pyrolysis, contribute to the rest of the biochar yield. Biochar finds application in the agricultural industry to improve crop yield, enhance water-retention capacity, soil acidity correction and plant pathogen control (Saeid and Chojnacka, 2019). The gross calorific value of biochar varies between 17.5 and 26.5 MJ/kg (Mierzwa-Hersztek et al., 2019; Dąbrowska et al., 2017). Biochar can be directly employed as a solid fuel in boilers, or it could be blended with conventional fossil fuels and co-fired for electricity generation (Pattiya, 2018). The ability to act as a good absorber of organic pollutants can be further enhanced by chemical or physical activation processes.

1.5.3 Non-condensable gas

The vapors formed by pyrolysis consists of compounds varying from C_1 to C_{15}, of which compounds above C_4 condense as bio-oil and C_1-C_3 contribute to non-condensable gas. The generally observed non-condensable gas components are H_2, CO, CO_2, CH_4, C_2H_4, C_2H_6, C_3H_6 and C_3H_8 (Pattiya, 2018). The composition of the non-condensable gases depends on the species and their biochemical composition (Dhyani and Bhaskar, 2017). Thermal cracking of cellulose carbonyl and carboxyl linkages accounts for the CO yield. Hemicellulose pyrolysis contributes to the CO_2 production due to the higher carboxyl content. Lignin, primarily composed of phenyl and methoxyphenol content, contributes to the production of H_2 and CH_4. The gases can be recycled back to the pyrolysis reactor to be used as a carrier gas. Owing to their combustible nature the gases can alternatively be employed for combustion purposes in energy and electricity production.

1.6 Literature Review

1.6.1 Chemical pretreatment techniques

The pre-processing of biomass prior to most of the energy conversion process, viz. fermentation, anaerobic digestion and gasification, is practiced as a means to improve the efficiency of energy conversion. For example, biomass is chemically treated with acid/alkali to improve cellulose accessibility before fermentation. Some of the commonly employed chemical-based treatment techniques and their subsequent impact on biomass features (chemical and structural) and the energy conversion process are discussed in this section.

Kim and Holtzapple (2005) investigated the chemical treatment of corn stover with $Ca(OH)_2$ in different environments and temperatures between 25 and 55 ℃ for up to 4 weeks. $Ca(OH)_2$ consumption was higher in the oxidative environment as delignification required the presence of oxygen. Deacetylation occurred in non-oxidative environment and was influenced primarily by temperature. Removal of acetyl groups occurred rapidly. However, the removal of lignin occurred gradually throughout the entire period of pretreatment. Higher content of hemicellulose and lignin were removed in non-oxidative and oxidative environments respectively. A maximum of 87.5% lignin was removed with oxidative environment at 55 ℃. Enzymatic digestibility increased substantially with lime pretreatment, and much higher activity was observed under oxidative environment. Although cellulose had higher stability than hemicellulose, degradation occurred rapidly once it dissolved in the treatment media.

Chen et al. (2009) comparatively examined the action of four chemical agents: dilute acid (H_2SO_4), lime ($Ca(OH)_2$), ammonia (NH_4OH) and sodium hydroxide

(NaOH) on the availability and accessibility of cellulose in corn stover for enzymatic digestibility. Each of these pretreatment techniques resulted in weight loss and varying degrees of hydrolysis of lignocellulosic compounds. H_2SO_4 treatment was most effective with 76% hemicellulose degradation, followed by ammonia treatment with 67.8% hemicellulose reduction. Cellulose degradation, varying between 2 and 8%, was minimal in all the pretreatment techniques. NaOH treatment showed a maximum lignin removal of 74%, thereby improving cellulose accessibility to enzymatic action. Enzymatic hydrolysis was carried out with 20 FPU/g substrate and 8% substrate concentration. H_2SO_4 treated biomass yielded the lowest reducing sugar yield of 24.6 g/L followed by lime and ammonia treatment with sugar yields of 37.9 and 42.8 g/L respectively. The hydrolysate from enzymatic action on alkali-treated biomass yielded the highest fermentable sugar yield of 64.1 g/L, making it the optimal pretreatment for ethanol production.

Dhabhai et al. (2013) studied the structural change of wheat straw biomass with dilute acid treatment. Wheat straw was treated with 0.5-2% H_2SO_4 at temperatures between 120 and 190 ℃ for time duration between 7-240 min. The acid-treated resulted in hydrolysis of hemicellulose and lignin, whose intensity increased with an increase in the severity of the process, which was reflected in the observed increase in cellulose content. The solubilization of biomass components resulted in an increase in surface area from 4 m^2/g up to a maximum of 7.1 m^2/g. However, surface area and pore volume started to drop at temperatures higher than 180 ℃ due to the shrinking and deformation of pores due to excessive pressure and high temperature. The increasing trends in crystallinity were attributed to the conversion of non-crystalline cellulose to glucose. Thermal degradation of crystalline cellulose at temperatures above 180 ℃ resulted in a

decrease in crystallinity. FTIR analysis showed small changes in aromatic C-H peaks corresponding to lignin, signifying the limited capacity of acid to solubilize lignin completely.

Singh et al. (2014) extensively investigated the various pretreatment techniques for effectively reducing sugar release by understanding the underlying mechanism behind each of the physical, chemical, and physicochemical pretreatments. Dilute acid treatment gave high sugar release, which revealed a significant reduction of the xylan fraction of biomass. However, the sugar release, which varied inversely with the concentration of acid treatment, was attributed to the simultaneous hydrolysis of cellulose at high temperatures. Alkali treatment comparatively resulted in much lower sugar release suggesting minimal hydrolysis of hemicellulose and cellulose. Alkali treated biomass were characterized by enhanced surface area, reduced crystallinity and breakdown of lignin structure. Oxidizing agent H_2O_2 improved the accessibility of cellulose for enzymatic treatment by acting as a swelling agent. Analysis of H_2O_2 treated biomass showed the degradation of lignin. Surfactant (SDS and Triton X-100) treatments resulted in higher sugar yield compared to alkali treatment. However, not much difference was observed between SDS and triton X-100 treatments.

Edmunds et al. (2017) studied the chemical treatment of switchgrass (*Panicum virgatum* L.) with chelating agents (EDTA and citric acid) and compared it with other conventionally used chemical agents, which include sulphuric acid, acetic acid and water. Mineral removal ranged between 40 and 87% when treated with chelating and chemical agents for 5 – 20 min. Treatment with citric, acetic acids and water did not vary significantly with duration of treatment. H_2SO_4 treatment gave a high removal efficiency of 70.8% with 5 min treatment time. However, with an increase in duration,

the degradation of biomass structure through hydrolysis of hemicellulose and cellulose affected the demineralization efficiency. The demineralization efficiency increased with EDTA treatment duration and reached its maximum of 87.3% with 20 min treatment. All chemical agents were influential in removing K, with efficiencies ranging between 95.5 and 99.6%. The demineralization pattern of Ca and Mg were similar, and removal efficiency in decreasing order of treatment media was H_2SO_4 > EDTA > citric acid > acetic acid > water. EDTA was most effective in the removal of Si of up to 75.2%. Due to the significant degradation observed with H_2SO_4 treatment, EDTA treatment was the most effective treatment for the removal of AAEMs.

Jamaldheen et al. (2018) compared various pretreatment techniques such as H_2SO_4 and NaOH coupled with microwave, ultrasound, autoclaving or heating at high temperatures to achieve maximum holocellulose content in *sorghum durra* stalk. Heating at high temperatures resulted in the degradation of holocellulose due to the exposure to dry heat. Among the two solvents used, it was observed that all NaOH treated biomass had higher holocellulose content than H_2SO_4 treated biomass due to its delignification ability, which is not associated with acid treatment. Of all the NaOH treatments, 1% NaOH coupled with autoclaving, gave the highest yield of 83.9 % holocellulose. However, NaOH was also found to hydrolyze hemicellulose, which was evident by the presence of arabinose in the filtrates of alkali-treated biomass. The absence of peaks at 1732 and 1515 cm^{-1} associated with lignin in FTIR analysis confirmed the delignification effect of NaOH, resulting in an increase in holocellulose content. By varying the duration of alkali treatment coupled with autoclaving between 10 and 30 min, it was observed that hemicellulose yield increased with time with a decrease in acid-insoluble lignin (ADL). The maximum holocellulose yield of 85.7%

and the lowest ADL of 2.1% was obtained with 1% NaOH treated coupled with autoclaving for 30 min.

Haykiri-Acma and Yaman (2019) studied the effect of phosphoric acid treatment on the structural, compositional and combustion characteristics of corn residue. Proximate analysis of the treated corn residue revealed an increase in fixed carbon at the expense of the volatile content. An increase in ash content was also observed, which was attributed to the introduction of phosphorus into biomass structure through the media employed for the acid treatment. Reduction in the crystallinity index from 0.25 in raw biomass to 0.06 in treated biomass showed the ability of the acid to alter the structure by increasing the amorphous fraction. The removal of hemicellulose and covalent bonds during acid treatment reduced the maximum burning rate by broadening the peaks. The removal of elements exhibiting catalytic activity could also account for the slow-burning. The treatment also resulted in a decrease in calorific value from 15.5 to 14.2 MJ/kg. A comparative study with other chemical agents showed that H_2SO_4, HNO_3 and NaOH also reduced the calorific value. However, treatment with H_2O, HCl and CH_3COOH aided in increasing the calorific value.

Javed (2020) studied the physiochemical structural modifications occurring in wheat straw with various acids and their impact on the thermal degradation characteristics. The acid treatment, which includes 5% H_2SO_4, HCl, CH_3COOH and a mixture of all three acids, resulted in a marginal decrease in moisture and an increase in fixed carbon. All treatments resulted in a significant reduction in ash content, with the maximum reduction observed in the mixed acid treatment. This reduction in ash content was attributed to the observed improvement in the HHV. The surface morphology of treated samples indicated the solubilizing effect of treatment media. The

solubilization of small particles was accounted for the observed reduction in surface area. TGA analysis revealed the shifting of cellulose degradation peak to a higher temperature. This observation indicated the washing off of AAEMs during treatment, thereby reducing the catalytic activity. The absence of AAEMs, especially potassium, resulted in increasing the char yield. Potassium enhances the char gasification by H_2O and CO_2 to form CO and H_2; hence the absence of potassium yielded higher char content.

The brief overview of the chemical treatment techniques and their effects on biomass discussed throughout this section are listed in Table 1.4 below.

Table 1.4: Summary of literature on chemical pretreatment techniques and effects on biomass

Biomass	Pretreatment media	Salient features	Reference
Corn stover	0.5 g $Ca(OH)_2$/g biomass in oxidative and non-oxidative environment. Temperature: 22-55 ℃. Duration: up to 4 weeks.	Removal of acetyl groups was rapid compared to removal of lignin, which occurred gradually throughout the pretreatment period. Non-oxidative treatment removed higher fraction of hemicellulose while treatment in oxidative environment resulted in higher delignification. A maximum of 87.5% lignin was removed.	Kim and Holtzapple, 2005
Corn stover	1.5% H_2SO_4, 0.4g/g $Ca(OH)_2$, 10% NH_4OH, 2% NaOH.	Maximum removal of cellulose, hemicellulose and lignin by NH_4OH, H_2SO_4 and NaOH respectively. Removal of lignin by NaOH exposed cellulose to enzyme activity, thereby yielding highest fermentable sugars for ethanol production.	Chen et al., 2009
Wheat straw	0.5-2% H_2SO_4. Temperature: 120-190 ℃. Duration: 7-240 min.	Hydrolysis of hemicellulose and lignin occurred, increasing surface area and pore volume at 120-180 ℃. Above 180 ℃, excessive temperature and pressure resulted in shrinking and deformation of pores. Cellulose fraction increased till 180 ℃ and then decreased, resulting in similar trend in the crystallinity index. Degradation of amorphous fraction of cellulose at low temperatures also contribute to variations in crystalline index.	Dhabhai et al., 2013
Parthenium hysterophorus	1-5% H_2SO_4 and NaOH, 0.5% SDS and Triton X-100, H_2O_2 + NaOH. Temperature: 120 ℃, 121 ℃ @ 15 psi pressure. Duration: 20, 30 & 40 min. L/S ratio: 10.	Dilute acid significantly reduced the xylan fraction of biomass. Increase in acid conc. reduced the sugar release. Alkali treatment enhanced surface area, reduced crystallinity but yielded less sugar. H_2O_2 treatment showed degradation of lignin. Both surfactants gave similar, but higher sugar yields than alkali treated biomass.	Singh et al., 2014

Biomass	Pretreatment media	Salient features	Reference
Switchgrass (*Panicum virgatum* L.)	EDTA, citric acid, CH_3COOH, H_2SO_4, H_2O. Duration: 5-20 min. L/S ratio: 20.	H_2SO_4 demineralization efficiency decreased with time due to structural damage to cellulose and hemicellulose. EDTA showed highest overall demineralization efficiency (87.3%). Decreasing order of the removal of Ca and Mg: H_2SO_4 > EDTA > citric acid > acetic acid > water EDTA showed highest Si removal efficiency.	Edmunds et al., 2017
Sorghum durra stalk	1% H_2SO_4 & 1% NaOH with ultrasound (10 min), microwave (180 W for 3 min), autoclaving (121 ℃, 15 psi for 20 min) or direct heating (121 ℃ for 30 min).	All NaOH treated biomass expressed higher holocellulose content than H_2SO_4 treated biomass. NaOH + Autoclaving gave highest holocellulose yield which increased with duration of reaction.	Jamaldheen et al., 2018
Corn residue	5 % H_3PO_4 Duration: 2 h.	Increase in fixed carbon, decrease in volatile content. Decrease in crystallinity index. Reduction in maximum degradation rate due to broadening of degradation temperature range. H_3PO_4, H_2SO_4, HNO_3, NaOH treatment decreased the calorific value, while H_2O, HCl and CH_3COOH treatment increased the calorific value over the raw biomass HHV.	Haykiri-Acma and Yaman, 2019
Wheat straw	5% H_2SO_4, HCl, CH_3COOH and mixture of all three acids. Duration: 2 h. L/S ratio: 15.	Increase in volatile content with significant decrease in ash content. Increase in HHV due to reduce in ash content and variation in biomass composition. TGA analysis revealed increased char yield due to reduction of ash during acid treatment, which aids in the gasification of char with primary gas products CO_2 and H_2O to form CO and H_2.	Javed, 2020

1.6.2 Effect of chemical pretreatment techniques on pyrolysis products of biomass

Pyrolysis of biomass essentially is the thermal breakdown of lignocellulosic components to smaller molecules, which in part condense to form bio-oil and the rest remain in the form of non-condensable gases. By modifying the structure and composition of these primary lignocellulosic components, the pyrolysis reaction can be partially controlled to follow favorable degradation mechanisms. This section includes recent literature, which studies the impacts and effects of various chemical pretreatments on lignocellulosic components, which control the dynamics of pyrolysis reactions. The pyrolysis of individual lignocellulosic components viz., cellulose, hemicellulose and lignin have also been included to gain insight into their individual contributions in pyrolysis.

Dobele et al. (2003) investigated the effects of treatment and impregnation of phosphoric acid on materials containing cellulose such as wastepaper, recycled pulp and birch wood towards production of 1,6-anhydrosaccharides. Impregnation of different materials revealed that microcrystalline cellulose and birch wood were the least and most effective in their ability to absorb and retain the acid respectively. The highest yield of levoglucosan (40%) was obtained with the pyrolysis of microcrystalline cellulose treated with 0.5% acid solution. Pyrolysis of 2% acid-treated cellulose, on the other hand, yielded high concentration of levoglucosenone (34%). The pyrolysis of recycled pulp showed a higher yield of levoglucosenone in all instances. The changes in cellulose structure during recycling and the acid treatment accounted for the dehydration reactions during pyrolysis, resulting in increased yield of levoglucosenone. Birch wood pyrolysis yielded a maximum of 15% levoglucosan with 0.5% acid treatment. Pyrolysis of 2% acid treatment gave a 17% levoglucosenone. The presence

of lignin in biomass can explain these observed results due to its radical scavenging action. The decline in lignin content with 2% acid treatment resulted in the preferred dehydration reaction route resulting in the increased production of levoglucosenone. Hence phosphoric acid technique can shift the pyrolysis reaction to produce higher levoglucosan or levoglucosenone favorably.

El-barbary et al. (2009) explored the effect of a wide range of acids (H_3PO_4, H_2SO_4) and alkaline (NaOH, $Ca(OH)_2$, NH_4OH, H_2O_2) treatments on the pyrolytic products of pine wood. Pyrolysis of the treated biomass was performed at a temperature of 450 °C in an augur reactor. Acid treatment yielded bio-oils with low pH, high acid value and viscosity. Removal of base metals during acid treatment and the increase in acid-catalyzed polymerization reaction resulted in a lower pH and an increase in viscosity. The increase in water content, a by-product of the polymerization reaction, reduced bio-oil heating value. In the case of alkali pretreatment, the high water content in bio-oils of up to 24% contributed significantly to reducing bio-oil viscosity. Bio-oil of pretreated biomass on comparison with bio-oil from untreated biomass were compositionally characterized with lower concentrations of hemicellulose and lignin-derived compounds due to the partial hydrolysis of the fundamental lignocellulosic components during pretreatment. Negligible changes were observed in the density of the bio-oils. FTIR analysis showed similar compounds in all bio-oils with higher hydrocarbon content observed in bio-oils derived from $Ca(OH)_2$, NaOH and H_2O_2 treated biomass.

Misson et al. (2009) performed the pretreatment of empty palm fruit bundles (EPFB) with NaOH and $Ca(OH)_2$ with and without the presence of H_2O_2. The study analyzed the treatment effect on the lignin fraction of EPFB and the composition

variations of bio-oil produced by the catalytic pyrolysis of treated EPFB. NaOH treatment resulted in a 7-fold decrease in the lignin content compared to $Ca(OH)_2$ treatment. $Ca(OH)_2$ treatment performed consecutively with H_2O_2 achieved a maximum of 44% degradation, whereas, with NaOH treatment coupled with consecutive H_2O_2 treatment, degradation reached close to 99%. FTIR analysis of the bio-oils from treated and untreated samples indicates the presence of peaks corresponding to specific bonds of alcohols, alkanes, alkenes, ketones, carboxylic acids, esters, aldehydes, phenols and other aromatic compounds. Composition analysis of the bio-oil from treated biomass revealed the increase in phenols, carboxylic acids, alkanes and alkenes.

Shen et al. (2010) investigated the mechanism of the formation of primary bio-oil and gaseous products from hemicellulose thermal degradation. Xylan degradation occurred predominantly between 250 ℃ and 400 ℃ with CO, CO_2 and methane evolution. Pyrolysis of xylan was carried out between 400 and 690 ℃ with a carrier flow rate of 600 L/h (residence time of 0.5 s). With an increase in temperature, char yield decreased, and gas yield increased. The bio-oil yield peaked at 475 ℃ and decreased gradually with an increase in temperature. The gas yield significantly increased above 475 ℃ at the expense of bio-oil yield. GC analysis showed the initial production of 1,4-anhydro-D-xylopyranose as the first product of xylan degradation. The anhydrosugars were consumed through six different pathways through subsequent reactions to form acetone, furfural, acetic acid, methane, H_2, CO and CO_2. Analysis of the gaseous products showed higher yields of CO and CO_2 over H_2 and CH_4. With an increase in temperature, CO production also increased. This was attributed to the

decomposition of xylan units, resulting in aldehyde fragments, which produces CO as one of the products through decarbonylation.

Patwardhan et al. (2011) investigated the pyrolytic behavior of lignin extracted from corn stover to provide mechanistic insight into the formation of products through Py-GC-MS/FID. Isolated lignin (through organosolv process) was pyrolyzed at 500 °C in a micro-furnace pyrolyzer with a vapor residence time of 15-20 ms. Pyrolysis of the lignin gave a char yield of 37%. CO_2 yield at 15.2% was the major component of the gas stream. Compositional analysis of bio-oil revealed the presence of phenol, acetic acid, 4-vinyl phenol, 2,6-dimethoxy phenol and 2-methoxy-4-vinyl phenol as the major components. Mechanistic analysis revealed the initial formation of monomeric compounds, which oligomerize to form larger compounds in the presence of acetic acid. An increase in pyrolysis temperature reduced the char yield with an increase in phenolic compounds, CO yield, and other low MW compounds. The observed phenomenon was attributed to the promotion of demethoxylation reaction with an increase in temperature. Pyrolysis of lignin doped with KCl, NaCl, $CaCl_2$ and $MgCl_2$ gave insignificant variations in yields, which was attributed to the resilience of lignin towards coordinating with mineral species.

Eom et al. (2011) investigated the demineralization impacts of acid and neutral solutions on the pyrolytic degradation products of *Popular albaglandulosa* (popular wood). Biochemical analysis of the treated biomass indicated that HCl showed significant changes in holocellulose and lignin content. Ash content demineralization efficiency in the decreasing order of treatment media was HCl > HF > Tap-H_2O > DI-H_2O. HCl and HF treatments were effective in the removal of K, Mg and Zn to a great extent. Consequently, a drop in the char yield was observed with all treated biomass.

Interestingly, HCl treatment, which recorded the maximum demineralization efficiency, produced higher char content among all the pretreatment techniques. The higher presence of lignin in HCl treated biomass resulted in the formation of lignin-derived char. Hydrolysis of hemicellulose during HCl treatment resulted in the absence of the DTG peak at 300 °C, corresponding to hemicellulose degradation. HCl treated biomass exhibited the highest degradation rate, followed by DI-H_2O treated biomass. Compositional analysis of bio-oils from treated biomass showed a reduction in acids, pyrans, furans and carbonyls with an increase in anhydrosugars yield. The increase in anhydrosugars, such as levoglucosan, was attributed to the demineralization effects accompanied by the presence of acid catalysts. Degradation pathways of lignocellulosic compounds showed a close relationship between inorganic elements in biomass and the pyrolysis product stream distribution.

Zhurinsh et al. (2013) investigated the impact of acid treatment of birch wood on the pyrolysis products such as levoglucosan, furfural and its derivatives. Birch wood was treated with 1-5% H_2SO_4 at temperatures varying between 100 and 180 °C. Increase in the treating acid concentration was marked by significant decrease in ketones and aldehydes in bio-oil. Enhancement of the thermal stability of biomass was also observed, attributed to the catalytic dehydration and condensation effects of H_2SO_4. The pyrolytic liquid yield peaked with 3% acid treatment. The increase in temperature of treatment significantly affected the bio-oil product distribution, especially at temperatures above 140 °C. The sugar yield dropped drastically at temperatures greater than 140 °C, and instead, levulinic acid was produced through acid-catalyzed decomposition. A decrease in furan content was observed with increase

in pretreatment temperature. The overall yield also decreased considerably with an increase in temperature with a yield of 48.2 wt.% when treated at 180 ℃.

Banks et al. (2014) compared the impact of treatment with deionized water, 1% HCl and 0.1% Triton X-100. Triton X-100 was the most promising treatment technique. Hence it was further studied by treating the biomass with four different concentration levels (0.1,0.25, 0.5 and 1%) and studying its effect on the properties of *Miscanthus x giganteus* and their subsequent pyrolysis product stream characteristics. Triton X-100 was found to exhibit excellent potential for mobilizing the removal of inorganic matter. Treatment with 1% Triton X-100 reduced the ash content in the biomass from 1.78% to 0.68%. However, the treatment did not record significant changes in the elemental ratios (C, H, N and O) and heating values. Triton X-100 treated biomass gave higher bio-oil yields at 76.21% compared to deionized water and HCl treated biomass, which yielded 62.44 and 64.13% bio-oil, respectively. A rise in the fraction of organics in the bio-oil was seen for Triton treated biomass. Char yield reduced with all pretreatments with significant changes observed with Triton X-100 treated samples. The reduction of ash played a substantial role in shifting the equilibrium towards the production of liquid bio-oil by reducing the cracking of organics to water and non-condensable gases except with HCl treatment where non-condensable gas yield increased at the expense of bio-oil yield.

Werner et al. (2014) compared the chemical and pyrolytic characteristics of xylan from beech wood with several other hemicelluloses, including galactomannan, glucomannan, arabinoxylan, arabinogalactan, β-glucan and xyloglucan. Thermogravimetric analysis showed hemicellulose based on glucon to be most thermally stable, and xylan was the least thermally stable sample. Glucomannan and

xylan produced a higher char yield of 2.2 and 2%, respectively. Consequently, they had the highest ash and carbon content. Gas analysis revealed that xylan decomposed with comparatively higher CO_2 formation. Anhydrosugars were formed with the pyrolysis of all hemicelluloses except with xylan. Cellulose and β-glucan gave the highest anhydrosugar yield.

Dong et al. (2015) compared the effect of various acid washing (HCl, H_2SO_4, HNO_3, HF) on the pyrolysis products of sawdust of mosa bamboo using Py-GC/MS. The washing was carried out with 3% acid concentration at room temperature for 2 h with a liquid to solid ratio of 70 (50 g in 3.5 L acid solution). HCl treatment resulted in the effective removal of inorganic content. The decreasing order of acid on the effectiveness of removing inorganics was HCl > HNO_3 > HF > H_2SO_4. The increase in sulfur with H_2SO_4 treatment was attributed to the acid residue or solution impurities. The reduction in inorganics and the treatment resulted in disruption of biomass structure. This aided in increasing the composition for thermal degradation resulting in increased total peak areas. Acid washing promoted the formation of sugars through the depolymerization reaction of hemicellulose and cellulose. Lignin-derived bio-oil components revealed the existence of guaiacyl and syringyl units as the major lignin units present in mosa bamboo. HCl treatment was most effective, resulting in the production of high phenolic content bio-oil. The presence of high content of sulfur in H_2SO_4 treated samples was attributed to the insignificant effect on the yield of methoxyeugenol.

Zheng et al. (2018) investigated the structural changes occurring to corncobs and its effects on the pyrolytic bio-oil chemical composition with acid, alkali and hydrogen peroxide treatment. FTIR and XRD analysis was employed to understand the

structural and chemical changes occurring during pretreatment. The disappearance or drop in the intensity of peaks in FTIR suggested reduction of specific components of the biomass, viz. the disappearance of signal at 1739 cm^{-1} with NaOH treatment indicated the removal of hemicellulose carbonyl groups. The reduction of the signal strength of peaks corresponding to the vibration of the aromatic structure shows the degradation of lignin by NaOH. H_2O_2 treatment had minimal impact on the corncob structure. XRD analysis revealed that all the pretreatment techniques increased the crystallinity index (CrI) of the biomass. This was attributed to the degradation of the less orderly small crystallites, while the larger crystallites were relatively unaffected by the treatment. This facilitated the increase in CrI and the average crystalline size. H_2SO_4 aided in increasing the levoglucosan yield in bio-oil. Aldehyde and ketone yields reduced as a result of the decrease of AAEM during the pretreatment process. The removal of AAEM, in addition to hydrolysis of hemicellulose and lignin during pretreatment, also contributed to the reduction in char yield.

Chen et al. (2019) studied the structural changes in agriculture waste (sweet sorghum biomass) when treated with dilute acid (HCl). The effects on pyrolytic behavior and bio-oil composition changes were also studied using TGA and GC-MS. The acid treatment at 25 ℃ for 4 h was influential in reducing ash content, H/C and O/C elemental ratios. Biochemical analysis revealed the enhanced content of cellulose and hemicellulose in the treated biomass. The average MW of bio-oil reduced from 123 in raw biomass to 118 g/mol in the acid-treated biomass, suggesting the formation of smaller molecules through secondary cracking reactions or the effect of residual acid catalyzing the breaking of internal bonds of cellulose during pyrolysis. Treatment of biomass with acid increased the bio-oil yield, reduced the water content, and improved

bio-oil pH. The treatment effectively improved the yield of certain rare chemicals such as D-allose, furfural and 2,3-dihydro-benzofuran.

Su et al. (2020) studied the pretreatment induced physicochemical changes in rice husk when treated with a dilute acid, phosphoric acid (H_3PO_4). The impact of the treatment on the quality of bio-oil and syngas was also studied. The dilute acid treatment led to significant reduction of inorganic metals: S, P, Cl and AAEMs. However, due to its minimal impact on the Si, the major inorganic element present in the biomass, the overall ash content reduced only marginally. With increase in temperature, the crystallinity index also increased, signifying the degradation of the amorphous fraction of biomass. Elemental analysis of the treated biomass showed minimal variation in the O/C and H/C ratios. The bio-oils had high moisture content of up to 96%. The breakdown of β-O-4 bond through pretreatment induced the depolymerization of lignin, resulting in the formation of monophenol units during pyrolysis. The organic phase primarily consisted of phenol, 2-methylphenol and 3-methylphenol. Pretreatment increased CO and decreased CO_2 production. However, no significant variations were observed with H_2 and CH_4 gas yields.

Lu et al. (2020) investigated the effects of acid and base agents on the properties of Chinese fir waste and its subsequent impacts on the pyrolysis product streams, bio-oil and biochar. The fir waste was treated with acids (HCl, H_3PO_4, HCOOH and CH_3COOH) and alkaline solutions (NH_3 and KOH). Solid yields from pretreatment varied between 74 and 95%, with the maximum degradation occurring with alkaline treatment. Acid treatments were more effective than alkaline treatments in removing AAEM (Ca, K, Mg and Na). Crystallinity analysis of treated biomass revealed increased crystallinity and crystal size with alkaline treatment. This was attributed to

the comparatively higher degradation of the short, less orderly cellulose crystallites in comparison with the larger, more orderly crystallites. The thermogravimetric analysis revealed a three-stage degradation: till 200 ℃, 200 to 500 ℃ and 500 to 800 ℃ attributing to moisture loss, lignocellulosic components and carbonization process, respectively. DTG and TG curves of the second stage showed the initial degradation from 150 to 300 ℃ to be due to hemicellulose and lignin. The next step between 300 and 500 ℃ was attributed to more thermally stable cellulose degradation. Pretreatment resulted in a minor increase in bio-oil yield at the expense of the biochar and gas yield. Bio-oil was characterized by an increase in acid (expect with alkali treatment) and phenolic content. The demineralization of biomass, crystallinity changes and the compositional modification of lignocellulosic components were reported to being the major causes affecting the pyrolysis product steam distribution and composition.

The salient features of the literatures discussed throughout this section is listed in Table 1.5 below.

Table 1.5: Summary of literature on the impact of chemical pretreatment techniques on pyrolysis products

Biomass	Pretreatment media	Pyrolysis conditions	Salient features	Reference
Microcrystalline cellulose, recycled pulp and birch wood	0.05 - 3% H_3PO_4 for 1 h at 100 °C. L/S ratio: 100	70 µg sample pyrolyzed at 500 °C for 10 s in a pyroprobe. Heating rate: 600 °C/s	Birch wood and microcrystalline cellulose were the highest and least effective materials that retained the acid. Pyrolysis of microcrystalline cellulose gave the highest yield of 40% levoglucosan and 34% levoglucosenone with 0.5% and 2% H_3PO_4 acid treatment respectively. Similar trends but with lower levels of 15% and 17% were observed with birch wood. The shifting of reaction mechanism towards dehydration reactions with samples treated with higher concentration of acid resulted in enhanced production of levoglucosenone.	Dobele et al., 2003
Pinus taeda (Loblolly pine wood)	Acids: H_3PO_4 & H_2SO_4; Alkali: NaOH, $Ca(OH)_2$, NH_4OH and H_2O_2 (at pH = 11) at 100/80 °C for 60 min	1 kg/h augur reactor. Pyrolysis temperature = 450 °C	Acid treatment results in removal of base metals and compounds of alkaline nature, thereby producing bio-oils with low pH. Acid-catalyzed polymerization reaction resulted in the formation of high molecular weight compounds in bio-oil, leading to an increase in viscosity. Alkali treatment enhanced the moisture content in bio-oils leading to a reduction in viscosity. No significant changes in density were observed.	El-barbary et al., 2009
Empty palm fruit bunches	100 mM NaOH, 100 mM $Ca(OH)_2$, H_2O_2 at 27 °C	30 g EPFB with 5% catalyst pyrolyzed at 300 °C in a semi-batch Stainless Steel reactor	NaOH was more effective in lignin solubilization than $Ca(OH)_2$. H_2O_2 aids in removal of lignin up to 99% when combined with NaOH treatment consecutively. Lignin degradation resulted in increase in char yield. Liquid (bio-oil) and non-condensable gas yield reduced. Pretreatment of the biomass resulted in increased phenols, carboxylic acids, alkanes and alkenes in the bio-oil.	Misson et al., 2009

Biomass	Pretreatment media	Pyrolysis conditions	Salient features	Reference
Hemicellulose extracted from beech		5 g pyrolyzed between 400 and 690 ℃. Nitrogen gas flow = 600 L/h. Residence time: 0.5 s	Xylan degradation occurred between 250 and 400 ℃. With increase in temperature of pyrolysis, char decreases and gas yield increases. Bio-oil production peaked at 475 ℃ and gradually decreased with increase in temperature. 6 distinct degradation pathways were identified, resulting in production of furfural, acetic acid, methane, H_2, CO and CO_2.	Shen et al., 2010
Lignin from corn stover through organosolv process		500 µg pyrolyzed at 500 ℃ in a micro-furnace pyrolyzer. Heating rate: 2000 ℃/s. Vapor residence time: 15-20 ms	Major bio-oil components from pyrolysis of lignin were phenol, acetic acid, 4-vinyl phenol, 2,6-dimethoxy phenol and 2-methoxy-4-vinyl phenol. Thermal degradation initially forms monomeric compounds, which oligomerize to form larger compounds facilitated by acetic acid. Increase in temperature reduces char, increases gas yield, increases phenolic compound yield. AAEM did not show any significant influence on pyrolysis of lignin.	Patwardhan et al., 2011
Populus albaglandulosa (Popular wood)	Acids: HCl, HF Neutral: DI-H_2O, Tap-H_2O.	0.25 mg biomass pyrolyzed at 550 ℃ for 10 s	Reduction in holocellulose content with HCl treatment. All pretreatment removed the inorganic ash content (especially K, Mg and Zn) in biomass. HCl treatment was most effective in demineralization efficiency. A multi-fold increase in levoglucosan in bio-oils of all pretreated biomass was observed. Bio-oils recorded a reduction in furans, acids, pyrans and carbonyls. Inorganic metal ash content plays a vital role in the pyrolysis product stream distribution and bio-oil composition.	Eom et al., 2011

Biomass	Pretreatment media	Pyrolysis conditions	Salient features	Reference
Birch wood (*Betula pendula*)	1 - 5% H_2SO_4 in paddle mixer for 10 min and hydrolysed through 2 different techniques at 100-190 ℃.	1 - 2 mg biomass pyrolyzed at 500 ℃. Heating rate: 600 ℃/s.	Increase in acid concentration reduced ketone and aldehyde yield in bio-oil. Overall bio-oil yield decreased with increase in acid concentration beyond 3%. Increase in pretreatment temperature beyond 140 ℃ caused acid-catalyzed decomposition of sugars to form levulinic acid. Overall bio-oil yield decreased with increase in temperature.	Zhurinch et al., 2013
Miscanthus x giganteus	Deionized water, 1% HCl and Triton X-100 (0.1, 0.25, 0.5 and 1%) at room temperature for 4 h.	1 kg/h fluidized bed reactor. Pyrolysis temperature = 535 ± 5℃. Residence time = < 1.1s.	Deionized water and Triton X-100 effectively reduced the inorganic matter in biomass with the latter being the more effective one. Pyrolysis of demineralized triton X-100 treated biomass yielded higher bio-oil and lower char and non-condensable gases. Triton X-100 treatment was effective in improving the bio-oil quality and stability by increasing the bio-oil organics content and reducing viscosity index.	Banks et al., 2014
Hemicellulose monomers, β-glucan, Cellulose		50 µg sample flash pyrolyzed at 450 ℃ for 0.2 min	Glucan-based hemicelluloses were most thermally stable; xylan was the least thermally stable. Glucomannan and xylan gave high char yields. Xylan decomposition yielded high CO_2. Anhydrosugars were produced through pyrolysis of all hemicelluloses except xylan.	Werner et al., 2014

Biomass	Pretreatment media	Pyrolysis conditions	Salient features	Reference
Mosa bamboo sawdust	3 wt.% HCl, H_2SO_4, HNO_3, HF at room temperature for 2 h L/S ratio: 70	0.5 mg biomass pyrolyzed in a pyroprobe at 550 °C. Heating rate: 20,000 °C/s	The decreasing order of demineralization effectiveness of acid is HCl > HNO_3 > HF > H_2SO_4. Cellulose and hemicellulose depolymerization resulted in increase in sugars in bio-oil. HCl treatment was most effective in increasing phenolics.	Dong et al., 2015
Corncobs	NaOH (1% & 2%) H_2SO_4 (1% & 2%), H_2O_2 (1%) at 80/100 °C.	0.3 mg biomass pyrolyzed at 500 °C in a pyroprobe reactor. Residence time: 20s.	NaOH treatment resulted in hydrolysis of hemicellulose and lignin. H_2SO_4 treatment caused the decomposition of hemicellulose fraction. XRD analysis showed the increase in crystallinity index and crystalline size of all pretreated biomass indicating the selective hydrolysis of less orderly smaller cellulose crystallites. Removal of AAEM and hydrolysis of certain lignocellulosic components resulted in increased levoglucosan yield (with H_2SO_4 treatment) and reduction in aldehyde and ketone yields.	Zheng et al., 2018
Sweet sorghum bagasse	0.1 mol/L HCl for 4 h at 25 °C under shaking at 800 rpm L/S ratio: 10	1 kg/h fluidized bed reactor. Pyrolysis temperature = 500 °C. Nitrogen gas flow = 50 L/min.	HCl treatment reduced ash, H/C and O/C ratios. Bio-oil of acid-treated samples had lower average MW. Bio-oil yield increased, water content reduced, pH increased. Yield of rare chemicals such as D-allose, furfural, 2,3-dihydro-benzofuran increased.	Chen et al., 2019

Biomass	Pretreatment media	Pyrolysis conditions	Salient features	Reference
Rice husk	10% H_3PO_4 for 4 h at 5 different temperatures (60, 80, 100, 120 and 140 °C).	2 g biomass pyrolyzed at 500 °C for 15 min.	Acid treatment reduced S, P, Cl and AAEM contents. Had little impact on Si removal. Minimal variation in H/C and O/C ratios. Acid treatment aided in β-O-4 bond cleavage resulting in formation of monophenols. Increase in CO and decrease in CO_2 production. Minimal change in CH_4 and H_2 production.	Su et al., 2020
Chinese fir	2 wt.% HCl, H_3PO_4, HCOOH, CH_3COOH, NH_3 and NaOH at 30 °C for 3 h L/S ratio: 10..	20 g biomass pyrolyzed until 450 °C for 30 min in a fixed bed reactor.	Acids exhibited much superior AAEM demineralization efficiencies compared to alkalis. Crystallinity variations was due to relative higher impact on small, less crystalline cellulose crystallites, especially with NaOH treatment Increased thermal stability was observed with treated biomass. A negative correlation between acidity of the bio-oil and those of the pretreatment agents was observed. An increased phenolic and acid concentration was recorded in bio-oil produced from pretreated biomass. Reduction in AAEM, variation in crystallinity and lignocellulosic composition were primary factors influencing the pyrolysis process.	Lu et al., 2020

1.6.3 Effect of alkali and alkaline earth metals (AAEM)

The inorganic components present in biomass behave as catalysts and affects the thermal degradation of biomass. The alkali and alkaline earth metals (Na, K, Mg and Ca) predominantly play a major role and generally constitute a major fraction of the inorganic matter of biomass. Several literatures on the impact of such AAEMs and chemical pretreatment techniques to inhibit their activity have been published in the last two decades. A brief overview of a few of those published works are described below.

Patwardhan et al. (2010) investigated the impact of several inorganic Na, K, Mg, Ca salts on cellulose pyrolysis to gain insight on the thermal degradation reactions. The analytical study revealed the primary impacts of inorganic salts on the yields of low MW compounds, furans and anhydrosugars. The catalytic activity of the inorganic salts led to the formation of higher low MW compounds resulting in the drop in levoglucosan, a primary cellulose derivative, yield. Alkali earth metals (K, Na) showed higher catalytic activity than alkaline earth metals (Mg, Ca), resulting in much lower levoglucosan yield. The yield of furans, formed through thermal dehydration reactions of cellulose, was enhanced with $MgCl_2$ infused cellulose. $MgCl_2$ also enhanced the production of levoglucosenone, a dehydration product of levoglucosan. The results also revealed that metal ions cause or catalyze the homolytic cleavage of cellulose bonds, leading to low MW compounds instead of heterocyclic scission of glycosidic linkages leading to the formation of anhydrosugars. One common observation with alkali and alkaline earth metals was the significant variation in pyrolysis products with even a small addition of AAEM salts.

Mourant et al. (2011) studied the impact of AAEMs on bio-oil product distribution. The study showed the presence of AAEMs in two forms: water-soluble AAEMs and acid-soluble (but water-insoluble) AAEMs. Acid soluble AAEMs were found to be chemical bonded to the lignocellulosic components, hence were not soluble with water treatment. In addition to the water-soluble AAEMs, acid treatment resulted in the removal of acid-soluble AAEMs (especially Ca). No significant variations were observed with bio-oil and biochar yield on the removal of AAEMs. However, drastic variations were observed with bio-oil physical and compositional properties. Removal of water-soluble AAEMs, accounting for 70% of total AAEMs, resulted in a marginal increase in sugars. Acid treated biomass yielded high quantities of sugars and lignin degradation products in the bio-oil. Water content in bio-oil was found to reduce by 5% with the removal of acid-soluble AAEMs. The observed increase in viscosity was attributed to the relative increase in the heavier components, facilitated by the removal of AAEMs.

Eom et al. (2012) performed a detailed study of the effect of various inorganic metals (Mg, Ca and K) on the pyrolysis of demineralized poplar wood (*Populus ablaglandulosa*). Four concentration levels (0.05, 0.1, 0.5 and 1%) each of $MgCl_2$, $CaCl_2$ and KCl were taken for the study. Pyrolysis of the impregnated poplar wood showed major changes in the char yield, maximum degradation rate and chemical composition of resulting bio-oils. Char yields gradually increased with an increase in the concentration of KCl. Calcium salt impregnation yielded low char. Potassium was found to suppress levoglucosan's formation with an increase in the formation of low molecular weight compounds such as glycolaldehyde, acetic acid, and butanedial. This was suggested to have occurred due to potassium promoting ring-opening cellulose

mechanism, resulting in the formation of C_2-C_4 compounds instead of anhydrosugars and furans. An increase in cyclopentenes was recorded with increasing potassium concentration. Mg-doped biomass, unlike K doped biomass, yielded higher levoglucosan up to 19.41wt.%. Potassium also exhibited a significant demethoxylation effect with lignin pyrolysis resulting in increased phenol, guaiacol and syringol in the resulting bio-oils. On the other hand, magnesium and calcium salts showed minimal catalytic effect limited to the variations observed with 3-methoxycatechol and 4-vinylguaiacol.

Collard et al. (2012) compared the effect of salts of iron [$Fe(NO_3)_3 \cdot 9H_2O$] and nickel [$Ni(NO_3)_2 \cdot 6H_2O$] individually on commercially available cellulose, xylan and lignin to understand their catalytic impacts on the pyrolysis of biomass. Pyrolysis of iron and nickel impregnated cellulose yielded increased char accompanied by an increase in gas yield (especially H_2 and CO_2), suggesting that the metal salts catalyze the decarboxylation and dehydration reactions. No significant changes in the char, gas and tar overall yields with xylan pyrolysis. However, a prominent (27 fold) furfural increase, formed by depolymerization of xylan, was observed with nickel impregnation at the expense of the yield of the C_1-C_3 compounds. The catalytic effect on lignin pyrolysis resulted in increased char and decreased tar yield. An increase in CO and H_2 yield combined with the observed effects on char and tar suggested the Ni and Fe salts catalyze the fragmentation of lignin. Pyrolysis of complete beech wood biomass matrix revealed iron to catalyze decarboxylation, dehydration and char formation mechanism. Nickel salts, on the other hand, enhanced xylan depolymerization and rearrangement of aromatic chains resulting in higher furfural in tar and char.

Jiang et al. (2013) studied the activity of AAEM on the pyrolysis characteristics of rice straw and the AAEM removal efficiency by a variety of chemical agents, which include deionized water, acetic acid (CH_3COOH), hydrochloric acid (HCl), sulphuric acid (H_2SO_4), nitric acid (HNO_3) and orthophosphoric acid (H_3PO_4). Proximate analysis of treated and untreated rice showed a significant reduction in ash fraction even with DI water showing that one-third of the ash content in rice husk was water-soluble. Strong acid treatment resulted in maximum AAEM removal of 99.7-99.8% K, 84.8-88.5% Na, 62.3-97.9% Ca and 98.6-99.2% Mg. Porosity analysis revealed an increase in pore volume and surface area and a reduction in the average pore diameter with H_2SO_4 treatment revealing the formation of a large number of micro and mesopores. TG analysis revealed two distinct peaks, which were attributed to the thermal degradation of hemicellulose and cellulose. Cellulose degradation peak temperature was much lower with samples treated with strong acid (HCL, H_2SO_4 and HNO_3). This was attributed to the inhibition of the thermal degradation of cellulose by Ca, which was found in low concentrations in strong acid-treated samples. FTIR analysis of gas emissions during pyrolysis showed the action of alkali metals to catalyze demethanization and dehydration reactions. Besides, FTIR analysis also revealed distinctive roles played by alkali and alkaline earth metals during the pyrolysis of biomass.

Hu et al. (2015) investigated the effect of AAEMs on rice husk pyrolysis by treating rice husk with water and 5% HCl solutions at 23 ℃ for 2 h prior to pyrolysis in a fluid bed reactor. Washing with water was influential in the removal of 92 and 84% of K and Na respectively. However, only 10 and 40% demineralization efficiencies of Ca and Mg were observed. Demineralization efficiencies above 98% were observed for

K and Mg with HCl treatment, and efficiencies greater than 85% were observed for Na and Cl removal. Treated biomass was found to give high bio-oil output with low solid biochar yields at low pyrolysis temperatures. This was due to the effect of AAEMs in promotion of the thermal degradation of tars in untreated biomass resulting in low bio-oil yield. However, this effect was not very significant at higher pyrolysis temperatures. Heavy aromatics, which are generally formed with high-temperature pyrolysis, experienced a notable increase with treated rice husk. This revealed that AAEMs played a significant role in the thermal breakdown of heavy aromatics. The non-condensable gas analysis also revealed that AAEMs enhanced the decarboxylation reactions resulting in the production of H_2 and CO_2.

Stefanidis et al. (2015) investigated the demineralization efficiency of acetic and nitric acids on various biomass species having low (0.68 wt.%) to high (9.08 wt.%) ash contents by varying the duration and temperature of treatment. Quantitative analysis of ash revealed the high concentration of K, Mg and Na in agricultural residues such as wheat and barley straw. Demineralization using water for 24 h at room temperature resulted in a 32% reduction in ash. However, an increase in temperature did not significantly increase the ash removal efficiency. Both HNO_3 and CH_3COOH aided in a significant reduction in ash in all biomass species up to 90%. However, HNO_3 was more effective than CH_3COOH in ash removal. Pyrolysis of the demineralized samples gave higher bio-oil yields with a reduction in biochar and gas outputs. The anhydrosugars yield improved considerably with a notable decrease in the lignin-based pyrolysis products. By varying the parameters, pyrolysis of biomass treated at the optimal conditions of 1% HNO_3 at 50 °C gave high-quality bio-oil with a higher organic fraction.

Banks et al. (2016) examined the influence of ash components on pyrolysis product stream characteristics by pyrolyzing potassium and phosphorus impregnated beech wood samples and analyzing their product stream yield and compositions. Both the ash metals negatively impacted the pyrolysis process by affecting bio-oil stability and reducing their yields. Potassium affected the degradation profile of hemicellulose and cellulose, resulting in their primary thermal degradation products such as levoglucosan, 2(5H)-furanone experiencing significant variations. Phosphorus impregnation resulted in increased levoglucosenone and 3-furaldehyde production, suggesting that phosphorus promoted the dehydration pathway during the pyrolysis process. With an increase in concentration of impregnating potassium salt above 1%, the produced bio-oil was not stable and resulted in phase separation. Stability assessment study revealed that bio-oils produced from samples impregnated with higher concentrations of salts experienced an increase in viscosity due to the polymerization due to the inorganic content in bio-oil. Major fractions of the inorganics resulted in biochar; however, a small fraction was detected in the liquid bio-oil.

Dalluge et al. (2017) examined the impact of infusion of acetate salts of AAEM on the pyrolysis of lignin isolated from corn stover. Char yields dramatically increased with alkali metals in comparison with alkaline metals. The increase in char yield was found to be directly related to the electropositivity of the infusion metal. The increase in light oxygenates in volatile aromatics with alkali metal-infused lignin suggests the scission of the lignin linkages. Alkali and alkaline metals showed opposite effects with the overall volatile aromatic yield. Alkali metals aided in an increase, whereas alkaline metals decreased the yield. Sodium showed the highest reactivity among other alkali metals, such as the observed 17% increase in volatile aromatics yield at 500 °C.

However, a drop in light oxygenates was observed over 500 ℃, which was postulated to occur due to their decomposition to carbon dioxide, methane and other gases. Low yields of methoxyphenol compounds were obtained due to the predominance of hydroxyphenyl lignin instead of syringol and guaiacol lignin in herbaceous crops. Hence, a maximum of 0.7% yield was obtained at 300 - 500 ℃ with sodium infused lignin.

Zafar et al. (2019) investigated the demineralization efficiencies of various leaching agents on corncobs to combat operational challenges in biomass-based boilers. The accumulation of ash (primarily AAEMs) with direct combustion of AAEM rich corncobs are linked to combustion, corrosion of boiler tubes, among many other issues. Corncobs were treated with three concentration levels (0.2, 0.3 and 0.4 M) of three acidic and basic agents (HCl, HNO_3 and NaOH). The ash reduction efficiency in decreasing order is HCl > HNO_3 > NaOH. The highest ash removal of 92.81% was achieved with 0.3M HCl treatment. Interestingly, NaOH treatment having the lowest ash removal showed the most effective sulfur removal. NaOH treated biomass exhibited the lowest H/C ratio with a notable increase in the calorific value of the biomass. HCl and HNO_3 treatments lead to an increase in H/C ratio and a decrease in calorific value. Hence, there exists a strong correlation between H/C ratio and calorific value. TGA analysis revealed the shifting of hemicellulose degradation peak. This positive shift was attributed to the absence of AAEMs, which facilitate the valorization of biomass components at temperatures much lower than their actual thermal degradation temperature.

The summary of the impact of AAEMs on biomass pyrolysis discussed throughout this section is listed in Table 1.6 below.

Table 1.6: Summary of literature on the effect of alkali and alkaline earth metals on pyrolysis of biomass

Biomass	Treatment/Impregnation	Salient features	Reference
Microcrystalline cellulose	Wet impregnation with chloride salts of Na, K, Mg & Ca, $Ca(OH)_2$, $CaCO_3$, $Ca(NO_3)_2$.	Small amounts of inorganic salts resulted in significant changes in pyrolytic products. Degradation of cellulose occurred primarily through homolytic or heterolytic cleavage of linkages. Alkaline metals promoted homolytic cleavage leading to an increase in furfural. Levoglucosan yield reduced to a lower extent with pyrolysis of alkali metal-infused cellulose.	Patwardhan et al., 2010
Mallee Wood	Treated with water and dilute HNO_3 (0.1 wt.%) at room temperature for 2 h L/S ratio: 10.	AAEMs existed in two forms: water-soluble AAEMs & acid-soluble AAEMs. Water-soluble AAEM constitutes 70% of total AAEMs. Acid-soluble AAEMs constitutes primarily of Ca salts. Removal of AAEMs contributed to significant changes in bio-oil physical and compositional properties.	Mourant et al., 2011
Demineralized poplar wood (*Populus ablaglandulosa*)	Wet impregnation with 4 concentration levels (0.05, 0.1, 0.5 and 1%) of KCl, $MgCl_2$ and $CaCl_2$ at 100 °C for 1 h.	*Effect of KCl*: Increased char yield. Suppressed levoglucosan yield by enhancing C_2-C_4 compound formation through direct ring-opening mechanisms of cellulose. Enhanced phenolic compound production from lignin pyrolysis. *Effect of $MgCl_2$ and $CaCl_2$*: Increased levoglucosan yield with $MgCl_2$. Minimal change effected in lignin pyrolysis products.	Eom et al., 2012
Commercial lignin, cellulose, xylan (extracted from beech wood)	Wet impregnation with metallic salts $[Fe(NO_3)_3.9H_2O]$ and $[Ni(NO_3)_2.6H_2O]$ at pH 1.5 and 6 respectively.	Iron salt catalyzed decarboxylation, dehydration and char formation mechanisms. Nickel salt primarily promoted the depolymerization of xylan, leading to improved furfural yield. Both iron and nickel salts improved the char and gas production with a drop in the tar production.	Collard et al., 2012

Biomass	Treatment/Impregnation	Salient features	Reference
Rice straw	Treatment with deionized water and 5 wt.% of acetic acid, HCl, H_2SO_4, HNO_3 & H_3PO_4 for 2 h at 25 °C. L/S ratio: 10.	Deionized water removed significant quantities of K and Na metals (water-soluble). H_2SO_4 treatment forms large number of micro and mesopores resulting in increase in pore volume and surface area with decrease in average pore diameter. Calcium inhibits the thermal degradation of cellulose Alkali and alkaline earth metals play distinctive roles in pyrolysis of biomass	Jiang et al., 2013
Rice husk	Treated with water and 5% HCl at 25 °C for 2 h. L/S ratio: 10.	Treatment with water removed significant quantities of K and Na. HCl treatment removed >98% K and Mg and >85% of Ca and Na. Treated biomass gave high bio-oil and low biochar yields. AAEMs aided in thermal breakdown of heavy aromatics and increased H_2 and CO_2 production.	Hu et al., 2015
Lignocel, oak & pine wood, wheat & barley straw, miscanthus and eucalyptus	Treated with 0.1 and 1% of HNO_3 and CH_3COOH at room temperature and 50°C for 2 and 4 h. L/S ratio: 20.	K, Mg and Na found in high concentration in agricultural residues. 32% reduction in ash with water treatment at room temperature for 24 h. Acid treatment effective in removal of up to 90% ash. HNO_3 more efficient than CH_3COOH in demineralization of biomass. Pyrolysis gave higher bio-oil with improved anhydrosugars yield. Decrease in lignin derived compounds in bio-oil.	Stefanidis et al., 2015

Biomass	Treatment/Impregnation	Salient features	Reference
Fagus sylvatica (Beech wood)	0.1-2% potassium acetate / phosphoric acid hand-mixed with biomass and water. Pyrolysis in a 1 kg/h fluidized bed reactor.	High concentration of potassium impregnation reduced stability of bio-oil which caused phase separation. Potassium enhanced the thermal decomposition through degradation pathway resulting in increase in levoglucosenone. Phosphorus affected degradation profiles of Increase in viscosity with time observed due to presence of small fraction of inorganics in bio-oil.	Banks et al., 2016
Lignin isolated from corn stover	Wet infusion with acetate salts of Li, Na, K, Ce, Mg, Ca, Ba and Cu.	Alkali infused lignin yielded more char than alkaline infused lignin. The increase in char yield had a direct relation to the infusing metal cation's electropositivity. Sodium was the most reactive among all the AAEM by yielding maximum variation in volatile aromatics and methoxyphenol compound yields	Dalluge et al., 2017
Corncob	Chemically treated with 0.2, 0.3 and 0.4M NaOH, HCl and HNO_3 at 25 – 27 ℃ for 2 h with shaking at 250 rpm. L/S ratio: 25.	Ash removal efficiency: HCl > HNO_3 > NaOH NaOH treatment exhibited the highest sulfur removal. NaOH treatment decreased H/C ratio, resulting in an increase in calorific value.	Zafar et al., 2019

1.7 Aim and Scope of the present study

Bio-oils are formed as the primary product of pyrolysis of lignocellulosic biomass. However, they cannot be directly used due to critical factors such as their high moisture content, acidity and high oxygen content (low HHV), which plague its application. To overcome these drawbacks, three fundamental approaches have been deliberated upon and carefully investigated by numerous researchers: (1) pretreatment of biomass prior to pyrolysis, (2) modification of the pyrolysis process by varying process parameters (reactor type, temperature, residence time, catalyst) and (3) treatment of bio-oil (hydrotreating, steam reforming, esterification, hydrodeoxygenation, emulsification, etc.). Despite the extensive research, which has been carried out in this field, comparatively fewer research has explored the pretreatment of biomass approach. Additionally, bio-oils are a source of many rare platform chemicals that are of high commercial value.

By modifying the structure and composition of biomass through pretreatment, studies have shown significant changes in the pyrolysis product distribution. The examination of literature in the earlier sections described (1) various chemical treatment techniques to modify biomass with favorable biochemical composition and properties, (2) effect of major biochemical components on the pyrolysis product stream, and (3) significant catalytic effect of minor inorganic metallic components affecting pyrolysis process.

This study has three primary objectives. The first objective is to understand the impact of various chemical pretreatment techniques on the physical and biochemical characteristics of lignocellulosic biomass. It was postulated that specific lignocellulosic biomass properties such as calorific value, equilibrium moisture content, elemental

(H/C and O/C) ratios could serve as markers for the improvement of biomass to enhance pyrolysis product yields.

The second objective is to develop techniques to enhance selective chemical yields in bio-oils selectively. Pyrolysis is known to produce certain rare chemicals that are extracted from bio-oil for their commercial value. Pretreatment results in the hydrolysis of specific lignocellulosic components. Through this component removal, the enhancement of certain chemicals in bio-oil can be achieved. However, due to pretreatment, there is an inevitable loss of biomass, which translates into an overall reduction in pyrolysis yields. Nevertheless, this approach may be cost-effective as it improves the selectivity of the pyrolysis reaction, resulting in the application of more straightforward extraction techniques instead of multiple complicated steps. Additionally, by mapping the changes in properties of bio-oils with changes in the physical properties of treated biomass, a deeper understanding of the effect of chemical treatment on pyrolysis can be achieved.

The third objective is aimed at gaining insight into the effect of the inherent inorganic ash. Although they exist in only small fractions, they act as catalysts and significantly shift product formation mechanisms. A clear understanding of the individual effects of each of these inorganic components, especially the alkali and alkaline earth metals (AAEMs), in biomass pyrolysis is required. It is a well-known fact that the same biomass species can have varying ash compositions in different regions. Hence the crucial information of catalytic effect of AAEMs could help filter biomass species with varying ash contents for specific applications such as the production of chemicals.

The objectives of this thesis are listed below

1. Investigation of various chemical pretreatment techniques to improve selective physical and biochemical properties of lignocellulosic biomass.
2. Pyrolysis of pretreated biomass to understand their impact on chemical composition and properties of bio-oil.
3. Understanding the impact of alkali and alkaline earth metal (AAEM) salts on the pyrolysis of lignocellulosic biomass.

The thesis comprises seven chapters (including the current one) that address the objectives as mentioned above. The overview of each of these chapters is given below:

Chapter 1 (the current chapter) has presented the energy scenario in the global and Indian scenario. The structure of lignocellulosic biomass and the various techniques for their conversion to useful energy including pyrolysis were presented. A review of literature on various chemical pretreatment techniques currently employed and their effects on biomass and pyrolysis products were discussed. Finally, the objectives and justifications of this study were outlined.

Chapter 2 explores the effect of diverse chemical (acids, alkali and surfactants) pretreatment techniques on a low lignin content invasive weed species *A. donax* to understand their impact on certain biomass physical properties, which play a greater role in influencing thermochemical reaction such as pyrolysis. Thermogravimetric analysis, which essentially is pyrolysis, was employed to provide valuable insights into the likely impact of chemical treatment on the pyrolysis process.

Chapter 3 examines the changes impacted on the physical properties of high lignin content *P. juliflora* biomass due to chemical pretreatment and compares them

with the results obtained with *A. donax* samples. *P. juliflora* differs greatly from *A. donax* in terms of its biochemical composition and metallic ash composition.

Chapter 4 investigates the impact of pretreatment on the composition and characteristic properties of the thermal degradation products of *A. donax* biomass. Gas chromatography mass spectroscopy analysis of the bio-oil was primarily used for understanding the impacts. The mapping of the observed changes in critical properties of treated biomass to the observations in bio-oil and biochar properties has been presented.

Chapter 5 presents the effect of chemical pretreatment on the composition and chemical properties of the pyrolysis products of *P. juliflora* biomass. The mapping of the observed changes in critical properties of treated biomass to the observations in bio-oil and biochar properties has been presented.

Chapter 6 presents the catalytic impacts of the alkali and alkaline earth metals (AAEM) on the pyrolysis of lignocellulosic biomass. The primary effect of various salts of magnesium and potassium in promoting specific carbohydrate and lignin degradation pathways has been presented. The effects of various salt anions on biomass pyrolysis have been highlighted.

Chapter 7 presents the broad conclusions of the thesis. Suggestions for future research in this field have also been included.

References

Abbasi, T., & Abbasi, S. A. (2010). Biomass energy and the environmental impacts associated with its production and utilization. *Renewable and sustainable energy reviews*, *14*(3), 919-937.

Agrela, F., Cabrera, M., Morales, M. M., Zamorano, M., & Alshaaer, M. (2019). Biomass fly ash and biomass bottom ash. In *New Trends in Eco-efficient and Recycled Concrete* (pp. 23-58). Woodhead Publishing.

Azeez, A. M., Meier, D., Odermatt, J., & Willner, T. (2010). Fast pyrolysis of African and European lignocellulosic biomasses using Py-GC/MS and fluidized bed reactor. *Energy & Fuels*, *24*(3), 2078-2085.

Banks, S. W., Nowakowski, D. J., & Bridgwater, A. V. (2014). Fast pyrolysis processing of surfactant washed Miscanthus. *Fuel Processing Technology*, *128*, 94-103.

Banks, S. W., Nowakowski, D. J., & Bridgwater, A. V. (2016). Impact of potassium and phosphorus in biomass on the properties of fast pyrolysis bio-oil. *Energy & Fuels*, *30*(10), 8009-8018.

Basu, P., & Basu, P. (2013). Chapter 1 - Introduction. *Biomass Gasification and Pyrolysis-Practical Design and Theory*, 1-25.

Bhaskar, T., Sera, A., Muto, A., & Sakata, Y. (2008). Hydrothermal upgrading of wood biomass: influence of the addition of K_2CO_3 and cellulose/lignin ratio. *Fuel*, *87*(10-11), 2236-2242.

Bodirlau, R., Teaca, C. A., & Spiridon, I. (2008). Chemical modification of beech

wood: Effect on thermal stability. *BioResources*, *3*(3), 789-800.

Bridgwater, A. V., & Bridge, S. A. (1991). A review of biomass pyrolysis and pyrolysis technologies. In *Biomass pyrolysis liquids upgrading and utilization* (pp. 11-92). Springer, Dordrecht.

Caillat, S., & Vakkilainen, E. (2013). Large-scale biomass combustion plants: An overview. In *Biomass Combustion Science, Technology and Engineering* (pp. 189-224). Woodhead Publishing.

Carrillo, M. A., Staggenborg, S. A., & Pineda, J. A. (2014). Washing sorghum biomass with water to improve its quality for combustion. *Fuel*, *116*, 427-431.

Chen, D., Gao, D., Capareda, S. C., Huang, S., & Wang, Y. (2019). Effects of hydrochloric acid washing on the microstructure and pyrolysis bio-oil components of sweet sorghum bagasse. *Bioresource technology*, *277*, 37-45.

Chen, M., Zhao, J., & Xia, L. (2009). Comparison of four different chemical pretreatments of corn stover for enhancing enzymatic digestibility. *Biomass and Bioenergy*, *33*(10), 1381-1385.

Chen, W., Chen, Y., Yang, H., Xia, M., Li, K., Chen, X., & Chen, H. (2017). Co-pyrolysis of lignocellulosic biomass and microalgae: products characteristics and interaction effect. *Bioresource technology*, *245*, 860-868.

Collard, F. X., Blin, J., Bensakhria, A., & Valette, J. (2012). Influence of impregnated metal on the pyrolysis conversion of biomass constituents. *Journal of Analytical and Applied Pyrolysis*, *95*, 213-226.

Czernik, S., & Bridgwater, A. V. (2004). Overview of applications of biomass fast

pyrolysis oil. *Energy & fuels*, *18*(2), 590-598.

Dąbrowska, M., Jaworek, M., Świętochowski, A., & Lisowski, A. (2017). Valuable energy of biochar from agricultural and forest waste streams. In *Rural development 2017: bioeconomy challenges: proceedings of the 8th international scientific conference, 23-24 November, 2017, Aleksandras Stulginskis University, 2017, p. 256-260*.

Dalluge, D. L., Kim, K. H., & Brown, R. C. (2017). The influence of alkali and alkaline earth metals on char and volatile aromatics from fast pyrolysis of lignin. *Journal of Analytical and Applied Pyrolysis*, *127*, 385-393.

Dhabhai, R., Chaurasia, S. P., & Dalai, A. K. (2013). Effect of pretreatment conditions on structural characteristics of wheat straw. *Chemical Engineering Communications*, *200*(9), 1251-1259.

Dhyani, V., & Bhaskar, T. (2018). A comprehensive review on the pyrolysis of lignocellulosic biomass. *Renewable Energy*, *129*, 695-716.

Dobele, G., Dizhbite, T., Rossinskaja, G., Telysheva, G., Meier, D., Radtke, S., & Faix, O. (2003). Pretreatment of biomass with phosphoric acid prior to fast pyrolysis: a promising method for obtaining 1, 6-anhydrosaccharides in high yields. *Journal of Analytical and Applied Pyrolysis*, *68*, 197-211.

Dong, Q., Zhang, S., Zhang, L., Ding, K., & Xiong, Y. (2015). Effects of four types of dilute acid washing on moso bamboo pyrolysis using Py–GC/MS. *Bioresource technology*, *185*, 62-69.

Dudley, B. (2019). BP Statistical Review of World Energy 2019 (68th edition). Available online at https://www.bp.com/content/dam/bp/business-

sites/en/global/corporate/pdfs/energy-economics/statistical-review/bp-stats-review-2019-full-report.pdf (Accessed on 15th July 2020)

Edmunds, C. W., Hamilton, C., Kim, K., Chmely, S. C., & Labbé, N. (2017). Using a chelating agent to generate low ash bioenergy feedstock. *Biomass and bioenergy*, *96*, 12-18.

El-barbary, M. H., Steele, P. H., & Ingram, L. (2009). Characterization of fast pyrolysis bio-oils produced from pretreated pine wood. *Applied biochemistry and biotechnology*, *154*(1-3), 3-13.

Eom, I. Y., Kim, J. Y., Kim, T. S., Lee, S. M., Choi, D., Choi, I. G., & Choi, J. W. (2012). Effect of essential inorganic metals on primary thermal degradation of lignocellulosic biomass. *Bioresource technology*, *104*, 687-694.

Eom, I. Y., Kim, K. H., Kim, J. Y., Lee, S. M., Yeo, H. M., Choi, I. G., & Choi, J. W. (2011). Characterization of primary thermal degradation features of lignocellulosic biomass after removal of inorganic metals by diverse solvents. *Bioresource technology*, *102*(3), 3437-3444.

Fivga, A. (2012). *Comparison of the effect of pretreatment and catalysts on liquid quality from fast pyrolysis of biomass* (Doctoral dissertation, Aston University).

Ghalia, M. A., & Dahman, Y. (2017). Synthesis and utilization of natural fiber-reinforced poly (lactic acid) bionanocomposites. In *Lignocellulosic Fibre and Biomass-Based Composite Materials* (pp. 313-345). Woodhead Publishing.

Hague, A. R. (1998). *The pretreatment and pyrolysis of biomass for the production of liquids for fuels and speciality chemicals* (Doctoral dissertation, Aston University).

Hallac, B. B., & Ragauskas, A. J. (2011). Analyzing cellulose degree of polymerization and its relevancy to cellulosic ethanol. *Biofuels, Bioproducts and Biorefining*, *5*(2), 215-225.

Haykiri-Acma, H., & Yaman, S. (2019). Effects of Dilute Phosphoric Acid Treatment on Structure and Burning Characteristics of Lignocellulosic Biomass. *Journal of Energy Resources Technology*, *141*(8).

Hu, S., Jiang, L., Wang, Y., Su, S., Sun, L., Xu, B., He, L., & Xiang, J. (2015). Effects of inherent alkali and alkaline earth metallic species on biomass pyrolysis at different temperatures. *Bioresource technology*, *192*, 23-30.

Izaurralde, R. C., Mcgill, W. B., & Williams, J. R. (2012). *Development and application of the EPIC model for carbon cycle, greenhouse-gas mitigation, and biofuel studies* (No. PNNL-SA-83721). Pacific Northwest National Lab.(PNNL), Richland, WA (United States).

Jamaldheen, S. B., Sharma, K., Rani, A., Moholkar, V. S., & Goyal, A. (2018). Comparative analysis of pretreatment methods on sorghum (Sorghum durra) stalk agrowaste for holocellulose content. *Preparative Biochemistry and Biotechnology*, *48*(6), 457-464.

Javed, M. A. (2020). Acid treatment effecting the physiochemical structure and thermal degradation of biomass. *Renewable Energy*, *159*, 444-450.

Jiang, L., Hu, S., Sun, L. S., Su, S., Xu, K., He, L. M., & Xiang, J. (2013). Influence of different demineralization treatments on physicochemical structure and thermal degradation of biomass. *Bioresource technology*, *146*, 254-260.

Kaur, A. (2016). Energy Statistics 2016 (Twenty Third Issue). Available online at

http://mospi.gov.in/sites/default/files/publication_reports/Energy_statistics_2016.pdf (Accessed on 25th May 2020)

Khullar, S. (2015). Report of the expert group on 175 GW RE by 2022. Available online at https://niti.gov.in/writereaddata/files/175-GW-Renewable-Energy.pdf (Accessed on 12th June 2020)

Kim, K. H., Singh, S., Custodis, V., & van Bokhoven, J. (2017). Role of free radicals in fast pyrolysis. In *Fast Pyrolysis of Biomass* (pp. 117-137).

Kim, M., Aita, G., & Day, D. F. (2010). Compositional changes in sugarcane bagasse on low temperature, long-term diluted ammonia treatment. *Applied biochemistry and biotechnology*, *161*(1-8), 34-40.

Kim, S., & Holtzapple, M. T. (2005). Lime pretreatment and enzymatic hydrolysis of corn stover. *Bioresource technology*, *96*(18), 1994-2006.

Labatut, R. A., & Pronto, J. L. (2018). Sustainable Waste-to-Energy Technologies: Anaerobic Digestion. In *Sustainable Food Waste-To-energy Systems* (pp. 47-67). Academic Press.

Lu, X., Han, T., Jiang, J., Sun, K., Sun, Y., & Yang, W. (2020). Comprehensive insights into the influences of acid-base properties of chemical pretreatment reagents on biomass pyrolysis behavior and wood vinegar properties. *Journal of Analytical and Applied Pyrolysis*, 104907.

Mhaske, P., & Sharma, S. K. (2019). Growth of electricity sector in India from 1947-2019. Available online at http://www.cea.nic.in/reports/others/planning/pdm/growth_2019.pdf (Accessed on 15th June 2020)

Mierzwa-Hersztek, M., Gondek, K., Jewiarz, M., & Dziedzic, K. (2019). Assessment of energy parameters of biomass and biochars, leachability of heavy metals and phytotoxicity of their ashes. *Journal of Material Cycles and Waste Management*, *21*(4), 786-800.

Ministry of New and Renewable Energy (MNRE), Government of India. (2020). Annual Report 2019-20. Available online at https://mnre.gov.in/img/documents/uploads/file_f-1585710569965.pdf (Accessed on 16th June 2020)

Misson, M., Haron, R., Kamaroddin, M. F. A., & Amin, N. A. S. (2009). Pretreatment of empty palm fruit bunch for production of chemicals via catalytic pyrolysis. *Bioresource technology*, *100*(11), 2867-2873.

Mourant, D., Wang, Z., He, M., Wang, X. S., Garcia-Perez, M., Ling, K., & Li, C. Z. (2011). Mallee wood fast pyrolysis: effects of alkali and alkaline earth metallic species on the yield and composition of bio-oil. *Fuel*, *90*(9), 2915-2922.

Pasangulapati, V., Ramachandriya, K. D., Kumar, A., Wilkins, M. R., Jones, C. L., & Huhnke, R. L. (2012). Effects of cellulose, hemicellulose and lignin on thermochemical conversion characteristics of the selected biomass. *Bioresource technology*, *114*, 663-669.

Pattiya, A. (2018). Fast pyrolysis. In *Direct Thermochemical Liquefaction for Energy Applications* (pp. 3-28). Woodhead Publishing.

Patwardhan, P. R., Brown, R. C., & Shanks, B. H. (2011). Understanding the fast pyrolysis of lignin. *ChemSusChem*, *4*(11), 1629-1636.

Patwardhan, P. R., Satrio, J. A., Brown, R. C., & Shanks, B. H. (2010). Influence of

inorganic salts on the primary pyrolysis products of cellulose. *Bioresource technology*, *101*(12), 4646-4655.

Raveendran, K., Ganesh, A., & Khilar, K. C. (1995). Influence of mineral matter on biomass pyrolysis characteristics. *Fuel*, *74*(12), 1812-1822.

Rajendran, K., Lin, R., Wall, D. M., & Murphy, J. D. (2019). Influential Aspects in Waste Management Practices. In *Sustainable Resource Recovery and Zero Waste Approaches* (pp. 65-78). Elsevier.

Saeid, A., & Chojnacka, K. (2019). Fertlizers: Need for new strategies. In *Organic Farming* (pp. 91-116). Woodhead Publishing.

Saleh, S. B., Hansen, B. B., Jensen, P. A., & Dam-Johansen, K. (2013). Influence of biomass chemical properties on torrefaction characteristics. *Energy & fuels*, *27*(12), 7541-7548.

Sannigrahi, P., Ragauskas, A. J., & Tuskan, G. A. (2010). Poplar as a feedstock for biofuels: a review of compositional characteristics. *Biofuels, Bioproducts and Biorefining*, *4*(2), 209-226.

Sanyal, T. K. (2020). Energy Statistics 2020 (Twenty Seventh Issue). Available online at http://mospi.gov.in/sites/default/files/publication_reports/ES_2020_240420m.pdf (Accessed on 11th May 2020)

Shen, D. K., Gu, S., & Bridgwater, A. V. (2010). Study on the pyrolytic behaviour of xylan-based hemicellulose using TG–FTIR and Py–GC–FTIR. *Journal of analytical and applied pyrolysis*, *87*(2), 199-206.

Singh, S., Khanna, S., Moholkar, V. S., & Goyal, A. (2014). Screening and optimization

of pretreatments for Parthenium hysterophorus as feedstock for alcoholic biofuels. *Applied energy*, *129*, 195-206.

Sluiter, J. B., Ruiz, R. O., Scarlata, C. J., Sluiter, A. D., & Templeton, D. W. (2010). Compositional analysis of lignocellulosic feedstocks. 1. Review and description of methods. *Journal of agricultural and food chemistry*, *58*(16), 9043-9053.

Stefanidis, S. D., Heracleous, E., Patiaka, D. T., Kalogiannis, K. G., Michailof, C. M., & Lappas, A. A. (2015). Optimization of bio-oil yields by demineralization of low quality biomass. *Biomass and Bioenergy*, *83*, 105-115.

Su, Y., Xu, D., Liu, L., Shi, L., Zhang, S., Xiong, Y., & Zhang, H. (2020). Simultaneous Catalytic Conversion of Acid Pretreated Biomass into High-quality Syngas and Bio-oil at Mild Temperature. *Energy & Fuels*, *34*(7), 8366-8375

Tabuti, J. R. S., Dhillion, S. S., & Lye, K. A. (2003). Firewood use in Bulamogi County, Uganda: species selection, harvesting and consumption patterns. *Biomass and Bioenergy*, *25*(6), 581-596.

Wang, H., Srinivasan, R., Yu, F., Steele, P., Li, Q., & Mitchell, B. (2011). Effect of acid, alkali, and steam explosion pretreatments on characteristics of bio-oil produced from pinewood. *Energy & Fuels*, *25*(8), 3758-3764.

Wang, S., & Luo, Z. (2016). *Pyrolysis of biomass* (Vol. 1). Walter de Gruyter GmbH & Co KG.

Werner, K., Pommer, L., & Broström, M. (2014). Thermal decomposition of hemicelluloses. *Journal of Analytical and Applied Pyrolysis*, *110*, 130-137.

World Bank. (n.d.). World Development Indicators Database,

Yang, X. J., Hu, H., Tan, T., & Li, J. (2016). China's renewable energy goals by 2050. *Environmental Development*, *20*, 83-90.

Yang, Y. (2014). *Energy production from biomass and saste derived intermediate pyrolysis oils* (Doctoral dissertation, Aston University)

Yu, J., Paterson, N., Blamey, J., & Millan, M. (2017). Cellulose, xylan and lignin interactions during pyrolysis of lignocellulosic biomass. *Fuel*, *191*, 140-149.

Zabed, H., Faruq, G., Sahu, J. N., Azirun, M. S., Hashim, R., & Nasrulhaq Boyce, A. (2014). Bioethanol production from fermentable sugar juice. *The Scientific World Journal*, *2014*.

Zafar, M. H., Kazmi, M., Tabish, A. N., Ali, C. H., Gohar, F., & Rafique, M. U. (2019). An investigation on the impact of demineralization of lignocellulosic corncob biomass using leaching agents for its utilization in industrial boilers. *Biomass Conversion and Biorefinery*, 1-7.

Zhang, Y., & Chen, W. T. (2018). Hydrothermal liquefaction of protein-containing feedstocks. In *Direct Thermochemical Liquefaction for Energy Applications* (pp. 127-168). Woodhead Publishing.

Zheng, A., Zhao, K., Li, L., Zhao, Z., Jiang, L., Huang, Z., Guoqiang, W., He, F., & Li, H. (2018). Quantitative comparison of different chemical pretreatment methods on chemical structure and pyrolysis characteristics of corncobs. *Journal of the Energy Institute*, *91*(5), 676-682.

Zhurinsh, A., Dobele, G., Rizhikovs, J., Zandersons, J., & Grigus, K. (2013). Effect of pretreatment conditions on the analytical pyrolysis products from birch wood lignocellulose. *Journal of Analytical and Applied Pyrolysis*, *103*, 227-231.

भारतीय प्रौद्योगिकी संस्थान गुवाहाटी
Indian Institute of Technology Guwahati

Chapter 2

Chemical pretreatment of low lignin content *A. donax* biomass to improve critical properties for pyrolysis

2.1 Introduction

Chemical treatment has largely been employed as a lignocellulosic biomass pre-processing technique for alcohol production through fermentation. In recent years, this treatment technique finds application in treating biomass for thermochemical applications as well. Numerous studies have shown the effectiveness of pretreatment to improve the yield of certain rare chemicals in pyrolysis or improve the quality of syngas in gasification.

This chapter explores various chemical agents for pretreatment of lignocellulosic biomass as a means to improve them for pyrolysis. No specific pretreatment technique can be ideal for all types of lignocellulosic biomass, as their composition varies with species, and in some cases, even with location (Surendra et al.,

2018). The chemical agents explored in this chapter include acids (sulphuric acid H_2SO_4, phosphoric acid H_3PO_4), alkali (sodium hydroxide NaOH) and surfactants (sodium dodecyl sulfate, Triton X-100). The effects of these treating media on certain biomass characteristics, which include calorific value, equilibrium moisture content, elemental (H/C and O/C) ratios have been investigated. These critical properties have been reported to have significant impact on biomass pyrolysis (Bridgwater and Peacocke, 2000; Czernik and Bridgwater, 2004; DiBlasi, 2008; Basu, 2018). Thermogravimetric analysis (TGA) of the pretreated biomass was used to gain further insight into the impact of treatment on the pyrolysis profile of each of the treated samples.

Arundo donax (*A. donax*), a fast-growing non-native invasive weed abundantly found in northeast India, was selected for the study (Saikia et al., 2015). It is non-native to India with an ability to grow in wetlands over a wide range of pH from 5.5 to 8.3 (Duke, 1976). *A. donax* is also known to reduce groundwater availability and cause displacement of native vegetation, thereby establishing the need to control its spread and growth.

2.2 Materials and Methods

2.2.1 Biomass gathering and processing

The biomass of *A. donax* was collected from the campus of our institute. Apart from the roots, the entire plant was utilized for the pretreatment. The collected biomass was initially chopped into smaller sections of 2-4 cm each to aid in the washing and drying processes. The biomass chips were washed with deionized water and dried at 60 °C for a duration of 24 h. They were then ground and filtered through a US mesh No. 20 (0.841 mm) and retained on a US mesh No. 270 (0.053 mm).

2.2.2 Chemical pretreatment experiments

Chemical pretreatment was carried out with a wide range of chemicals consisting of mild acids (H_2SO_4, H_3PO_4), alkali (NaOH) and surfactants (SDS, Triton X-100). The dried biomass was treated with the solvents with a solid-liquid ratio of 1:20 to ensure adequate solid-liquid interaction for a duration of 20 min at a temperature of 90 ℃. Three solvent concentration levels of 1, 3 and 5% were taken for acid (v/v) and alkali (w/v) treatment, whereas 0.5% of SDS (w/v) and Triton X-100 (v/v) was selected. After the chemical treatment, the biomass was filtered out and washed with deionized water until a neutral pH of wash-water was attained. The pretreated biomass was dried for a duration of 24 h at 60 ℃ and stored in airtight boxes. The mass loss during the chemical process was recorded.

2.2.3 Proximate and ultimate (elemental) analysis of untreated biomass

Proximate analysis of the raw biomass was carried out as per ASTM standard D7582-15 (ASTM D7582-15, 2015) using a thermogravimetric analyzer (Hitachi STA7200). The brief procedure is explained below. 1 g of the powdered biomass was taken in the platinum pan and loaded into the TGA apparatus and heated to 107 ℃. The weight loss in the sample during the heating process was taken as the moisture content. The volatile matter was calculated by recording the weight difference when heated to 900 ℃ in an inert (nitrogen) environment. The residual mass at 900 ℃ corresponds to fixed carbon and inorganic ash content. By shifting the furnace environment from inert to oxidizing after cooling to 600 ℃, the fixed carbon is eliminated, leaving behind only the inorganic metallic ash. The elemental concentrations of carbon (C), hydrogen (H), nitrogen (N), sulphur (S) and oxygen (O) in biomass were determined with an elemental analyzer (EuroVector EA 3000, Italy). L-cystine was used as a standard for calibration

in 5 tin capsules. Around 0.1 mg of the powdered untreated and treated biomass was taken in tin capsules, which were heated at 980 ℃ with helium gas as carrier gas and oxygen as combustion gas. Callidus™ software was used for the estimation of elemental compositions. The impact of pretreatment on the biomass quality was assessed using van Krevelen diagram or coalification diagram, which essentially is a plot of elemental ratios H/C versus O/C.

2.2.4 Metal concentration by ICP-MS analysis

The trace metal content analysis of biomass was carried out using an Inductively Coupled Plasma Mass Spectroscopy (Agilent 7800 Quadrupole ICP-MS) and a Milestone Ethos UP Microwave digester. Around 0.1 g of raw biomass was taken along with 6 ml conc. HNO_3, 2 ml conc. HCl and 2 ml H_2O_2 in a microwave digestion vessel. The mixture was digested in a microwave processor at 1200 W with a ramp duration of 15 min till it reaches 210 ℃ and a hold time of 25 min. The contents were transferred entirely into a volumetric flask, and deionized water was used to make up the total volume to 50 ml. This solution was used for analysis using ICP-MS.

2.2.5 Surface metallic composition by FESEM-EDX

The surface analysis of biomass for metallic composition was performed using Field Emission Scanning Electron Microscope / Energy Dispersive X-Ray Spectroscopy (FESEM-EDX, Zeiss, Sigma-300, Germany). The biomass samples were oven dried at 80 ℃ for 6 h and sputter coated with gold. The surface analysis was carried out at 25 ℃.

2.2.6 Equilibrium moisture content of treated and untreated biomass

The moisture retention capacity of the biomass was measured with the help of a high precision semi-micro weighing balance (Sartorius CPA225D, Göttingen,

Germany) having an accuracy of ±0.00003 g. Initially, the untreated and pretreated biomass were kept in an environment with 22 ± 1 ℃ and an approximate RH of 60%. A small amount of untreated and treated biomass was taken in an empty silica crucible and dried at 105 ℃ for 24 h. The weights of the dried biomass were then measured. The moisture retention capacity of the biomass was calculated by using the formula:

$$\text{Moisture content}(\%) = \frac{\text{Initial wt. of biomass} - \text{Final wt. of biomass}}{\text{Initial wt. of biomass}} \times 100$$

2.2.7 Gross calorific value

The gross calorific value of the samples was determined using Parr 1341 Plain Jacket Oxygen Bomb Calorimeter (Parr Instrument Company, USA) coupled with Parr 6775 digital thermometer and Parr 2901 ignition unit. ASTM standard test method (ASTM D5865-20, 2013) was followed. Benzoic acid pellets of known calorific value were used for standardization.

2.2.8 Biochemical compositional analysis

The fiber fractionation of the untreated and the treated biomass was analyzed using various protocols. The holocellulose content was determined using the chloride method described by Browning (1967). Neutral detergent fiber (NDF) and acid detergent fiber (ADF) were analyzed using the procedure followed by Van Soest (Van Soest, 1963a; Van Soest, 1963b). The hemicellulose content is the difference of NDF and ADF. Lignin content was determined using the TAPPI standard protocol (TAPPI, 1992). The complete biochemical analysis procedure employed in this study has been included in Annexure A.

2.2.9 X-Ray Diffraction analysis

The diffraction analysis of the untreated and the pretreated biomass was carried out using a Rigaku Smartlab diffractometer with a D/teX Ultra250 1D detector to evaluate the impact of pretreatment techniques. The measurements were recorded at 45 kV and 112 mA using a Cu-Kα (λ = 1.54Å) radiation. The scan range was 5-90° (2θ), with a scan speed of 21°/min (2θ) and a step size of 0.02° (2θ). The crystallinity (%) and crystalline size were calculated using Scherrer equation (Bhuiyan et al., 2000).

$$\text{Crystalline size} = \frac{K \times \lambda}{\beta \cos\theta}$$

Notation: K = Scherrer constant; λ = X-ray wavelength; β = FWHM (Full width at half maximum); θ = XRD peak position.

2.2.10 Fourier-transform infrared spectroscopy analysis

ATR-FTIR analysis was undertaken by using a Shimadzu IRAffinity-1 (Shimadzu, Japan) equipped with a Quest ATR Device (Specac, USA). All samples were analyzed with 100 scans from 500-4000 cm^{-1} with a 4 cm^{-1} resolution. Before analysis, the samples were dried and ground.

2.2.11 Thermogravimetric analysis

The thermal gravimetric study of the raw and pretreated samples was carried out using a thermal gravimetric analyzer (Hitachi STA7200), having a sensitivity of 0.2 μg. Powder samples weighing 5-7 mg was taken in a platinum pan. The platinum pan was placed inside the ceramic furnace and thermally analyzed. The analysis was carried in an inert (nitrogen) environment with a flow rate of 100 ml/min from 30 to 900 ℃ at 10 ℃/min heating rate. The change in weight of the powder sample with time is measured.

2.3 Results and discussion

2.3.1 Characterization of *A. donax* biomass

The raw biomass (green) had an average moisture content of 72.30 ± 4.30%. Individual analysis of the stem and foliage revealed moisture content of 75.24 ± 1.01% and 67.38 ± 2.19%, respectively. The proximate analysis of the untreated raw biomass showed a moisture content of 9.46 ± 0.07%, volatiles content of 75.78 ± 0.78%, fixed carbon content of 8.38 ± 0.93% and an ash content of 6.38 ± 1.65%. The results were found to be identical to a previous study on *A. donax* (Saikia et al., 2015) who reported volatiles, fixed carbon and ash content of 74.3%, 11.7% and 5.35%, respectively. Inductively coupled plasma - mass spectroscopy (ICP-MS) analysis of the ash showed the presence of metals like Mg, Mn, Cu and Zn (as previously reported by Bonanno, 2012), and their concentrations are shown in Table 2.1. FESEM-EDX surface elemental analysis revealed the presence of Cr, Cd, Mn and Si in relatively higher concentrations compared to Ni, Al, As and Mg. The EDX images of *A. donax* is given in Annexure 2.

Table 2.1: Metal concentration in *A. donax* identified using ICP-MS

	Mg	Cr	Mn	Co	Ni	Cu	Zn	As
Concentration (ppm)	624.28	1.23	31.56	0.09	0.61	26.99	25.41	0.02
	Mo	Cd	Pb	K	Ca	Na	Al	Fe
	2.91	0.01	3.15	12763.76	614.45	0.02	0.1	1516.82

2.3.2 Residual weight and biochemical composition of pretreated biomass

The solid yield Sy and the biochemical composition of the untreated and pretreated biomass are given in Table 2.2.

Table 2.2: Biochemical compositional analysis of untreated and treated *A. donax* biomass

Type of treatment	Solid Yield S_Y	Cellulose (w/w %)	Hemicellulose (w/w %)	Lignin (w/w %)
Untreated	-	41.33	27.20	9.69
1% H_2SO_4	66.43±0.01	53.80	21.11	6.01
3% H_2SO_4	54.88±0.42	63.36	9.24	8.33
5% H_2SO_4	54.53±9.95	67.35	4.82	7.89
1% H_3PO_4	77.08±2.88	46.01	31.14	8.85
3% H_3PO_4	74.29±0.58	49.83	27.43	6.93
5% H_3PO_4	72.47±2.79	52.48	24.49	5.03
1% NaOH	58.08±1.04	61.18	20.71	5.42
3% NaOH	48.85±0.71	79.69	5.19	3.60
5% NaOH	42.41±1.99	82.52	3.30	1.54
0.5% SDS	79.17±1.85	46.23	34.86	4.07
0.5% Triton X-100	76.62±1.61	45.60	35.54	5.62

Acids typically react with the hemicellulose and lignin components of lignocellulosic biomass. Role of sulphuric acid in xylan hydrolysis is more pronounced than delignification, whereas phosphoric acid is a relatively mild solvent with minimal solubilization of hemicellulose (Meng et al., 2016). In accordance with the relative difference in reactivity of acids towards lignocellulosic components, H_2SO_4 and H_3PO_4 treatments reduced hemicellulose from 27.20% w/w to 4.82% w/w, and 24.49% w/w, respectively. Cellulose solubility was minimal, and hence the resulting concentration of cellulose increased from 41.33% w/w to a max of 67.35% w/w and 52.48% w/w for H_2SO_4 and H_3PO_4 treatments, respectively. Alkali (NaOH) treatments, which are widely known for their ability to break up the lignin structure (delignification process), finds major application in paper and pulp industries due to their need for high purity cellulose. A steep reduction in lignin concentration in biomass from 9.69 to 1.54% w/w

was observed when pretreated with 5% NaOH solution. The alkali-treated biomass also exhibited high concentrations of cellulose of up to 82.52% w/w due to the near-total solubilization of hemicellulose and lignin. The surfactants SDS and Triton X-100 showed similar lignin degradation properties but did not show any reaction with hemicellulose resulting in high hemicellulose concentrations. The order of reactivity of solvent on hemicellulose is NaOH > H_2SO_4 > H_3PO_4 > SDS > Triton X-100. In case of lignin, the order of reactivity is NaOH > SDS > H_3PO_4 > Triton X-100 > H_2SO_4.

Considering the biomass as a whole, pretreatment with varying concentrations of sulphuric acid and sodium hydroxide resulted in solubilization of lignocellulosic components in the range from 33 to 45% w/w and 42 to 58% w/w, respectively. The severity of treatment media in terms of the solid yield on the biomass as a whole in decreasing order can be expressed as NaOH > H_2SO_4 > H_3PO_4 > Triton X-100 > SDS.

2.3.3 Equilibrium moisture content and calorific value

The untreated biomass after drying and grinding had an equilibrium moisture content of 9.68 ± 1.24%. Fig. 2.1 shows a comparative plot of two parameters: equilibrium moisture content and calorific value, which are considered critical physical parameters for thermochemical reactions.

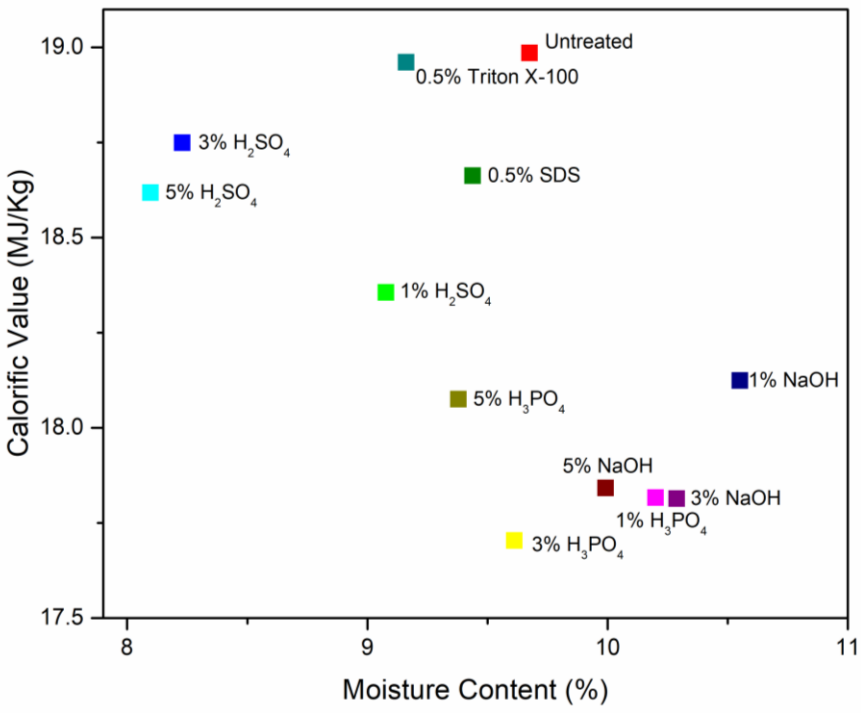

Figure 2.1: Combined plot of moisture content and calorific value of untreated and treated *A. donax* samples

Chemical agents essentially disrupt the covalent carbohydrate-lignin bonds and the glycosidic polysaccharide linkages, and also cause the solubilization of certain lignocellulose components. As a result, the calorific value, which is a measure of bond energy, gets affected. Generally, pretreatment of biomass results in a reduction in calorific value. However, in some cases, the low strength bonds are broken during pretreatment, with minimal damage to higher strength bonds. This results in increasing the calorific value of the resulting pretreated biomass. Equilibrium moisture content is critical because pore size and volume are significantly affected during pretreatment process. This could either increase or decrease the moisture content adsorbed from the environment prior to pyrolysis. The impact of high moisture content is complex as it affects pH, viscosity and efficiency of thermochemical process by increasing the

amount of energy required to heat it up to the required temperature for thermal degradation to occur (Bridgwater, 1999). Moisture content and calorific value have been clubbed together in this plot as they have correlations between them: High moisture content has a direct negative impact on the calorific value (Czernik and Bridgwater, 2004). Minimal reduction in calorific value and low equilibrium moisture content of the treated biomass is preferred in thermochemical reactions as low calorific value results in high gaseous output. The pretreated biomass samples whose points fall in the upper left quadrant of the plot are preferred for pyrolysis. Fig. 3.1 shows that 3 and 5% H_2SO_4 and Triton X-100 treated samples fall in this region. A 14.9%, 16.3% and 5.3% reduction in equilibrium moisture content and likewise 1.24%, 1.93% and 0.13% reduction in calorific value was observed in case of biomass treated with 3%, 5% H_2SO_4 and 0.5% Triton X-100, respectively. Conversely, NaOH treated biomass exhibited an increase in equilibrium moisture content. This is attributed to the increased accessibility of lignocellulosic framework as a result of lignin solubilization. The minimal change in calorific value with Triton X-100 treatment was in concurrence with previous result of Banks et al. (2014) for Triton X-100 treated biomass of *Miscanthus*. Alkali and phosphoric acid-treated biomass showed the maximum loss in calorific value up to 6.17 and 6.75%, respectively due to relatively higher degradation of lignin. Overall, it was observed that biomass properties after alkali and phosphoric acid treatment fell in the lower right quadrant of the plot, which is not considered favorable for pyrolysis.

2.3.4 Elemental analysis

The van Krevelen diagram or coalification diagram (O/C ratio vs. H/C ratio) for untreated and treated *A. donax* biomass is shown in Fig. 2.2.

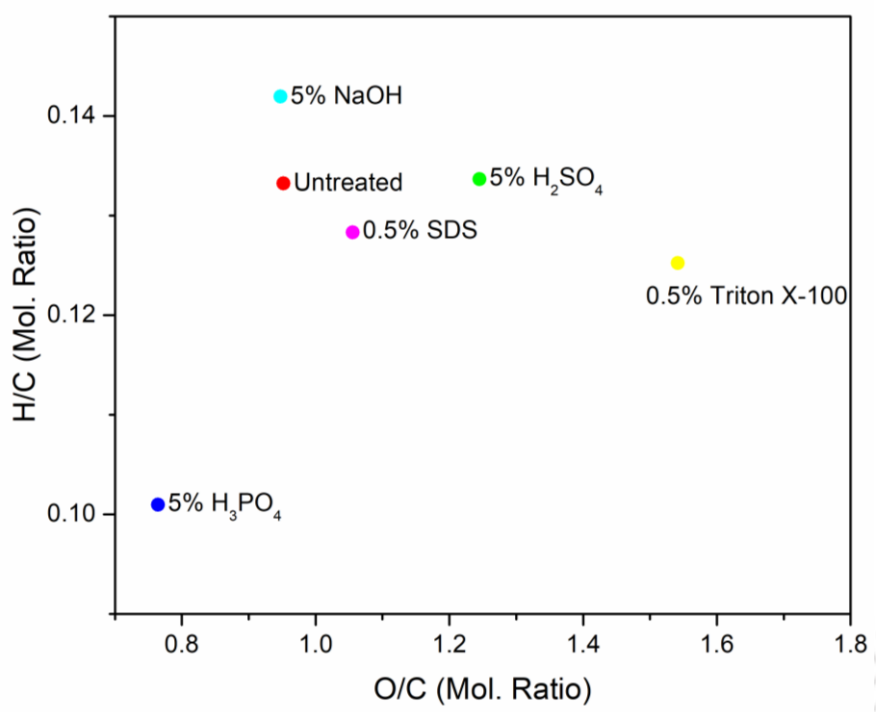

Figure 2.2: Van Krevelen diagram of untreated and treated *A. donax* samples

Based on the biomass compositions, the pyrolysis characteristics and product distribution can be explained. The relative abundance of elemental components: C, H and O can give valuable information related to the thermochemical process product streams. Among all sources of hydrocarbon fuels, lignocellulosic biomass records the highest oxygen content (Basu, 2018). Oxygen does not necessarily contribute to the heating value of biomass; instead, it negatively influences pyrolysis processes by increasing water content in bio-oil and reduces the heat efficiency of the process, which was explained earlier. Bio-oil oxygenates also have a direct impact on bio-oil stability (Meng et al., 2015); hence biomass with smaller O/C ratios is more suitable for pyrolysis. High O/C ratio could indicate the presence of ether group (C-O-C) and carboxyl groups (R-COOH), which on pyrolysis favors the production of CO_2 and CO,

thereby increasing the gas yield. A lower H/C ratio could favor high char production (Wei et al., 2006). Hence, pretreated biomass with high H/C and low O/C ratios are deemed as suitable for high liquid yield. Untreated biomass exhibited H/C and O/C ratios of 0.133 and 0.952, respectively. Biomass treated with alkali (5% NaOH) results in an increase in H/C ratio from 0.133 to 0.142, with a marginal decrease in the O/C ratio from 0.952 to 0.948. Treated biomass having lower O/C are reported to have high calorific value due to enriched carbon content. But contrary to this postulate, H_3PO_4 treated samples in this study, having the lowest O/C ratio, exhibited reduction in calorific value by 4.8 to 6.7%. This was attributed to the large reduction in H/C ratio, which contributes to HHV. However, the significant decrease in O/C ratio from 0.952 to 0.764 is expected to yield more stable bio-oil having low moisture content and oxygenates.

2.3.5 Thermogravimetric analysis

The thermogravimetric analysis of biomass before and after treatment was performed to get an in-depth understanding of the influence of pretreatment on thermal degradation characteristics. This analysis is also used for the prediction of the pyrolytic behavior of treated biomass.

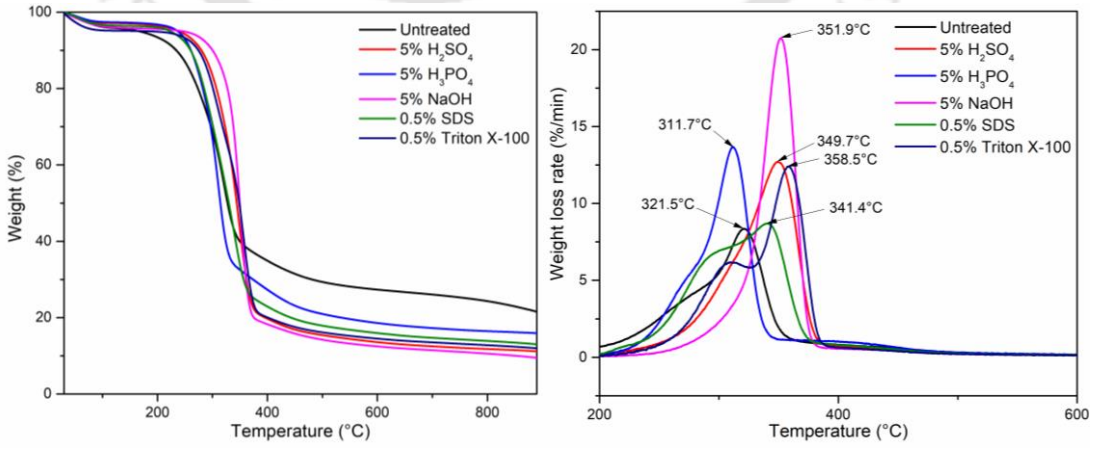

(a) (b)

Figure 2.3: (a) TGA plot of untreated and treated *A. donax* samples (b) DTG plot of untreated and treated *A. donax* samples

Table 2.3: Thermogravimetric parameters of untreated and treated *A. donax* biomass

Feedstock	T_i[a] (°C)	T_{max}[b] (°C)	T_f[c] (°C)	DTG_{max}[d] (wt%/min)	CY[e] (wt%)
Untreated	151.5	321.5	352.2	8.41	21.32
5% H_2SO_4	202.9	349.7	360.7	12.75	11.07
5% H_3PO_4	214.4	311.7	336.2	13.72	15.87
5% NaOH	243.4	351.9	368.6	20.78	9.39
0.5% SDS	194.9	341.4	368.6	8.75	12.96
0.5% Triton X-100	218.1	358.5	377.0	12.47	11.88

Notation: [a] T_i, onset temperature of degradation; [b] T_{max}, maximum weight loss temperature; [c] T_f, final temperature of degradation; [d] DTG_{max}, rate of change in mass corresponding to T_{max}; [e] CY, Char yield at 900 °C

Fig. 2.3(a) and (b) presents the TG and DTG curves of treated and untreated *A. donax* biomass, and Table 2.3 summarizes their characteristic properties.

Initial observations showed a positive shift in the onset temperature of degradation (T_i) of all the pretreated samples. Lignin is the first lignocellulosic component to decompose due to its comparative low degradation temperature. The reduced lignin content in the pretreated biomass could explain the delayed onset of degradation. Comparing the TG curves of acid (H_3PO_4 and H_2SO_4) treated biomass, it was also observed that although T_i of H_3PO_4 (214.4 °C) occurred after that of H_2SO_4 treated biomass (202.9 °C), the degradation was much faster (and thus ended quicker) in H_3PO_4 treated biomass. This occurs due to two reasons: the relatively low concentration of lignin in H_3PO_4 treated biomass delaying the onset of degradation and the substantially higher concentration of hemicellulose in H_3PO_4 treated biomass. This phenomenon of faster degradation and steep decrease in weight with temperature was observed in all treated biomass having higher concentrations of cellulose and hemicellulose, especially in NaOH and H_3PO_4 treated biomass. The DTG plot of few

pretreated samples shown in Fig. 2.3(b) revealed two peaks: the first one resembling a shoulder peak and the other one being a sharp peak. The first peak occurring in the 275 - 325 ℃ range corresponds primarily to the degradation of hemicellulose and partially of that of lignin, which can be explained based on the biochemical compositional analysis shown in Table 2.2. The first peak is clearly distinguishable in the case of biomass pretreated with SDS, Triton X-100, and H_3PO_4. These three samples have a high hemicellulose content of 34.86, 35.54 and 24.49% respectively; whereas H_2SO_4 and NaOH treated samples exhibited low concentration of 4.82 and 3.30% respectively. From this, it can be inferred that a relationship exists between the first shoulder peak and hemicellulose degradation (Eom et al., 2011; Wang and Luo, 2016). The second sharp peak occurs between 300 and 365 ℃ is due to the thermal degradation of cellulose (Zheng et al., 2018). The order of the peaks are due to the increasing order of thermal stability of the lignocellulosic components with lignin easily degradable and cellulose being the most stable of the three components (Yang et al., 2007). For the second peak, the decreasing order in the rate of gravimetric change observed is 5% NaOH > 5% H_3PO_4 > 0.5% Triton X-100 = 5% H_2SO_4 > 0.5% SDS = untreated. This data trend closely resembles cellulose content. Alkali (NaOH) treated samples exhibited the highest cellulose content (greater than 85%) among all the pretreatment techniques, which explains the reason why the degradation rate is the highest for 5% NaOH treated sample at 20.78 wt.%/℃ at 351.9 ℃ (corresponding to the second peak). Untreated biomass has the lowest degradation rate at 8.41 %/℃. DTG of the pretreated samples also revealed significant shifts in the temperature corresponding to max degradation rate varying from 311.7 ℃ for H_3PO_4 treated biomass to 358.5 ℃ for Triton X-100 treated biomass. The positive shift from 321.5 to 351.9 ℃ in the case of alkali pretreatment has been reported to arise from the transformation of naturally occurring

cellulose I to cellulose II. The interaction of the –OH group in cellulose II is comparatively stronger, which requires higher energy for thermal degradation (Yue, 2011).

The residual solid yield (CY) at 900 ℃, which is also summarized in Table 2.3, includes the char yield along with the ash content of the biomass. The CY of pretreated samples was found to decrease in the order 5% H_3PO_4 > 0.5% SDS > 0.5% Triton X-100 > 5% H_2SO_4 > 5% NaOH. In a similar study on the pretreatment of corncobs by H_2SO_4 and NaOH, Zheng et al. (2018) have attributed the reduction in char yield to the catalytic effect of AAEM in biomass, and the variations in concentrations of lignin and hemicellulose in pretreated biomass, which produce more char compared to cellulose. Raw untreated biomass had the highest char content of 21.32 wt.%, whereas char content of pretreated biomass was 15.87 wt.%. This is attributed to the washing off of the AAEM metals in the biomass. Similar results have also been reported by previous authors (Davidsson et al., 2002; Aho et al., 2013).

2.3.6 XRD analysis

The crystallinity parameters of the samples, viz. crystallinity (%), crystalline size and FWHM at the peak, are presented in Table 2.4.

Table 2.4: Crystalline properties of untreated and treated *A. donax* biomass

Parameter	Pretreatment Condition					
	Untreated	5% H_2SO_4	5% H_3PO_4	5% NaOH	0.5% SDS	0.5% Triton X-100
Crystallinity (%)	60.70	73.86	76.80	52.68	74.78	78.23
FWHM (degree)	2.34	2.27	2.27	2.11	2.30	2.23
Crystalline size (nm)	3.62	3.73	3.73	4.01	3.68	3.79

The untreated biomass was found to have crystallinity and crystal size of 60.7% and 3.62 nm, respectively. Pretreatment studies indicated an increase in the crystallinity and crystalline size. The cellulose component of lignocellulosic biomass consists of the crystalline and the amorphous part. Crystalline fraction consists of cellulose chains, which are well and orderly packed alongside by strong hydrogen bonds, whereas, in the amorphous fraction, the cellulose chain arrangement is loose. Hence, amorphous cellulose is more susceptible for reaction than the crystalline part (Yu and Wu, 2010). Acid and surfactant treatment yielded an increase in crystallinity and crystal size. Similar rise in crystallinity from 50% to 62% was observed with the 5% H_2SO_4 acid treatment of *P. hysterophorus* (Singh et al., 2014). The changes could be due to the fast-reacting amorphous components: amorphous part of cellulose, hemicellulose and lignin while having limited or no reactivity with the crystalline cellulose (Singh et al., 2014). Further, the higher reactivity of less orderly and small crystalline structure compared to the larger crystalline cellulose structures resulted in increase in crystalline size in pretreated biomass (Zheng et al., 2018). Alkali-treated samples showed a reduction in crystallinity with increase in crystal size. This trend has already been reported by previous authors (Yue, 2011). This is attributed to transformation of parallel arrangement of cellulose microfibrils (cellulose I) to anti-parallel arrangement of cellulose microfibrils (cellulose II), which is less crystalline in nature. This transformation is hypothesized to occur due to the intermingling of parallel microfibrils during the swelling caused by the alkali solution.

2.3.7 FTIR analysis

FTIR spectral analysis was used to deduce the changes occurring in the chemical and structural composition of biomass during the pretreatment. FTIR spectra of treated and untreated biomass are shown in Fig. 2.4 and signal labels summarized in Table 2.5.

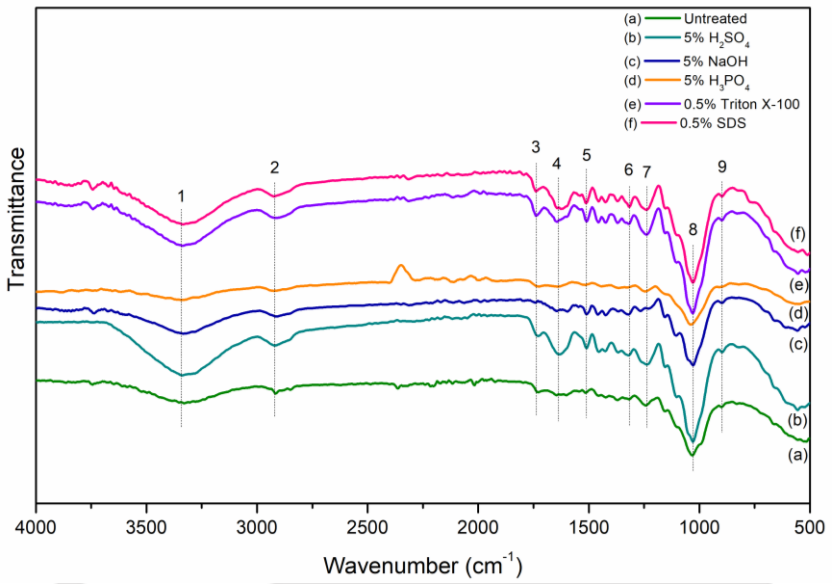

Figure 2.4: FTIR spectra of untreated and treated *A. donax* biomass

Table 2.5: Characterization of signal labels in FTIR spectra (Singh et al., 2014)

Signal label No.	Band position (cm^{-1})	Assignment
1	3348	O-H stretching
2	2900	C-H stretching
3	1738	C=O stretching due to carbohydrate linkage to lignin
4	1640	C=O stretching vibration in conjugated carbonyl of lignin
5	1510	Aromatic ring vibration (related to lignin removal)
6	1314	C-H vibration in carbohydrate
7	1238	Hemicellulose–lignin linkage
8	1026	C=O stretch in carbohydrate
9	897	Band of carbohydrate

The disappearance and reduction intensity of band occurs after pretreatment due to the selective solubilization of components of lignocellulosic biomass. The peak at 3348 cm^{-1} (1) is assigned to the OH stretching, and samples pretreated with 5% H_2SO_4, 0.5% Triton X-100 and SDS showed a remarkable increase in the intensity when compared with untreated samples (He et al., 2008). The peak at around 2900 cm^{-1} (2) is due to C-H stretching and is generally associated with the alkane group of compounds (Misson et al., 2009; Yan et al., 2016). Considerable variation in the intensities of peaks in fingerprint region of 1800-800 cm^{-1} was also observed. The band at 1738 cm^{-1} (3) is suggested to be associated with the acetyl group of hemicellulose (Meng et al., 2016). The disappearance of this band was observed in the case of alkali (NaOH) treated biomass, which concurs with the near-complete solubilization of hemicellulose during alkali treatment. The band was clearly distinguishable in case of surfactant (SDS and Triton) treated samples, which could be attributed to the minimal impact of surfactants on the hemicellulose part of biomass. The band at 1640 cm^{-1} (4) is attributed to residual (or adsorbed) moisture in the pores formed in biomass as a result of pretreatment (Amir et al., 2013). The band at 1510 cm^{-1} (5), assigned to the aromatic skeletal structure in lignin, is commonly taken as lignin reference (Pandey and Pitman, 2003; Meng et al., 2016). Alkali (NaOH) and weak acid (H_3PO_4) treated samples having low concentrations of lignin showed a decrease in intensity of this band. Small peaks detected between 1450 and 1360 cm^{-1} also correspond to C-H stretching, which is associated with alkane group of compounds (Misson et al., 2009). The bands at 1314 cm^{-1} (6), 1026 cm^{-1} (8) and 897 cm^{-1} (9), which are associated with C-H vibration, C-O stretch and C-H deformation in cellulose, did not record much variation for all pretreatment techniques.

2.4 Conclusion

This chapter has explored the effect of diverse chemical (acids, alkali and surfactants) pretreatment techniques on a low lignin content invasive weed species *A. donax* to understand their impact on certain biomass physical properties, which play a greater role in influencing thermochemical reaction such as pyrolysis. The analyzed properties included the biochemical composition, elemental analysis, equilibrium moisture content and calorific value of biomass samples. Thermogravimetric analysis, which essentially is pyrolysis, offered valuable insights into the likely impact of chemical treatment on the pyrolysis process. Alkali treatment caused significant mass loss compared to acid and surfactant treatments due to its comparatively severe hydrolysis effect on the hemicellulose and lignin fractions of the biomass. The resulting alkali-treated samples were cellulose-rich, which was evident with the sharp cellulose degradation peak within a narrow temperature range observed during thermogravimetric studies. The biochemical composition also revealed stark differences among different acid treatments (H_2SO_4 and H_3PO_4), which resulted in significant variation in their differential thermograms (DTGs). The lowest O/C ratio, a characteristic feature of high-grade fuels, was exhibited by H_3PO_4 treated samples. However, significant reduction in H/C caused reduction in the calorific value. On the other hand, the highest calorific value coupled with low moisture content was exhibited by H_2SO_4 treated samples, which could potentially improve the energy efficiency of pyrolysis process. H_3PO_4 and NaOH treated samples produced the maximum and lowest solid yields during thermal analysis (TGA), respectively. The production of char was found to be closely associated with the lignin and hemicellulose content. The

inorganic ash, which mostly consisted of alkali and alkaline earth metals, also influenced the char output due to its catalytic activity.

From the study, it can be inferred that chemical pretreatment could be employed as a promising technique for improvement of biomass for pyrolysis, and the physical properties discussed above could serve as critical markers for analyzing and screening various biomass species.

References

Aho, A., DeMartini, N., Pranovich, A., Krogell, J., Kumar, N., Eränen, K., Holmbom, B., Salmi, T., Hupa. M., & Murzin, D. Y. (2013). Pyrolysis of pine and gasification of pine chars–Influence of organically bound metals. *Bioresource technology*, *128*, 22-29.

Amir, R. M., Anjum, F. M., Khan, M. I., Khan, M. R., Pasha, I., & Nadeem, M. (2013). Application of Fourier transform infrared (FTIR) spectroscopy for the identification of wheat varieties. *Journal of food science and technology*, *50*(5), 1018-1023.

ASTM D7582-15. (2015). Standard Test Methods for Proximate Analysis of Coal and Coke by Macro Thermogravimetric Analysis. ASTM International, West Conshohocken, PA.

ASTM D5865-13. (2013). Standard Test Method for Gross Calorific Value of Coal and Coke. ASTM International, West Conshohocken, PA.

Banks, S. W., Nowakowski, D. J., & Bridgwater, A. V. (2014). Fast pyrolysis processing of surfactant washed *Miscanthus*. *Fuel Processing Technology*, *128*, 94-103.

Basu, P. (2018). Biomass gasification, pyrolysis and torrefaction: practical design and theory. Academic press.

Bhuiyan, M. T. R., Hirai, N., & Sobue, N. (2000). Changes of crystallinity in wood cellulose by heat treatment under dried and moist conditions. *Journal of Wood Science*, *46*(6), 431-436.

Bonanno, G. (2012). *Arundo donax* as a potential biomonitor of trace element contamination in water and sediment. *Ecotoxicology and Environmental Safety, 80*, 20-27.

Bridgwater, A. V. (1999). Principles and practice of biomass fast pyrolysis processes for liquids. *Journal of analytical and applied pyrolysis, 51*(1-2), 3-22.

Bridgwater, A. V., & Peacocke, G. V. C. (2000). Fast pyrolysis processes for biomass. *Renewable and sustainable energy reviews*, *4*(1), 1-73.

Browning, B. L. (1967). Methods of wood chemistry. Volumes I & II. John Wiley & Sons, New York, USA.

Czernik, S., & Bridgwater, A. V. (2004). Overview of applications of biomass fast pyrolysis oil. *Energy & fuels*, *18*(2), 590-598.

Davidsson, K. O., Korsgren, J. G., Pettersson, J. B. C., & Jäglid, U. (2002). The effects of fuel washing techniques on alkali release from biomass. *Fuel*, *81*(2), 137-142.

Di Blasi, C. (2008). Modeling chemical and physical processes of wood and biomass pyrolysis. *Progress in energy and combustion science*, *34*(1), 47-90.

Duke, J. A. (1976). Perennial weeds as indicators of annual climatic parameters. *Agricultural Meteorology*, *16*(2), 291-294.

Eom, I. Y., Kim, K. H., Kim, J. Y., Lee, S. M., Yeo, H. M., Choi, I. G., & Choi, J. W. (2011). Characterization of primary thermal degradation features of lignocellulosic biomass after removal of inorganic metals by diverse solvents. *Bioresource technology*, *102*(3), 3437-3444.

He, Y., Pang, Y., Liu, Y., Li, X., & Wang, K. (2008). Physicochemical characterization

of rice straw pretreated with sodium hydroxide in the solid state for enhancing biogas production. *Energy & Fuels*, *22*(4), 2775-2781.

Meng, J., Moore, A., Tilotta, D. C., Kelley, S. S., Adhikari, S., & Park, S. (2015). Thermal and storage stability of bio-oil from pyrolysis of torrefied wood. *Energy & Fuels*, *29*(8), 5117-5126.

Meng, X., Sun, Q., Kosa, M., Huang, F., Pu, Y., & Ragauskas, A. J. (2016). Physicochemical structural changes of poplar and switchgrass during biomass pretreatment and enzymatic hydrolysis. *ACS Sustainable Chemistry & Engineering*, *4*(9), 4563-4572.

Misson, M., Haron, R., Kamaroddin, M. F. A., & Amin, N. A. S. (2009). Pretreatment of empty palm fruit bunch for production of chemicals via catalytic pyrolysis. *Bioresource technology*, *100*(11), 2867-2873.

Pandey, K. K., & Pitman, A. J. (2003). FTIR studies of the changes in wood chemistry following decay by brown-rot and white-rot fungi. *International biodeterioration & biodegradation*, *52*(3), 151-160.

Saikia, R., Chutia, R. S., Kataki, R., & Pant, K. K. (2015). Perennial grass (*Arundo donax L.*) as a feedstock for thermo-chemical conversion to energy and materials. *Bioresource technology*, *188*, 265-272.

Singh, S., Khanna, S., Moholkar, V. S., & Goyal, A. (2014). Screening and optimization of pretreatments for *Parthenium hysterophorus* as feedstock for alcoholic biofuels. *Applied energy*, *129*, 195-206.

Surendra, K. C., Ogoshi, R., Zaleski, H. M., Hashimoto, A. G., & Khanal, S. K. (2018). High yielding tropical energy crops for bioenergy production: Effects of plant

components, harvest years and locations on biomass composition. *Bioresource technology*, *251*, 218-229.

TAPPI. (1992). Technical association of the pulp and paper industry. Georgia, USA: Atlanta.

Van Soest, P. J. (1963a). Use of detergents in the analysis of fibrous feeds. I. Preparation of fiber residues of low nitrogen content. *Journal of the association of Official Agricultural Chemists*, *46*(5), 825-829.

Van Soest, P. J. (1963b). Use of detergents in the analysis of fibrous feeds. 2. A rapid method for the determination of fiber and lignin. *Journal of the Association of Official Agricultural Chemists*, *46*(5), 829-835.

Wang, S., & Luo, Z. (2016). *Pyrolysis of biomass* (Vol. 1). Walter de Gruyter GmbH & Co KG.

Wei, L., Xu, S., Zhang, L., Zhang, H., Liu, C., Zhu, H., & Liu, S. (2006). Characteristics of fast pyrolysis of biomass in a free fall reactor. *Fuel processing technology*, *87*(10), 863-871.

Yan, L., Pu, Y., Bowden, M., Ragauskas, A. J., & Yang, B. (2016). Physiochemical characterization of lignocellulosic biomass dissolution by flowthrough pretreatment. *ACS Sustainable Chemistry & Engineering*, *4*(1), 219-227.

Yang, H., Yan, R., Chen, H., Lee, D. H., & Zheng, C. (2007). Characteristics of hemicellulose, cellulose and lignin pyrolysis. *Fuel*, *86*(12-13), 1781-1788.

Yu, Y., & Wu, H. (2010). Significant differences in the hydrolysis behavior of amorphous and crystalline portions within microcrystalline cellulose in hot-

compressed water. *Industrial & Engineering Chemistry Research*, *49*(8), 3902-3909.

Yue, Y. (2011). A comparative study of cellulose I and II fibers and nanocrystals. *LSU Master's Theses*. 764.

Zheng, A., Zhao, K., Li, L., Zhao, Z., Jiang, L., Huang, Z., Guoqiang, W., He, F., & Li, H. (2018). Quantitative comparison of different chemical pretreatment methods on chemical structure and pyrolysis characteristics of corncobs. *Journal of the Energy Institute*, *91*(5), 676-682.

Chapter 3

Chemical pretreatment of high lignin content *P. juliflora* biomass to improve critical properties for pyrolysis

3.1 Introduction

The last chapter investigated the impact of chemical pretreatment on invasive weed *A. donax*. It is well known that due to extensive variations observed in the structure and composition of different biomass species, no specific pretreatment technique produces the same effect in all biomass species. Hence investigating the effect of chemical pretreatment on other biomass species with considerably different biochemical composition and structure is essential to gain better insight into the effect of pretreatment.

The invasive weed *Prosopis juliflora* (*P. juliflora)* was selected for the study for their significant compositional variation compared to *A. donax*. *P. juliflora* exhibited the following significant variations in biochemical composition compared to *A. donax*:

(1) 43% less inorganic ash content, (2) 46% less hemicellulose and (3) 108% more lignin content. *P. juliflora*, a fast-growing exogenous species, were planted en masse in the 19th century due to acute fuelwood shortage and still is extensively used in the rural regions of the south Indian state of Tamilnadu for firewood and charcoal production (Chandrasekaran et al., 2017; Simon and Peterson, 2019). However, in the last 2 decades due to its encroachment into agricultural lands, water bodies and even forest lands, there is an urgent need for its control to preserve the native ecosystem. Multiple efforts are also undertaken by local, district and national administration to control its growth and spread.

The hardwood biomass was treated with the same set of chemical agents used in our previous chapter. The variation in critical pyrolytic characteristics of the biomass, which include calorific value, equilibrium moisture content and elemental ratios, were closely monitored and compared with the findings of *A. donax* biomass. Quantitative variations in composition were also analyzed. Thermal profiles of the pretreated samples through TGA gave crucial information about their pyrolysis behavior, which were compared with those of *A. donax* biomass explained in the previous chapter.

3.2 Materials and Methods

3.2.1 Biomass gathering and processing

The woody biomass *P. juliflora* for this study was collected directly in powder form from sawmills in Thoothukudi district, Tamil Nadu, India. A broad size spectrum ranging from wood chips to fine powder was obtained from which wood chips were discarded directly. Screened power passing through a 0.841 mm (US mesh 20) were

taken for the study. The powdered biomass was dried in an electric oven to expel the unbound moisture and stored in airtight containers.

3.2.2 Chemical pretreatment experiments

Chemical pretreatment was carried out as explained in the earlier section 2.2.2 with a wide range of chemicals consisting of acids (H_2SO_4, H_3PO_4), alkali (NaOH) and surfactants (SDS, Triton X-100). 100 g of the untreated powdered biomass was pretreated with each of the pre-treating agents. The mass loss during pretreatment was recorded and the oven dried pretreated biomass samples were stored in airtight containers.

3.2.3 Proximate, ultimate (elemental) and ash analysis of untreated biomass

The proximate analysis of raw biomass, which involves quantification in terms of moisture content, volatile content, fixed carbon and ash was carried out in accordance with ASTM standard D7582-15 (ASTM D7582-15, 2015). The ash content of biomass primarily consisting of alkali and alkaline earth metals (AAEM) among other metallic species were determined using an Inductively Coupled Plasma Mass Spectroscopy (ICP-MS). The procedure involves solubilization of the raw biomass in a solution consisting of a mixture of solubilizing agents. The filtered solution containing the inorganic metals is used for the ICP-MS analysis. The elemental concentrations of carbon (C), hydrogen (H), nitrogen (N), sulphur (S) and oxygen (O) in biomass were determined with an elemental analyzer (EuroVector EA 3000, Italy). The experimental procedures for the proximate analysis, ultimate analysis and ash component analysis were mentioned earlier in sections 2.2.3 and 2.2.4.

3.2.4 Equilibrium moisture content, gross calorific value and biochemical compositional analysis of treated and untreated biomass

Each of the chemically treated biomass samples and the untreated biomass were analyzed for their moisture retention capacity or equilibrium moisture content, gross calorific value and biochemical composition using the same procedure mentioned in sections 2.2.5, 2.2.6 and 2.2.7 using standard techniques (ASTM D5865-20, 2013). The complete biochemical analysis procedure employed in this study based on previous studies (Van Soest, 1963a; Van Soest, 1963b; Browning, 1967; TAPPI, 1992) has been included in Annexure A.

3.2.5 X-Ray Diffraction analysis

The procedure employed in our earlier chapter (section 2.2.8) for the diffraction analysis was adopted in this chapter. The crystallinity (%) was calculated as described by Kim and Holtzapple (2006) using the formula given below:

$$\text{Crystallinity (\%)} = \frac{I_{cr} - I_{am}}{I_{cr}} \times 100$$

Notation: I_{cr} = Intensity of diffraction at $2\theta = 22.6°$; I_{am} = Intensity of the background scatter at $2\theta = 18.7°$. It is widely known that I_{cr} and I_{am} also corresponds to the crystalline and amorphous fractions of the biomass respectively (Segal et al., 1959).

3.2.6 Thermogravimetric analysis

The thermal gravimetric study of the raw and pretreated samples was carried out using a thermal gravimetric analyzer (Hitachi STA7200) as mentioned earlier in section 2.2.10. The change in weight of the powder sample with time was measured.

3.3 Results and discussion

3.3.1 Characterization of *P. juliflora* biomass

The proximate analysis of the untreated raw biomass showed a moisture content of 7.27 ± 0.06%, volatiles content of 72.62 ± 0.56%, fixed carbon content of 16.46 ± 0.26% and an ash content of 3.65 ± 0.36%. On comparison with *A. donax*, significant variations were observed with the fixed carbon and ash content. *P. juliflora* exhibited twice the fixed carbon content and 50% of the ash content observed with *A. donax* samples. Previous studies on the same biomass species reported similar volatile, fixed carbon and ash contents of 69.8%, 19.1% and 3.24% respectively (Chandrasekaran et al., 2017). ICP-MS (Inductively coupled plasma - mass spectroscopy) analysis of the ash, which comprises the metallic fraction of biomass, showed the presence of numerous metals, whose concentrations are shown in Table 3.1.

Surface elemental analysis with FESEM-EDX revealed high concentrations of Cr, Mn, Cd and Co. However, ICP-MS analysis, which recorded the bulk concentration, showed high concentrations of Ca, Fe, K. Al and Na. The EDX images of *P. juliflora* is given in Annexure B.

Table 3.1: Metal concentration in *P. juliflora* identified using ICP-MS

	Mg	Cr	Mn	Co	Ni	Cu	Zn	As
Concentration (ppm)	87.6	4.47	4	0.14	0.54	1.71	5.18	0.11
	Mo	Cd	Pb	K	Ca	Na	Al	Fe
	0.31	0.01	0.23	1820.52	5501.77	668.11	1794.91	2706.58

3.3.2 Residual weight and biochemical composition of pretreated biomass

The action of chemical agents on the various lignocellulosic components lead to varying levels of their degradation or solubilization in the media. The overall biomass solid yield (S_Y) and individual compositions of the biochemical components of the untreated and treated biomass samples are given in Table 3.2.

The overall solid yield after pretreatment ranged between 65 and 82% w/w. Acid treatment comparatively gave higher solid yield than alkali treatments. Among the acid treatments, H_3PO_4 was much less harsh on the biomass compared to H_2SO_4 resulting in higher solid yield. The solid yield varied between 75.8 and 79.2% w/w with H_2SO_4 treatment and between 80.1 and 82.2% with H_3PO_4 treatment. NaOH was the most severe of all the treatments resulting in 65 – 69.8% w/w solid yield. However, the solid yield was much higher than that was observed with *A. donax* biomass, which gave a solid yield of 42.4% (w/w) for 5% NaOH treatment. Similar patterns were observed with the other chemical treatments as well, which illustrate the difference in the arrangement of the lignocellulosic components in various biomass resulting in their varying resistance to chemical agents. The primary effect of acids was observed with the solubilization of polysaccharide chains with the hydrolysis of hemicellulose occurring to a greater extent compared to cellulose. The severe hemicellulose hydrolysis by H_2SO_4 resulted in reducing its fraction from 14.63% to 0.48%. H_3PO_4 caused a less severe effect with 8% hemicellulose in the treated biomass. Although cellulose degradation also occurred, the far intense effect on hemicellulose resulted in an increase in the pretreated biomass cellulose fraction from 42.13% to a maximum of 48.86%. The substantial increase of lignin from 20.2% to 33.6% with H_2SO_4 treatment revealed the true extent of hemicellulose hydrolysis. As observed earlier with *A. donax*

biomass, alkali treatment had a significant detrimental effect on hemicellulose and lignin hydrolysis resulting in the relative increase in cellulose concentration. Hemicellulose concentration decreased from 14.63% up to 3.44% with 5% (w/v) NaOH treatment. The lignin fraction reduced from 12.88% to 5.92%. This resulted in increasing the cellulose concentration from 42.13% up to 69.16%. Other studies with the same biomass species treated with 5% (w/v) NaOH had a maximum cellulose concentration of 72.27% (Saravanakumar et al., 2014a). However, the same treatment with *A. donax* in similar conditions resulted in a higher cellulose concentration of 82.52% from 41.33% in the raw untreated biomass. These results coupled with the relatively higher solid yield in *P. juliflora* show the limited effectiveness of chemical treatment due to its high lignin content resulting in its resistance for hydrolysis to occur. Treatment with surfactants also resulted in hemicellulose solubilization resulting in a marginal increase in cellulose and lignin.

Table 3.2: Biochemical compositional analysis of untreated and treated *P. juliflora* biomass

Type of treatment	Solid Yield S_Y	Cellulose (w/w %)	Hemicellulose (w/w %)	Lignin (w/w %)
Untreated	-	42.13	14.63	20.2
1% H_2SO_4	79.21	42.40	11.29	29.76
3% H_2SO_4	77.21	46.72	0.90	30.62
5% H_2SO_4	75.84	48.86	0.48	33.63
1% H_3PO_4	82.21	36.56	15.28	26.86
3% H_3PO_4	80.07	46.04	10.31	25.04
5% H_3PO_4	81.83	45.44	8.00	23.88
1% NaOH	69.80	61.39	13.84	12.88
3% NaOH	67.00	65.31	11.24	9.78
5% NaOH	64.96	69.16	3.44	5.92
0.5% SDS	77.14	47.42	8.21	23.52
0.5% Triton X-100	81.16	42.07	10.05	26.18

The order of reactivity of treatment medium on hemicellulose was: H_2SO_4 > NaOH > H_3PO_4 > SDS > Triton X-100. The lignin reactivity in descending order was: NaOH > SDS > H_3PO_4 > Triton X-100 > H_2SO_4. Overall similar trends of selective degradation were observed with both *A. donax* and *P. juliflora*. However, the intensities of the degradation varied to great extents due to their varying biochemical compositions.

3.3.3 Equilibrium moisture content and calorific value

The untreated *P. juliflora* biomass had a much higher equilibrium content (compared to *A. donax*) of 11.03 ± 0.13%. The calorific value recorded to be 17.8 MJ/kg was relatively low on comparison to other biomass species having similar features (Demirbaş, 2001; Prasad et al., 2015). Although the favourable conditions for high calorific content were present in the biomass, viz. high lignin content and low ash content, the presence of high moisture content offsets the benefits (Krajnc, 2015).

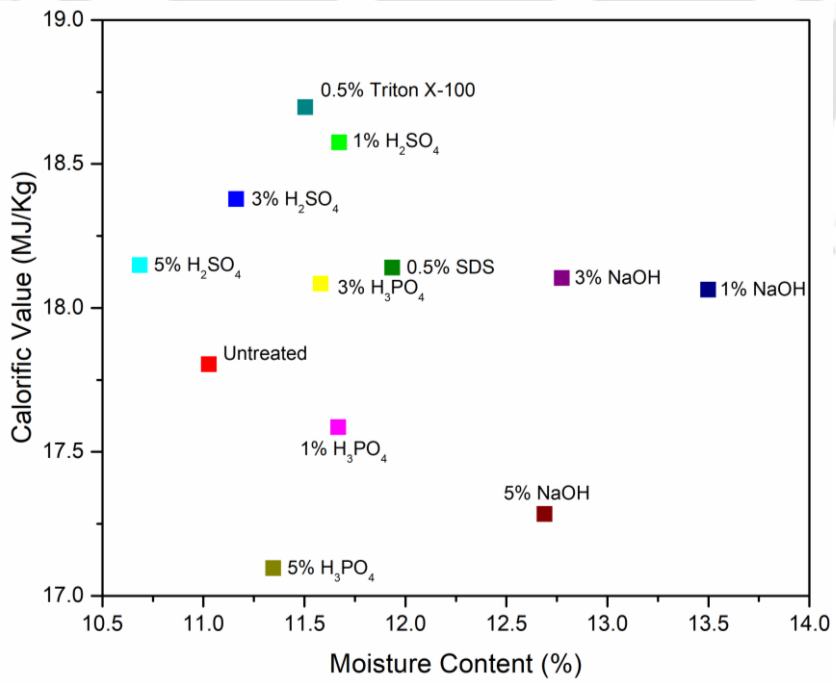

Figure 3.1: Combined plot of moisture content and calorific value of untreated and treated *P. juliflora* samples

Fig. 3.1 shows a comparative plot of two critical physical parameters: equilibrium moisture content and calorific value of the treated and untreated biomass. The calorific value of biomass varies to a great extent with the equilibrium moisture content of the biomass. An increase in moisture content in the biomass has a negative effect on the biomass resulting in the decrease in calorific value. Hence due to their relationship, a combined plot is essential for better understanding. The calorific value of most of the treated biomass samples varying from 17.10 to 18.70 MJ/kg were found to be higher than that of the untreated biomass. The presence of high energy lignin bonds and the rupture of a higher fraction of low energy bonds is likely to have caused the increase in the overall calorific biomass. This was affirmed with high lignin content samples, viz. H_2SO_4 and Triton X-100 treated samples, exhibiting the highest calorific values ranging between 18.15 and 18.70 MJ/kg. Meanwhile, NaOH treatment which had a significant delignification effect resulted in a minor increase or decrease in calorific value. All chemical treatments on *P. juliflora* biomass resulted in an increase in equilibrium moisture content except with high concentrations of H_2SO_4. Increasing H_2SO_4 concentration used for treatment reduced the moisture content of the treated samples. Nevertheless, it was accompanied by a decrease in the calorific value. Optimization of the concentration of acid concentration could aid in balancing the opposing effects. Alkali treatment in particular had considerable effect on the biomass resulting in substantial increase in the equilibrium moisture content by 15 to 22%. Similar observations were also made with *A. donax* samples which was attributed to the easy accessibility of moisture aided by the degradation of lignin framework. However, the higher fraction of lignin in 1% and 3% NaOH treated samples counteracts the drawbacks of high equilibrium moisture content and contributes to a higher calorific value. H_3PO_4 treated samples demonstrated an increase in moisture content and a

decrease in calorific value which are generally not preferred for thermochemical feedstocks. Overall it was observed that acid and surfactant treatment could aid the pyrolysis reaction through reduced energy requirement and improved bio-oil yield.

3.3.4 Elemental analysis

Each of the treated samples along with the raw biomass were classified using the Van Krevelen diagram which is commonly used for classification of different types of coal and feedstocks for thermal conversion to energy. Fig. 3.2 depicts the van Krevelen diagram for untreated and treated *P. juliflora* biomass samples.

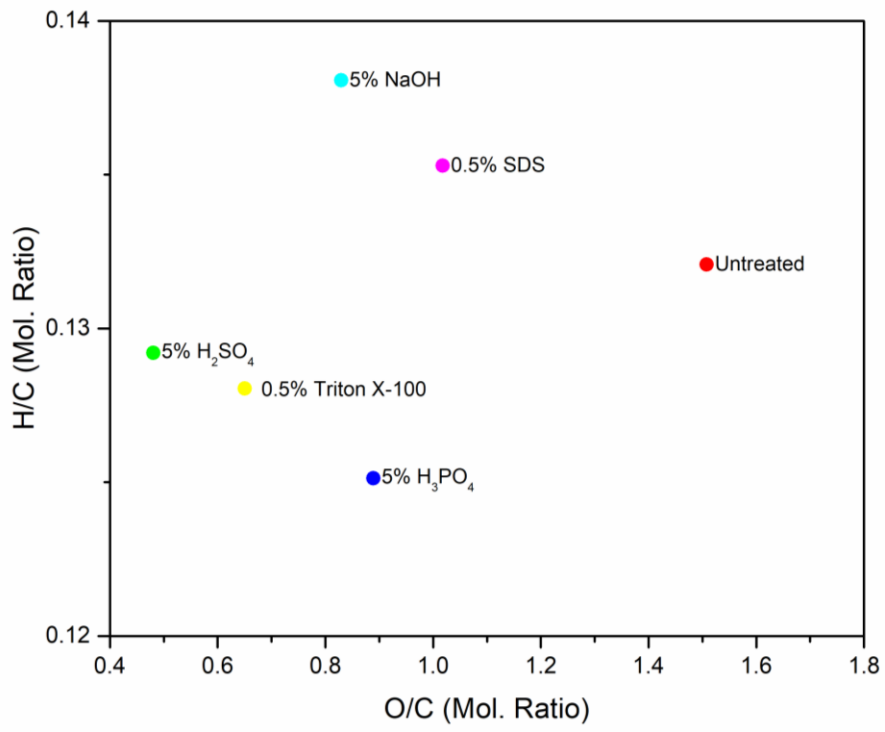

Figure 3.2: Van Krevelen diagram of untreated and treated *P. juliflora* samples

The elemental analysis of *P. juliflora* showed lower carbon and hydrogen and higher oxygen compared to *A. donax*. Hence, the biomass species showed similar H/C ratio (0.133 in *A. donax* and 0.132 in *P. juliflora* raw samples) but significantly higher O/C ratio (0.95 in *A. donax* and 1.51 in *P. juliflora* raw samples). Chemical treatment

of *P. juliflora* samples gave similar H/C results to that observed with *A. donax* samples. NaOH and H_3PO_4 treatments yielded the highest (0.138) and lowest (0.125) H/C ratios, respectively. The treated and untreated samples had a O/C ratio ranging widely from 0.48 with H_2SO_4 treatment to 1.51 with untreated sample. With O/C ratio directly related to production of CO_2 and CO during pyrolysis, the wide variation could result in significant shift in non-condensable gas yield with pretreatment. Additionally, the reduction of oxygen in biomass could aid in bio-oils with lower moisture.

Carbon enrichment of biomass, indicated by decrease in H/C and O/C ratios, is closed associated with the HHV of the biomass (Channiwala and Parikh, 2002; Pudasainee et al., 2020). Hydrogen content also contributes greatly as indicated in numerous studies (Maksimuk et al., 2020). Hence treatment techniques which causes significant decrease in H/C ratio are not the most optimal for pyrolysis. H_2SO_4, NaOH and Triton X-100 treated samples recorded reduction in both O/C and H/C ratios. However, NaOH treatment causes a large reduction in H/C ratio, which resulted in 2.9% reduction in the calorific value of 5% NaOH treated sample. But due to the significant reduction in O/C ratio, few samples (1 & 3% NaOH treated samples) also showed a marginal 1.4 to 1.7% increase in calorific value, as shown in the previous section. The other H_2SO_4 and Triton X-100 treated samples showed a marginal decrease in H/C ratio with substantial decrease in O/C ratio, due to which they had the highest calorific values.

3.3.5 Thermogravimetric analysis

The thermal decomposition behaviour of treated samples can be assessed and compared with that of untreated samples with the aid of thermogravimetic analysis. Though the observed behaviour, vital information related to pyrolysis of the substance

can be obtained and analyzed. Fig. 3.3(a) and (b) presents the TG and DTG curves of treated and untreated *P. juliflora* biomass, and Table 3.3 summarizes their characteristic properties.

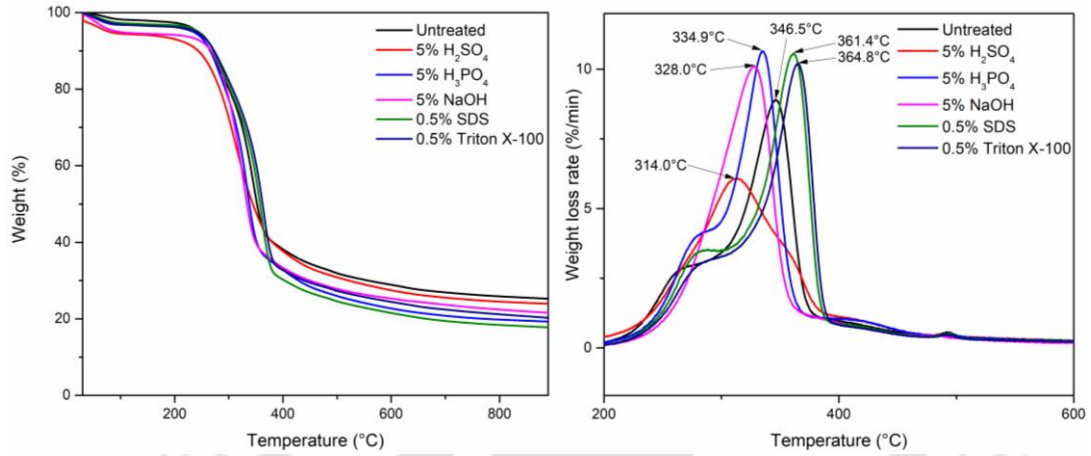

(a) (b)

Figure 3.3: (a) TGA plot of untreated and treated *P. juliflora* samples (b) DTG plot of untreated and treated *P. juliflora* samples

Table 3.3: Thermogravimetric parameters of untreated and treated *P. juliflora* biomass

Feedstock	T_i[a] (°C)	T_{max}[b] (°C)	T_f[c] (°C)	DTG_{max}[d] (wt%/min)	CY[e] (wt%)
Untreated	182.9	346.5	372.8	8.89	25.20
5% H_2SO_4	151.3	314.0	368.8	6.08	23.90
5% H_3PO_4	166.8	334.9	362.5	10.65	19.23
5% NaOH	181.5	328.0	355.4	10.10	21.54
0.5% SDS	182.9	361.4	381.8	10.56	17.75
0.5% Triton X-100	191.3	364.8	390.5	10.20	20.22

Notation: [a] T_i, onset temperature of degradation; [b] T_{max}, maximum weight loss temperature; [c] T_f, final temperature of degradation; [d] DTG_{max}, rate of change in mass corresponding to T_{max}; [e] CY, Char yield at 900 °C

Of the biochemical components, lignin has the lowest decomposition temperature of around 160 °C (Yang et al., 2007). Hence, changes in the initial onset temperature (T_i) of pretreated samples could be related to its decomposition. H_2SO_4 and

H_3PO_4 treated samples, which exhibited a lower T_i exhibited higher lignin content. And as observed with *A. donax* biomass, T_i of H_2SO_4 (151.3 °C) was lower than the T_i of H_3PO_4 (166.8 °C) treated samples. A distinctive feature of the DTG curves are the two distinctive peaks: the first shoulder peak corresponding to hemicellulose degradation, and the other sharp peak signifying degradation of cellulose (Eom et al., 2011). The second sharp peak was observable in all untreated and treated samples but only a few samples exhibited the first peak. The hemicellulose-based first peak was clearly distinguishable in the DTG of raw sample in addition to H_3PO_4, SDS and Triton X-100 treated samples, which had a higher hemicellulose content (> 8%). The absence of the first peak in H_2SO_4 and NaOH treated samples was attributed to their low hemicellulose fraction of 0.48% and 3.44%, respectively. The second sharp peak which occurs in the 275° – 325 °C range was due to the degradation of cellulose. Nevertheless, it is found to be influenced by lignin, which binds the cellulose and hemicellulose together thereby supressing their thermal degradation. This was clearly observed with NaOH treated *A. donax* and *P. juliflora* samples, which had the highest cellulose content among all treated samples. NaOH treated *A. donax* sample exhibited a significantly higher peak mass degradation (DTG_{max}) on comparison with the other treated samples. This phenomenon was not observed with NaOH treated *P. juliflora* samples, whose DTG_{max} was lower than those of H_3PO_4 and SDS treated samples, due to the relatively higher lignin content (5.92%). The significantly higher content of lignin in most of *P. juliflora* treated samples inhibited the degradation of cellulose resulting in limiting DTG_{max} to between 10 and 11 wt%/min.

The char yield (CY) from untreated *P. juliflora* samples was 25.2%, which was marginally higher than that obtained from untreated *A. donax* (21.32%). The decreasing

order of CY is untreated > H_2SO_4 (23.9%) > NaOH (21.54%) > Triton X-100 (20.22%) > H_3PO_4 (19.23%) > SDS (17.75%). The reduction in CY with pretreatment was considerably lower than that for *A. donax* biomass. The high fraction of lignin in *P. juliflora* biomass, which contributes significantly to char production, could account for the observed CY (Gupta et al., 2016). Additionally, the low ash content of *P. juliflora* suggests the abundance of ash-free content in the char yield.

3.3.6 XRD analysis

Crystalline properties derived from X-ray Diffraction (XRD) studies of untreated and treated *P. juliflora* samples are displayed in Table 3.4.

Table 3.4: Crystalline properties of untreated and treated *P. juliflora* biomass

Parameter	Pretreatment Condition					
	Untreated	5% H_2SO_4	5% H_3PO_4	5% NaOH	0.5% SDS	0.5% Triton X-100
Crystallinity (%)	35.85	46.13	43.84	46.26	41.71	34.71
FWHM (degree)	2.4	2.13	2.07	1.88	2.08	2.2
Crystalline size (nm)	3.53	3.97	4.09	4.50	4.07	3.85

Spectral analysis of untreated *P. juliflora* samples showed it be less crystalline than *A. donax*. Pretreatment with chemical agents caused selective hydrolysis of the crystalline and non-crystalline fractions of the biomass causing variations in their spectral properties. Acid treatment showed similar increasing patterns of crystallinity and crystalline size as observed with acid-treated *A. donax* samples. The rationale behind the observed patterns have been discussed in the previous chapter. Alkali treatment increased the crystallinity from 35.85% to 46.26%, which was in contract to the decreasing trend observed with *A. donax* samples. Similar increase in crystallinity

with the alkali treatment of the same biomass have also been reported (Saravanakumar et al., 2014b). The presence of much lower cellulose fraction in alkali treated samples and the limited effectiveness of alkali treatment on *P. juliflora* samples, as discussed in previous section, could have limited the hydrolysis to the smaller polysaccharide crystallites. This was apparent with the significant increase in the average crystalline size from 3.53 to 4.50. All treatments besides Triton X-100 enhanced the crystallinity of the biomass. Although a growth in the average crystalline size was observed, high concentration of lignin which contributes to the amorphous nature of the biomass could have contributed to the observed crystallinity decrease.

3.4 Conclusion

This chapter has examined the changes induced in the physical properties of *P. juliflora* biomass due to chemical pretreatment, and has compared them with similar results obtained with *A. donax* samples, described in previous chapter. The occurrence of elevated levels of lignin in the biomass largely suppressed the hydrolysis of cellulose and hemicellulose polysaccharides. This, to a great extent, transpired to be the cause of much of the changes in physicochemical properties of *P. juliflora*. In general, the hydrolysis inhibition resulted in lowering the weight loss from 20.9-57.6% in *A. donax* to 17.8-35% in *P. juliflora* during chemical treatment. Acid (H_2SO_4) treatment, which largely hydrolyses xylan, yielded high lignin content samples having higher calorific value, low moisture content and very favorable O/C and H/C ratios. Alkali treated samples, which were not as cellulose-rich as NaOH treated *A. donax* samples, exhibited a comparatively lower degradation rate when thermally analyzed. Furthermore, significantly high equilibrium moisture content with 5% NaOH treated samples, and its

low lignin content contributed to its low HHV. Major reduction in the O/C value with acid treatment, especially with H_2SO_4 treatment, which exhibited an O/C ratio of 0.48, could translate into generation of bio-oil with low oxygenates, thereby improving its quality. The chemical treatments did not significantly affect the char yield (as observed with *A. donax* samples) due to the high fraction of lignin in *P. juliflora* biomass, which contributes largely to the solid yield.

References

ASTM D7582-15. (2015). Standard Test Methods for Proximate Analysis of Coal and Coke by Macro Thermogravimetric Analysis. ASTM International, West Conshohocken, PA.

ASTM D5865-13. (2013). Standard Test Method for Gross Calorific Value of Coal and Coke. ASTM International, West Conshohocken, PA.

Browning, B. L. (1967). Methods of wood chemistry. Volumes I & II. John Wiley & Sons, New York, USA.

Chandrasekaran, A., Ramachandran, S., & Subbiah, S. (2017). Determination of kinetic parameters in the pyrolysis operation and thermal behavior of Prosopis juliflora using thermogravimetric analysis. *Bioresource technology*, *233*, 413-422.

Channiwala, S. A., & Parikh, P. P. (2002). A unified correlation for estimating HHV of solid, liquid and gaseous fuels. *Fuel*, *81*(8), 1051-1063.

Demirbaş, A. (2001). Relationships between lignin contents and heating values of biomass. *Energy conversion and management*, *42*(2), 183-188.

Eom, I. Y., Kim, K. H., Kim, J. Y., Lee, S. M., Yeo, H. M., Choi, I. G., & Choi, J. W. (2011). Characterization of primary thermal degradation features of lignocellulosic biomass after removal of inorganic metals by diverse solvents. *Bioresource technology*, *102*(3), 3437-3444.

Gupta, N. K., Prakash, P., Kalaichelvi, P., & Sheeba, K. N. (2016). The effect of temperature and hemicellulose-lignin, cellulose-lignin, and cellulose-hemicellulose on char yield from the slow pyrolysis of rice husk. *Energy*

Sources, Part A: Recovery, Utilization, and Environmental Effects, *38*(10), 1428-1434.

Krajnc, N. (2015). *Wood fuels handbook*. Food and Agriculture Organization of the United Nations.

Kim, S., & Holtzapple, M. T. (2006). Effect of structural features on enzyme digestibility of corn stover. *Bioresource technology*, *97*(4), 583-591.

Maksimuk, Y., Antonava, Z., Krouk, V., Korsakova, A., & Kursevich, V. (2020). Prediction of higher heating value based on elemental composition for lignin and other fuels. *Fuel*, *263*, 116727.

Prasad, L., Subbarao, P. M. V., & Subrahmanyam, J. P. (2015). Experimental investigation on gasification characteristic of high lignin biomass (Pongamia shells). *Renewable Energy*, *80*, 415-423.

Pudasainee, D., Kurian, V., & Gupta, R. (2020). Coal: Past, Present, and Future Sustainable Use. In *Future Energy* (pp. 21-48). Elsevier.

Saravanakumar, S. S., Kumaravel, A., Nagarajan, T., & Moorthy, I. G. (2014b). Effect of chemical treatments on physicochemical properties of *Prosopis juliflora* fibers. *International Journal of Polymer Analysis and Characterization*, *19*(5), 383-390.

Saravanakumar, S. S., Kumaravel, A., Nagarajan, T., & Moorthy, I. G. (2014a). Investigation of physico-chemical properties of alkali-treated *Prosopis juliflora* fibers. *International Journal of Polymer Analysis and Characterization*, *19*(4), 309-317.

Segal, L. G. J. M. A., Creely, J. J., Martin Jr, A. E., & Conrad, C. M. (1959). An empirical method for estimating the degree of crystallinity of native cellulose using the X-ray diffractometer. *Textile research journal*, *29*(10), 786-794.

Simon, G. L., & Peterson, C. (2019). Disingenuous forests: A historical political ecology of fuelwood collection in South India. *Journal of Historical Geography*, *63*, 34-47. doi: 10.1016/j.jhg.2018.09.003

TAPPI. (1992). Technical association of the pulp and paper industry. Georgia, USA: Atlanta.

Van Soest, P. J. (1963a). Use of detergents in the analysis of fibrous feeds. I. Preparation of fiber residues of low nitrogen content. *Journal of the association of Official Agricultural Chemists*, *46*(5), 825-829.

Van Soest, P. J. (1963b). Use of detergents in the analysis of fibrous feeds. 2. A rapid method for the determination of fiber and lignin. *Journal of the Association of Official Agricultural Chemists*, *46*(5), 829-835.

Yang, H., Yan, R., Chen, H., Lee, D. H., & Zheng, C. (2007). Characteristics of hemicellulose, cellulose and lignin pyrolysis. *Fuel*, *86*(12-13), 1781-1788.

Indian Institute of Technology Guwahati

Chapter 4

Impact of chemical pretreatment on the pyrolytic products of *A. donax* biomass

4.1 Introduction

The fragmentation and depolymerization of the core elements of lignocellulosic biomass, viz. cellulose, hemicellulose, and lignin, during pyrolysis results in the generation of > 300 compounds (Staš et al., 2014). A fraction of these compounds is feedstock for numerous industrial processes and products, and many others have high commercial value. Methoxy and dimethoxy phenol derivatives such as cresols, guaiacols, and isoeugenol find major application in food, paint and pharmaceutical industries (Stoikos, 1991). Wang et al. (2015) observed that pyrolysis of corncobs treated with H_2SO_4 resulted in a multi-fold increase in yield of furfural, which is a highly versatile chemical with global market of 370,000 tons with a growth rate of 3.1%. Furfural finds numerous applications in the manufacture of around 80 chemicals (Dalvand et al., 2018). Pyrolysis of birch wood treated with dilute phosphoric acid generated bio-oils with enhanced 1,6-anhydrosaccharides, which opens up possibilities

of their application in chemical and medical industry due to their optical activity (Dobele et al., 2003). Lu et al. investigated the application of alkali pretreatment of herbaceous biomass for enhancing the production of 4-vinylphenol that finds application in organic transistors and adhesives (Lu et al., 2019). Two specific challenges, which inhibit the utilization of bio-oils for various applications are: (1) the relatively low concentration of specific desired compounds in bio-oil, and (2) effective extraction (or separation) and purification of these compounds from a mixture of a wide range of compounds in bio-oil that include phenols, ketones, ethers, acids, furans, and aldehydes.

A possible solution to aforementioned issue is pretreatment, i.e. specifically modifying, reducing or removing individual components of the lignocellulosic biomass by employing specific treatment techniques prior to pyrolysis. This would, in effect, remove or enhance the precursor lignocellulosic fraction, which would either lead to the reduction or enhancement of the generation of specific compounds or compound groups by pyrolysis. Furthermore, reduction of the concentration of certain undesirable compounds in the bio-oil may render extraction of desired components easier through more straightforward extraction techniques. This current chapter analyzes the effect of the previously studied chemical pretreatments on the pyrolysis product stream characteristics. Besides, this chapter also endeavours to map the changes in product (bio-oil, biochar and non-condensable gas) yield and composition to changes in biomass properties (biochemical composition, H/C and O/C ratios), which could form pivotal criteria and yardsticks in screening biomass samples and pretreatment techniques for specific applications.

4.2 Materials and Methods

4.2.1 Fixed bed pyrolysis reactor

For the pyrolysis of the treated and untreated biomass, a semi-batch fixed bed batch reactor was designed and assembled. The 600 cc capacity high-temperature reactor fabricated using high-grade stainless steel parts can withstand up to 1000 ℃.

The reactor was constructed with a 20 cm long 2” schedule 40 tube having an OD of 60.33 mm and ID of 52.5 mm with significantly higher thickness for safety reasons. One end of the tube was TIG welded with a SS316 plate of 5 mm thickness. The other end was TIG welded with a 2” class 150 weld neck raised face flange. An accompanying 2” class 150 blind flange was used to close the end. A steel wire gauze reinforced compressed asbestos fibre gasket was placed between the weld neck and blind flange to make the reactor leak-free during the high-temperature operations. The reactor was housed inside a 4 kW electric furnace capable of heating at close to 40 ℃/min, which resulted in a heating rate of 25 ℃/min in the interior of the reactor. The reactor setup is shown in Fig. 4.1. The schematic reactor setup is also shown in Fig. 4.2.

The blind flange has an inlet and outlet for the passage of inert nitrogen gas and bio-oil vapor laden carrier nitrogen gas, respectively. The flow of carrier nitrogen gas can be controlled using a gas flowmeter. The outlet of the reactor was linked to the vapor condensation system. The condensation system consists of a set of metal water jackets with the bio-oil flow lines passing through them. Cold water (at 7 to 10 ℃) was continuously circulated through the water jackets, which surround the bio-oil vapor flow lines. At the lower end of each of the metal water jackets, the bio-oil collection funnels are placed. The condensed pyrolytic bio-oil vapors were collected below the

condensation system in glass funnels so that the oil can be tapped out for analysis whenever required.

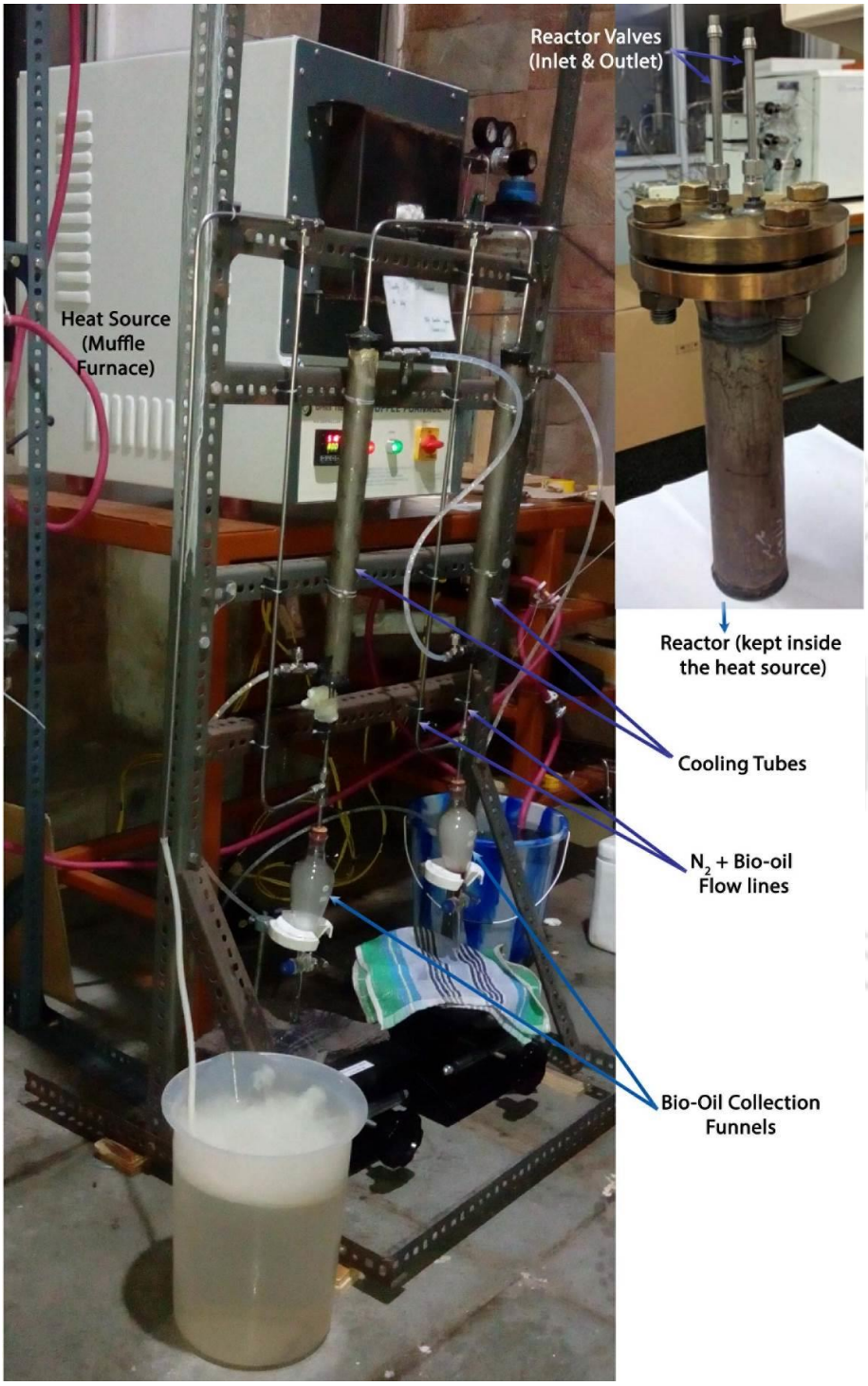

Figure 4.1: Semi-batch pyrolysis reactor setup

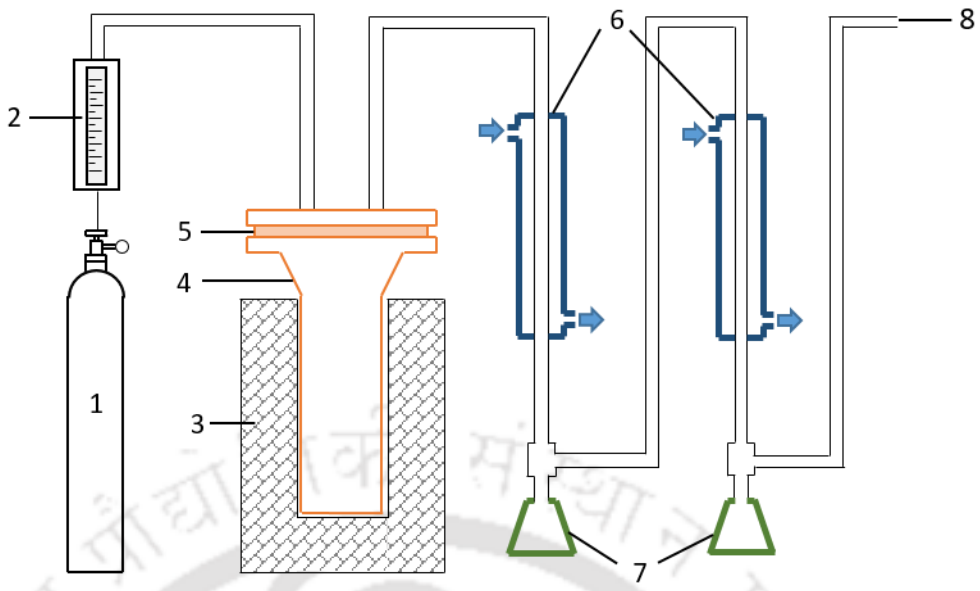

Figure 4.2: Schematic of the Semi-batch pyrolysis reactor. Components: (1) N_2 gas cylinder, (2) Flowmeter, (3) Furnace, (4) High temperature reaction vessel, (5) Gasket, (6) Condensers, (7) Bio-oil collection funnels, and (8) To scrubber & exhaust

4.2.2 Pyrolysis of treated and raw untreated biomass samples

For each of the pyrolysis runs, 50 g of biomass was taken in the reactor and initially purged with nitrogen gas for 10-15 min to expel off the oxygen present inside the reactor. The heating process for pyrolysis was then initiated with a 100 ml/min carrier (nitrogen) flow rate. Once the reactor reached 600 ℃, the reactor was isothermally maintained at that temperature for 2 h before the cooling cycle starts. The reactor was opened once the reactor temperature drops below 80 ℃ to recover the solid residue (also known as biochar). The condensed bio-oil and biochar were then analyzed.

4.2.3 Analysis of bio-oil using GC-MS

Gas Chromatography-Mass Spectroscopy (GC–MS) analysis of pyrolytic oil was performed on a Varian 450-GC interfaced to a 240-MS ion trap mass detector. The MS detection was carried out with a mass to charge range from 50 to 1000 amu. A 30 m × 0.25 mm Agilent J&W VF-5ms column having a film thickness of 0.25 μm was

used for the separation of compounds. The GC oven was initially maintained at 80 ℃ for 2 min, then increased at a rate of 8 ℃/min to 140 ℃, then heated at 4 ℃/min to 280 ℃. Once the oven reaches 280 ℃, it was isothermally maintained for 2 min. High purity helium gas was used as the carrier gas with a fixed flow rate of 1 ml/min. The injection point temperature was fixed at 250 ℃. Injector split ratio of 10:1 was used. The pyrolytic oil was initially centrifuged, and the heavier organic phase was separated and dissolved in acetone. The small fraction of undissolved components, including small particles of char, are filtered out using a 0.2 µm PTFE membrane filter. This acetone-dissolved bio-oil was used for analysis using GC-MS to study the chemical composition quantitatively. A fixed quantity of 5 µL was used for each analysis.

4.3 Results and Discussion

The treatment of biomass with chemical agents resulted in the targeted breakdown of specific lignocellulosic constituents of biomass. The effect of the eleven pretreatment experiments on the biochemical composition, equilibrium moisture content, calorific value, crystallinity and crystal size of *A. donax* biomass has been discussed in the previous chapters.

The quantified product streams of pyrolysis: bio-oil, biochar and non-condensable gases, with their physical properties, are tabulated in Table 4.1.

Table 4.1: Properties of product streams of pyrolysis of untreated and treated *A. donax* biomass

	Pyrolysis of untreated *A. donax*	Pyrolysis of *A. donax* treated with										
		1% H_2SO_4	3% H_2SO_4	5% H_2SO_4	1% H_3PO_4	3% H_3PO_4	5% H_3PO_4	1% NaOH	3% NaOH	5% NaOH	0.5% SDS	0.5% Triton X-100
Pyrolysis yield (% w/w)												
Bio-oil	31.35	44.25	40.33	34.51	46.20	41.49	44.96	45.53	46.79	46.66	45.70	42.29
Biochar	25.68	18.99	19.57	20.40	22.46	22.63	22.32	17.66	17.26	17.94	21.00	20.00
Non-condensable gases [a]	42.97	36.76	40.1	45.09	31.34	35.88	32.72	36.81	35.95	35.40	33.30	37.71
Bio-oil properties												
pH	3.49	3.08	2.98	2.98	2.90	2.80	2.74	2.42	2.20	2.27	2.17	2.80
Density (g/cm^3)	1.10	1.10	1.10	1.12	1.10	1.10	1.10	1.09	1.12	1.13	1.10	1.09
Biochar properties												
O/C ratio	0.109	0.065	0.074	0.064	0.078	0.091	0.071	0.069	0.084	0.075	0.076	0.061
H/C ratio	0.018	0.014	0.006	0.013	0.019	0.017	0.018	0.021	0.014	0.015	0.011	0.020

[a] by difference

4.3.1 Effect of pretreatment on the overall yield of pyrolysis products

Pyrolysis of untreated *A. donax* biomass gave a low bio-oil yield of 31.35% w/w. A positive impact of the chemical treatment on pyrolysis process was the marked increase in quantitative bio-oil yield. The highest yields of 46.79% and 46.66% w/w were observed with 3% and 5% NaOH treated samples, respectively. Furthermore, it was observed that NaOH treated biomass exhibited the highest cellulose content, which could contribute to the high bio-oil yield (Wang and Luo, 2016). The high H/C ratio of the NaOH treated samples also predicted high bio-oil yield earlier. Small insignificant variations in bio-oil yield were observed with varying NaOH concentration treatments. But with acid-treated biomass, the generation of bio-oil decreased considerably with an increase in the concentration of treatment media. This trend was more distinct with strong acid (H_2SO_4) than with weak acid (H_3PO_4). The bio-oil yield from untreated and treated biomass varied in the following order: native (untreated) < H_2SO_4 < Triton X-100 < SDS < H_3PO_4 < NaOH. Bio-oil from untreated biomass had a pH value of 3.49 and a density of 1.10 g/cm^3. The density of bio-oil from pretreated biomass was almost similar - ranging from 1.09 to 1.13 g/cm^3. The pH of bio-oils from treated biomass ranged from 2.20 to 3.08, with the lowest pH values obtained for bio-oils from NaOH and SDS treated biomass. The decrease in the ash content associated with chemical pretreatment plays an important role in reducing the pH of bio-oil. Major fraction of the alkali and alkaline earth metals (AAEM), which constitute a large portion of ash, gets washed off during pretreatment. This results in rise of the acidic fractions of the biomass which is manifested in the properties of bio-oils, thereby resulting in bio-oils with low pH.

Solid (biochar) yield, on the contrary, reduced for all 11 samples of pretreated biomass. Biochar includes the minerals (ash) and carbonaceous residues formed during pyrolysis. The mineral (ash) content of untreated *A. donax* accounting for 6.38 % w/w was found to mainly consist of AAEM such as potassium (K), magnesium (Mg) and calcium (Ca). Studies have shown that the washing of AAEM occurs during pretreatment. Jiang et al. (2013) recorded the tremendous AAEM demineralization effect of H_2SO_4 of up to 99.8% of K, 88.5% of Na, 95.7% of Ca and 98.6% of Mg. H_3PO_4 also showed similar results except for Ca, where a 62.3% reduction was observed. This demineralization effect of treatment media could contribute to the low biochar yields. Interestingly, it was also observed that biochar did not record significant change for different concentrations of H_3PO_4 and NaOH. On the contrary, the biochar yield increased with increasing concentrations of H_2SO_4, even though AAEM content reduced. The proportional increase of lignin in treated biomass with the concentration of H_2SO_4 treatment media could enhance the char yield as pyrolysis of lignin typically produces biochar to a greater extent compared to cellulose and hemicellulose (Raveendran et al., 1995). The biochar yield from treated biomass in increasing order was as follows: NaOH < H_2SO_4 < Triton X-100 < SDS < H_3PO_4 < untreated biomass, which exactly matched with the order of char yield obtained when studied with thermogravimetric analysis (TGA) as shown previously in Table 2.3(a).

In addition to the bio-oil and biochar, pyrolysis results in the production of a gaseous product stream consisting mainly of CO, CO_2, CH_4, H_2 and lower hydrocarbons (C_2-C_4 compounds) in minor quantities. The yield of non-condensable gases reduced in most instances except with 5% H_2SO_4 treated biomass.

Identification and quantification of pyrolytic compounds face many challenges due to the presence of a wide range of molecular weight compounds, non-volatile compounds, non-availability of spectra and standards of compounds and the instability of the bio-oil. This has resulted in the unavailability of a single stand-alone technique for the complete qualitative and quantitative analysis of bio-oils.

Bio-oils have been reported to contain more than 300 compounds which have been identified by GC-MS and GC-FID with a variety of GC columns (Staš et al., 2014) and up to 857 compounds by GC x GC-TOFMS (Tessarolo et al., 2013). In this thesis, 47 individual compounds in bio-oil were identified with GC-MS analysis. These individual components were classified into three groups: aromatic, non-aromatic and heterocyclic compounds. The identified compounds, based of the study by Staš et al. (2014), were sorted into nine sub-groups (under the three main groups mentioned above) as: (1) Phenols (phenol, cresols, alkylphenols, etc.), (2) Benzenediols (resorcinol, catechol and their derivatives), (3) Methoxy, dimethoxy phenol derivatives, (4) Aromatic non-oxygenates and (5) Aromatics oxygenates under aromatic compounds; (6) Carboxylic acids (mainly acetic acid), (7) Ketones (cyclopentenones, cyclohexenones, etc.), (8) Other non-aromatics under non-aromatic compounds; and (9) Furans under heterocyclic compounds. Table 4.2 lists the bio-oil compounds identified through GC-MS in our study along with their categorization into the nine sub-groups. Additionally, another categorization based on the lignocellulosic precursor components, viz. carbohydrate (C) or lignin (hydroxyphenol lignin, guaiacol lignin, syringol lignin and other aromatics) is included.

Table 4.2: Pyrolytic liquid compounds identified through GC-MS analysis with their retention time, classification and source

Peak No.	Residence Time (min)	IUPAC compound name	Source[a,b]	Group[c]	Formula	MW
1	3.42	acetic acid	C	Acids	$C_2H_4O_2$	60
2	3.93	(E)-pent-3-en-2-one / methyl propenyl ketone	C	Ketones	C_5H_8O	84
3	4.2	2,5-dimethylfuran	C	Furans	C_6H_8O	96
4	4.97	toluene / methylbenzene	L	Non-oxygenated aromatics	C_7H_8	92
5	5.96	furan-2-carbaldehyde / furfural	C	Furans	$C_5H_4O_2$	96
6	6.11	furan-2-ylmethanol / furfuryl alcohol	C	Furans	$C_5H_6O_2$	98
7	6.36	1,3-xylene / m-xylene / 1,3-dimethylbenxene	L	Non-oxygenated aromatics	C_8H_{10}	106
8	6.94	styrene / vinylbenzene	L	Non-oxygenated aromatics	C_8H_8	104
9	7.19	2-methylcyclopent-2-en-1-one	C	Ketones	C_6H_8O	96
10	7.54	cyclohexanone / cyclohexyl ketone	C	Ketones	$C_6H_{10}O$	98
11	8.21	5-methylfuran-2-carbaldehyde / 5-methyIfurfural	C	Furans	$C_6H_6O_2$	110
12	8.47	phenol	L-H	Phenols	C_6H_6O	94
13	8.57	benzene-1,3-diol / 3-hydroxyphenol / resorcinol	L	Benzenediols	$C_6H_6O_2$	110
14	9.03	2,2-diethyl-3-methyl-1,3-oxazolidine	C		$C_8H_{17}NO$	143
15	9.49	2-hydroxy-3-methylcyclopent-2-en-1-one	C	Ketones	$C_6H_8O_2$	112
16	9.73	2,3-dimethylcyclopent-2-en-1-one	C	Ketones	$C_7H_{10}O$	110
17	9.99	2-methylphenol / o-cresol	L-H	Phenols	C_7H_8O	108
18	10.43	4-methylphenol / p-cresol	L-H	Phenols	C_7H_8O	108
19	10.78	2-methoxyphenol / guaiacol	L-G	Methoxyphenol derivatives	$C_7H_8O_2$	124
20	11.43	3-ethyl-2-hydroxycyclopent-2-en-1-one	C	Ketones	$C_7H_{10}O_2$	126
21	11.58	1-methyl-2,3-dihydro-1H-indene / 1-methylindan	L	Non-oxygenated aromatics	$C_{10}H_{12}$	132
22	12.02	3,5-dimethylphenol	L-H	Phenols	$C_8H_{10}O$	122
23	12.44	2-ethylphenol	L-H	Phenols	$C_8H_{10}O$	122
24	12.77	4-ethylbenzene-1,3-diol / 4-ethylresorcinol	L	Benzenediols	$C_8H_{10}O_2$	138
25	13.09	2-methoxy-4-methylphenol / 4-methylguaiacol / creosol	L-G	Methoxyphenol derivatives	$C_8H_{10}O_2$	138

Peak No.	Residence Time (min)	IUPAC compound name	Source[a,b]	Group[c]	Formula	MW
26	13.33	benzene-1,2-diol / 2-hydroxyphenol / pyrocatechol / catechol	L	Benzenediols	$C_6H_6O_2$	110
27	13.79	2,3-dihydro-1-benzofuran / coumaran	L	Oxygenated aromatics	C_8H_8O	120
28	13.99	1,2-dimethoxy-4-methylbenzene / 3,4-dimethoxytoluene	L	Oxygenated aromatics	$C_9H_{12}O_2$	152
29	14.77	3-methylbenzene-1,2-diol / 3-methylcatechol	L	Benzenediols	$C_7H_8O_2$	124
30	14.97	3-methoxybenzene-1,2-diol / 3-methoxycatechol	L	Benzenediols	$C_7H_8O_3$	140
31	15.16	4-ethyl-2-methoxyphenol / 4-ethylguaiacol	L-G	Methoxyphenol derivatives	$C_9H_{12}O_2$	152
32	15.43	1-(2,6-dihydroxyphenyl)ethanone / 2-acetylresorcinol	L	Benzenediols	$C_8H_8O_3$	152
33	15.71	2,3-dihydroinden-1-one / 1-indanone	L	Oxygenated aromatics	C_9H_8O	132
34	15.86	(5-formylfuran-2-yl)methyl acetate / 5-acetoxymethylfurfural	C	Furans	$C_8H_8O_4$	168
35	16.20	1-(2-hydroxy-5-methylphenyl)Ethanone	L-H	Phenols	$C_9H_{10}O_2$	150
36	17.08	2,6-dimethoxyphenol / syringol	L-S	Methoxyphenol derivatives	$C_8H_{10}O_3$	154
37	17.21	2-methoxy-4-prop-2-enylphenol / eugenol	L-G	Methoxyphenol derivatives	$C_{10}H_{12}O_2$	164
38	17.47	1-(2,5-dihydroxyphenyl)propan-1-one	L	Phenols	$C_9H_{10}O_3$	166
39	18.65	2-methoxy-6-prop-2-enylphenol	L-G	Methoxyphenol derivatives	$C_{10}H_{12}O_2$	164
40	19.57	1,2,4-trimethoxybenzene	L-S	Oxygenated aromatics	$C_9H_{12}O_3$	168
41	19.86	2-methoxy-4-(prop-1-enyl)-phenol / trans-isoeugenol	L-G	Methoxyphenol derivatives	$C_{10}H_{12}O_2$	164
42	20.18	2-methoxy-4-propylphenol / 4-propylguaiacol	L-G	Methoxyphenol derivatives	$C_{10}H_{14}O_2$	166
43	21.67	1-ethyl-4-phenylbenzene / 4-ethylbiphenyl	L	Non-oxygenated aromatics	$C_{14}H_{14}$	182
44	22.04	1-(4-hydroxy-3-methoxyphenyl)propan-2-one / 4-hydroxy-3-methoxyphenyl acetone	L-G	Methoxyphenol derivatives	$C_{10}H_{12}O_3$	180
45	22.93	1-(3,4-dimethoxyphenyl)ethanone	L	Methoxyphenol derivatives	$C_{10}H_{12}O_3$	180
46	23.95	1-phenylpropylbenzene / 1,1-diphenylpropane	L	Non-oxygenated aromatics	$C_{15}H_{16}$	196
47	23.77	2,6-dimethoxy-4-prop-2-enylphenol / 4-allylsyringol	L-S	Methoxyphenol derivatives	$C_{11}H_{14}O_3$	194

[a] (Dalluge et al., 2017; Eom et al., 2012; Fivga, 2012); [b] C: Carbohydrate, L-H: Hydroxylphenol lignin, L-G: Guaiacol lignin, L-S: Syringyl lignin, L: Other aromatics; [c] (Staš et al., 2014)

The gas chromatography spectra of bio-oil produced by pyrolysis of untreated biomass is shown in Fig. 4.3 and the identified compounds of each of the marked peaks is listed in Table 4.3. The spectra of untreated biomass show several clear peaks. The spectra of the bio-oils obtained by pyrolysis of treated biomass samples have been included in Annexure C. The comparison of the spectra showed that the chemical pretreatment resulted in the reduction of the intensities of various peaks. Overall, it was observed from the quantitative analysis that pretreatment of biomass did not result in the disappearance of compounds but resulted in the variation in intensities of the peaks, whose areas under the peak are a direct measure of the concentrations of the component concentrations. The components were identified by matching the obtained mass spectra corresponding to every peak with standard NIST mass spectra. The quantified components of bio-oils, obtained through pyrolysis of treated and native biomass, is shown in Table 4.4. The effect of chemical pretreatment on the bio-oil components derived from carbohydrate and lignin fractions and discussed in subsequent sections.

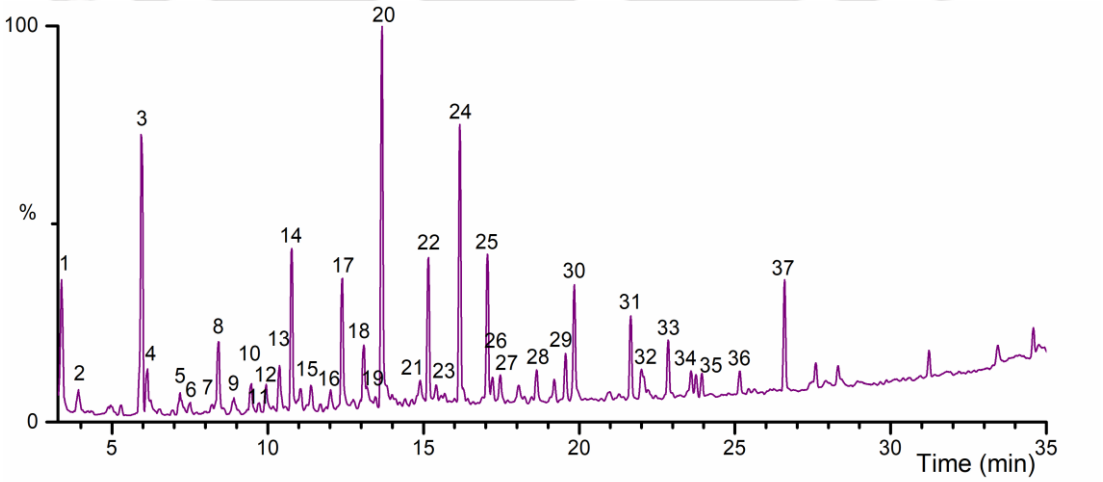

Figure 4.3: Chromatogram of bio-oil from pyrolysis of raw untreated *A. donax* by GC-MS analysis

Table 4.3: Identified chemicals from pyrolysis of raw untreated *A. donax*

1: acetic acid
2: (E)-pent-3-en-2-one / methyl propenyl ketone
3: furan-2-carbaldehyde / furfural
4: furan-2-ylmethanol / 2-furanmethanol
5: 2-methylcyclopent-2-en-1-one
6: cyclohexanone / cyclohexyl ketone
7: 5-methylfuran-2-carbaldehyde / 5-methylfurfural
8: phenol
9: 2,2-diethyl-3-methyl-1,3-oxazolidine
10: 2-hydroxy-3-methylcyclopent-2-en-1-one / cyclotene
11: 2,3-dimethylcyclopent-2-en-1-one
12: 2-methylphenol / o-cresol
13: 4-methylphenol / p-cresol
14: 2-methoxyphenol / guaiacol
15: 3-ethyl-2-hydroxycyclopent-2-en-1-one
16: 3,5-dimethylphenol
17: 2-ethylphenol
18: 2-methoxy-4-methylphenol / 4-methylguaiacol / creosol
19: benzene-1,2-diol / 2-hydroxyphenol / pyrocatechol / catechol
20: 2,3-dihydro-1-benzofuran / coumaran
21: 3-methoxybenzene-1,2-diol / 3-methoxycatechol
22: 4-ethyl-2-methoxyphenol / 4-ethylguaiacol
23: 1-(2,6-dihydroxyphenyl)ethanone / 2-acetylresorcinol
24: 1-(2-hydroxy-5-methylphenyl)ethanone / 2-hydroxy-5-methylacetophenone / o-acetyl-p-cresol
25: 2,6-dimethoxyphenol / syringol
26: 2-methoxy-4-prop-2-enylphenol / 4-allyl-2-methoxyphenol / eugenol
27: 1-(2,5-dihydroxyphenyl)propan-1-one
28: 2-methoxy-6-prop-2-enylphenol / 2-allyl-6-methoxyphenol
29: 1,2,4-trimethoxybenzene
30: 2-methoxy-4-(prop-1-enyl)-phenol / trans-isoeugenol
31: 1-ethyl-4-phenylbenzene / 4-ethylbiphenyl
32: 1-(4-hydroxy-3-methoxyphenyl)propan-2-one / 4-hydroxy-3-methoxyphenyl acetone
33: 1-(3,4-dimethoxyphenyl)ethanone
34, 36, 37: 2,6-dimethoxy-4-prop-2-enylphenol / 4-allylsyringol
35: 1-phenylpropylbenzene / 1,1-diphenylpropane

Table 4.4: Bio-oil product distribution from pyrolysis of untreated and treated *A. donax*

Compound name	Yield (% v/v)					
	Untreated	5% H_2SO_4	5% H_3PO_4	3% NaOH	0.5% SDS	0.5% Triton X-100
Carboxylic acids						
acetic acid	4.06	1.20	4.59	3.30	-	9.88
	4.06	**1.20**	**4.59**	**3.30**	-	**9.88**
Ketones						
3-penten-2-one	0.97	-	0.78	6.29	-	1.61
2-methyl-2-cyclopenten-1-one	1.21	0.62	0.72	1.61	-	0.43
1-cyclohexanone	0.49	1.11	0.89	2.37	-	0.65

2-hydroxy-3-methyl-2-cyclopenten-1-one	1.02	1.48	1.06	3.59	0.69	1.28
2,3-dimethyl-2-cyclopenten-1-one	0.32	0.11	-	0.48	-	0.21
3-ethyl-2-hydroxy-2-cyclopenten-1-one	1.29	0.64	0.98	2.95	-	0.44
	5.29	**3.96**	**4.42**	**17.29**	**0.69**	**4.62**
Others						
2,2-diethyl-3-methyl-oxazolidine	0.99	0.73	1.69	1.89	0.81	0.54
	0.99	**0.73**	**1.69**	**1.89**	**0.81**	**0.54**
Furans						
2,5-dimethylfuran	-	-	0.65	1.64	-	0.81
furfural	9.65	19.89	18.83	15.49	17.93	9.33
2-furanmethanol	1.67	0.47	0.41	3.00	1.32	0.74
5-methyl-2-furaldehyde	0.29	2.98	0.59	4.03	-	1.55
5-acetoxymethyl-2-furaldehyde	-	-	0.73	-	0.48	0.40
	11.61	**23.35**	**21.21**	**24.16**	**19.73**	**12.82**
Phenols						
phenol	3.13	1.81	1.58	0.82	0.75	1.57
2-methylphenol (o-cresol)	1.02	1.37	0.51	2.08	-	0.67
4-methylphenol (p-cresol)	1.84	1.70	1.53	0.98	0.78	1.84
3,5-dimethylphenol	0.73	-	-	-	-	-
2-ethylphenol	4.51	3.57	4.07	0.71	2.44	5.74
1-(2-hydroxy-5-methylphenyl)ethanone	9.16	5.35	8.06	3.44	4.78	8.23
1-(2,5-dihydroxyphenyl)propan-1-one	1.06	0.43	0.59	0.84	-	0.92
	21.45	**14.23**	**16.34**	**8.88**	**8.74**	**18.96**
Benzenediols						
resorcinol	-	-	-	-	-	-
catechol	0.54	-	-	-	-	-
3-methoxybenzene-1,2-diol	1.25	-	1.25	-	-	-
1-(2,6-dihydroxyphenyl)ethanone	0.59	-	-	-	-	0.37
	2.39	-	**1.25**	-	-	**0.37**
Methoxyphenol derivatives						
guaiacol	5.79	3.08	2.31	3.47	1.38	2.36
creosol	1.89	5.58	4.60	3.42	2.04	3.37
4-ethyl-2-methoxyphenol	4.57	2.96	3.60	3.17	2.51	5.06
syringol	4.62	2.24	1.41	1.53	1.02	1.66
eugenol	0.77	0.66	0.62	0.81	-	0.84
2-allyl-6-methoxyphenol	1.07	0.64	0.68	0.39	-	0.86
trans-isoeugenol	4.31	2.75	3.20	3.08	1.30	3.20
4-propylguaiacol	-	0.75	-	-	29.91	-
1-(4-hydroxy-3-methoxyphenyl)propan-2-one	1.39	1.25	4.80	0.54	-	0.34
1-(3,4-dimethoxyphenyl)Ethanone	1.80	1.04	-	1.00	-	0.93
4-allylsyringol	5.10	3.50	3.64	1.76	1.48	3.61
	31.31	**24.46**	**24.87**	**19.17**	**39.65**	**22.23**

Aromatic non-oxygenates						
toluene	-	-	0.49	0.90	-	0.76
1,3-xylene	-	-	0.08	-	-	0.44
styrene	-	-	0.18	-	-	-
1-methyl-2,3-dihydro-1*H*-indene	-	-	-	-	-	-
1-phenylpropylbenzene	0.72	0.64	0.27	-	-	0.43
1-ethyl-4-phenylbenzene	2.81	9.02	2.36	0.90	3.21	1.84
	3.54	**9.66**	**3.38**	**1.80**	**3.21**	**3.46**
Aromatic oxygenates						
2,3-dihydro-1-benzofuran	12.76	8.19	10.52	3.96	4.72	10.20
2,3-dihydroinden-1-one	-	-	-	-	-	-
1,2,4-trimethoxybenzene	1.63	2.39	1.72	1.82	0.89	1.61
	14.39	**10.58**	**12.25**	**5.78**	**5.62**	**11.80**

4.3.2 Effect of pretreatment on carbohydrate degradation bio-oil products

The carbohydrate fraction of biomass, composed of cellulose and hemicellulose, constitutes close to 70% by weight of *A. donax* biomass. Pyrolysis of the saccharide polymers results in formation of a number of non-aromatic compounds such as furans, ketones and carboxylic acids. A comparative plot on the effect of pretreatment on each of these group of chemicals formed through pyrolysis are shown in Fig. 4.4

Furans are well documented to be the products of the depolymerization reactions of D-glucose units in cellulose. Collard and Blin (2014) suggested that furan formation occurs by the rupture of the bond between the C_1 carbon atom and the oxygen atom of the chain, followed by the cyclization between the same oxygen atom and the C_2 carbon atom. This leads to the formation of a C=C double bond, and with the elimination of some oxygenated groups results in the formation of furan ring. This mechanism suggests the initial formation of 5-hydroxymethylfurfural (5-HMF). The rupture of weak bonds of 5-HMF can lead to the formation of furfural, 2-furanmethanol, 5-methylfurfural. Furfural is also reported to be one of the pyrolytic products of

hemicellulose generated by the dehydration of depolymerized xylan, which are polysaccharides found in hemicellulose (Shen et al., 2010). Furan yield in untreated biomass was 11.6% v/v and recorded an increase in all the 11 pretreated samples. The furan yield increased to 20.2 - 25.1% v/v for acid-treated biomass; 14.6 - 24.2% v/v for alkali-treated samples and to 19.7% v/v and 12.8% v/v for SDS and Triton X-100 treated biomass respectively. The individual concentrations of furfural and 5-methylfurfural recorded an increase with pretreatment of samples. Hence, pretreatment of biomass, specifically with acid, could be employed to improve the yield of furfural, one of the high-value chemicals with diverse applications. Higher concentration of acid employed for the treatment yielded higher furfural yield. However, with H_3PO_4 treatment, the yield was found to increase with concentration initially and reached a maximum of 21.2% v/v with 3% H_3PO_4 but dropped to 18.8% v/v with 5% H_3PO_4 media.

One of the other products formed by the thermal decomposition of hemicellulose is acetic acid (Banks et al., 2014). Acetic acid plays a major role in the stability of bio-oil as acid-catalysed polymerization reactions result in increasing the viscosity of bio-oils and phase separation (Meng et al., 2014). This invariably degrades the quality of bio-oil and limits its application. The highest acetic acid content of 9.88% v/v was observed with Triton X-100 treatment. The high concentration of hemicellulose in Triton X-100 treated biomass could account for the observed increase in acetic acid. Similar results were also reported by Banks et al. (2014), who observed the increase in acetic acid yield with increase in the concentration of Triton X-100 treatment solution. The relation between the hemicellulose content and acetic acid yield was also observed with H_2SO_4 treated biomass, which was one of the solvents effective in the hydrolysis

of hemicellulose. Lower the hemicellulose in H_2SO_4 treated biomass, lower was the acetic acid yield. The lowest acetic acid yield of 1.2% v/v was observed with 5% H_2SO_4 treatment. Acetic acid was not detected with 5% NaOH treatment, which gave the lowest hemicellulose content of all the pretreated samples.

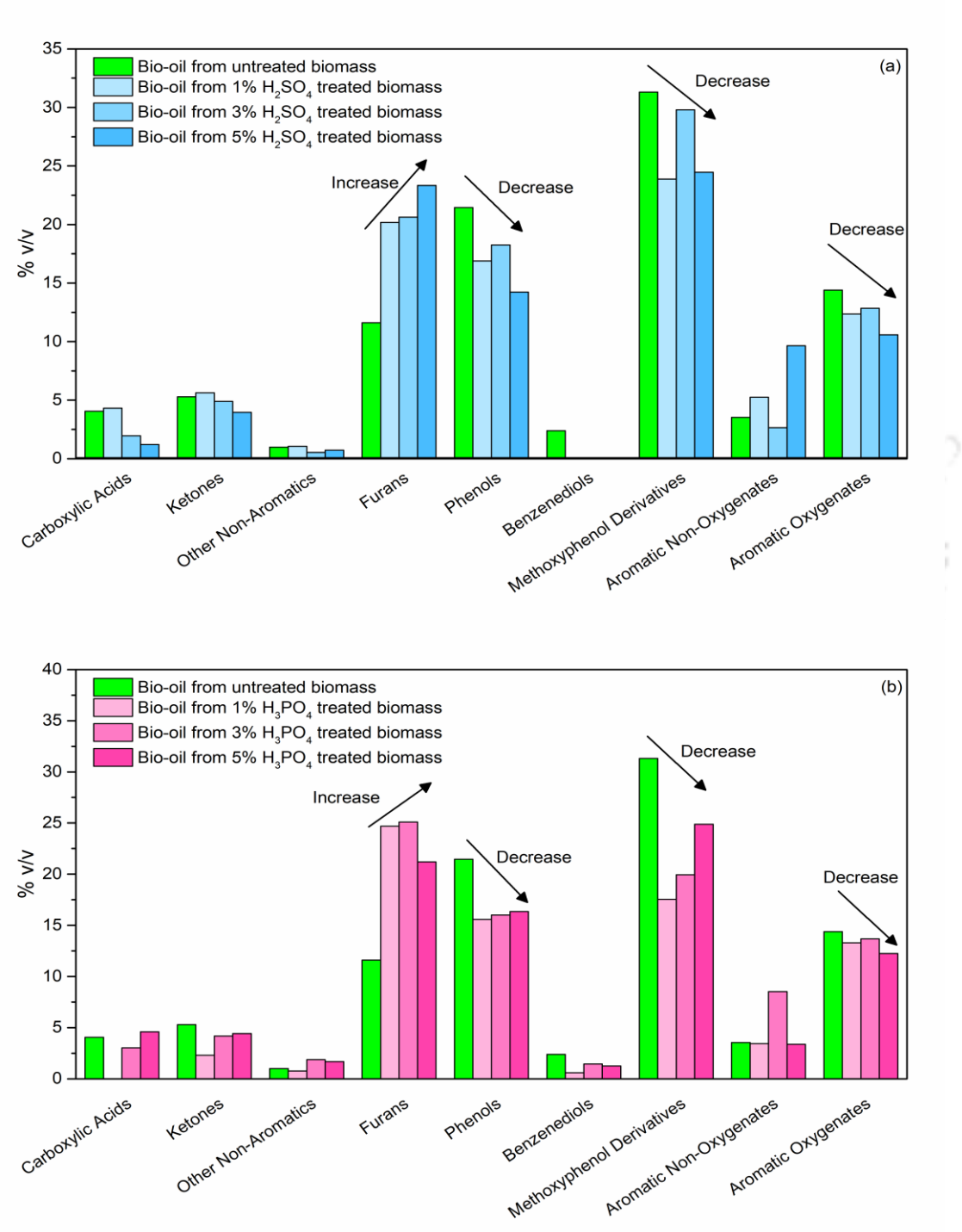

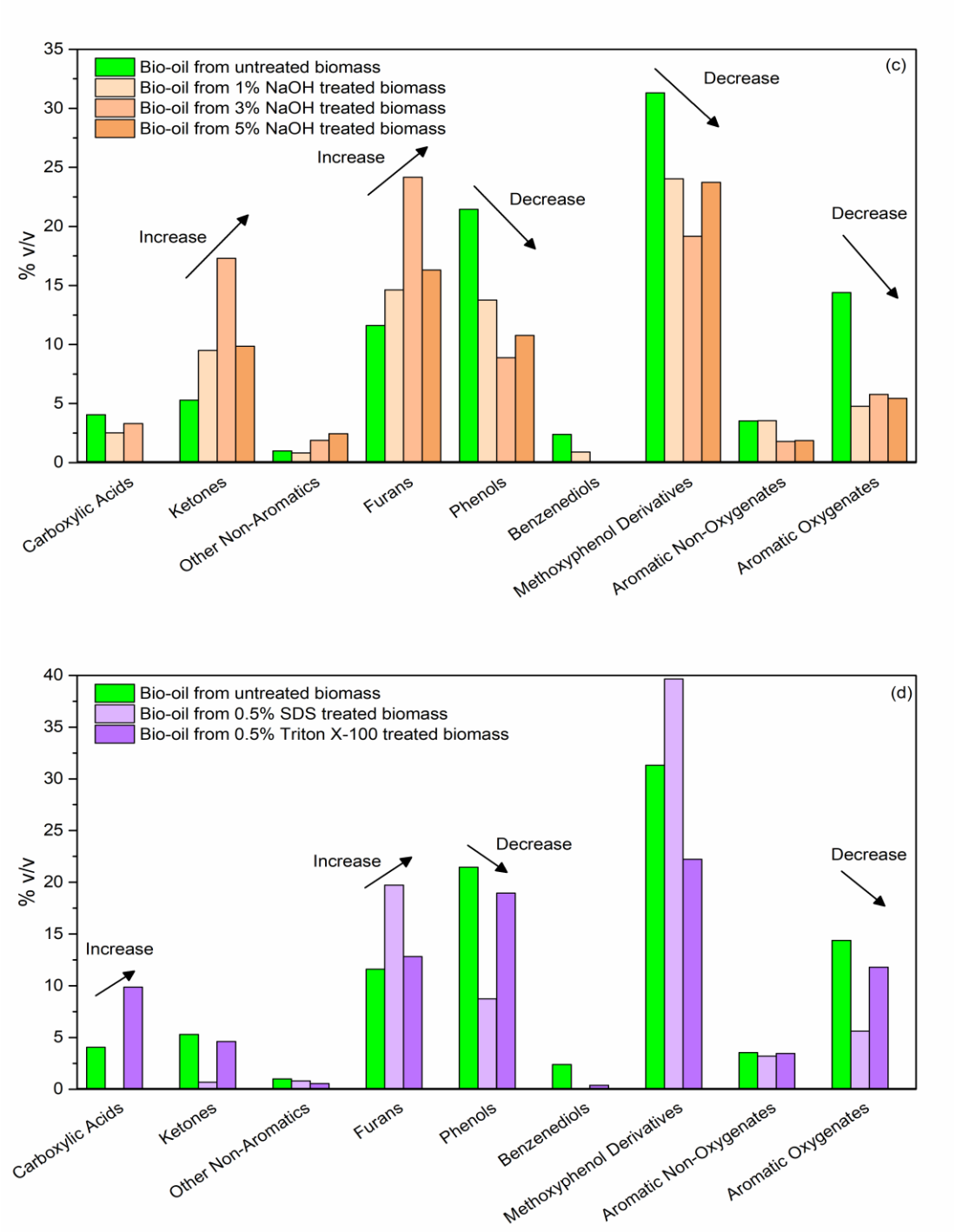

Figure 4.4: Comparison of the chemical composition of bio-oils obtained from (a) H_2SO_4 treated biomass, (b) H_3PO_4 treated biomass, (c) NaOH treated biomass and (d) SDS & Triton X-100 treated biomass.

4.3.3 Effect of pretreatment on lignin degradation bio-oil products

Lignin is a complex polymer comprising of 3 monomer units: guaiacyl (G), syringol (S) and *p*-hydroxyphenol (H) linked by carbon-carbon, ether and ester bonds. The commonly identified linkages in lignin are α-O-4, β-O-4, 4-O-5, β-β, β-5, β-1 and 5-5. Nakamura et al. (2008) reported that ether bonds involving alkyl chains: α-O-4 and β-O-4 are comparatively less weak than the aryl linkages. The rupture of these weak α-O-4 and β-O-4 links at moderately low temperatures between 200 °C and 250 °C results in the formation of methoxyphenol derivatives such as guaiacols and eugenol. At much higher temperatures of 300 °C, the α-aryl, β-aryl and aryl-aryl linkages rupture, resulting in the formation of phenolic compounds with alkyl chains, viz. o-cresol, p-cresol and other organic compounds, which fall under the category of phenols.

The total phenolic content in bio-oil obtained from untreated biomass contributes to around 52% (21% phenols and 31% methoxyphenol derivatives). From the data in Fig. 4.4, it is evident that the yield of phenols and methoxyphenol derivatives showed a reduction trend across all pretreatment techniques with the exception of SDS treated biomass, which displayed a significant increase in methoxyphenol derivatives. Phenols in bio-oil decreased in the range of 12.3-14.2%, 12.4-16.0%, 8.9-13.8%, 8.7% and 19.0% with biomasses treated with H_2SO_4, H_3PO_4, NaOH, SDS and Triton X-100, respectively. The methoxyphenol content for pretreated biomasses varied between 23.9-29.8% for H_2SO_4, 17.4-24.9% for H_3PO_4, 18.9-24.0% for NaOH, 39.7% for SDS and 22.2% for Triton X-100.

All pretreatment techniques bring about a reduction in lignin content (varying between 8.7 and 84.1%), and this reduction is partially accountable for the decrease in the yields. SDS treated biomass exhibit the maximum reduction of phenols and an

increase in methoxyphenol content. From this, it can be deduced that SDS treated biomass resulted in minimal degradation of the guaiacyl and syringyl units in lignin. On the contrary, Bio-oil from Triton X-100 treated biomass exhibited the lowest methoxyphenol derivatives and the highest phenols content. This signifies higher degradation occurs at higher temperature, which is in agreement with the positive shift observed in the Derivative Thermogravimetric (DTG) curve of Triton X-100 treated biomass (Fig. 2.3(b)).

Alkali treatment, a common and widely applied process for delignification, was one of the treatments producing oils with the lowest phenol and methoxyphenol content. Nevertheless, bio-oils obtained from alkali-treated biomass expressed an enhancement in certain guaiacyl-derived compounds such as 2-methoxy-4-methylphenol (creosol) and 2-methoxy-4-ethylphenol (4-ethylguaiacol) and eugenol (Chen et al., 2015). Similar increases in creosol and eugenol yields were observed in bio-oils obtained from H_2SO_4 treated samples. This suggests a higher reactivity of lignin S-units over lignin G-units in plant biomass with strong acid (H_2SO_4) and alkaline (NaOH) solution, consequently resulting in a relatively higher content of G-units in pretreated biomass, eventually resulting in the enhancement of guaiacyl-derived components in bio-oil. Other bio-oils obtained from H_2SO_4 treated biomass did not record any significant difference in individual or total concentrations of phenolic compounds in comparison with oils obtained from H_3PO_4 treated biomass.

The bio-oil components formed through the thermal degradation of biomass, which is in effect the pyrolysis of multiple individual components, cannot be wholly attributed to their individual degradation reactions alone but also the interaction between the components. Hosoya et al. (2009) suggested a pathway to explain the

formation of benzenediols at the expense of lignin-derived phenolic compounds with the aid of cellulose derivatives. This pathway involves the homolysis of alkoxy (-O-alkyl) links of methoxyphenol compounds, followed by the H-donation from cellulose-derived volatiles, to form benzenediols and alkyl compounds. Pyrolysis of untreated biomass yielded 2.4% v/v of benzenediols consisting of benzene-1,2-diol (catechol), 3-methoxycatechol and 2-acetylresorcinol. Bio-oils from all the treated biomass revealed a reduction in benzenediols, with a few bio-oils showing either complete absence or very low concentrations (below detectible limits) of benzenediols, which could be due to two probable reasons. The prime reason could be, as explained before, the chemical treatments resulting in the hydrolysis and degradation of lignin, which is the pre-cursor to most benzene-based compounds found in bio-oils. The other reason could be the higher thermal stability exhibited by biomass post treatment. Pyrolysis occurring at higher temperatures has shown the gas-phase degradation of catechol to form CO and acetylene. From this, it can be deduced that pretreated biomass having higher thermal stability could produce bio-oils with lower benzenediol content. The DTG curves in our earlier chapter (Fig. 2.3(b)) show a positive shift in degradation peak temperatures for biomass treated with H_2SO_4, NaOH, SDS and Triton X-100. Bio-oils from H_2SO_4 and surfactant treated biomass recorded very insignificant quantities of benzenediols: 0.37% v/v in Triton X-100 and 0.09% v/v with 1% H_2SO_4 treatment. In contrast, H_3PO_4 treated biomass exhibited a negative shift in the peak degradation temperature and the bio-oils from all H_3PO_4 treated biomass recorded the highest presence of benzenediols up to a concentration of 1.26 % v/v.

A major proportion of the aromatic composition of bio-oils is characterized by the presence of the phenolic ring. The rest is composed of components such as

alkylbenzenes (toluene, xylene, styrene) and benzene rings with various functional groups. These are classified under aromatic oxygenates and non-oxygenates based on the presence or absence of oxygen in their chemical structure. The presence of oxygenates in bio-oil is one of the primary reason which curtails its application in the field of energy generation and transportation fuel. High oxygen content in bio-oils results in lower energy density when compared with hydrocarbon fuels, thereby requiring further deoxygenation processing for application as transportation fuel (Czernik and Bridgwater, 2004). Another consequence of high oxygen content is the instability of bio-oil leading to its phase separation. Bio-oils from untreated biomass exhibited a high proportion of oxygenates to non-oxygenates. The increase in aromatic non-oxygenates as observed in oils from H_2SO_4 and H_3PO_4 treated biomass can be attributed to the variation of concentration of 1-ethyl-4-phenylbenzene ($C_{14}H_{14}$), whose reaction mechanism of formation is unknown.

The major compounds contributing to the aromatic oxygenates were 2,3-dihydro-1-benzofuran and 1,2,4-trimethoxybenzene. The bio-oils from pyrolysis of biomass with all pretreatments recorded a decrease in the aromatic oxygenates content. This drop was mainly attributed to the reduction in the concentration of 2,3-dihydro-1-benzofuran. A maximum reduction of ~ 73% in aromatics content was observed in the bio-oils from treated samples. Hu et al. (2015) also observed reduction in 2,3-dihydro-1-benzofuran content with HCl treatment and an increase in pyrolysis temperature. The improvement in thermal stability of the treated biomass, notably with NaOH treatment, observed from the DTG analysis resulted in the positive shift in pyrolysis degradation temperature. This phenomenon could account for the observed decrease in concentrations of different components of bio-oil.

4.3.4 Effect of pretreatment on biochar and non-condensable gas yield

The properties of biochar are tabulated in Table 4.1. The hydrogen to carbon (H/C) ratio in char showed a decrease with most of the treatment techniques. The increase in the H/C ratios in Triton X-100 treated samples shows the presence of thermally stable compounds such as pyridines in the char. The oxygen to carbon (O/C) ratios decreased with all pretreatment methods. The decrease in both the H/C and O/C ratios indicates the increase in the carbonaceous nature of the char which results in the improvement in char quality. This was reflected in the high calorific value of the biochars. The calorific value of the biochars varied between 27.56 and 30.55 MJ/kg, which is almost comparable with that of high-grade coal, which HHV ranges from 24.4 to 37.2 MJ/kg (Schweinfurth, 2002). Hence, biochars have enormous applications in power generation (as blending agent with coal) in thermal power plants for the production of electricity. Recent studies have also shown biochar blended with soil improved crop yields, water holding capacity of soil and acidity correction of soil, which are among numerous other benefits (Saeid and Chojnacka, 2019).

The pyrolysis of the raw untreated biomass gave a non-condensable gas yield of 42.97% w/w. The lowest gas yields were observed with H_3PO_4 treated samples. Consequently, H_3PO_4 treated samples exhibited the lowest O/C ratio (0.762). In contrast, H_2SO_4 treated samples which exhibited a higher O/C ratio of 1.245, gave the highest gas yield of 45.09% w/w. From this, we can confirm the correlation between the biomass O/C ratio and gas production during pyrolysis. However, Triton X-100 samples characterized with the highest O/C ratio produced a low gas yield. This could be attributed to the high thermal stability of the treated sample.

4.4 Conclusion

This chapter investigated the impact of pretreatment on the composition and characteristic properties of the thermal degradation products of *A. donax* biomass. Acid treatment resulting in reduction of hemicellulose (for H_2SO_4) and lignin (for H_3PO_4) exhibited a substantial increase in the furan yield with concurrent decrease in phenol and methoxyphenol derivatives. Alkali treatment was effective in reducing the oxygenate content of the biomass. The efficacy of alkaline media in biomass delignification resulted in a reduction in the production of lignin-based phenolic compounds. Among the bio-oils from treated samples, the highest phenolic (18.96% v/v) and methoxyphenol yield (39.65% v/v) was realized with surfactants Triton X-100 and SDS treatments respectively. Strong correlations were discovered between the critical properties (biochemical composition, H/C and O/C ratios) of treated samples and the quantified pyrolysis product stream (bio-oil, biochar and non-condensable gas) and their key properties. Variations in the O/C ratio had a significant influence on the non-condensable gas yield. However, the combination of all critical properties was essential in understanding the mechanisms behind possible variations. The observations from the TGA thermograms proved beneficial in providing insight into certain product formation mechanisms such as those of phenols and methoxyphenol groups. The study also revealed the formation of compounds such as benzenediols through the interaction of primary decomposition fractions of various individual lignocellulosic components. Pretreatment also improved the biochar quality by reducing the H/C and O/C ratios, thereby improving their calorific value.

References

Banks, S. W., Nowakowski, D. J., & Bridgwater, A. V. (2014). Fast pyrolysis processing of surfactant washed Miscanthus. *Fuel Processing Technology*, *128*, 94-103.

Collard, F. X., & Blin, J. (2014). A review on pyrolysis of biomass constituents: Mechanisms and composition of the products obtained from the conversion of cellulose, hemicelluloses and lignin. *Renewable and Sustainable Energy Reviews*, *38*, 594-608.

Czernik, S., & Bridgwater, A. V. (2004). Overview of applications of biomass fast pyrolysis oil. *Energy & fuels*, *18*(2), 590-598.

Dalluge, D. L., Kim, K. H., & Brown, R. C. (2017). The influence of alkali and alkaline earth metals on char and volatile aromatics from fast pyrolysis of lignin. *Journal of Analytical and Applied Pyrolysis*, *127*, 385-393.

Dalvand, K., Rubin, J., Gunukula, S., Wheeler, M. C., & Hunt, G. (2018). Economics of biofuels: Market potential of furfural and its derivatives. *Biomass and Bioenergy*, *115*, 56-63.

Dobele, G., Dizhbite, T., Rossinskaja, G., Telysheva, G., Meier, D., Radtke, S., & Faix, O. (2003). Pre-treatment of biomass with phosphoric acid prior to fast pyrolysis: a promising method for obtaining 1, 6-anhydrosaccharides in high yields. *Journal of Analytical and Applied Pyrolysis*, *68*, 197-211.

Eom, I. Y., Kim, J. Y., Kim, T. S., Lee, S. M., Choi, D., Choi, I. G., & Choi, J. W. (2012). Effect of essential inorganic metals on primary thermal degradation of lignocellulosic biomass. *Bioresource technology*, *104*, 687-694.

Fivga, A. (2012). *Comparison of the effect of pretreatment and catalysts on liquid quality from fast pyrolysis of biomass* (Doctoral dissertation, Aston University).

Hosoya, T., Kawamoto, H., & Saka, S. (2009). Solid/liquid-and vapor-phase interactions between cellulose-and lignin-derived pyrolysis products. *Journal of Analytical and Applied Pyrolysis*, *85*(1-2), 237-246.

Hu, S., Jiang, L., Wang, Y., Su, S., Sun, L., Xu, B., He, L., & Xiang, J. (2015). Effects of inherent alkali and alkaline earth metallic species on biomass pyrolysis at different temperatures. *Bioresource technology*, *192*, 23-30.

Jiang, L., Hu, S., Sun, L. S., Su, S., Xu, K., He, L. M., & Xiang, J. (2013). Influence of different demineralization treatments on physicochemical structure and thermal degradation of biomass. *Bioresource technology*, *146*, 254-260.

Meng, J., Moore, A., Tilotta, D., Kelley, S., & Park, S. (2014). Toward understanding of bio-oil aging: accelerated aging of bio-oil fractions. *ACS Sustainable Chemistry & Engineering*, *2*(8), 2011-2018.

Nakamura, T., Kawamoto, H., & Saka, S. (2008). Pyrolysis behavior of Japanese cedar wood lignin studied with various model dimers. *Journal of Analytical and Applied Pyrolysis*, *81*(2), 173-182.

Raveendran, K., Ganesh, A., & Khilar, K. C. (1995). Influence of mineral matter on biomass pyrolysis characteristics. *Fuel*, *74*(12), 1812-1822.

Saeid, A., & Chojnacka, K. (2019). Fertilizers: Need for new strategies. In Organic Farming (pp. 91-116). Woodhead Publishing.

Schweinfurth, S. P. (2002). *Coal - A Complex Natural Resource: An Overview of*

Factors Affecting Coal Quality and Use in the United States (Vol. 1143). US Department of the Interior, US Geological Survey.

Shen, D. K., Gu, S., & Bridgwater, A. V. (2010). Study on the pyrolytic behaviour of xylan-based hemicellulose using TG–FTIR and Py–GC–FTIR. *Journal of analytical and applied pyrolysis*, *87*(2), 199-206.

Staš, M., Kubička, D., Chudoba, J., & Pospíšil, M. (2014). Overview of analytical methods used for chemical characterization of pyrolysis bio-oil. *Energy & Fuels*, *28*(1), 385-402.

Stoikos, T. (1991). Upgrading of biomass pyrolysis liquids to high-value chemicals and fuel additives. In *Biomass Pyrolysis Liquids Upgrading and Utilization* (pp. 227-241). Springer, Dordrecht.

Tessarolo, N. S., dos Santos, L. R., Silva, R. S., & Azevedo, D. A. (2013). Chemical characterization of bio-oils using comprehensive two-dimensional gas chromatography with time-of-flight mass spectrometry. *Journal of chromatography A*, *1279*, 68-75

Wang, S., & Luo, Z. (2016). *Pyrolysis of biomass* (Vol. 1). Walter de Gruyter GmbH & Co KG.

Wang, X., Leng, S., Bai, J., Zhou, H., Zhong, X., Zhuang, G., & Wang, J. (2015). Role of pretreatment with acid and base on the distribution of the products obtained via lignocellulosic biomass pyrolysis. *RSC Advances*, *5*(32), 24984-24989.

Chapter 5

Impact of chemical pretreatment on the pyrolytic products of *P. juliflora* biomass

5.1 Introduction

The previous chapter investigated the effect of chemical pretreatment on the pyrolysis of low lignin content *A. donax* biomass. However, with huge variations observed in compositions of lignocellulosic biomass with different species, location, soil types and environmental conditions, undertaking identical studies with other biomass species possessing considerably varying compositional characteristics would be valuable and essential to encompass the impact of chemical pretreatment on biomass pyrolysis accurately (Lewandowski et al., 2003; Hodgson et al., 2010).

The pretreatment of *P. juliflora* biomass samples, having diverse biochemical and ash composition, helped further demonstrate the broad effects of chemical agents to a greater extent in our earlier chapter 3. Through the pyrolysis of treated *P. juliflora* samples, this chapter aims to gather additional information on the impact of biomass

pre-processing (using chemical agents) on the products generated through the thermochemical process.

5.2 Materials and methods

5.2.1 Pyrolysis of raw and treated biomass samples

Pyrolysis of each treated (acid and alkali) and untreated *P. juliflora* samples was carried out using the same semi-batch pyrolysis setup used earlier for the pyrolysis of *A. donax* samples. All instrumental conditions and procedures used in the previous chapter (with *A. donax* samples) remained the same for experiments performed with treated *P. juliflora* samples as well. 50 g of biomass sample was used for each of the pyrolysis experiments.

5.2.2 Analysis of bio-oil using GC-MS

The produced bio-oil collected in the funnels was processed and analyzed for their chemical composition using GCMS using the same procedure mentioned in the previous section 4.2.2. Slight modifications in the GC instrumentation were incorporated. The old VF-5ms column was replaced with a new VF-5ms column with the same dimensions (30 m x 0.25 mm x 0.25 µm) during the annual maintenance of the equipment. Hence, minor variations in the residence time of the bio-oil components were observed.

5.3 Results and Discussion

The quantified product streams of pyrolysis: bio-oil, biochar and non-condensable gases, with their physical properties, are tabulated in Table 5.1.

Table 5.1: Properties of product streams of pyrolysis of untreated and treated *P. juliflora* biomass

	Pyrolysis of untreated *P. juliflora*	Pyrolysis of *P. juliflora* treated with								
		1% H_2SO_4	3% H_2SO_4	5% H_2SO_4	1% H_3PO_4	3% H_3PO_4	5% H_3PO_4	1% NaOH	3% NaOH	5% NaOH
Pyrolysis yield (% w/w)										
Bio-oil	29.70	33.30	37.06	32.02	38.50	35.59	34.83	32.73	34.66	38.25
Biochar	28.30	28.77	29.49	32.06	29.77	31.91	32.57	28.46	27.49	31.06
Non-condensable gases [a]	42.00	37.93	33.45	35.92	31.73	32.5	32.6	38.81	37.85	30.69
Bio-oil properties										
pH	3.42	2.70	2.86	1.79	2.76	2.56	2.80	3.35	3.47	3.02
Density (g/cm^3)	1.10	1.06	1.06	1.06	1.08	1.07	1.06	1.04	1.04	1.04
Biochar properties										
O/C ratio	0.088	0.046	0.023	0.025	0.052	0.043	0.032	0.027	0.029	0.027
H/C ratio	0.013	0.019	0.013	0.015	0.020	0.017	0.024	0.022	0.017	0.018

[a] by difference

5.3.1 Effect of pretreatment on the overall yield of pyrolysis products

The pyrolysis of *P. juliflora* yielded a bio-oil yield of 29.7% w/w. The bio-oil generation with all the chemically (acid and alkali) pretreated samples increased with yields varying between 32.02 and 38.50%. The highest bio-oil yields of 38.50% and 38.25% w/w were exhibited by biomass samples treated with 1% H_3PO_4 and 5% NaOH. Increase in the pretreating acid and alkali concentrations demonstrated varying increase and decrease trends in quantitative bio-oil yield. With acid treatment, an increase in the concentration of treating media initially resulted in higher bio-oil yield followed by a drop in the yield. The peak bio-oil yields were observed with 3% H_2SO_4 and 1% H_3PO_4 treated samples. However, with NaOH treated biomass, the increase in concentration of treating media resulted in a constant increase in bio-oil yield, with 5% NaOH treated samples giving higher bio-oil yield than 1 and 3% NaOH treated samples. The increasing order of bio-oil yield from untreated and treated biomass samples was observed to be untreated < H_2SO_4 < NaOH < H_3PO_4. The order was much similar to the order observed with the other biomass (*A. donax*) species. However, the pretreatment induced enhancement in liquid production was much lower than previously observed with *A. donax* biomass, which recorded a maximum increase of up to 49.3%. The characteristic higher fraction of lignin (20.2%) in *P. juliflora*, whose thermal degradation products contribute to a major fraction (>70%) of the bio-oil, could account for the observed disparity in the increase in bio-oil production. As lignin contributes to biochar yield more than other lignocellulosic components (cellulose and hemicellulose), an increase in its fraction in biomass will naturally result in increased biochar yield causing a drop in the bio-oil yield (Raveendran et al., 1995). The bio-oil produced from the raw untreated *P. juliflora* biomass was found to have a pH of 3.42 and a density of 1.10 g/cm^3. Bio-oils from acid-treated biomass exhibited pH values

varying from 2.56 to 2.86. The removal of alkaline earth and base metals facilitated by the acid treatment could have aided in increasing the acidity of bio-oil, as was also observed with *A. donax* treated samples. However, the shift in pH of bio-oils with alkali treatment was contrary to earlier observations. The bio-oils from alkali-treated samples had a pH varying between 3.02 and 3.47, which were higher compared to acid-treated samples. The results were, however, in agreement with the study performed by Hassan et al. (2009). They attributed it to the removal of certain acidic and alkaline groups in biomass by treating acid and alkali solutions. The removal of acidic groups of hemicellulose (uronic acid and acetyl substitutions) with alkali treatment could have resulted in increasing the pH of bio-oil as observed with 3% NaOH treated samples. Bio-oils produced from the treated samples exhibited a marginal reduction in density similar to the effect observed with *A. donax* biomass. The density was found to vary between 1.04 and 1.08 g/cm^{3,} with bio-oils from alkali-treated samples having the lowest density followed by acid-treated biomass bio-oils.

Pyrolysis of lignocellulosic biomass produces carbon-rich biochar, which includes the inorganic material (ash) of the biomass, as one of the by-products. The raw *P. juliflora* biomass gave a char yield of 28.30% w/w, which was much higher than what was observed with *A. donax* biomass (25.68% w/w). The considerably lower fraction of metallic ash in *P. juliflora*, which contributes to the biochar yield, shows the predominance of residues of the pyrolysis of major lignocellulosic components (cellulose, hemicellulose and lignin). The elemental analysis also showed the char to be of high quality with relatively higher carbon content than the char obtained with the pyrolysis of *A. donax* biomass. This was reflected with significantly lower O/C and H/C content (0.088% and 0.013% respectively) in comparison to those of *A. donax* biomass

(0.109% and 0.018% respectively). All the chemical pretreatment techniques resulted in an increasing the char yield except 3% NaOH treatment. All acid treatments yielded higher char yields with an increase in concentration. Among the chars produced from acid-treated samples, H_3PO_4 gave higher yields than H_2SO_4. The biochar yield in increasing order is untreated < NaOH < H_2SO_4 < H_3PO_4.

The gas yield, which primarily consists of non-condensable C1-C4 compounds and other gases such as H_2, decreased with all pretreatments. The decrease in the non-condensable gas yield ranged from 7.6% with 1% NaOH treatment to 26.9% with 5% NaOH treatment. The effect of chemical pretreatment on the yields of each of the pyrolysis products viz., bio-oil, biochar and non-condensable gas streams are explained in detail in the upcoming sections.

The GC spectra of the bio-oil obtained from untreated *P. juliflora* biomass sample is shown in Fig. 5.1. The identification and quantification of the peak and their areas were performed as mentioned in the previous chapter. The key for the notations indicating the 43 identified peaks is given in Table 5.2. The GC spectra and their identified peaks for the bio-oils from treated samples are included in Annexure C. Table 5.3 shows the comparison of the relative concentration of the compounds identified in each of the bio-oils. However, the table includes only the bio-oils obtained by the untreated and one of each of the acid and alkali-treated biomass samples. The complete table is nevertheless included in Annexure D.

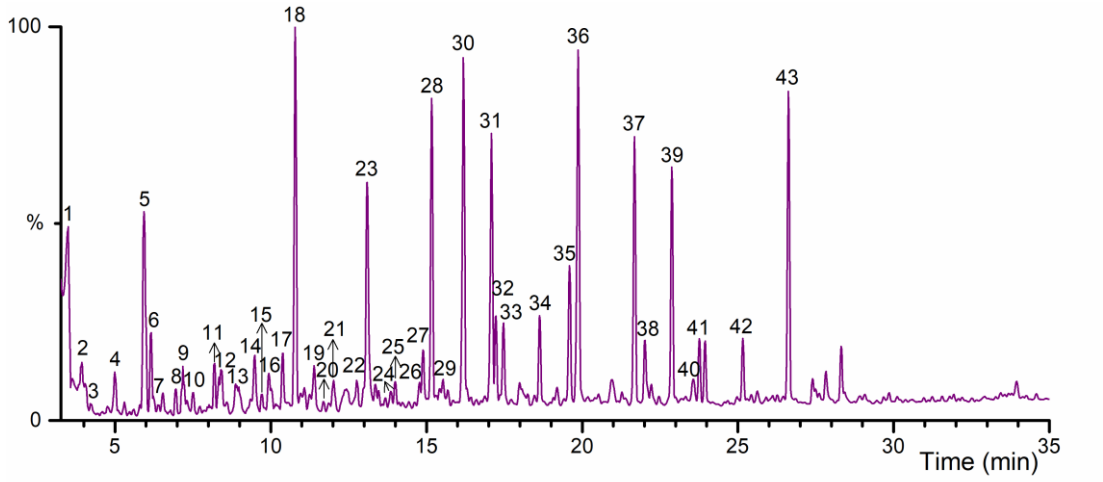

Figure 5.1: Chromatogram of bio-oil from pyrolysis of raw untreated *P. juliflora* by GC-MS analysis

Table 5.2: Identified chemicals from pyrolysis of raw untreated *P. juliflora*

1: acetic acid
2: (E)-pent-3-en-2-one / methyl propenyl ketone
3: 2,5-dimethylfuran
4: toluene / methylbenzene
5: furan-2-carbaldehyde / furfural
6: furan-2-ylmethanol / 2-furanmethanol
7: 1,3-xylene / m-xylene / 1,3-dimethylbenxene
8: styrene / vinylbenzene
9: 2-methylcyclopent-2-en-1-one
10: cyclohexanone / cyclohexyl ketone
11: 5-methylfuran-2-carbaldehyde / 5-methylfurfural
12: phenol
13: 2,2-diethyl-3-methyl-1,3-oxazolidine
14: 2-hydroxy-3-methylcyclopent-2-en-1-one / cyclotene
15: 2,3-dimethylcyclopent-2-en-1-one
16: 2-methylphenol / o-cresol
17: 4-methylphenol / p-cresol
18: 2-methoxyphenol / guaiacol
19: 3-ethyl-2-hydroxycyclopent-2-en-1-one
20: 1-methyl-2,3-dihydro-1H-indene / 1-methylindan
21: 3,5-dimethylphenol
22: 4-ethylbenzene-1,3-diol / 4-ethylresorcinol
23: 2-methoxy-4-methylphenol / 4-methylguaiacol / creosol
24: 2,3-dihydro-1-benzofuran / coumaran
25: 1,2-dimethoxy-4-methylbenzene / 3,4-dimethoxytoluene
26: 3-methylbenzene-1,2-diol / 3-methylcatechol / 3-methyl-pyrocatechol
27: 3-methoxybenzene-1,2-diol / 3-methoxycatechol
28: 4-ethyl-2-methoxyphenol / 4-ethylguaiacol
29: 1-(2,6-dihydroxyphenyl)ethanone / 2-acetylresorcinol
30: 1-(2-hydroxy-5-methylphenyl)ethanone / 2-hydroxy-5-methylacetophenone / o-acetyl-p-cresol
31: 2,6-dimethoxyphenol / syringol
32: 2-methoxy-4-prop-2-enylphenol / 4-allyl-2-methoxyphenol / eugenol
33: 1-(2,5-dihydroxyphenyl)propan-1-one
34: 2-methoxy-6-prop-2-enylphenol / 2-Allyl-6-methoxyphenol
35: 1,2,4-trimethoxybenzene

36: 2-methoxy-4-(prop-1-enyl)-phenol / trans-isoeugenol
37: 1-ethyl-4-phenylbenzene / 4-ethylbiphenyl
38: 1-(4-hydroxy-3-methoxyphenyl)propan-2-one / 4-hydroxy-3-methoxyphenyl acetone
39: 1-(3,4-dimethoxyphenyl)ethanone
40, 42, 43: 2,6-dimethoxy-4-prop-2-enylphenol / 4-allylsyringol
41: 1-phenylpropylbenzene / 1,1-diphenylpropane

Table 5.3: Bio-oil product distribution from pyrolysis of untreated and treated *P. juliflora*

Compound name	Yield (% v/v)			
	Untreated	5% H_2SO_4	5% H_3PO_4	3% NaOH
Carboxylic acids				
acetic acid	6.39	-	-	-
	6.39	-	-	-
Ketones				
3-penten-2-one	0.89	-	-	-
2-methyl-2-cyclopenten-1-one	0.99	1.63	1.79	1.32
1-cyclohexanone	0.73	0.38	0.61	0.27
2-hydroxy-3-methyl-2-cyclopenten-1-one	1.57	0.62	0.83	0.99
2,3-dimethyl-2-cyclopenten-1-one	0.32	-	-	-
3-ethyl-2-hydroxy-2-cyclopenten-1-one	1.00	1.40	0.70	0.56
	5.49	**4.03**	**3.93**	**3.13**
Others				
2,2-diethyl-3-methyl-oxazolidine	0.56	0.46	1.16	1.96
	0.56	**0.46**	**1.16**	**1.96**
Furans				
2,5-dimethylfuran	0.15	-	-	-
furfural	4.82	-	-	-
2-furanmethanol	1.48	-	-	-
5-methyl-2-furaldehyde	0.78	3.61	4.55	0.15
	7.24	**3.61**	**4.55**	**0.15**
Phenols				
phenol	0.86	2.36	1.81	2.11
2-methylphenol (o-cresol)	0.66	1.22	0.72	0.98
4-methylphenol (p-cresol)	0.85	1.95	1.42	1.53
3,5-dimethylphenol	0.59	1.58	0.74	1.10
2-ethylphenol	-	0.98	0.66	1.40
1-(2-hydroxy-5-methylphenyl)ethanone	6.70	1.55	3.52	7.00
1-(2,5-dihydroxyphenyl)propan-1-one	1.63	0.95	1.42	2.37
	11.29	**10.60**	**10.27**	**16.49**
Benzenediols				
3-methoxybenzene-1,2-diol	1.08	-	-	-
1-(2,6-dihydroxyphenyl)ethanone	0.16	-	-	-

4-ethylbenzene-1,3-diol	0.43	-	-	-
3-methylbenzene-1,2-diol	0.41	-	-	-
	2.08	**-**	**-**	**-**
Methoxyphenol derivatives				
guaiacol	6.81	7.02	6.26	10.80
creosol	5.34	12.66	10.03	6.39
4-ethyl-2-methoxyphenol	6.44	5.48	6.57	9.63
syringol	5.06	3.37	2.49	6.42
eugenol	1.49	1.02	1.04	0.91
2-allyl-6-methoxyphenol	1.49	0.30	0.75	0.82
trans-isoeugenol	6.93	1.41	5.34	4.39
4-propylguaiacol	-	4.36	4.18	-
1-(4-hydroxy-3-methoxyphenyl)propan-2-one	1.51	6.83	5.49	4.19
1-(3,4-dimethoxyphenyl)ethanone	4.18	0.51	1.21	3.27
4-allylsyringol	7.46	1.51	4.50	4.12
	46.72	**44.46**	**47.86**	**50.93**
Aromatic non-oxygenates				
toluene	0.93	-	-	-
1,3-xylene	0.26	-	-	-
styrene	0.46	-	-	-
1-methyl-2,3-dihydro-1*H*-indene	0.17	-	-	-
1-phenylpropylbenzene	1.06	0.53	0.80	1.27
1-ethyl-4-phenylbenzene	4.90	1.90	2.81	4.45
	7.79	**2.44**	**3.61**	**5.72**
Aromatic oxygenates				
2,3-dihydro-1-benzofuran	0.30	1.63	1.10	0.23
1,2-dimethoxy-4-methylbenzene	0.39	-	-	-
1,2,4-trimethoxybenzene	2.46	4.08	4.54	3.19
	3.14	**5.72**	**5.65**	**3.42**

5.3.2 Effect of pretreatment on carbohydrate degradation products

The pyrolysis of the carbohydrate fraction of *P. juliflora* biomass resulted in the formation of compounds, which accounted for 19.7% of the 90.7% identified peak areas of the GC spectra.

The primary products of the thermal degradation of carbohydrates include carboxylic acids and furans. The pyrolysis of raw untreated *P. juliflora* gave a higher carboxylic acid (6.39% v/v) and lower furan yield (7.24% v/v). The GCMS analysis of the bio-oils from the treated samples and subsequent spectral analysis of its peaks could

not detect the presence of prominently occurring compounds such as acetic acid and furfural. The replacement of the column could have caused the merging of these peaks with the solvent peak as furfural and acetic acid generally get eluted immediately after the solvent. Nevertheless, the other detected furan peaks and other parameters such as the pH provide essential information to understand the impact of chemical treatment on pyrolysis.

Acid treatment resulted in an increase in the yield of 5-methyl-2-furaldehyde, formed through the cracking of primary thermal degradation product 5-HMF, as observed with *A. donax* biomass (Collard and Blin, 2014). The change in pH of bio-oils from acid-treated samples followed the similar trends observed with *A. donax* biomass. On the other hand, bio-oil from alkali-treated samples exhibited a strong deviation from the observed trend with increased pH and a decrease in 5-methyl-2-furaldehyde yield. To gain insight into the contrasting observations, a comparative analysis of the kinetics of the thermal degradation of alkali-treated *A. donax* and *P. juliflora* samples in sections 2.3.5 and 3.3.5 was undertaken. The analysis of the carbohydrate degradation regimes of the TGA curves revealed vast differences. *A. donax* sample was characterized with high carbohydrate degradation temperature (351.9 ℃), signifying improved thermal stability with the sharp degradation occurring within a narrow temperature window. The degradation with *P. juliflora* biomass, on the other hand, occurred at a much lower temperature (328 ℃) over a much wider temperature range. This resulted in the significantly rapid carbohydrate thermal degradation of alkali-treated *A. donax* (20.78 %/min) over *P. juliflora* (10.1 %/min). The significant changes in the degradation kinetics suggest major variations in the pyrolytic mechanisms resulting in significant changes in the bio-oil chemical composition and characteristic properties. However, the

precise changes in biomass properties or degradation mechanism, which resulted in the significant changes in properties could not be ascertained due to the complex nature of biomass and their pyrolytic degradation reactions.

5.3.3 Effect of pretreatment on lignin degradation products

Pyrolysis of the high lignin content raw *P. juliflora* biomass produced bio-oil composed of around 71% v/v from lignin-derived compounds. Likewise, lignin-derived composed compounds also contributed to around 73% v/v of bio-oil from raw *A. donax* biomass. However, a major fraction (46.72% v/v) of *P. juliflora* bio-oil was composed of methoxyphenol derivatives, while hydroxyphenol yield was much lower at around 11.29% v/v. This signifies significant guaiacol and syringyl type monomers in the lignin structure of the lignocellulosic biomass. On the other hand, *A. donax* bio-oil was composed of 31.31% v/v methoxyphenol derivatives and 21.45% v/v phenol derivatives, suggesting a higher fraction of hydroxyphenol type monomer units.

The comparative quantitative plot of the various lignin-derived bio-oil compounds categorized under sub-categories viz. phenols, methoxyphenol derivatives, benzenediols, aromatic non-oxygenates and aromatic oxygenates is presented in Fig. 5.2 below.

Preliminary observation of the effect of chemical treatment on the variation in yields of *P. juliflora* lignin-derived compounds revealed its limited impact in comparison to the observed impact on *A. donax* biomass. The chemical treatment on *A. donax* biomass resulted in a reduction in lignin fraction and a concurrent reduction in yields of phenols and methoxyphenol yields in bio-oils.

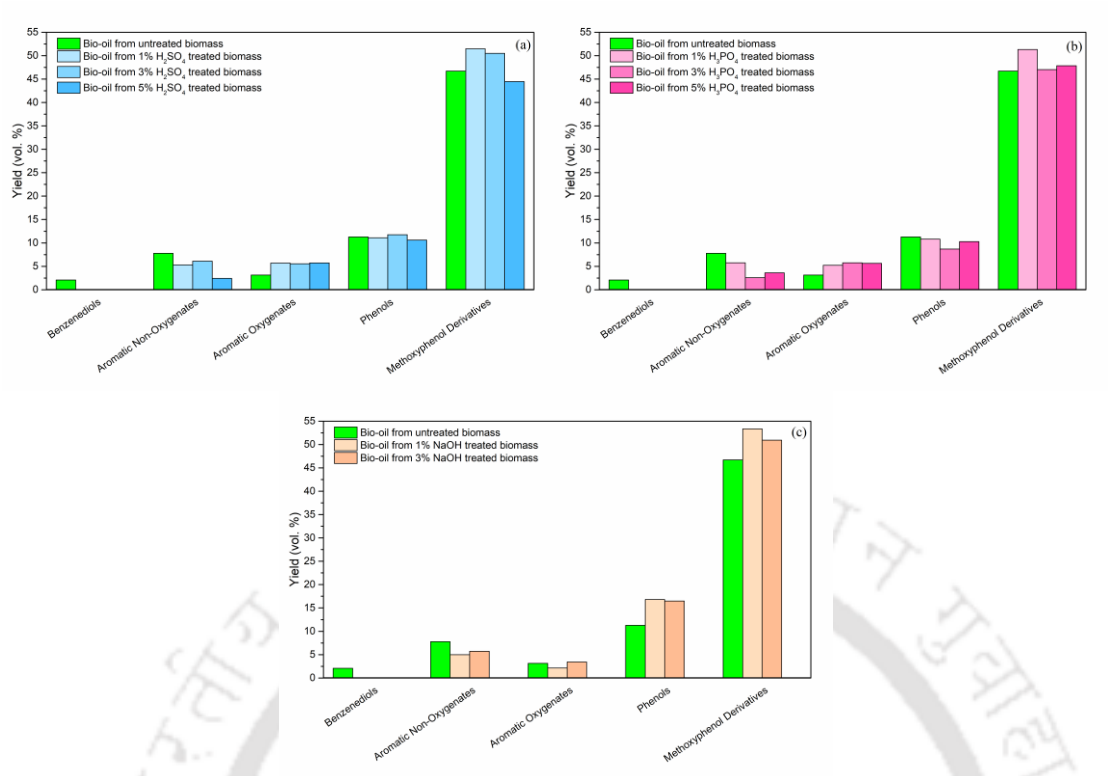

Figure 5.2: Comparison of the lignin-derived chemical composition of bio-oils obtained from (a) H_2SO_4 treated biomass, (b) H_3PO_4 treated biomass and (c) NaOH treated biomass.

Pyrolysis of untreated biomass gave a phenol yield of 11.29% v/v. Acid treatment did not lead to substantial changes with H_2SO_4 and H_3PO_4 treated samples yielding 10.60-11.75% v/v and 8.68-10.82% v/v respectively. The severe effect of acids on hemicellulose compared to lignin observed with *P. juliflora* biomass resulted in an overall increase in lignin in the resulting samples up to 33.6% w/w. This significant increase is likely to have averted the fall in phenol yield observed previously with *A. donax* samples. Alkali treated samples on pyrolysis, however, gave a much higher phenolic yield of 16.49-16.81% v/v. The compounds 1-(2-hydroxy-5-methylphenyl)ethanone and phenol contributed significantly to the observed increase. Wang et al. (2019) showed substantial generation of 1-(2-hydroxy-5-methylphenyl)ethanone from lignin at low degradation temperatures, which decreased with an increase in temperature. TGA analysis of alkali-treated *A. donax* and *P. juliflora*

samples showed the latter to exhibit a lower T_i temperature (181.5 °C for *P. juliflora*, 243.4 °C for *A. donax*), which corresponds to the initiation of lignin degradation (Table 2.3 and 3.3). Thus the low T_i temperature coupled with the comparatively higher lignin fraction in *P. juliflora* samples could potentially have caused the enhanced phenolic yield in alkali-treated samples.

The methoxyphenol derivative fraction of bio-oils, which contributed to 46.72% v/v of total peak area, sustained a 1-14% variation with chemical pretreatment. The lowest variations were observed with acid treatment with overall yields of 44.46-51.46% v/v with H_2SO_4 treatment and 47.04-51.31% v/v with H_3PO_4 treatment. Alkali treatment gave a marginally higher yield of 50.93-53.36% v/v. The changes in the individual components, however, exhibited significant positive and negative shifts in yield. An increase in the guaiacyl (L-G) compounds: guaiacol, creosol, 4-ethyl-2-methoxyphenol and 1-(4-hydroxy-3-methoxyphenyl)propan-2-one; and a decrease in syringyl (L-S) compounds: syringol and 4-allylsyringol were observed. Similar results observed previously with *A. donax* biomass was attributed to the higher reactivity of syringyl lignin compared to guaiacyl lignin, resulting in its hydrolysis with chemical treatment (Chen et al., 2015). Another interesting observation was the more significant increase in the fundamental low MW bio-oil compounds of the L-G and L-S groups, viz. guaiacol and syringol, over the other compounds with alkali treatment. Alkali treatment has shown to have a lower demineralization effect in comparison to acid treatments (Zafar et al., 2020). The residual ash content, consisting of alkali and alkaline earth metals, has also shown potential towards the generation of low MW compounds such as guaiacol and syringol (Nowakowski et al., 2007). These factors could have contributed to the enhanced presence of these compounds in the bio-oils.

Benzenediols, which contribute to a small fraction of 2.08% v/v in the untreated *P. juliflora* bio-oils, were either not present or below detectible limits in the treated biomass bio-oils.

The lignin derivatives which do not fall under the methoxyphenol phenol, phenols or benzenediols were categorized into aromatic oxygenates and aromatic non-oxygenates. *P. juliflora* biomass yielded comparatively lower aromatic oxygenates (3.14% v/v) compared to *A. donax* biomass, which contributed to 14.39% v/v of the peak area of bio-oil. This was attributed to the production of 2,3-dihydro-1-benzofuran in very low concentrations compared to *A. donax* biomass, which could have occurred to the significant differences in their lignin structure. With acid treatment, an increase in its concentration was observed, which seems contrary to the observation with *A. donax* and Hu et al. (2015). The possible justification could be the relative concentration of lignin in the treated biomass samples: acid treatment of *A. donax* biomass caused a relative decrease in its lignin content while it resulted in a relative increase with *P. juliflora* samples. The reduction of lignin with alkali treatment, resulting in the generation of low concentrations of 2,3-dihydro-1-benzofuran, supports the justification of its relation to the concentration of lignin in the precursor material. The other contributor was 1,2,4-trimethoxybenzene, whose variation trend with treated biomass matched the pattern of 2,3-dihydro-1-benzofuran. The aromatic non-oxygenates constituted 7.79% v/v in the untreated *P. juliflora* bio-oil. Bio-oils obtained from all the chemically treated samples exhibited a decrease in non-oxygenates fraction, which was partially due to the absence of some compounds such as toluene, styrene and 1,3-xylene in the treated sample bio-oils.

5.3.4 Effect of pretreatment on biochar and non-condensable gas yields

The pyrolysis of untreated *P. juliflora*, in addition to the bio-oil, also yielded 28.3% w/w biochar and 42% w/w non-condensable gases. The characteristic high lignin fraction of the biomass resulted in a marginally higher solid biochar yield at the expense of the liquid bio-oil yield. The biochar also had a low O/C ratio of 0.088, which is comparatively lower than the *A. donax* biochar (0.109). The H/C ratio (0.013) was also found to be lower, which indicated the biochar to be highly carbonaceous. The variation trends of biochar O/C ratio were similar with both biomass species in the following decreasing order: untreated < H_3PO_4 < NaOH < H_2SO_4. The variation in the biochar yield was minimal and varying between 27.49% w/w and 32.57% w/w. The TGA char yield showed previously in Table 3.3 also predicted similar marginal variations in the yield as opposed to the *A. donax* biomass, which exhibited a significant shift from biochar to bio-oil. The char yields with the highest concentrations (5% v/v) of acid treatment gave higher char yield than the untreated biomass. The high fraction of lignin in the treated biomass samples is presumed to be the likely reason for this enhanced yield.

The highest (42% w/w) and lowest (30.69% w/w) non-condensable gas by-production was from untreated and 5% NaOH treated biomass respectively. Although 5% NaOH treated sample gave the lowest gas yield, the average gas yield from H_3PO_4 treated samples (32.28% w/w) was much lower than that of NaOH (35.78% w/w) as observed previously with *A. donax* treated samples.

5.4 Conclusion

This chapter studied the effect of chemical pretreatment on biomass pyrolysis by comparing the analytical properties of bio-oil and biochar obtained from chemically treated *P. juliflora* samples with those from chemically treated *A. donax* samples. A comprehensive overview of the impacts on pyrolytic products effected through the various chemical (acid and alkali) treatments on the precursor substrate was acquired. An appreciable number of the variation in chemical and physical properties of bio-oil and biochar were linked to the high lignin followed by the low hemicellulose fractions in the native *P. juliflora* species. The observed shift in bio-oil chemical composition with acid treatment was comparable and analogous to the variations noted previously with *A. donax* biomass. Substantial differences between the degradation kinetics of alkali-treated *A. donax* and *P. juliflora* species, due to possible variations in the lignin and metallic ash, caused varying trends of bio-oil properties and composition. Contrary to *A. donax* pyrolysis, biochar yields increased with most pretreatment techniques attributed to the high char contributing lignin in the native biomass. The biochar from *P. juliflora* treated samples had much lower O/C ratios than *A. donax* samples, indicating their high carbonaceous nature.

References

Collard, F. X., & Blin, J. (2014). A review on pyrolysis of biomass constituents: Mechanisms and composition of the products obtained from the conversion of cellulose, hemicelluloses and lignin. *Renewable and Sustainable Energy Reviews*, *38*, 594-608.

El-barbary, M. H., Steele, P. H., & Ingram, L. (2009). Characterization of fast pyrolysis bio-oils produced from pretreated pine wood. *Applied biochemistry and biotechnology*, *154*(1-3), 3-13.

Hodgson, E. M., Lister, S. J., Bridgwater, A. V., Clifton-Brown, J., & Donnison, I. S. (2010). Genotypic and environmentally derived variation in the cell wall composition of Miscanthus in relation to its use as a biomass feedstock. *Biomass and Bioenergy*, *34*(5), 652-660.

Hu, S., Jiang, L., Wang, Y., Su, S., Sun, L., Xu, B., He, L., & Xiang, J. (2015). Effects of inherent alkali and alkaline earth metallic species on biomass pyrolysis at different temperatures. *Bioresource technology*, *192*, 23-30.

Lewandowski, I., Clifton-Brown, J. C., Andersson, B., Basch, G., Christian, D. G., Jørgensen, U., Jones, M. B., Riche, A. B., Schwarz, K. U., Tayebi, K., & Teixeira, F. (2003). Environment and harvest time affects the combustion qualities of Miscanthus genotypes. *Agronomy Journal*, *95*(5), 1274-1280.

Nowakowski, D. J., Jones, J. M., Brydson, R. M., & Ross, A. B. (2007). Potassium catalysis in the pyrolysis behaviour of short rotation willow coppice. *Fuel*, *86*(15), 2389-2402.

Raveendran, K., Ganesh, A., & Khilar, K. C. (1995). Influence of mineral matter on

biomass pyrolysis characteristics. *Fuel, 74*(12), 1812-1822.

Wang, L., Li, J., Chen, Y., Yang, H., Shao, J., Zhang, X., Yu, X., & Chen, H. (2019). Investigation of the pyrolysis characteristics of guaiacol lignin using combined Py-GC× GC/TOF-MS and in-situ FTIR. *Fuel, 251*, 496-505.

Zafar, M. H., Kazmi, M., Tabish, A. N., Ali, C. H., Gohar, F., & Rafique, M. U. (2019). An investigation on the impact of demineralization of lignocellulosic corncob biomass using leaching agents for its utilization in industrial boilers. *Biomass Conversion and Biorefinery*, 1-7.

Chapter 6

Role of AAEM on the pyrolysis of *A. donax* and *P. juliflora* biomass

6.1 Introduction

In addition to primary lignocellulosic components such as polysaccharides (cellulose and hemicellulose) and lignin, minerals such as sodium, magnesium, potassium, manganese, copper, calcium and iron are also present in plant biomass. The mineral content in biomass ranges from as low as 0.2-3.5% in wood-based biomass to 0.7-23.5% in agricultural waste (Dhyani and Bhaskar, 2018). These minerals occurring in compound form are essential during the growth phase of plants. These minerals, which do not volatilize in the temperature regimes generally employed for pyrolysis, significantly affects the pyrolysis process and are also found to disrupt product formation equilibriums. Hu et al. (2015) reported that a simple washing of rice husk with water and HCl (5%) at 25 ℃ caused alkali earth metals demineralization varying between 84 and 99.7%, which effected a tremendous increase in levoglucosan yield from 0.7% up to 41% in bio-oil and significantly increased the bio-oil yield during

pyrolysis. Another interesting study by Mourant et al. (2011) showed that AAEMs occur in two forms: water-soluble and acid-soluble (but water-insoluble), with the latter playing a significant role in suppressing the production of anhydrosugars. The study also reported a decrease in water in bio-oil and light organic compounds with pyrolysis of acid-treated *Eucalyptus loxopheba*. Further studies of the effect of AAEMs on thermal decomposition of individual components, viz. cellulose, hemicellulose and lignin, have shown to affect the pyrolysis temperature, catalyze the breakdown of lignin skeletal structure, modify char and non-condensable gas yields (Shimada et al., 2008; Mahadevan et al., 2016; Dalluge et al., 2017).

The typical approach of researchers to discern their effect was by comparing the pyrolysis products of demineralized and AAEM-infused demineralized biomass. Nevertheless, the standard approach to obtain demineralized biomass through water/acid wash has also been recorded to cause degradation of other lignocellulosic components viz., cellulose and hemicellulose. Based on the distinctive ash composition of *P. juliflora*, an alternate approach to explore the impact of AAEM on biomass pyrolysis has been undertaken in this study. Through this approach, the impact due to changes in lignocellulosic biomass during water/acid washing is eliminated. The stark variation in AAEM concentrations of *A. donax* and *P. juliflora* species was employed to understand their effect on lignocellulosic biomass pyrolysis better.

6.2 Materials and methods

6.2.1 Impregnation of AAEM salts into biomass matrix

Alkali and alkaline earth metals in the form of acetates, chlorides and oxides were infused into biomass samples. Acetate and chloride salts of potassium

(CH_3COOK, KCl) and the chloride and oxide salts of magnesium ($MgCl_2$, MgO) were used in the study. 2 wt% of the salts were individually mixed with the oven-dried *P. juliflora* and *A. donax* biomass into a homogenous mixture. This dry impregnation approach was adopted instead of the conventional technique of addition of salts in aqueous form. The AAEM doped biomass samples were labelled as AD-KAc, AD-KCl, AD-MgO, AD-MgCl, PJ-KAc, PJ-KCl, PJ-MgO and PJ-MgCl. The raw biomass was labelled as AD(control) and PJ(control).

6.2.2 Pyrolysis of salt impregnated biomass

The pyrolysis experimental setup used for pyrolysis of AAM laden biomass samples has been discussed in detail in section 4.2.1. Equal amounts (75 g) of each of the prepared biomass samples were used for the pyrolysis. After loading each of the samples, the reactor was heated to 600 ℃ and held isothermally for 2 h before the cooling process. The reactor was opened to recover the biochar only after the temperature reached below 80 ℃ to prevent sudden ignition.

6.2.3 Analysis of bio-oil using GCMS

The same procedure employed in bio-oil analysis mentioned in earlier section 4.2.3 was used.

6.3 Results and discussion

The metal makeup of ash components of *P. juliflora* and *A. donax* revealed the presence of minor elements such as Cr, Mn, Co, Ni, Cu, Zn, As, Mo, Cd and Pb with cumulative content of 0.002 and 0.009 wt% respectively. The AAEM, which falls under the major elements, collectively contributed to 0.81 and 1.4 wt% of the *P. juliflora* and

A. donax biomass dry weight. The decreasing order of the composition of AAEMs in *P. juliflora* was Ca (0.55 wt%) > K (0.18 wt%) > Na (0.07 wt%) > Mg (0.009 wt%). Potassium (K), a mineral required for multiple essential plant processes, is generally found in higher concentrations in wood fuels (0.09–0.54%) and agricultural residues (0.56–3.24%) (Miles et al., 1995; Masiá et al., 2007). Potassium content in *P. juliflora* at 0.18 wt% lies close to the lower end of the generally observed range. Significantly low Mg content, well below the generally observed range, was also recorded. The Mg content generally varies between 0.08 and 0.33 wt% in agricultural residue and between 0.09 and 0.14 wt% in wood fuels. On the other hand, *A. donax* samples exhibited significantly different composition. The decreasing order of the composition of AAEMs in *A. donax* was K (1.28 wt%) > Mg (0.06 wt%) > Ca (0.06 wt%) > Na (<0.0001 wt%). *A. donax* showed significantly high K content well above the generally observed range and Mg content was close to the lower end of the generally observed range.

The conventional technique for studying the effect of AAEM on biomass pyrolysis involves three steps: (1) demineralization of biomass, (2) infusion of demineralized biomass with various AAEM salts and (3) pyrolysis of AAEM infused biomass samples. The demineralization of biomass is generally carried out with mild acids or dilute strong acids. Secondly, the common approach for infusing AAEM salts into the biomass matrix involves soaking the biomass in the aqueous salt solution for a set period following by drying of the salt-laden biomass slurry in an oven. These demineralization and infusion techniques would not only introduce the target AAEM to the biomass but might also cause variations or degradation of the biochemical component structure. This was evident with the analysis of Jiang et al. (2013), who

observed significant variation in thermal characteristics even with water-washed rice straw. The thermogravimetric curves of water washed rice straw were similar to those of mild acid (acetic and phosphoric acid) treated rice straw, signifying the impact of degradation of biomass. Hence the conventional technique for demineralization, which involved either water or acid washing, is likely to cause significant compositional and structural variation. As a result, the overall changes observed with pyrolysis and its products, which will likely be a blend of the effects of AAEM salts and lignocellulosic degradation, potentially interferes in efforts to identify mineral effects on pyrolysis specifically. Hence a modification in the techniques employed is essential. The relatively lower content of K and 10-fold lower content of Mg compared to the generally observed range in the native *P. juliflora* biomass has special significance for this study as it reduces the inherent catalytic effect on the pyrolysis and eliminates the need for its demineralization. Additionally, dry impregnation approach was used in this study, as mentioned in earlier section 6.2.1, which ensures the observable changes are due to AAEM salt addition. Fig. 6.1 shows the concentrations of K and Mg in AAEM infused biomass samples.

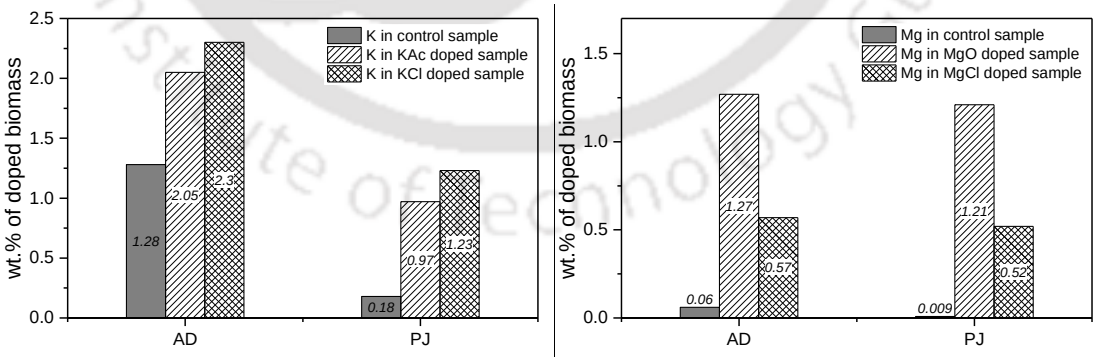

Figure 6.1: Concentration of K and Mg in control and AAEM infused biomass samples

The pyrolysis of salt infused *P. juliflora* samples and the results of the analysis the resultant pyrolysis products (bio-oil and biochar) were primarily used to discern the effect of AAEM salts in biomass pyrolysis.

The quantitative analysis of the pyrolytic product of the raw and AAEM doped biomass samples is given in Fig. 6.2.

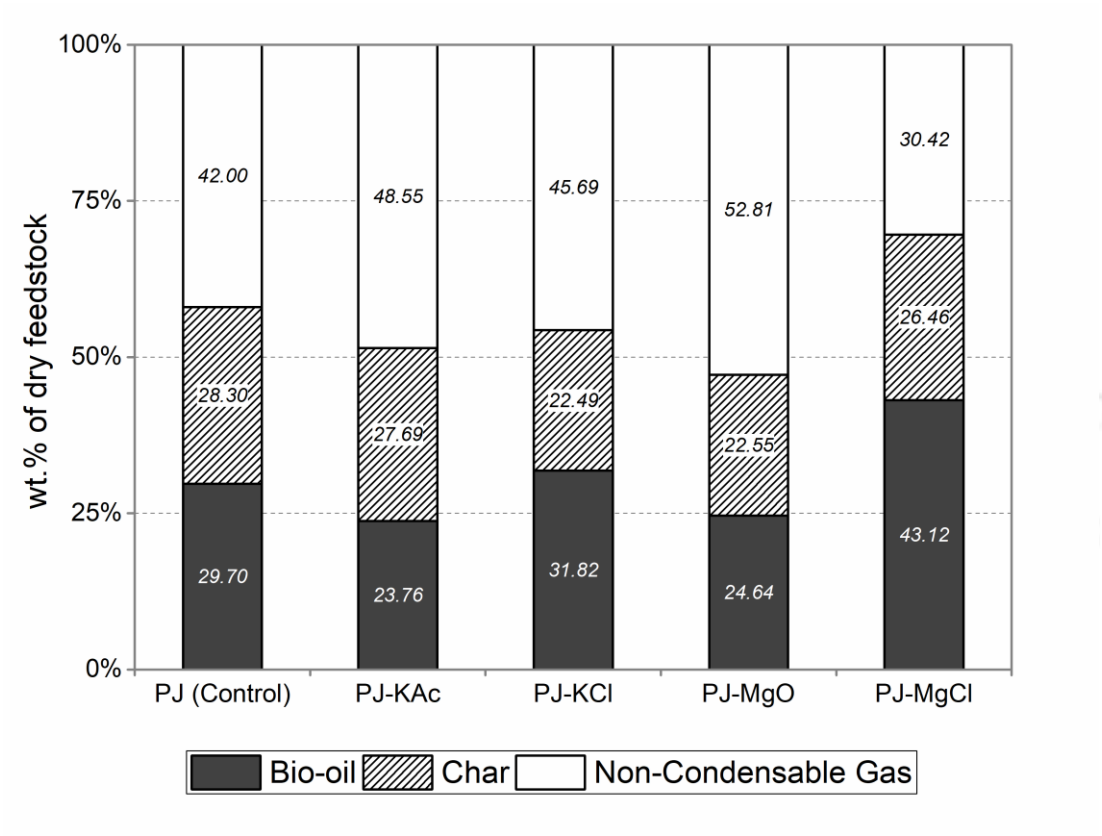

(a)

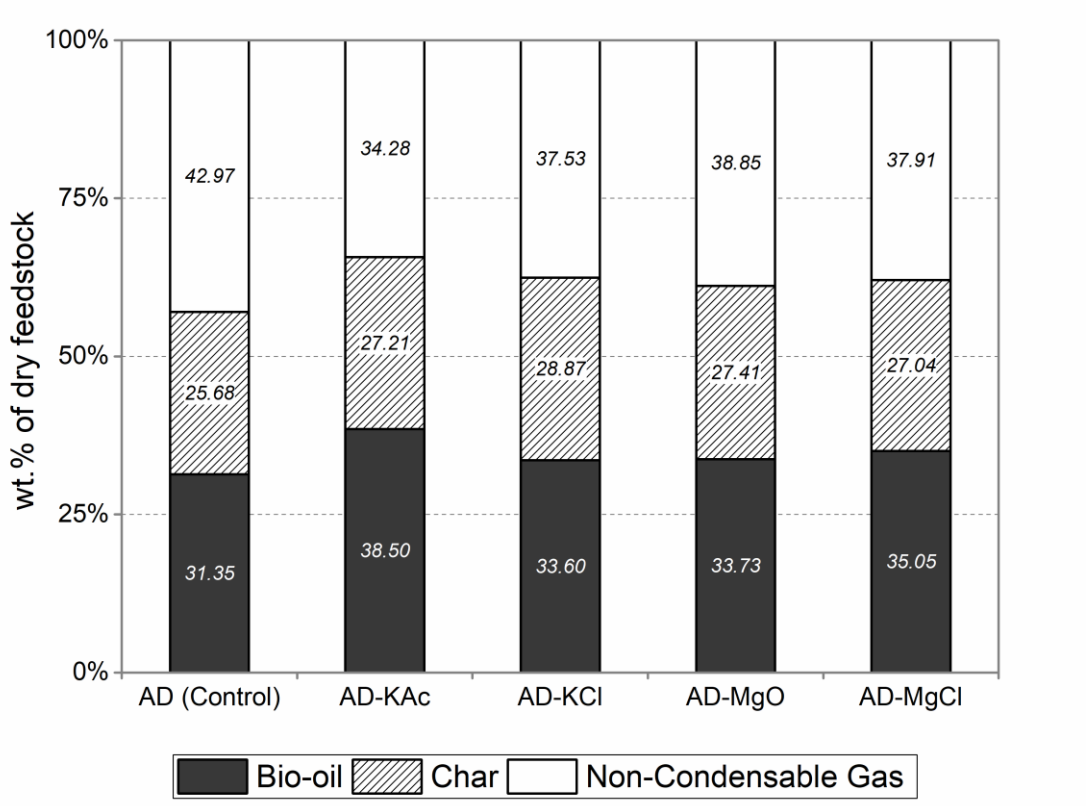

(b)

Figure 6.2: Bio-oil, biochar and gas yields form pyrolysis of K and Mg doped *P. juliflora* and *A. donax* samples

AAEM salts had interestingly different effects in PJ and AD biomass samples. An increase in gas yield with a reduction in bio-oil and biochar yields was observed with PJ biomass except with $MgCl_2$ doped samples. With AD biomass, however, the bio-oil and char yield increased with a decrease in gas production.

6.3.1 Effect of AAEM salts on bio-oil composition

The raw biomass samples PJ(control) and AD(control) on pyrolysis gave similar bio-oil yields of 29.7 and 31.35% w/w. The infusion of AAEM salts influenced the pyrolysis process resulting in significant variations in overall bio-oil yield with PJ biomass. The acetate and oxide salt doped biomass showed a 20 and 17% drop in the liquid output respectively. The chloride salts showed the opposite trend with PJ-MgCl

with a major 45% increase in liquid bio-oil production. AD biomass, on the other hand, recorded minimal changes, which could be due to the existence of significant K and Mg salts in the ash. However, since bio-oils are formed through the condensation of numerous chemicals formed through different thermal degradation mechanisms, the quantification of the individual components and gaining fundamental insight into their production mechanism is essential to understand the impact of AAEM salts on the observed difference in bio-oil yield. The bio-oil chemical composition analysis through GC-MS revealed the presence of 45 compounds, which were listed earlier in Table 4.2. The GC-MS quantitative analysis of the bio-oils are given in detail in Annexure D.

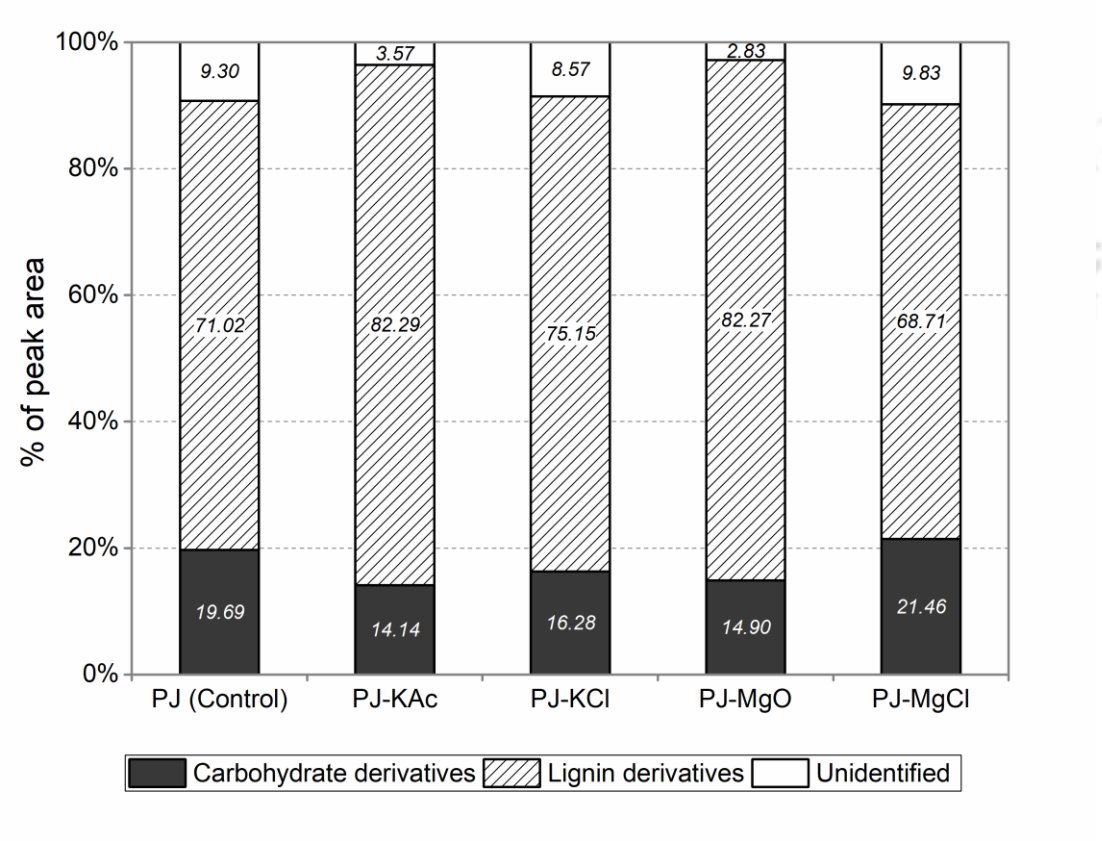

(a)

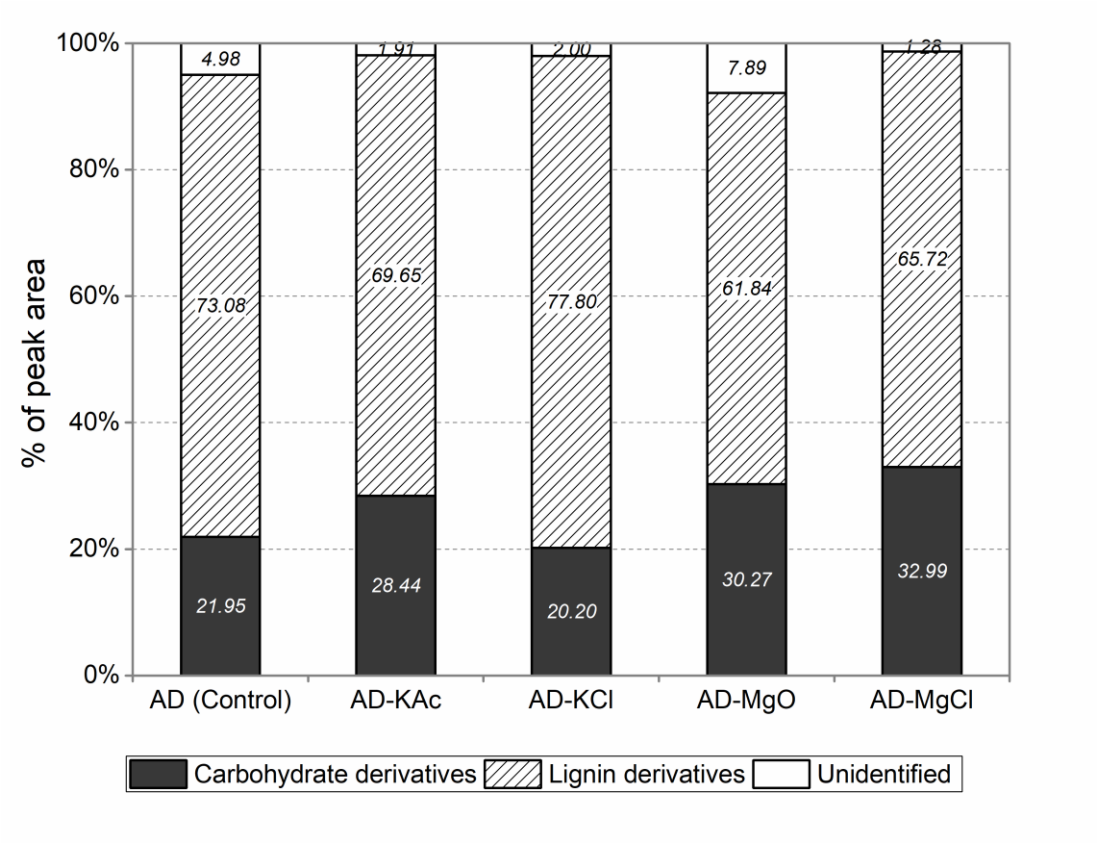

(b)

Figure 6.3: Classification of bio-oil peak areas on the basis of precursor materials

Fig. 6.3 classifies the mass spectroscopy identified peak area on the basis of the source component (carbohydrate and lignin) in biomass. Of the identified 45 compounds, 13 were carbohydrate derivatives, and the rest 32 were lignin derivatives. The peak areas of the carbohydrate and lignin degradation products accounted for 19.69 and 71.02% in PJ(control), 21.95 and 73.08% in AD(control) respectively. The observed variation with AAEM salt infusion are explained in subsequent sections. Certain compounds, with a cumulative 2-10% peak area detected by GC-MS, could not be identified using the NIST library.

6.3.1.1 Effect of K and Mg salts on pyrolytic degradation of carbohydrate

The alkali and alkaline earth metals had major impacts on the carbohydrate degradation products through variation in ring-opening and rearrangement

mechanisms, which impacted the yield of carboxylic acids, furans and non-aromatic ketones. Fig. 6.4 shows the composition of chemicals resulting from carbohydrate pyrolysis in the presence of AAEM salts.

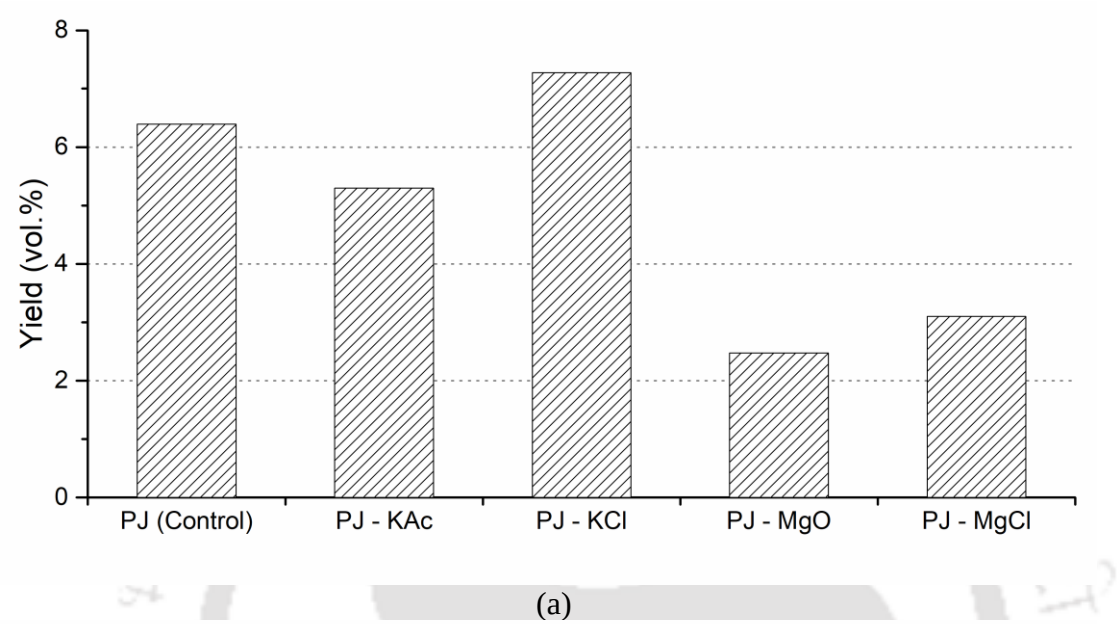

(a)

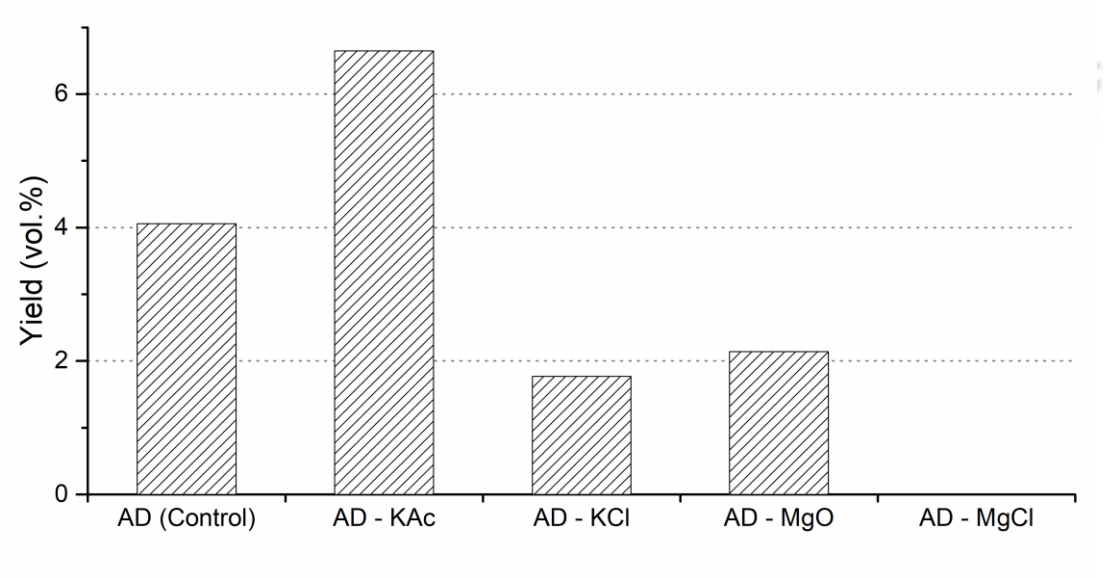

(b)

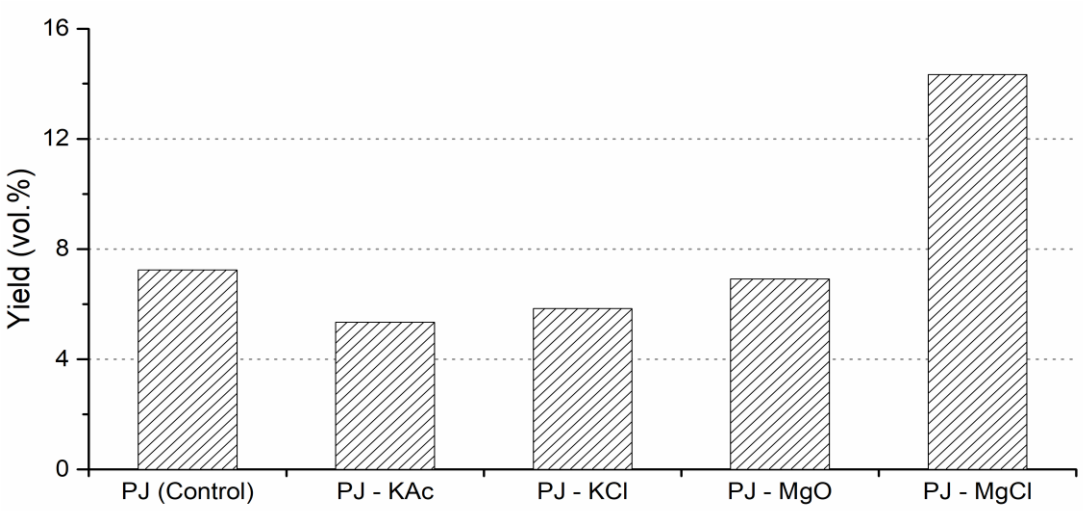
Yield (vol.%)
16
12
8
4
0
PJ (Control)
PJ - KAc
PJ - KCl
PJ - MgO
PJ - MgCl

(c)

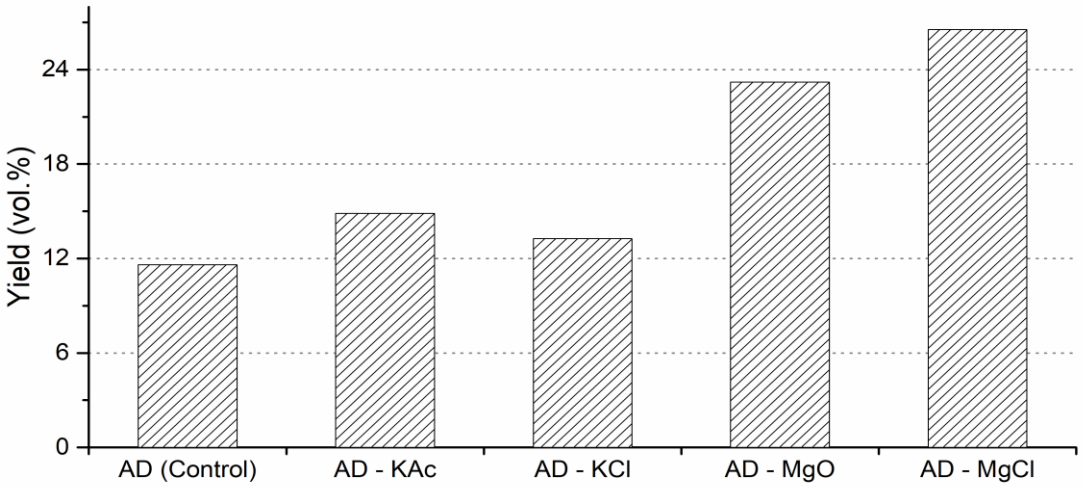
Yield (vol.%)
24
18
12
6
0
AD (Control)
AD - KAc
AD - KCl
AD - MgO
AD - MgCl

(d)

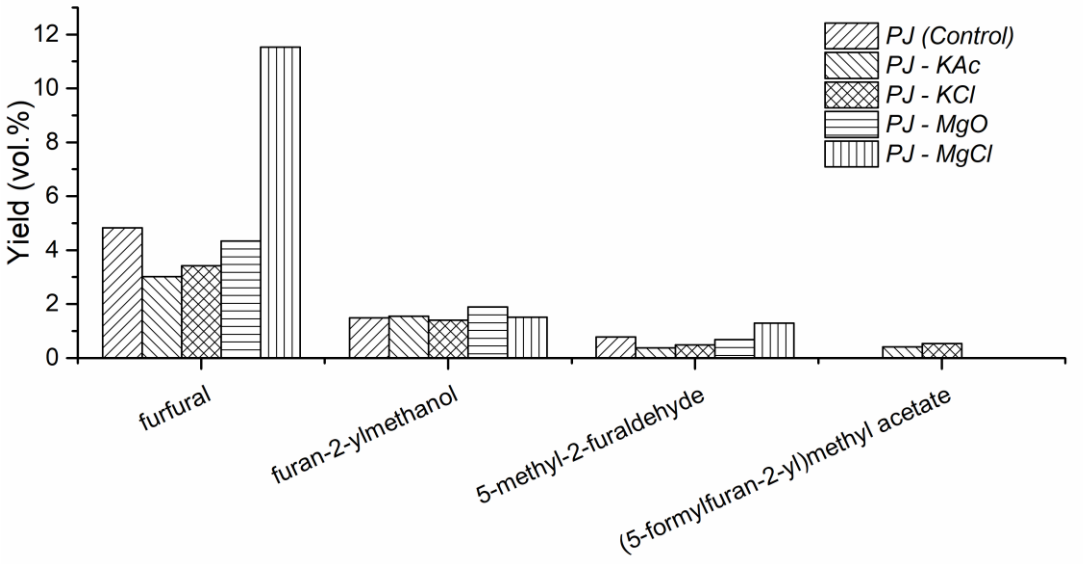
Yield (vol.%)
12
10
8
6
4
2
0
PJ (Control)
PJ - KAc
PJ - KCl
PJ - MgO
PJ - MgCl
furfural
furan-2-ylmethanol
5-methyl-2-furaldehyde
(5-formylfuran-2-yl)methyl acetate

(e)

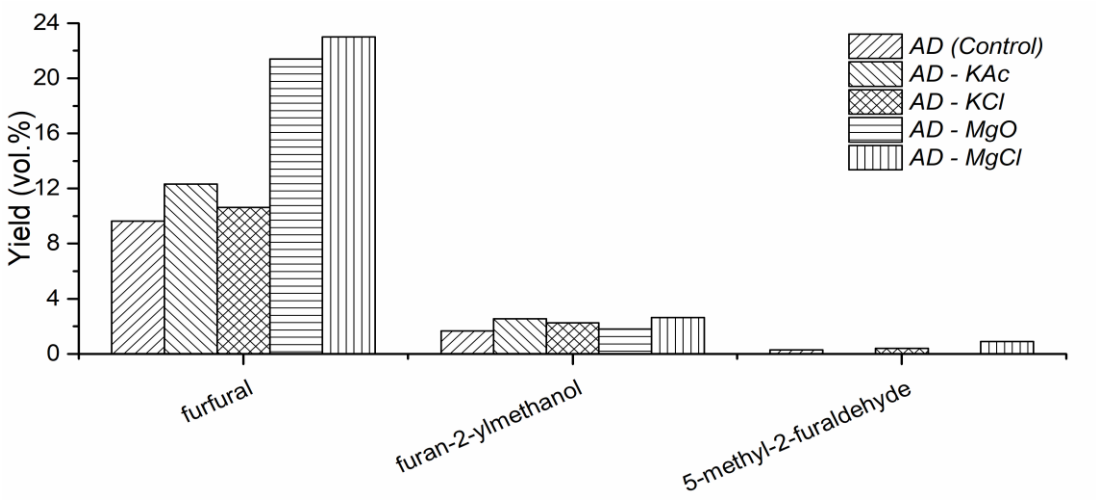
Yield (vol.%)
24
20
16
12
8
4
0
AD (Control)
AD - KAc
AD - KCl
AD - MgO
AD - MgCl
furfural
furan-2-ylmethanol
5-methyl-2-furaldehyde

(f)

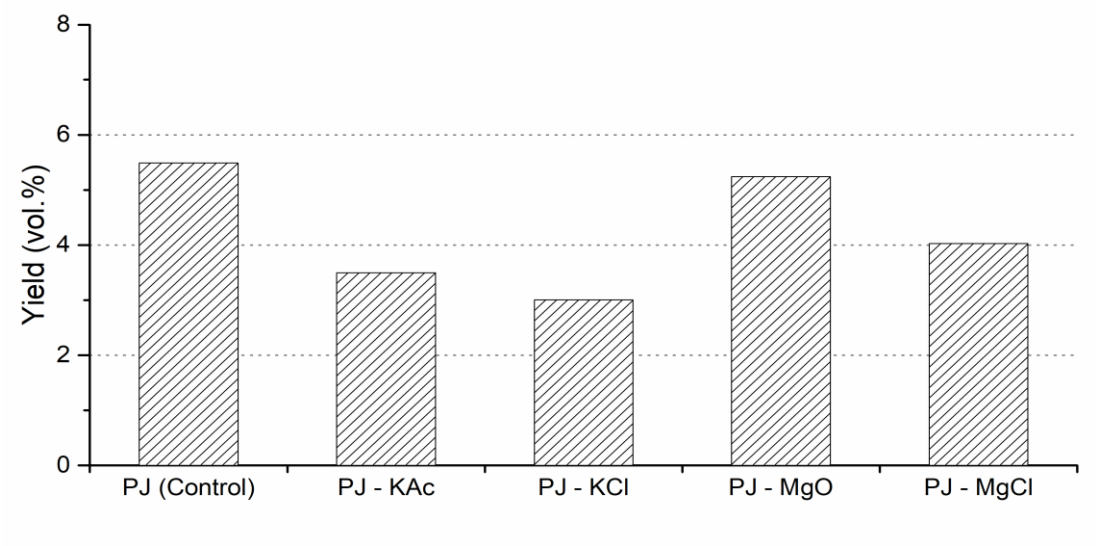
Yield (vol.%)
8
6
4
2
0
PJ (Control)
PJ - KAc
PJ - KCl
PJ - MgO
PJ - MgCl

(g)

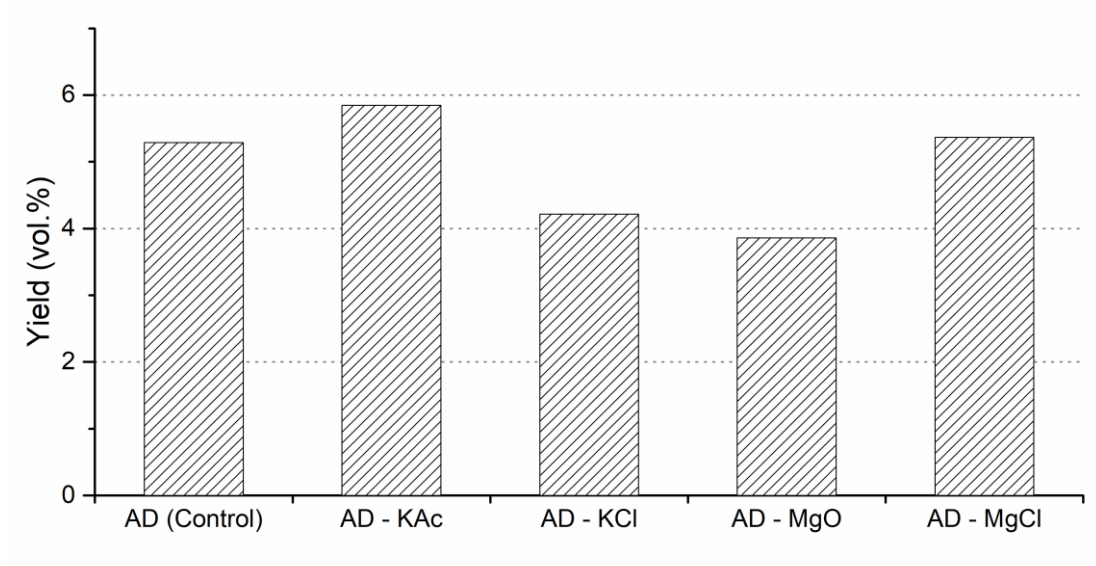
Yield (vol.%)
6
4
2
0
AD (Control)
AD - KAc
AD - KCl
AD - MgO
AD - MgCl

(h)

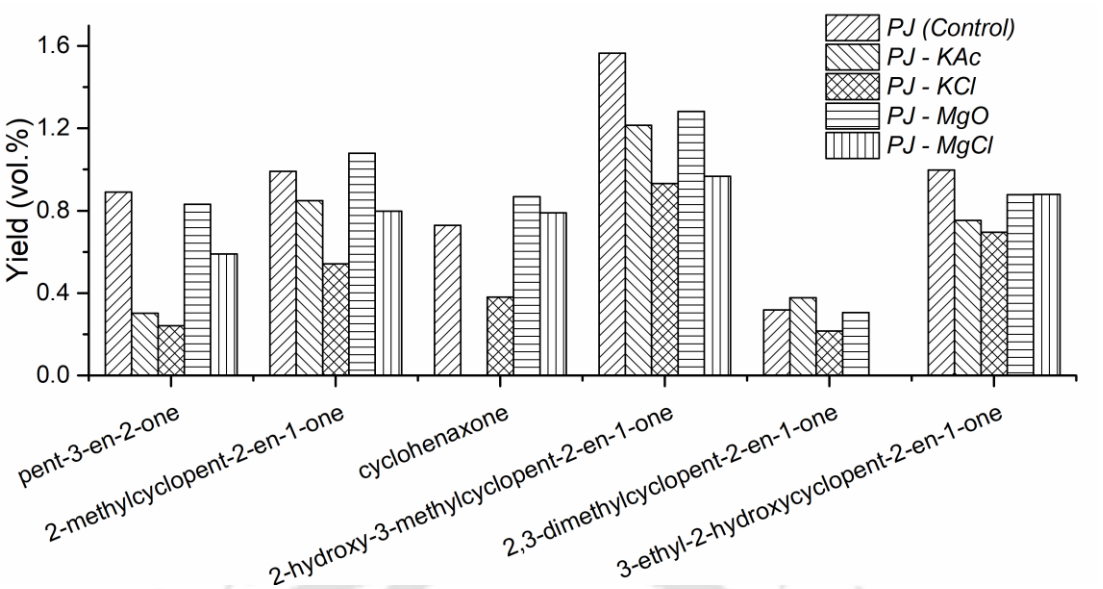

(i)

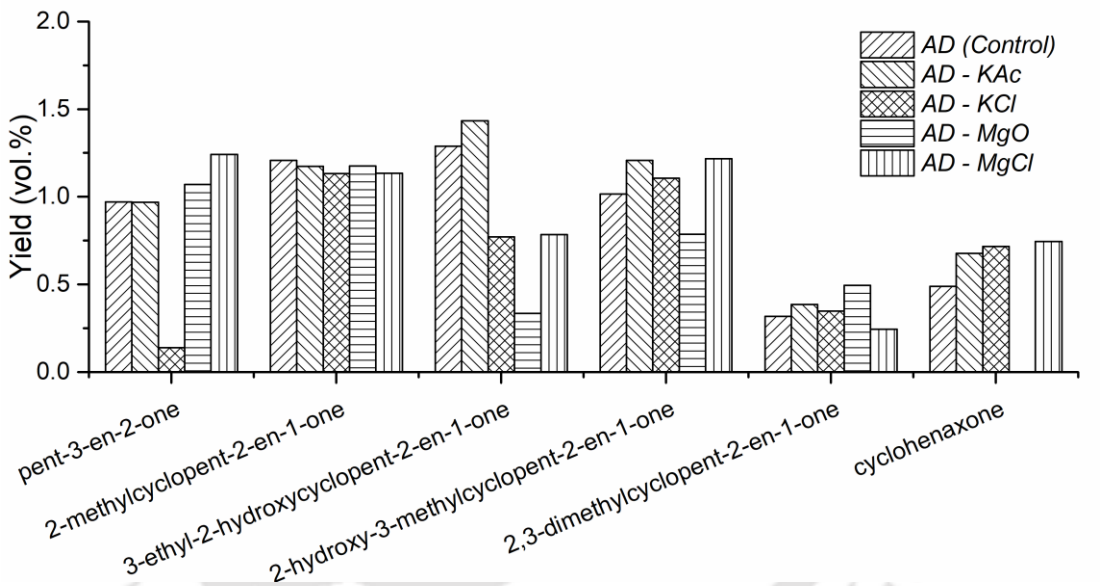

(j)

Figure 6.4: Carbohydrate derived pyrolytic bio-oil components: Effect of AAEM salts on the (a), (b) acetic acid yield; (c), (d) overall furan yield; (e), (f) individual furan compounds; (g), (h) overall ketone yield; and (i), (j) individual ketone compounds.

Acetic acid was the only carboxylic acid detected in the bio-oil samples. It is widely accepted that the pH of bio-oil reflects its relative abundance of carboxylic acids. Although other bio-oil components such as phenolics and sugars contribute to the acidity, their share is around 15-30%, with the rest 70% derived from carboxylic

acids (Oasmaa et al., 2010). The acetate and oxide salts resulted in reducing the acetic acid production in PJ biomass, as shown in Fig 6.4(a), which was reflected in the increase in pH from 3.42 in PJ(control) to 3.74 and 3.59 in PJ-KAc and PJ-MgO bio-oils respectively. In contrast, the pH decreased from 3.49 in AD(control) to 3.28 in AD-KAc due to the increase in acetic acid production. The addition of KCl promoted the production of acetic acid from 6.39% v/v in PJ(control) to 7.27% v/v in PJ-KCl. Consequently, it resulted in decreasing the pH to 3.34. The low molecular weight (MW) compounds such as acetic acid are formed through ring fission and dehydration reactions and potassium is known to promote these reactions (Nowakowski and Jones, 2008). Both PJ-MgCl and AD-MgCl bio-oil exhibited the lowest pH of 2.77, although they recorded low acetic acid contents. This could be due to the presence of other unidentified acids in the bio-oil, such as formic acid and propionic acid, which were identified in bio-oil obtained from *P. juliflora* biomass species by other researchers (Chandran et al., 2020).

Furans are formed through the ring-opening reaction of 6 membered glucose monomer followed by rearrangement, cyclization and dehydration of the C_5 to C_6 pyrolysis fragments (Mettler et al., 2012). Furan compounds detected in PJ and AD pyrolysis include furfural ($C_5H_4O_2$), furfuryl alcohol ($C_5H_6O_2$), 2,5-dimethylfuran (C_6H_8O), 5-methyl-2-furaldehyde ($C_6H_6O_2$) and 5-acetoxymethyl-2-furaldehyde ($C_8H_8O_4$). The C_5 compounds furfural and furfuryl alcohol made up the major fraction of the quantified furan content. $MgCl_2$ significantly increased the furan yield from 7.2 to 14.8% v/v and from 11.6 to 26.5% v/v in PJ and AD respectively. Furfural production increased 2-fold from 4.8% v/v in PJ(control) to 11.5% v/v in PJ-MgCl and from 9.6% v/v in AD(control) to 23% v/v in AD-MgCl. The characteristic property of $MgCl_2$ to

catalyze dehydration reactions was also highlighted by Patwardhan et al. (2010), who observed a substantial increase in furfural even with the addition of a small quantity (0.1 wt.%) of the alkaline earth metal chloride. Although KCl is known to catalyze dehydration reactions, a decrease in the furan yield was observed with PJ biomass. The competing property of KCl to also promote fragmentation of glucose monomers to form lower MW compounds such as acetic acid as observed above could account for the drop in furan yield (Eom et al., 2012). However, AD biomass showed a marginal increase in furfural concentration in potassium doped samples. This was attributed to the inherent Mg in the raw biomass which aided in production of furfural.

Non-aromatic ketones in bio-oil are primarily composed of cyclopentenones such as 2-methylcyclopent-2-en-1-one and 2-hydroxy-3-methylcyclopent-2-en-1-one. The cyclopentenone structure is formed through the C1-O ring-opening, followed by the coupling of C1 and C5 radicals of the glucose monomer (Kojima et al., 2015). The decreasing order of ketone content in bio-oils was PJ-MgO (5.24% v/v) > PJ-MgCl (4.03% v/v) > PJ-KAc (3.50% v/v) > PJ-KCl (3.00% v/v). Mg salts showed a higher selectivity towards the formation of ketones. Interestingly PJ-MgO bio-oil, which exhibited the highest ketone yield, also exhibited the lowest acetic acid production, which correlates with the finding of Mahadevan et al. (2016), who also reported the effect of alkaline earth metal oxides in suppressing acid production through ketonization reactions. On the contrary, alkali earth metals exhibited much less selectivity towards ketone production. However, significantly higher ketone production was observed with AD-KAc and AD-KCl bio-oils. Hence it was inferred that alkali earth metals (K) in the presence of inherent alkaline earth metals (Mg) as in AD biomass

promoted the cyclization of pyrolysis ring-opening fractions, resulting in an enhancement in furan and cycloketone production.

6.3.1.2 Effect of K and Mg salts on pyrolytic degradation of lignin

Compounds obtained through the thermal breakdown of lignin fraction contributed to more than 70% v/v of the 90.7 and 95% v/v detected and identified PJ(control) and AD(control) bio-oil composition respectively. Pyrolysis of AAEM infused *P. juliflora* biomass resulted in an increase in the 5-16% range except for PJ-MgCl, which recorded a marginal 3% decrease. The detected phenolic, methoxyphenol derivatives and other aromatic compounds derived from lignin were categorized into 4 groups: hydroxylphenol type (L-H) including phenol, o-cresol, p-cresol and 1-(2-hydroxy-5-methylphenyl)ethanone; guaiacol type (L-G) including 2-methoxyphenol, 2-methoxy-4-methylphenol, 4-ethyl-2-methoxyphenol and 2-methoxy-4-(prop-1-enyl)-phenol; syringol type (L-S) including 2,6-dimethoxyphenol, 2,6-dimethoxy-4-prop-2-enylphenol and 1,2,4-trimethoxybenzene; and the other lignin-derived aromatic hydrocarbons (L) including 1,3-xylene, styrene, 1-ethyl-4-phenylbenzene and 2,3-dihydro-1-benzofuran. L-G and L-S type products originate from the guaiacyl and syringyl monomer units in the original lignin fraction. L-G and L-S units contribute a major fraction of 30.02 and 14.97% respectively, of the overall bio-oil components from raw untreated *P. juliflora*, suggesting the predominance of guaiacyl and syringyl units in the hardwood with an approximate ratio of 2:1.

The effect of AAEM salts on the overall syringols and guaiacols yields and their individual component relative fractions are shown in Fig. 6.5. Although AAEM salt-induced changes were observed, they did not affect the chemical distribution of lignin derivatives to the extent observed with carbohydrate derived bio-oil compounds. This

shows the predominant effect of the inorganic ash on carbohydrate fraction over the lignin fraction of lignocellulosic biomass. This could be attributed to the limited ability of mineral species to interact with aromatic rings, which constitute lignin (Patwardhan et al., 2011).

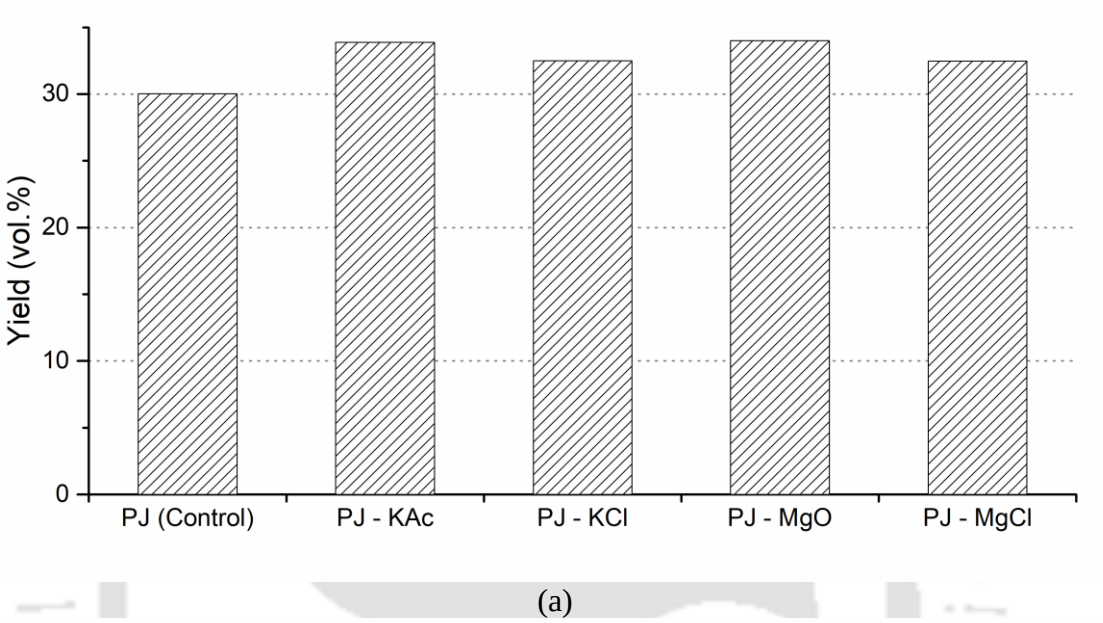

(a)

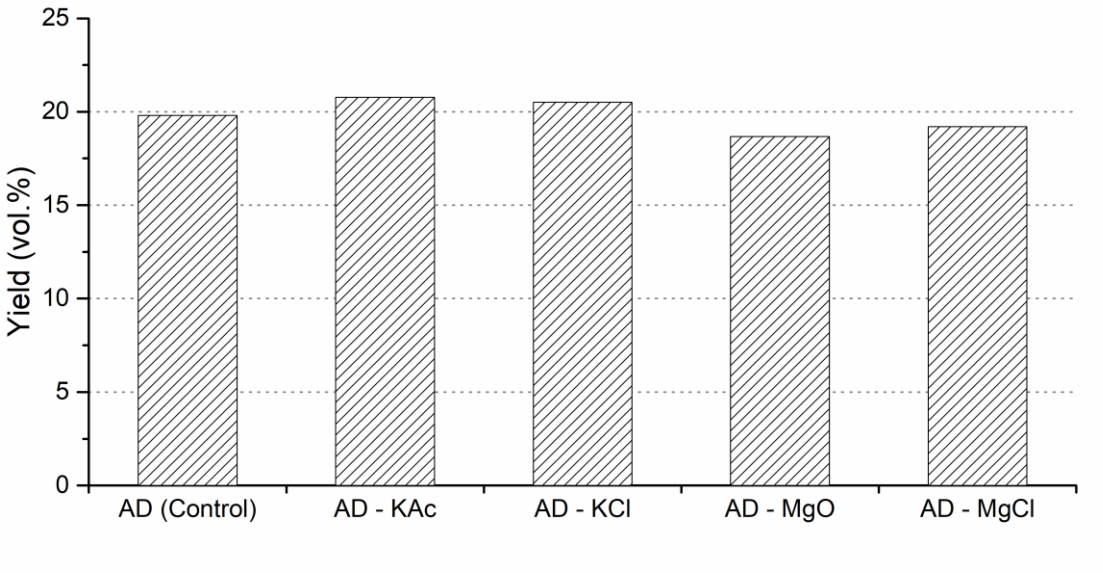

(b)

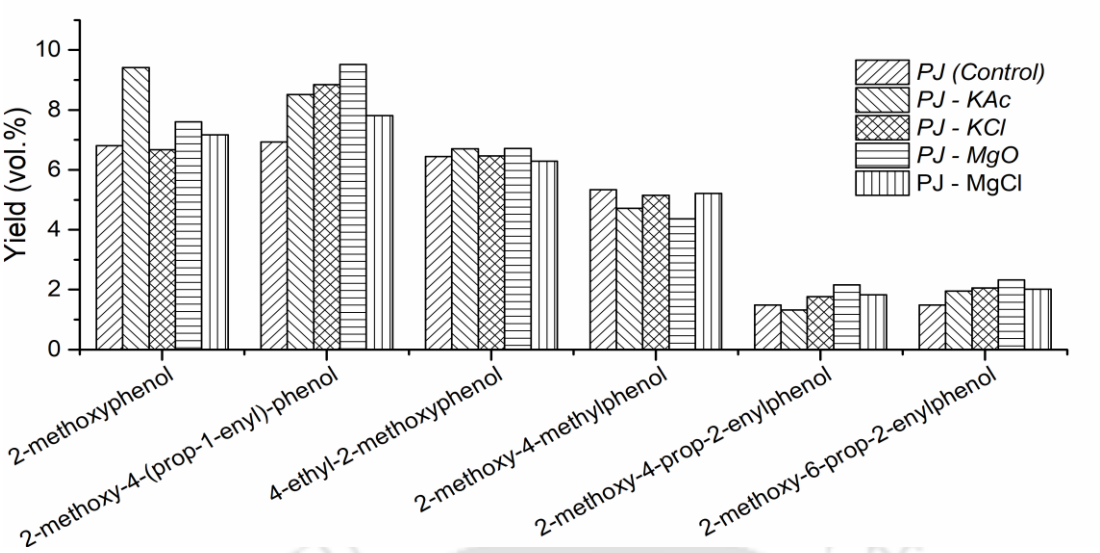
Yield (vol.%)
0
2
4
6
8
10
PJ (Control)
PJ - KAc
PJ - KCl
PJ - MgO
PJ - MgCl
2-methoxyphenol
2-methoxy-4-(prop-1-enyl)-phenol
4-ethyl-2-methoxyphenol
2-methoxy-4-methylphenol
2-methoxy-4-prop-2-enylphenol
2-methoxy-6-prop-2-enylphenol

(c)

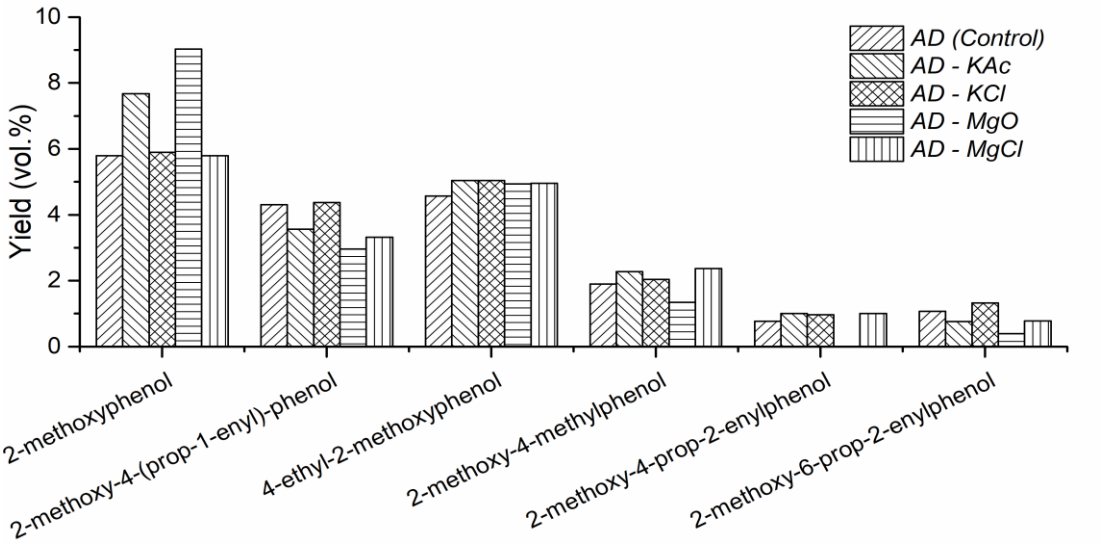
Yield (vol.%)
0
2
4
6
8
10
AD (Control)
AD - KAc
AD - KCl
AD - MgO
AD - MgCl
2-methoxyphenol
2-methoxy-4-(prop-1-enyl)-phenol
4-ethyl-2-methoxyphenol
2-methoxy-4-methylphenol
2-methoxy-4-prop-2-enylphenol
2-methoxy-6-prop-2-enylphenol

(d)

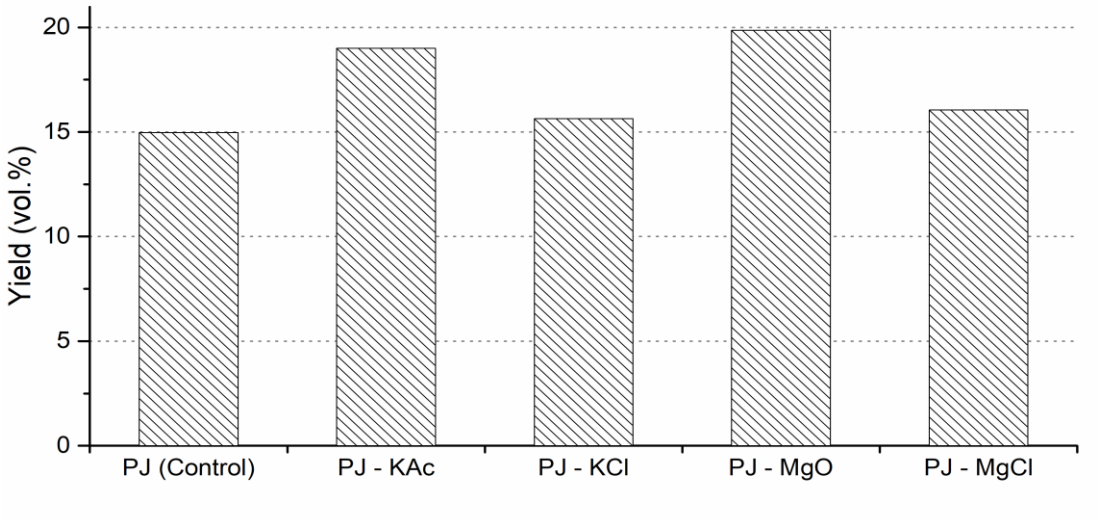
Yield (vol.%)
0
5
10
15
20
PJ (Control)
PJ - KAc
PJ - KCl
PJ - MgO
PJ - MgCl

(e)

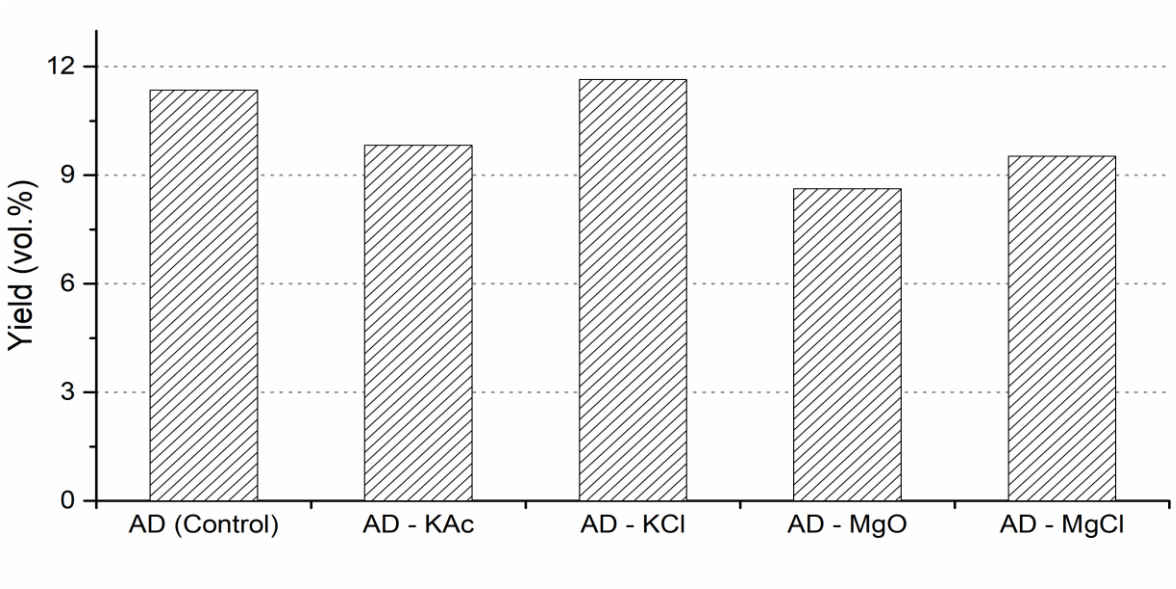
Yield (vol.%)
0
3
6
9
12
AD (Control)
AD - KAc
AD - KCl
AD - MgO
AD - MgCl

(f)

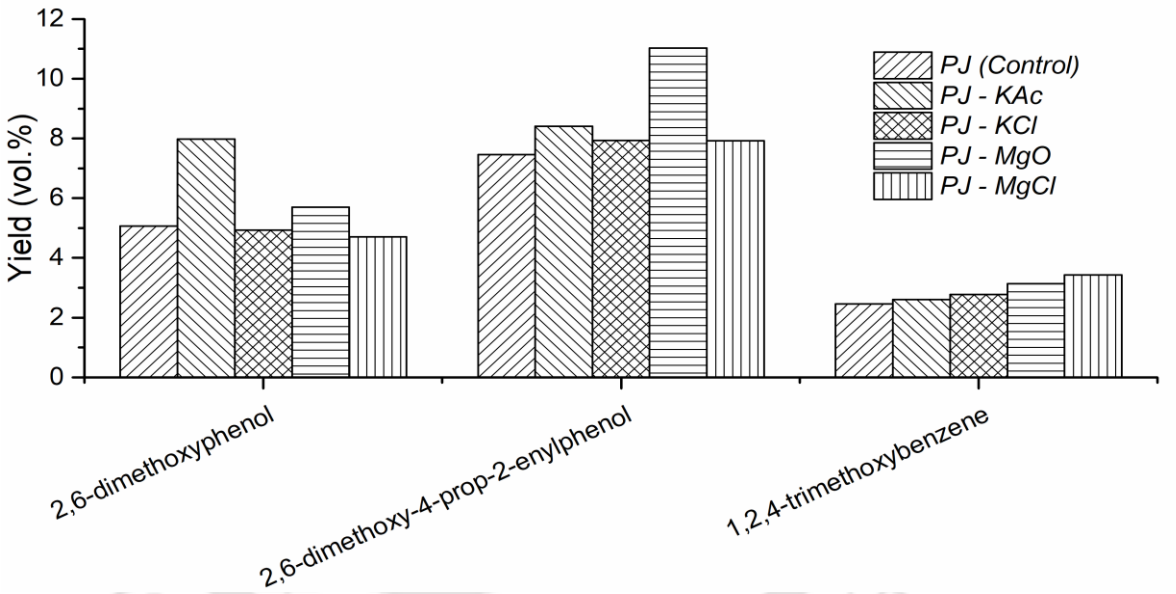
Yield (vol.%)
0
2
4
6
8
10
12
PJ (Control)
PJ - KAc
PJ - KCl
PJ - MgO
PJ - MgCl
2,6-dimethoxyphenol
2,6-dimethoxy-4-prop-2-enylphenol
1,2,4-trimethoxybenzene

(g)

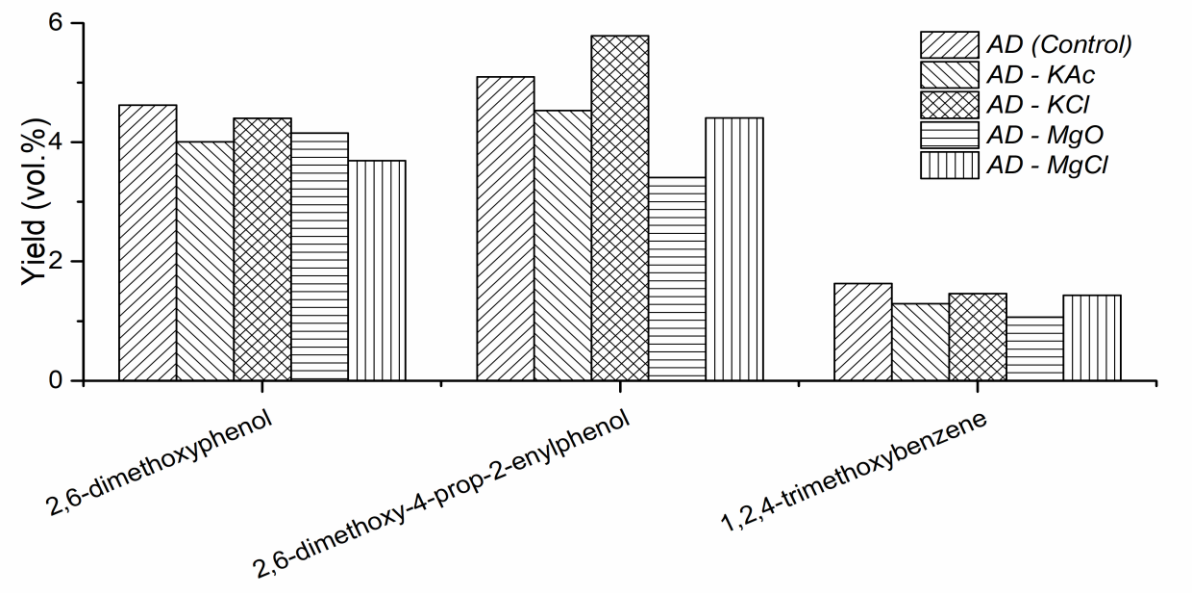

(h)

Figure 6.5: Lignin derived pyrolytic bio-oil components: Effect of AAEM salts on the (a), (b) overall guaiacol yield; (c), (d) individual guaiacol compounds; (e), (f) overall syringol yield; and (g), (h) individual syringol compounds.

Both the alkali and alkaline earth metal salt promoted the release of methoxyphenol derivatives (guaiacols and syringols) from the lignin structure or prevented the $–OCH_3$ side-chain cleavage. This was observed to a greater extent with the acetate and oxide salts over the chloride salts in PJ bio-oils. This is consistent with the observation of Dalluge et al. (2017), who reported an increase in methoxy side chain groups with lignin doped with potassium acetate.

Syringols increased significantly by 27-32% with JP-KAc and JP-MgO, while a 4-7% increase was observed with JP-KCl and JP-MgCl. Likewise, Guaiacols followed similar trends with a 13% increase with JP-KAc and JP-MgO and 8% rise with JP-KCl and JP-MgCl. This resulted in reducing the ratio of guaiacols to syringols from 2.0 in PJ(control) to 1.78 and 1.71 in PJ-KAc and PJ-MgO respectively. An interesting study by Asmadi et al. (2011) revealed the increase in reactivity of phenolic substrate with the number of methoxy side chains. Dalluge et al. (2014) further

observed a 50% additional decrease in syringol yield compared to guaiacols with pyrolysis of red oak whose AAEM were passivated using sulphuric acid. Hence, the observed dissimilarity in the level of increase between L-S and L-G was due to relative differences in their reactivities and the effect of AAEM. This was further substantiated by the reduction in the char, which is formed from polymerization of radicals formed by the breakdown of methoxyphenol derivatives (Asmadi et al., 2011). Although PJ-KAc and PJ-MgO showed alike incremental variations in the cumulative L-G and L-S yield, as shown in Fig. 6.5(a) and (e), they were attributed to vastly different mechanisms. The increase in 2-methoxyphenol ($C_7H_8O_2$; MW: 124) and 2,6-dimethoxyphenol ($C_8H_{10}O_3$; MW: 154), the lowest MW and primary forms of L-G and L-S respectively, was observed with PJ-KAc. However, the concentration of lower MW compounds did not seem to vary with PJ-MgO notably. Nevertheless, an increase with higher MW compounds such as 2-methoxy-4-(prop-1-enyl)-phenol ($C_{10}H_{12}O_2$; MW: 162) and 2,6-dimethoxy-4-prop-2-enylphenol ($C_{11}H_{14}O_3$; MW: 194) were primarily responsible for the increase in L-G and L-S yield in PJ-MgO. The impact of potassium on the enhanced production of low MW lignin compounds was also reported by Nowakowski et al. (2007). This highlights the principle variation in the mechanistic approach of alkali (K) and alkaline (Mg) earth metals towards the depolymerization of lignin. The observed increase in the concentration of basic lignin monomers (2-methoxyphenol and 2,6-dimethoxyphenol) suggests that alkali earth metals promote cleavage of intermolecular lignin linkages. Interestingly variations were observed within the various salts of AAEM, which are shown in Fig. 6.5(c) and 6.5(g). The chloride salts did not seem to alter the chemical distribution of lignin-derived compounds, which is in agreement with the study by Patwardhan et al. (2011), who observed insignificant variation in pyrolysis of lignin with chloride salts of AAEMs.

The observed contrast in catalytic activity is speculated to be due to the inability of the chloride salts over the acetate salt to decompose in the temperature regimes employed for pyrolysis and release the catalytically active form of the AAEM (Dalluge et al., 2017).

The infusion of K and Mg salts into AD biomass with high AAEM content did not affect the L-G and L-S yields to a great extent as shown in Fig. 6.5(b), (d), (f) and (h). L-S compounds exhibited a drop in yield as opposed the observation in PJ biomass. However, the extent of the drop was similar to the rise observed in PJ biomass. As observed in PJ biomass, the addition of chloride salts in AD biomass showed only marginal variations.

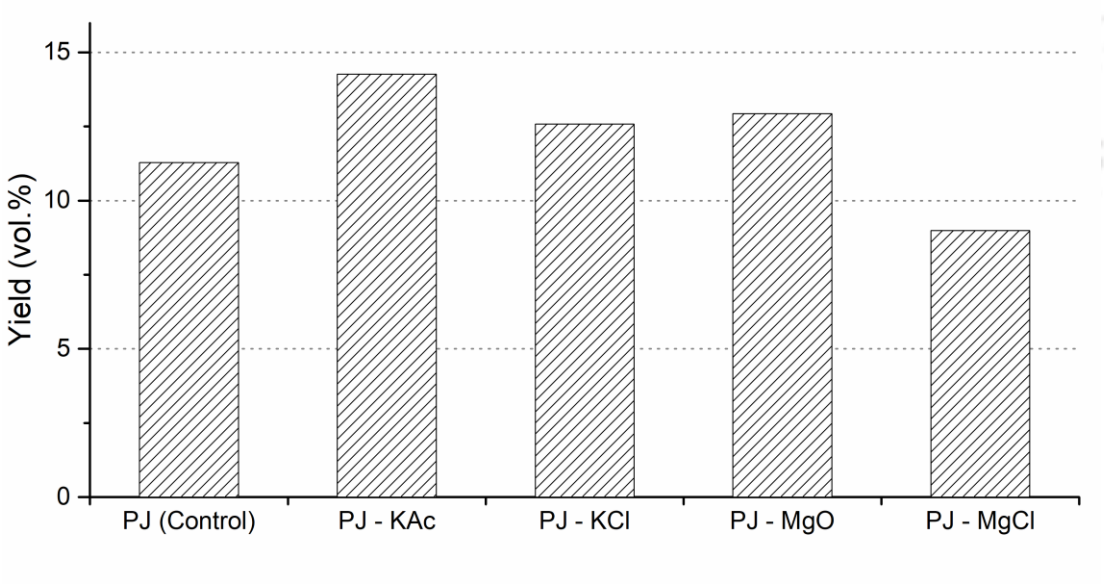

(a)

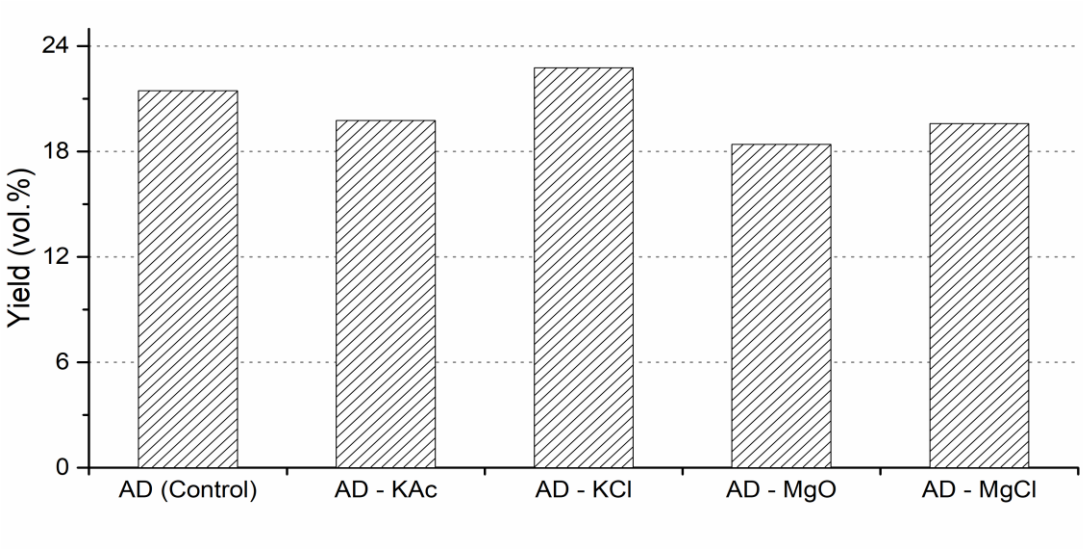
Yield (vol.%)
24
18
12
6
0
AD (Control)
AD - KAc
AD - KCl
AD - MgO
AD - MgCl

(b)

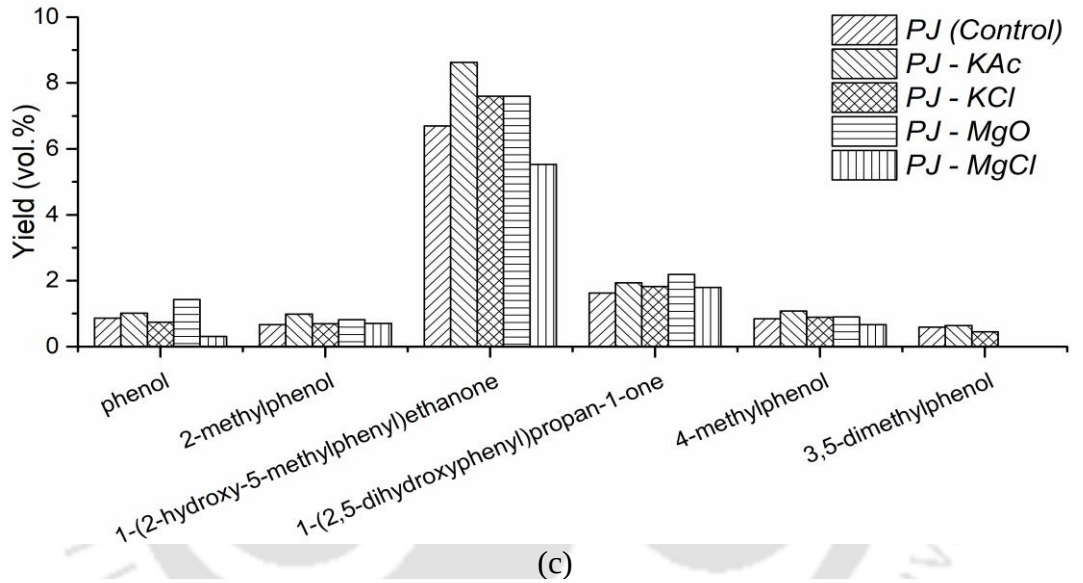
Yield (vol.%)
10
8
6
4
2
0
PJ (Control)
PJ - KAc
PJ - KCl
PJ - MgO
PJ - MgCl
phenol
2-methylphenol
1-(2-hydroxy-5-methylphenyl)ethanone
1-(2,5-dihydroxyphenyl)propan-1-one
4-methylphenol
3,5-dimethylphenol

(c)

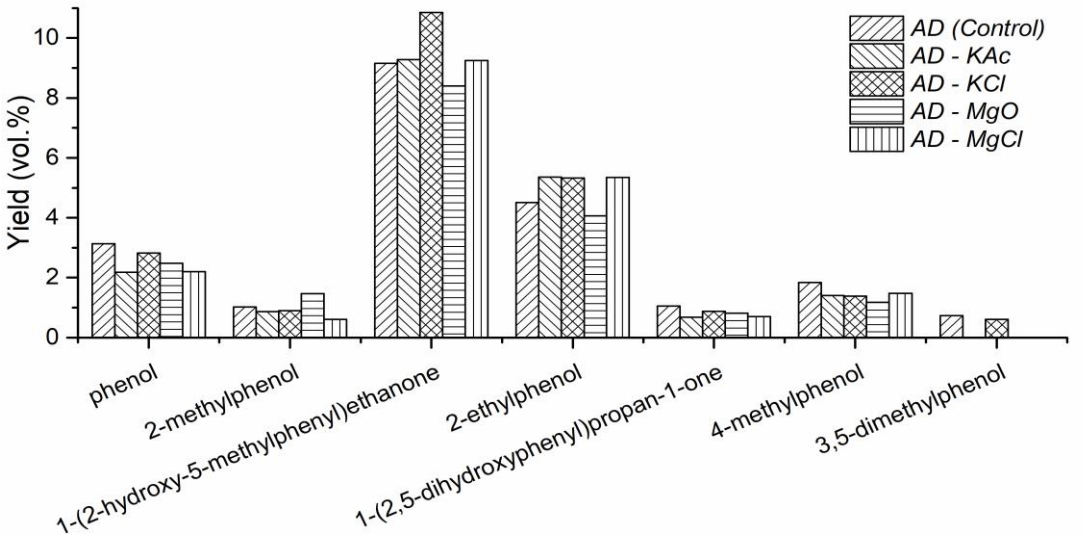
Yield (vol.%)
10
8
6
4
2
0
AD (Control)
AD - KAc
AD - KCl
AD - MgO
AD - MgCl
phenol
2-methylphenol
1-(2-hydroxy-5-methylphenyl)ethanone
2-ethylphenol
1-(2,5-dihydroxyphenyl)propan-1-one
4-methylphenol
3,5-dimethylphenol

(d)

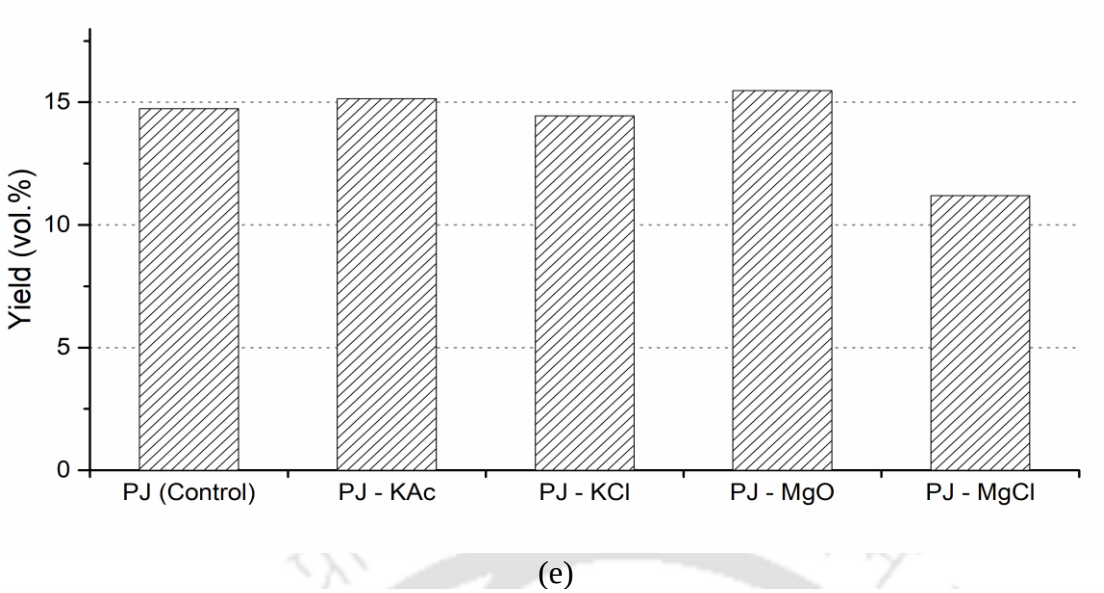
Yield (vol.%)
0
5
10
15
PJ (Control)
PJ - KAc
PJ - KCl
PJ - MgO
PJ - MgCl

(e)

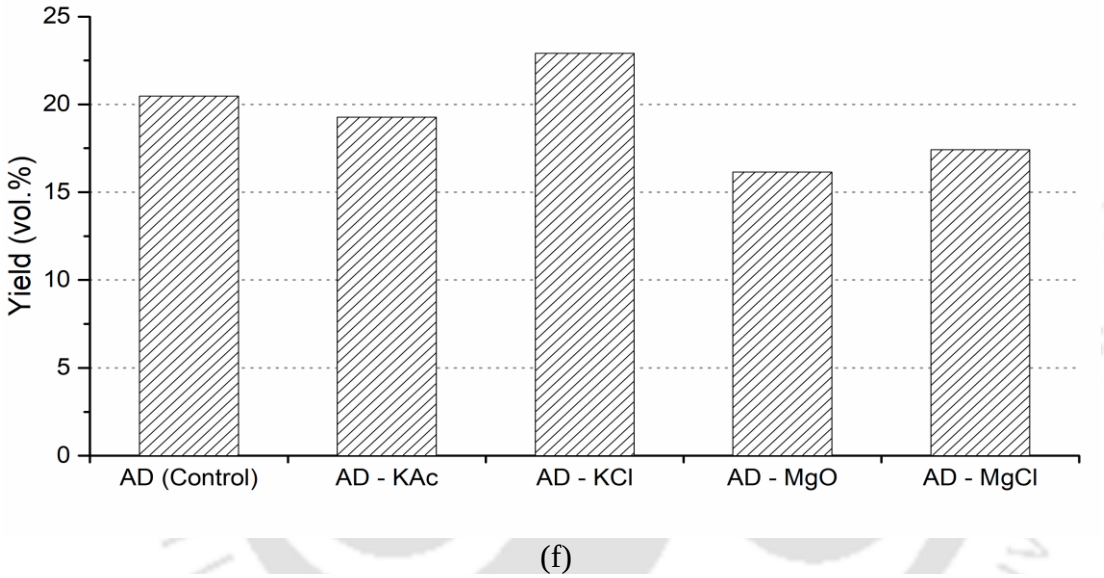
Yield (vol.%)
0
5
10
15
20
25
AD (Control)
AD - KAc
AD - KCl
AD - MgO
AD - MgCl

(f)

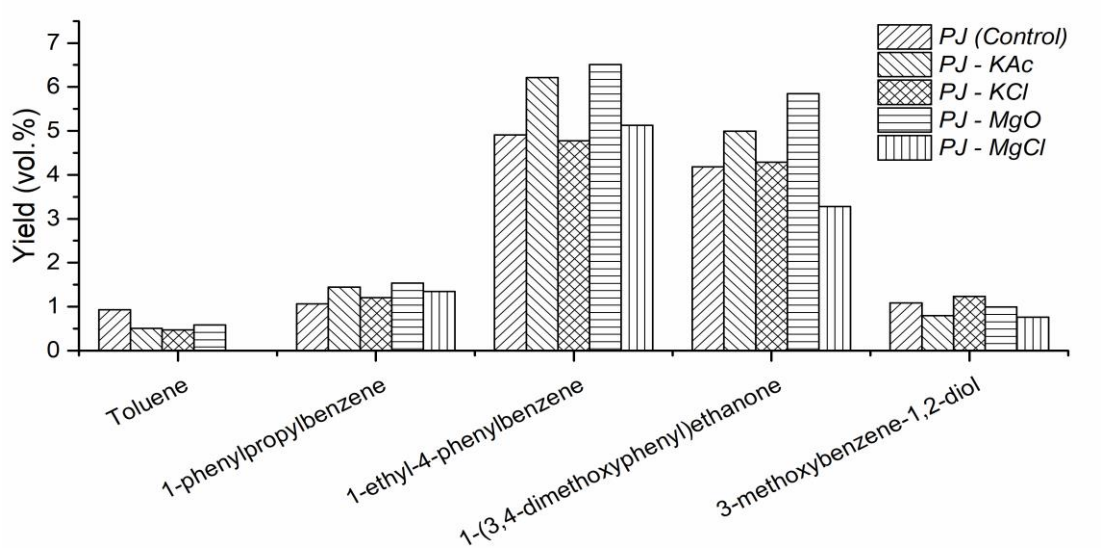
Yield (vol.%)
0
1
2
3
4
5
6
7
PJ (Control)
PJ - KAc
PJ - KCl
PJ - MgO
PJ - MgCl
Toluene
1-phenylpropylbenzene
1-ethyl-4-phenylbenzene
1-(3,4-dimethoxyphenyl)ethanone
3-methoxybenzene-1,2-diol

(g)

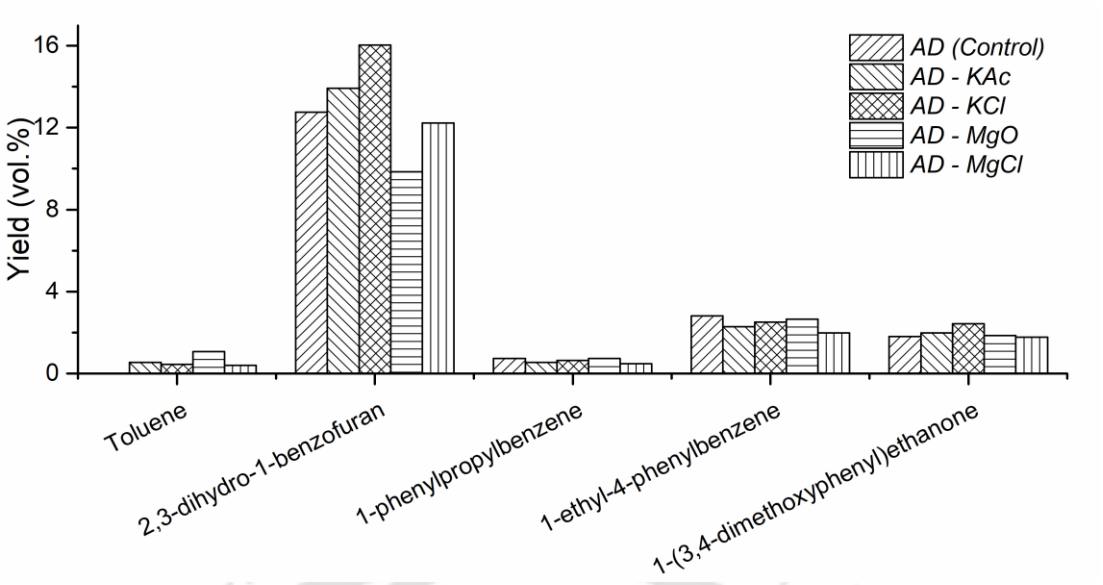

(h)

Figure 6.6: Lignin derived pyrolytic bio-oil components: Effect of AAEM salts on the (a), (b) overall hydroxyphenol yield; (c), (d) individual hydroxyphenol compounds; (e), (f) overall other aromatics yield; and (g), (h) individual other aromatics compounds.

L-H units originate from the p-hydroxyphenyl units in lignin structure, constitute 11.29% v/v and 21.45% v/v of the PJ(control) and AD(control) bio-oils respectively. The decreasing order of L-H units in bio-oil produced from AAEM-laden biomass was PJ-KAc (14.27% v/v) > PJ-MgO (12.93% v/v) > PJ-KCl (12.58% v/v) > PJ-MgCl (8.99% v/v). Similar results were also observed with AD biomass with potassium salts showing higher L-H yields than the magnesium salts. Fig. 6.6(a), (b), (c) and (d) shows the overall yield of hydroxyphenyl type compounds and their individual compositions. A major fraction in both AD and PJ biomass was constituted of 1-(2-hydroxy-5-methylphenyl)ethanone, an intermediate compound formed by the cleavage of the α-O-4 bond with the evolution of methanol, among other compounds (Wang et al., 2019). Much of the observed variation in overall L-H yield was attributed to the variation in concentrations of 1-(2-hydroxy-5-methylphenyl)ethanone and phenol.

The other aromatic compounds formed during pyrolysis of lignin include alkyl benzenes, alkenyl benzenes and benzenediols among other compound groups. They constitute 14.74% v/v in PJ(control), of which high MW compounds viz., 1-ethyl-4-phenylbenzene ($C_{14}H_{14}$; MW: 182) and 1-(3,4-dimethoxyphenyl)ethanone ($C_{10}H_{12}O_3$; MW: 180) contribute a significant fraction. 1-ethyl-4-phenylbenzene was the only polycyclic aromatic hydrocarbon (PAH) compound identified in the bio-oil, and very few works of literature have reported their presence in bio-oil. However, they were detected in high concentrations in our study in PJ biomass but found in low concentrations with AD bio-oils. Instead another low MW compound 2,3-dihydro-1-benzofuran (C_8H_8O; MW: 120) was found in high concentration of 10-16% v/v in AD bio-oils. Fig. 6.6(e), (f), (g) and (h) show the overall and individual yield of the other aromatics detected in bio-oil. It was observed that the addition of CH_3COOK and MgO improved the selectivity towards the higher MW compounds in PJ biomass. However, no significant variations were observed with their overall yield except with PJ-MgCl.

6.3.2 Effect of AAEM on biochar and non-condensable gas yields

Among the lignocellulosic components, lignin contributes to the char yield to a greater extent compared to cellulose and hemicellulose. Hence effect of AAEM salts on lignin degradation mechanism reflects to a great extent on the char and non-condensable gas yield. Among the AAEM salts, PJ-KAc produced the highest char yield, which could be attributed to the cleavage of intermolecular lignin linkages promoted by potassium acetate resulting in the production of low MW guaiacol and syringyl compounds as explained earlier. Similar effect was also observed by Mahadevan et al. (2016). Although the trend of biochar quantity produced with AAEM doped biomass was in accordance with other studies, it was observed that the char yield

from AAEM-laden biomass was always lower than that of the raw biomass. This could be due to the different dry impregnation approach employed in this study without the use of the chemical demineralization. However, further study will be required to understand the observed phenomenon. PJ-MgCl showed a drastic shift towards bio-oil production at the expense of non-condensable gas. However, a minimal reduction in char yield was also observed.

6.4 Conclusion

The catalytic impact of the salts of AAEMs on the primary carbohydrate and lignin pyrolysis reaction were studied. The primary variation with carbohydrate pyrolysis was realized by promoting cyclization reaction after ring-opening and rearrangement mechanisms by alkaline earth metals resulting in the enhanced production of furans and cycloketones. Alkali earth metal salts advocated the formation of products through ring fission and dehydration reactions resulting in increased carboxylic acid production. The alkali and alkaline earth metals catalyzed the thermal decomposition of lignin through the production of low (C_7-C_8) and high (C_{10}-C_{11}) MW methoxyphenol derivatives respectively. Overall, the AAEM salts seemed to considerably catalyze the degradation of carbohydrates compared to the degradation of lignin. In addition, the chloride salts of AAEMs significantly catalyzed the thermal decomposition reactions of carbohydrates compared to the oxide and acetate salts. However, the contrary was observed with lignin pyrolysis. The observed stark variations with different anions highlighted their role in biomass pyrolysis.

References

Asmadi, M., Kawamoto, H., & Saka, S. (2011). Thermal reactivities of catechols/pyrogallols and cresols/xylenols as lignin pyrolysis intermediates. *Journal of Analytical and Applied Pyrolysis*, *92*(1), 76-87.

Chandran, R., Kaliaperumal, R., Balakrishnan, S., Britten, A. J., MacInnis, J., & Mkandawire, M. (2020). Characteristics of bio-oil from continuous fast pyrolysis of Prosopis juliflora. *Energy*, *190*, 116387.

Dalluge, D. L., Daugaard, T., Johnston, P., Kuzhiyil, N., Wright, M. M., & Brown, R. C. (2014). Continuous production of sugars from pyrolysis of acid-infused lignocellulosic biomass. *Green chemistry*, *16*(9), 4144-4155.

Dalluge, D. L., Kim, K. H., & Brown, R. C. (2017). The influence of alkali and alkaline earth metals on char and volatile aromatics from fast pyrolysis of lignin. *Journal of Analytical and Applied Pyrolysis*, *127*, 385-393.

Dhyani, V., & Bhaskar, T. (2018). A comprehensive review on the pyrolysis of lignocellulosic biomass. *Renewable Energy*, *129*, 695-716.

Eom, I. Y., Kim, J. Y., Kim, T. S., Lee, S. M., Choi, D., Choi, I. G., & Choi, J. W. (2012). Effect of essential inorganic metals on primary thermal degradation of lignocellulosic biomass. *Bioresource technology*, *104*, 687-694.

Hu, S., Jiang, L., Wang, Y., Su, S., Sun, L., Xu, B., He, L., & Xiang, J. (2015). Effects of inherent alkali and alkaline earth metallic species on biomass pyrolysis at different temperatures. *Bioresource technology*, *192*, 23-30.

Jiang, L., Hu, S., Sun, L. S., Su, S., Xu, K., He, L. M., & Xiang, J. (2013). Influence of different demineralization treatments on physicochemical structure and thermal degradation of biomass. *Bioresource technology*, *146*, 254-260.

Kojima, Y., Kato, Y., Akazawa, M., Yoon, S. L., & Lee, M. K. (2015). Pyrolysis characteristic of kenaf studied with separated tissues, alkali pulp, and alkali lignin. *Biofuel Res. J*, *8*, 317-323.

Mahadevan, R., Adhikari, S., Shakya, R., Wang, K., Dayton, D., Lehrich, M., & Taylor, S. E. (2016). Effect of alkali and alkaline earth metals on in-situ catalytic fast pyrolysis of lignocellulosic biomass: a microreactor study. *Energy & Fuels*, *30*(4), 3045-3056.

Masiá, A. T., Buhre, B. J. P., Gupta, R. P., & Wall, T. F. (2007). Characterising ash of biomass and waste. *Fuel Processing Technology*, *88*(11-12), 1071-1081.

Mettler, M. S., Vlachos, D. G., & Dauenhauer, P. J. (2012). Top ten fundamental challenges of biomass pyrolysis for biofuels. *Energy & Environmental Science*, *5*(7), 7797-7809.

Miles, T. R., Miles, Jr, T. R., Baxter, L. L., Bryers, R. W., Jenkins, B. M., & Oden, L. L. (1995). Alkali deposits found in biomass power plants: A preliminary investigation of their extent and nature. Volume 1. United States.

Mourant, D., Wang, Z., He, M., Wang, X. S., Garcia-Perez, M., Ling, K., & Li, C. Z. (2011). Mallee wood fast pyrolysis: effects of alkali and alkaline earth metallic species on the yield and composition of bio-oil. *Fuel*, *90*(9), 2915-2922

Nowakowski, D. J., Jones, J. M., Brydson, R. M., & Ross, A. B. (2007). Potassium catalysis in the pyrolysis behaviour of short rotation willow coppice. *Fuel*, *86*(15), 2389-2402.

Nowakowski, D. J., & Jones, J. M. (2008). Uncatalysed and potassium-catalysed pyrolysis of the cell-wall constituents of biomass and their model compounds. *Journal of Analytical and Applied Pyrolysis*, *83*(1), 12-25.

Oasmaa, A., Elliott, D. C., & Korhonen, J. (2010). Acidity of biomass fast pyrolysis bio-oils. Energy & Fuels, 24(12), 6548-6554.

Patwardhan, P. R., Brown, R. C., & Shanks, B. H. (2011). Understanding the fast pyrolysis of lignin. *ChemSusChem*, *4*(11), 1629-1636.

Patwardhan, P. R., Satrio, J. A., Brown, R. C., & Shanks, B. H. (2010). Influence of inorganic salts on the primary pyrolysis products of cellulose. *Bioresource technology*, *101*(12), 4646-4655.

Shimada, N., Kawamoto, H., & Saka, S. (2008). Different action of alkali/alkaline earth metal chlorides on cellulose pyrolysis. *Journal of Analytical and Applied Pyrolysis*, *81*(1), 80-87.

Wang, L., Li, J., Chen, Y., Yang, H., Shao, J., Zhang, X., Yu, H., & Chen, H. (2019). Investigation of the pyrolysis characteristics of guaiacol lignin using combined Py-GC× GC/TOF-MS and in-situ FTIR. *Fuel*, *251*, 496-505.

Chapter 7

Overview and Scope for Future Work

7.1 Overview

Two invasive biomass species, *Arundo donax* and *Prosopis juliflora*, with widely varying biochemical compositions, were chemically treated with acids, alkali and surfactant to improve certain critical physicochemical and thermochemical properties, which could lead to improvement of the pyrolysis products. The diverse effects of the pretreatment on the lignocellulosic matrix using different agents were observed in terms of variation of biochemical composition, equilibrium moisture content, calorific value, O/C and H/C elemental ratios. The properties of the treated samples demonstrated the ability of chemical agents in improving biomass properties. Biomass with diverse biochemical compositions showed significant variations in properties with chemical treatment, which to a great extent was attributed to their lignin contents that inhibited the hydrolysis of cellulose and hemicellulose polysaccharides.

The treated biomass samples were pyrolyzed in a semi-batch pyrolysis unit. The products (bio-oil and biochar) were analyzed to understand the impact of the chemical

pretreatment on the pyrolysis process. A good proportion of the observed changes in pyrolysis product stream yields, chemical composition of bio-oils and calorific value of biochar were mapped to the changes in the critical properties of biomass. The inhibiting nature of lignin on the effectiveness of chemical agents also influenced the pyrolysis process by varying the quantitative product streams of bio-oil and biochar.

The impact of alkali and alkaline earth metals in biomass pyrolysis was also investigated as they are one of the components in the lignocellulosic biomass matrix. Although they are generally present in small quantities in lignocellulosic biomass, their catalytic effects significantly affect the pyrolysis products by altering the product formation mechanisms. The study also revealed the distinctive effects of anions in addition to the AAEM cations.

The major findings of the current thesis are summarized below.

Chapter 1 presents the general introduction to the central theme of the thesis. The structural components of biomass and the various thermal and biochemical techniques employed for its conversion to other forms of energy were discussed. Review of key pieces of literature on various biomass pretreatment techniques, effects on treatment on biomass biochemical properties and pyrolytic products, impact of ash content on biomass pyrolysis were presented for the convenience of readers.

Chapter 2 explored the effect of various chemical pretreatment techniques on low-lignin content *A. donax* species. Samples of the biomass were treated with varying concentrations of acid (H_2SO_4, H_3PO_4), alkali (NaOH) and surfactant (Triton X-100, SDS) at 90 ℃ for 20 min. The residue was filtered, washed with water and dried at 60 ℃. Alkali treatment produced the lowest solid yield, but the samples were cellulose-

rich. H_2SO_4 treatment yielded high calorific value and low moisture content feedstock. Biomass with low O/C ratio, which is a characteristic feature of high-grade fuels, was exhibited by samples treated with H_3PO_4. The work also discussed the ability to employ certain physical characteristics as makers for screening various biomass species.

Chapter 3 studied the impact of varying biomass biochemical composition on the structural and morphological properties of biomass during chemical pretreatment. The objective was achieved by performing various pretreatment experiments on high-lignin content *P. juliflora* species and comparing them with the effect on low-lignin content *A. donax* species. High lignin content was found to suppress cellulose and hemicellulose hydrolysis, which lessened the impact of chemical treatment, and it transpired to the cause of much of the observed changes. H_2SO_4 treatment yielded higher lignin content biomass which had higher calorific value, low moisture content and favorable O/C and H/C ratios for improved pyrolysis.

Chapters 4 and 5 analyzes the impacts of chemical pretreatment on pyrolysis product stream characteristics. Each of the treated samples were pyrolyzed in a semi-batch pyrolysis reactor at 600 ℃, and the bio-oil vapors were condensed and analyzed using GC-MS. Much of the observed variations in the bio-oil composition were found to be correlated to changes in the physical properties of biomass with pretreatment. The significant lignin hydrolysis by alkaline solution resulted in a reduction in the production of lignin-based phenolic compounds. Variations in the O/C ratio had a significant influence on the non-condensable gas yield. The high fraction of lignin in *P. juliflora* biomass caused an increase in biochar yields with most pretreatment techniques, which were not observed with *A. donax* treated samples. Reduction of H/C and O/C ratios of biochar with pretreatment resulted in improving their calorific value.

Chapter 6 studied the catalytic effect of acetate, chloride and oxide salts of AAEM on biomass pyrolysis through a novel approach wherein low ash & AAEM content feedstocks were infused with AAEM salts and pyrolyzed. The changes in bio-oil composition and bio-char properties were investigated to understand the effect of the salt in biomass pyrolysis. AAEM salts were broadly found to catalyze carbohydrate degradation to a greater extent compared to lignin degradation. Among the carbohydrate degradation products, alkaline earth metals were found to enhance the production of furans and ketones, while alkali earth metals catalyzed carboxylic acid production. The results also revealed variations in bio-oil product composition with different anions of the same AAEM cation.

7.2 Scope for Future Work

The research work presented in this thesis can be taken ahead and some suggestions for it are given below:

1. The effect of other chemical treatments such as ammonia fiber expansion (AFEX), organosolv and ionic solution treatment could also be employed. The physicochemical techniques involving the use of processes such as autoclaving, microwave, ultrasound with chemical agents could also be investigated.
2. Pyrolysis of the chemically treated biomass could be carried out using state of the art fast pyrolysis techniques, which are optimized for higher liquid yield. The product distribution is likely to vary to a certain extent due to variations in the thermal kinetics. The experiments in this thesis were carried out using batch fixed bed reactor. Variations in the reactor configurations (such as

bubbling/turbulent fluidized bed, moving bed, spouted bed) can give higher yields and better quality products.

3. Various biomass species could be screened for low ash and AAEM content for use in studies related to identifying the effects of metallic ash components.
4. Various combinations of salts of AAEM could be infused into biomass with low AAEM content and pyrolyzed to get a clearer understanding of their individual and synergies with other AAEMs during lignocellulosic biomass pyrolysis. Special catalysts for the pyrolysis have already been reported in literature. Improvement in these catalysts is also a major research avenue for the pyrolysis process.
5. The bio-oil is reported to have very small shelf life due to high content of oxygenates. Storage stability studies of the bio-oils formed through pyrolysis of chemically treated and additive mixed biomass could help in understanding the stability of the oils with time. Accelerated and natural aging techniques could be employed for this aging study.

भारतीय प्रौद्योगिकी संस्थान गुवाहाटी
Indian Institute of Technology Guwahati

Annexure A

The biochemical composition of biomass, which includes cellulose, hemicellulose, lignin and ash were quantitatively analysed using TAPPI protocols (TAPPI, 1992). The produces employed by browning and van soest were also employed for the analysis (Browning, 1967; Van Soest, 1963a; Van Soest, 1963b). The step-by-step procedure is mentioned below.

Determination of holocellulose content

A small quantity (2 g) of the powdered biomass was taken along with 100 ml deionized water in a 250 ml flask. The flask was placed in a heated water bath at 70 °C. After a duration of 30 min, 1.5 g sodium chlorite ($NaClO_2$) and 5 ml of 10% (v/v) acetic acid (CH_3COOH) were added to the flask and mixed together. After the passing of another 30 min, 5 ml of 10% (v/v) acetic acid was added to the mixture in the flask. Mixing of the content of the flask was done every 10 min. 1.5 g sodium chlorite and 5 ml of the dilute acetic acid were added every hour for the next 4 h. The biomass turned to almost white signifying the solubility of the lignin fraction. The mixture was filtered using a sintered glass crucible after the contents of the flask was cooled to below 10 °C. The best suited crucible between grade 1 and 5 (which refers to the porosity range of the crucible) was selected based on the average size of the raw biomass. The filtered biomass was washed with water multiple times to remove all traces of the treating chemicals. Finally the residue was washed with acetone and air-dried.

The fraction of the filtered biomass residue with respect to the quantity of the raw biomass taken equals the holocellulose content.

Determination of hemicellulose content

The protocols used by van soest (1963a; 1963b) for quanitifying the neutral detergent fiber (NDF) and acid detergent fiber (ADF) contents were used for determining the hemicellulose content

Hemicellulose content = NDF – ADF

Quantification of neutral detergent fiber (NDF)

Neutral detergent solution was initially prepared. 18.61 g disodium ethylene diamine tetraacetate (EDTA), 6.81 g sodium borate decahydrate ($Na_2B_4O_7.10H_2O$) and 4.56 g anhydrous disodium hydrogen phosphate (Na_2HPO_4) was taken in a beaker and dissolved in distilled water by heating. 30 g sodium lauryl sulphate (SLS) and 10 ml 2-ethoxyethanol was taken in another beaker with distilled water and heated until solubilized. Both solutions were then mixed together and volume was made up to 1 L using distilled water. The pH was around 6.9 to 7.1.

0.5 to 1 g of the raw biomass was taken with 100 ml cold neutral detergent solution, 0.5 g sodium sulphite and 2 ml decahydronaphthalene in a refluxing flask and heated to boiling. The heating level was then reduced so prevent foaming and reflexing was continued for 1 h. The solution was filtered using a sintered glass crucible. The residue collected in the crucible was rinsed with hot water (90-100 °C) multiple times till a clear filtrate was obtained. The residue was washed with acetone and dried at 100 °C for a minimum of 8 h and then weighed. The neutral detergent fiber was calculated as per the formula mentioned below.

$$\text{Neutral detergent fiber (NDF)} = \frac{\text{Weight of glass crucible with residue} - \text{Weight of empty glass crucible}}{\text{Weight of raw biomass}} \times 100$$

Quantification of acid detergent fiber (ADF)

Acid detergent solution was prepared by dissolving 20 g cetyl trimethylammonium bromide (CTAB) in 1 L of 1 N sulphuric acid at 20 ℃.

1 g of raw biomass was taken with 100 ml cold acid detergent solution and 2 ml decahydronaphthalene in a reflexing flask and heated to boiling. The heating level was then reduced so prevent foaming and reflexing was continued for 1 h. The solution was filtered using a sintered glass crucible. The residue collected in the crucible was rinsed with hot water (90-100 ℃) multiple times till a clear filtrate was obtained. The residue was washed with acetone till no more color was lost. The residue was washed with acetone and dried at 100 ℃ for a minimum of 8 h and then weighed. The acid detergent fiber was calculated as per the formula mentioned below.

$$\text{Acid detergent fiber (ADF)} = \frac{\text{Weight of glass crucible with residue} - \text{Weight of empty glass crucible}}{\text{Weight of raw biomass}} \times 100$$

Determination of cellulose content

The difference between the holocellulose and hemicellulose content was taken as the cellulose content.

Determination of lignin content

1 g of the raw biomass was taken in a beaker and 10 ml of 72% H_2SO_4 was added to it and left for 5 to 10 min. The mixture was then transferred into a refluxing flask and

volume of the solution was made up to 300 ml using distilled water. The entire contents was refluxed for 3 h. After cooling the solution, it was filtered using a sintered glass crucible. The residue was rinsed with hot distilled water to remove the acid and dried at 100 ℃ overnight. The weight of the residue corresponds to the lignin and ash content

$$\text{Lignin} + \text{Ash content}(\%) = \frac{\text{Weight of glass crucible with residue} - \text{Weight of empty glass crucible}}{\text{Weight of raw biomass}} \times 100$$

Ash (metallic) content was calculated separately. 1 g of biomass dried at 105 ℃ was taken in a crucible. The crucible was ignited between 900 and 950 ℃ in a muffle furnace for 3 h. The crucible is cooled to 100 ℃ and weighed. The weight of the residue corresponds to the ash content.

$$\text{Ash content}\ (\%) = \frac{\text{Weight of residue after ignition of biomass at 900 ℃}}{\text{Weight of raw biomass at 105 ℃}} \times 100$$

References

Browning, B. L. (1967). Methods of wood chemistry. Volumes I & II. John Wiley & Sons, New York, USA.

TAPPI. (1992). Technical association of the pulp and paper industry. Georgia, USA: Atlanta.

Van Soest, P. J. (1963a). Use of detergents in the analysis of fibrous feeds. I. Preparation of fiber residues of low nitrogen content. *Journal of the association of Official Agricultural Chemists*, *46*(5), 825-829.

Van Soest, P. J. (1963b). Use of detergents in the analysis of fibrous feeds. 2. A rapid method for the determination of fiber and lignin. *Journal of the Association of Official Agricultural Chemists*, *46*(5), 829-835.

Annexure B

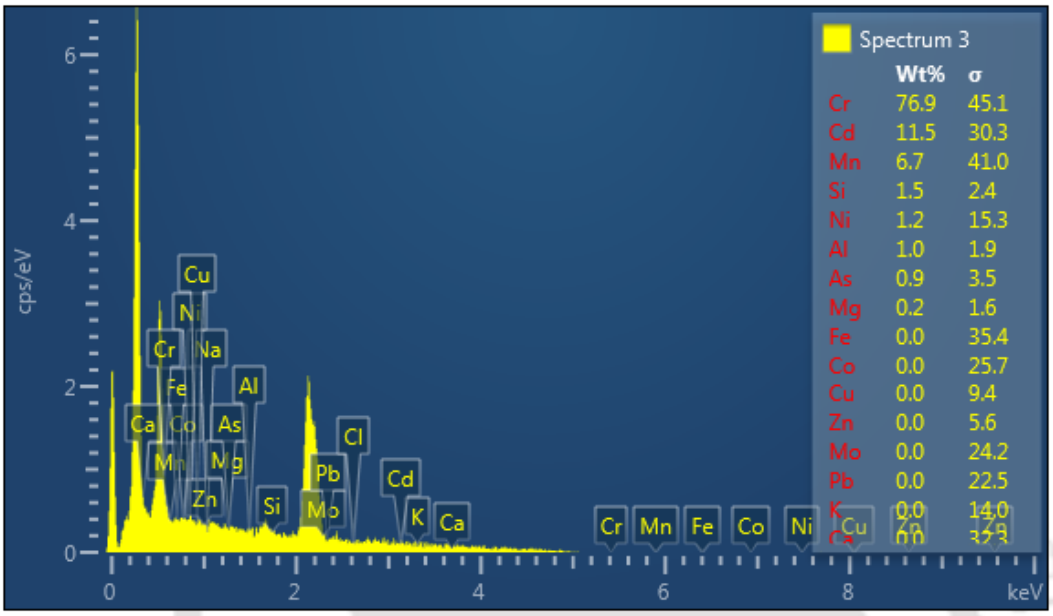

Figure B.1: EDX spectra of raw untreated *A. donax* biomass

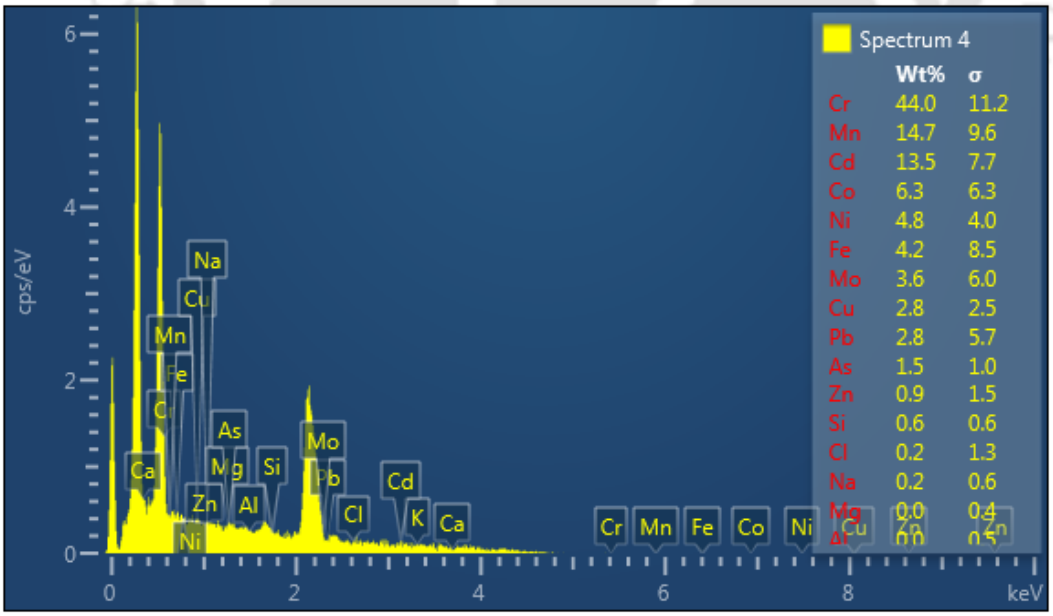

Figure B.2: EDX spectra of raw untreated *P. juliflora* biomass

Annexure C

Table C.1: Identified chemicals from pyrolysis of *A. donax* and *P. juliflora* biomass

1: acetic acid
2: (E)-pent-3-en-2-one / methyl propenyl ketone
3: 2,5-dimethylfuran
4: toluene / methylbenzene
5: furan-2-carbaldehyde / furfural
6: furan-2-ylmethanol / 2-furanmethanol
7: 1,3-xylene / m-xylene / 1,3-dimethylbenxene
8: styrene / vinylbenzene
9: 2-methylcyclopent-2-en-1-one
10: cyclohexanone / cyclohexyl ketone
11: 5-methylfuran-2-carbaldehyde / 5-methylfurfural
12: phenol
13: 2,2-diethyl-3-methyl-1,3-oxazolidine
14: 2-hydroxy-3-methylcyclopent-2-en-1-one / cyclotene
15: 2,3-dimethylcyclopent-2-en-1-one
16: 2-methylphenol / o-cresol
17: 4-methylphenol / p-cresol
18: 2-methoxyphenol / guaiacol
19: 3-ethyl-2-hydroxycyclopent-2-en-1-one
20: 1-methyl-2,3-dihydro-1H-indene / 1-methylindan
21: 3,5-dimethylphenol
22: 2-ethylphenol
23: 4-ethylbenzene-1,3-diol / 4-ethylresorcinol
24: 2-methoxy-4-methylphenol / 4-methylguaiacol / creosol
25: benzene-1,2-diol / 2-hydroxyphenol / pyrocatechol / catechol
26: 2,3-dihydro-1-benzofuran / coumaran
27: 1,2-dimethoxy-4-methylbenzene / 3,4-dimethoxytoluene
28: 3-methoxybenzene-1,2-diol / 3-methoxycatechol
29: 4-ethyl-2-methoxyphenol / 4-ethylguaiacol
30: 1-(2,6-dihydroxyphenyl)ethanone / 2-acetylresorcinol
31: 2,3-dihydroinden-1-one / 1-indanone
32: (5-formylfuran-2-yl)methyl acetate / 5-acetoxymethylfurfural
33: 1-(2-hydroxy-5-methylphenyl)ethanone / 2-hydroxy-5-methylacetophenone / o-acetyl-p-cresol
34: 2,6-dimethoxyphenol / syringol
35: 2-methoxy-4-prop-2-enylphenol / 4-allyl-2-methoxyphenol / eugenol
36: 1-(2,5-dihydroxyphenyl)propan-1-one
37: 2-methoxy-6-prop-2-enylphenol / 2-allyl-6-methoxyphenol
38: 1,2,4-trimethoxybenzene
39: 2-methoxy-4-(prop-1-enyl)-phenol / trans-isoeugenol
40: 2-methoxy-4-propylphenol / 4-propylguaiacol
41: 1-ethyl-4-phenylbenzene / 4-ethylbiphenyl
42: 1-(4-hydroxy-3-methoxyphenyl)propan-2-one / 4-hydroxy-3-methoxyphenyl acetone
43: 1-(3,4-dimethoxyphenyl)ethanone
44, 46, 47: 2,6-dimethoxy-4-prop-2-enylphenol / 4-allylsyringol
45: 1-phenylpropylbenzene / 1,1-diphenylpropane

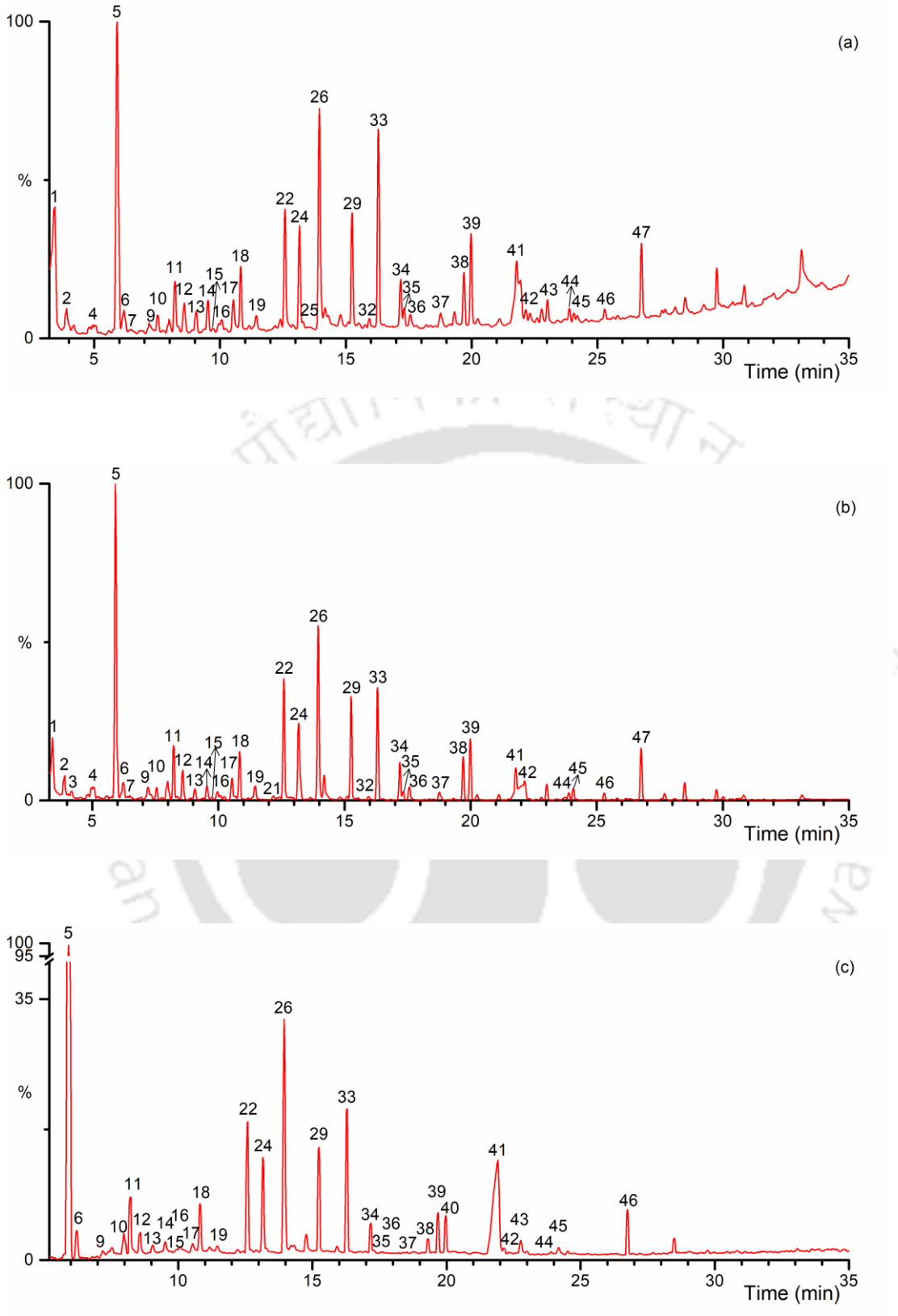

Figure C.1: GC Spectra of bio-oil from pyrolysis of *A. donax* treated with (a) 1% H_2SO_4, (b) 3% H_2SO_4 and (c) 5% H_2SO_4

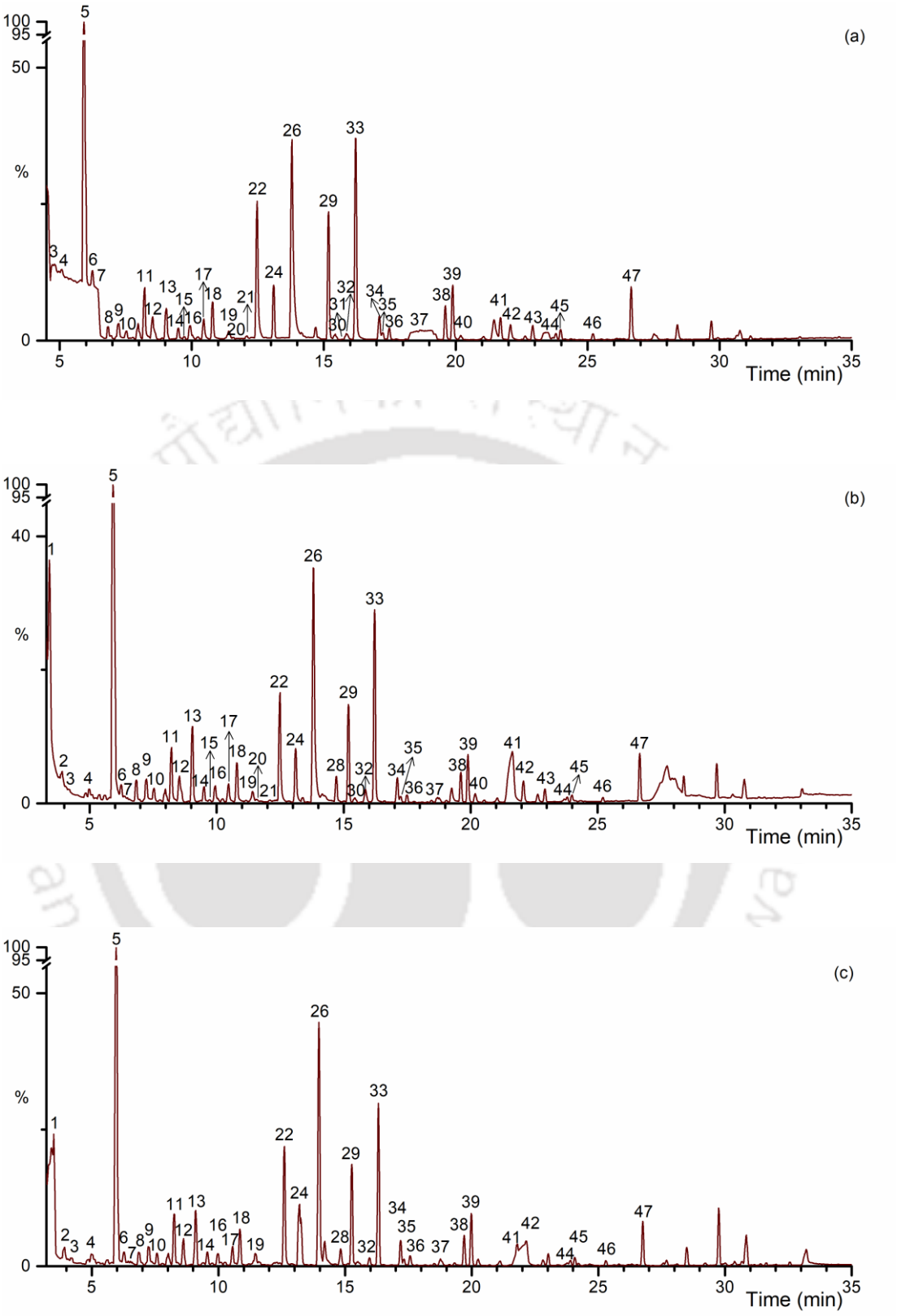

Figure C.2: GC Spectra of bio-oil from pyrolysis of *A. donax* treated with (a) 1% H_3PO_4, (b) 3% H_3PO_4 and (c) 5% H_3PO_4

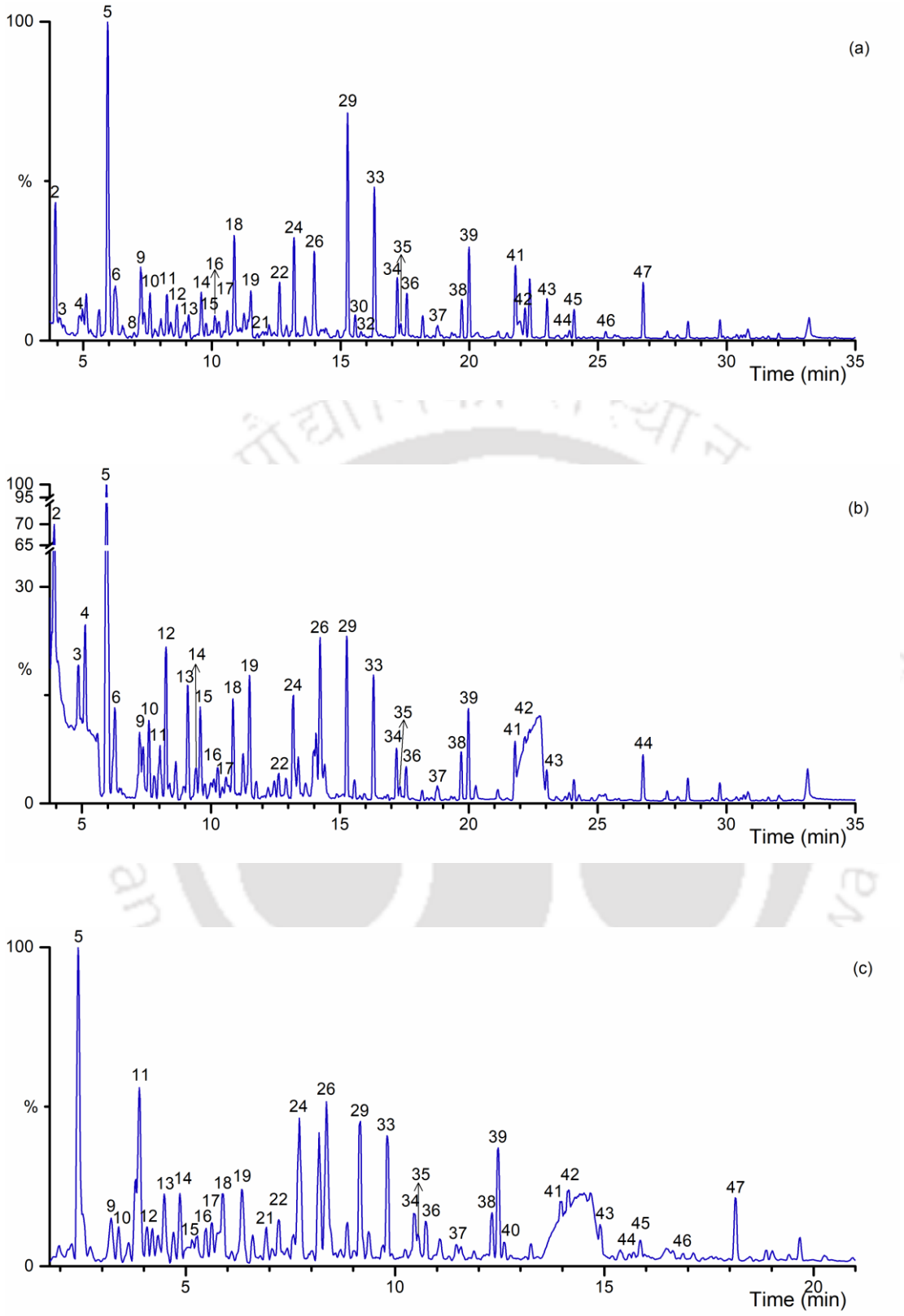

Figure C.3: GC Spectra of bio-oil from pyrolysis of *A. donax* treated with (a) 1% NaOH, (b) 3% NaOH and (c) 5% NaOH

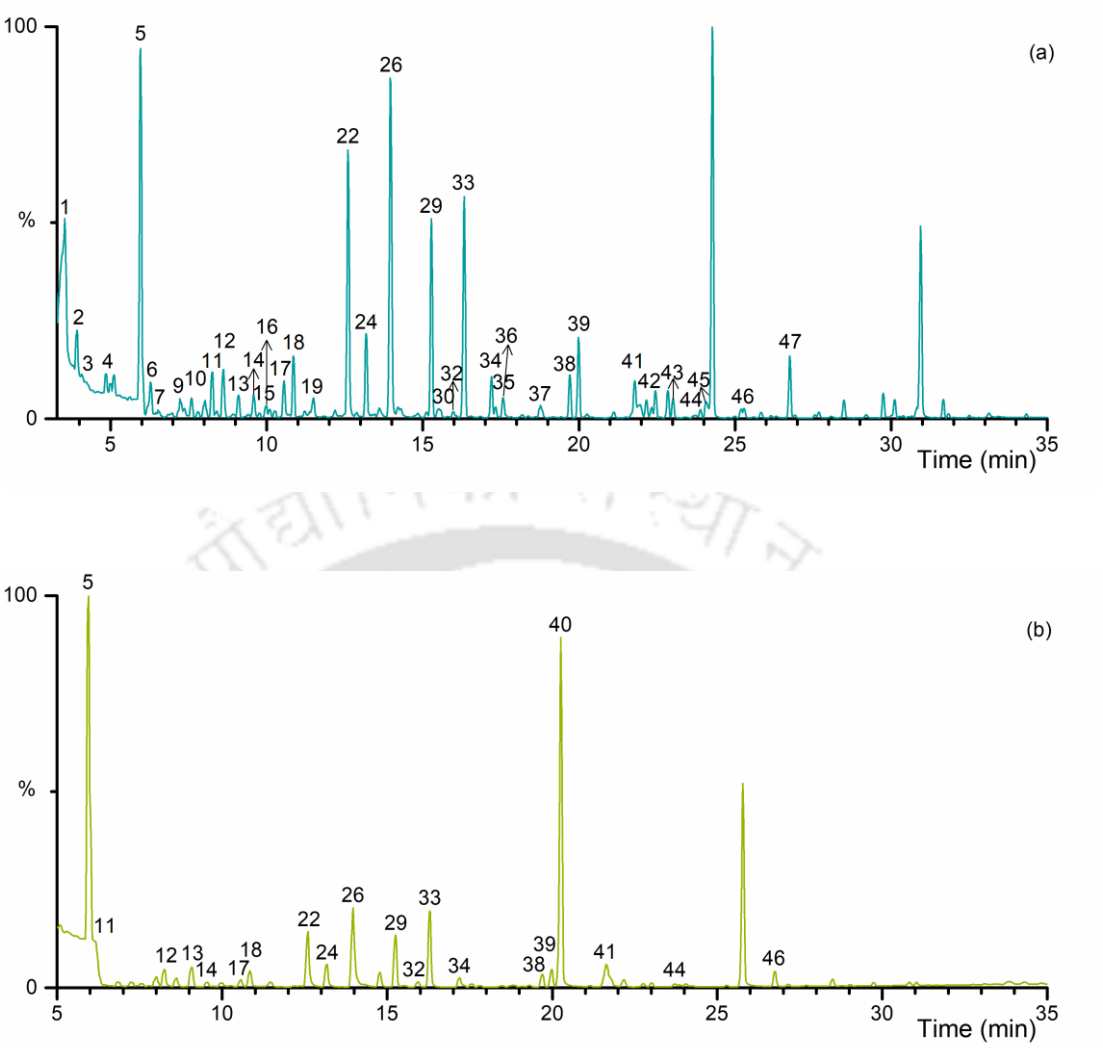

Figure C.4: GC Spectra of bio-oil from pyrolysis of *A. donax* treated with (a) 0.5% Triton X-100 and (b) 0.5% SDS

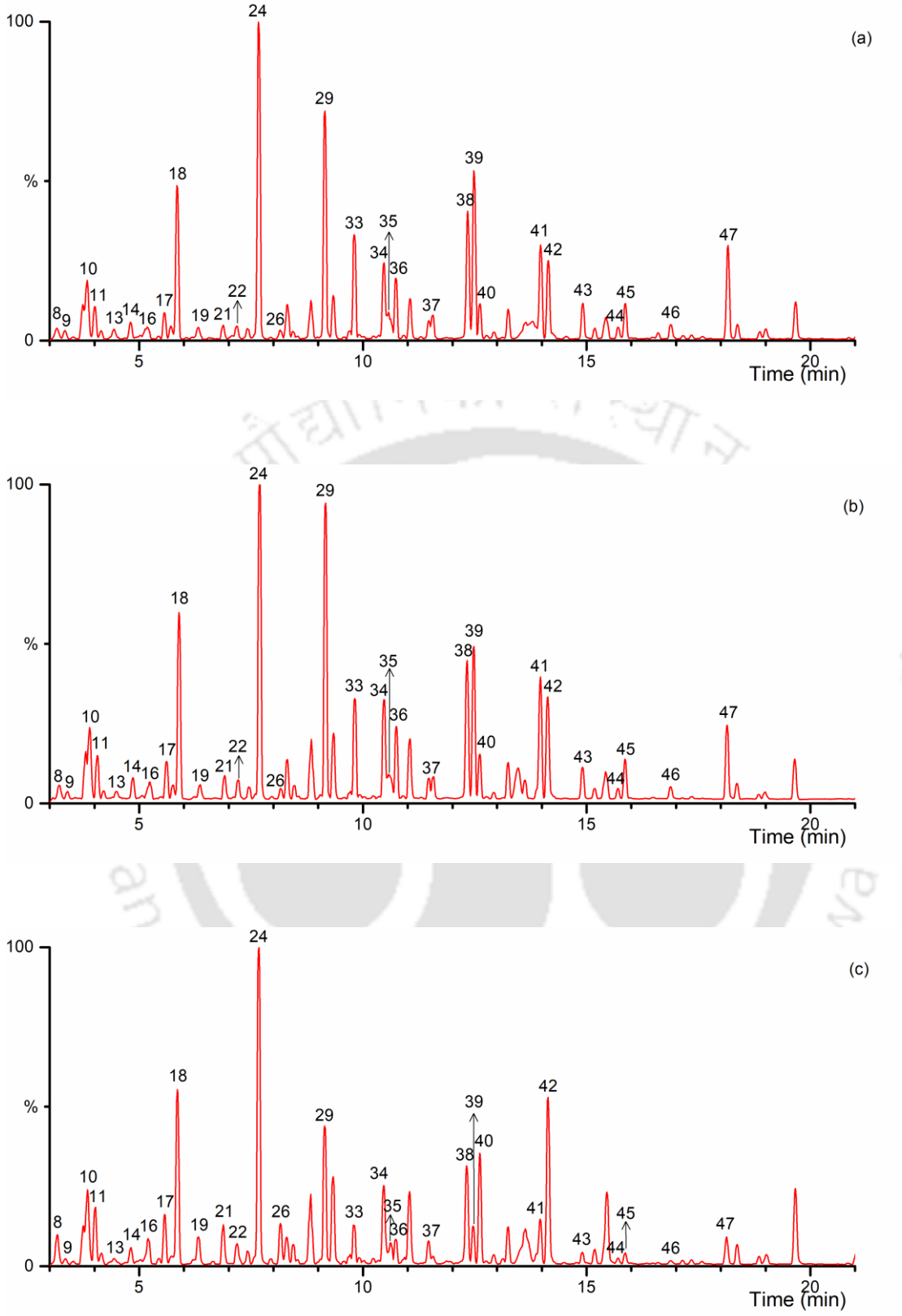

Figure C.5: GC Spectra of bio-oil from pyrolysis of *P. juliflora* treated with (a) 1% H_2SO_4, (b) 3% H_2SO_4 and (c) 5% H_2SO_4

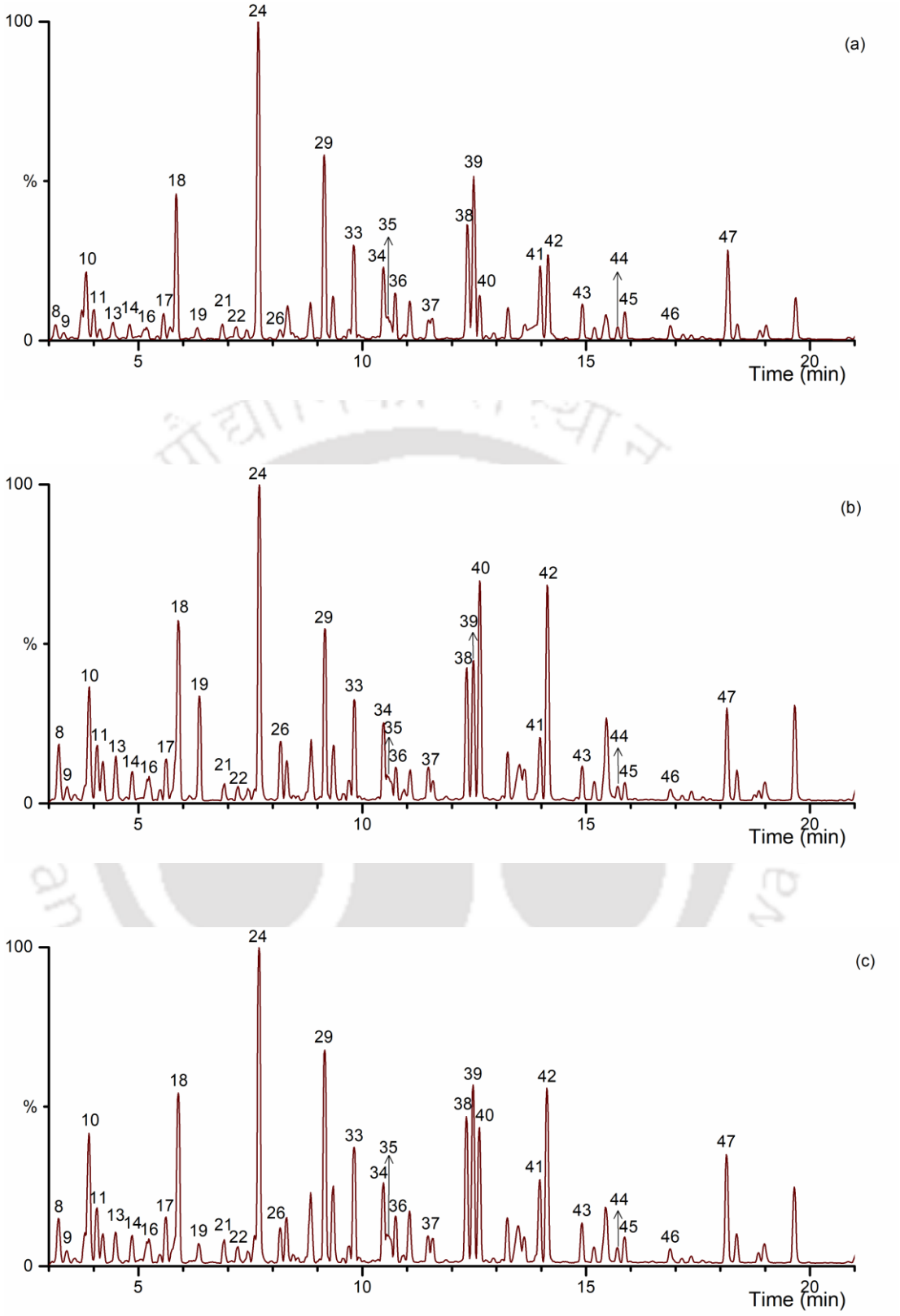

Figure C.6: GC Spectra of bio-oil from pyrolysis of *P. juliflora* treated with (a) 1% H_3PO_4, (b) 3% H_3PO_4 and (c) 5% H_3PO_4

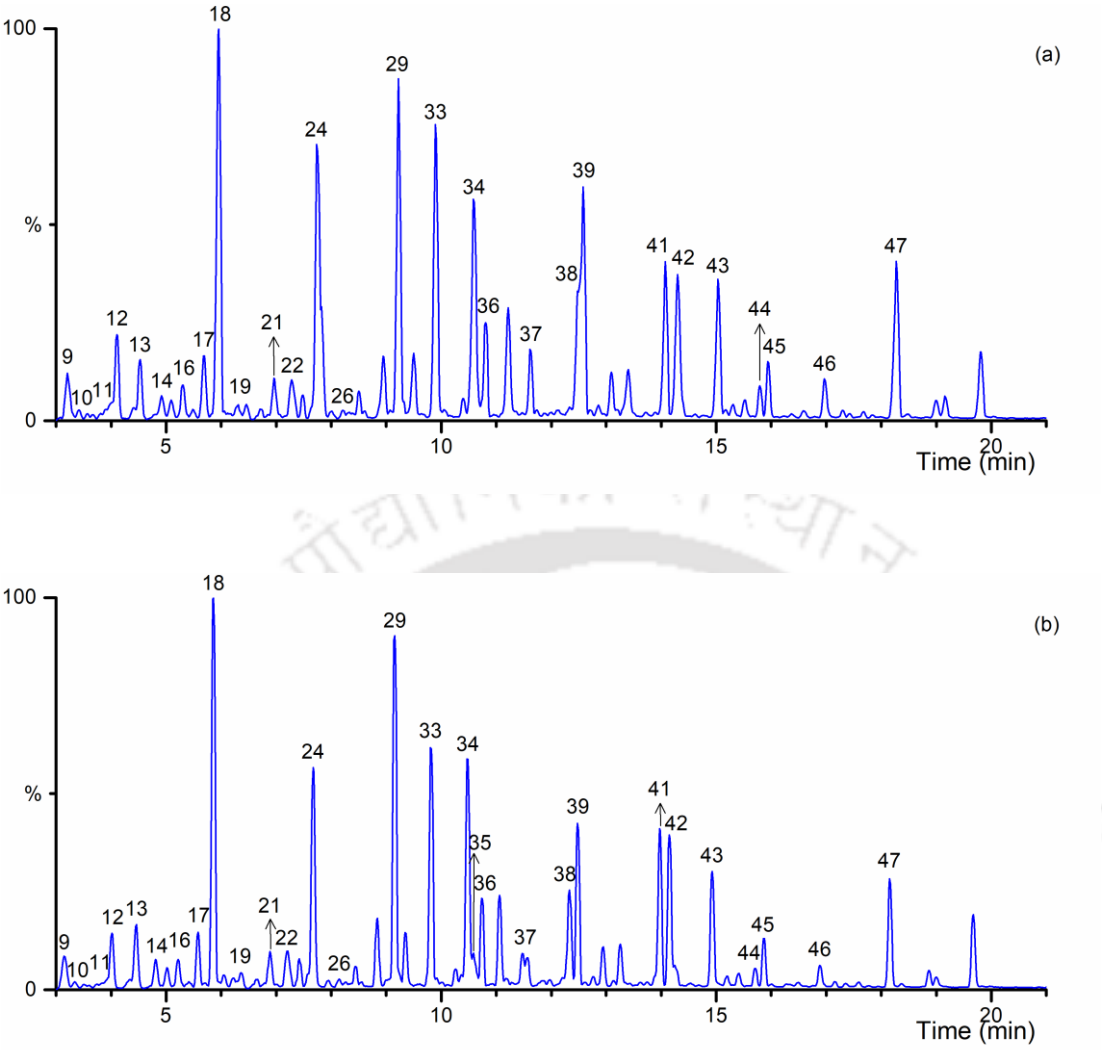

Figure C.7: GC Spectra of bio-oil from pyrolysis of *P. juliflora* treated with (a) 1% NaOH and (b) 3% NaOH

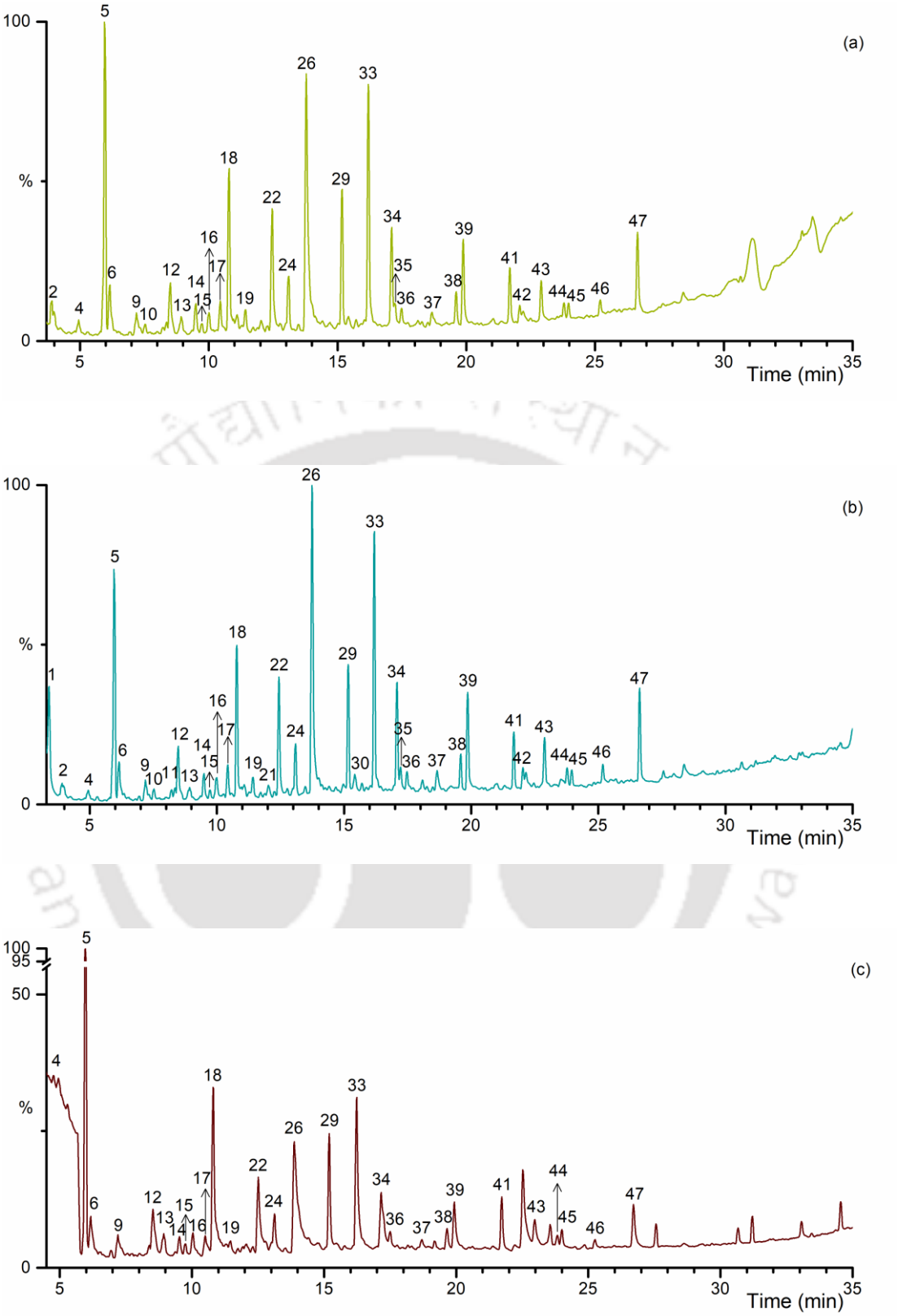
(a)
100
%
0
5
10
15
20
25
30
35
Time (min)
(b)
(c)
95
50

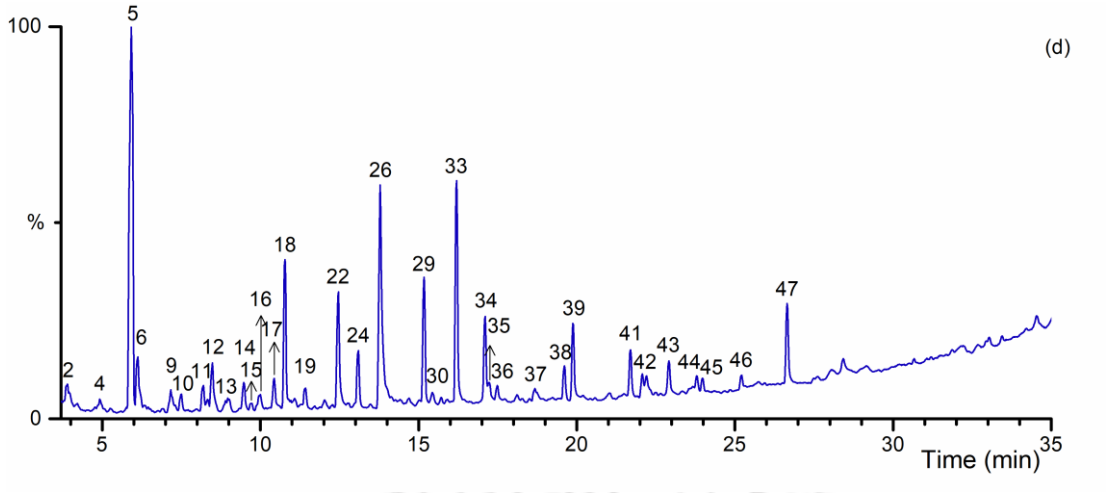

Figure C.8: GC Spectra of bio-oil from pyrolysis of *A. donax* doped with (a) 2% CH_3COOK, (b) 2% KCl (c) 2% MgO and (d) 2% $MgCl_2$

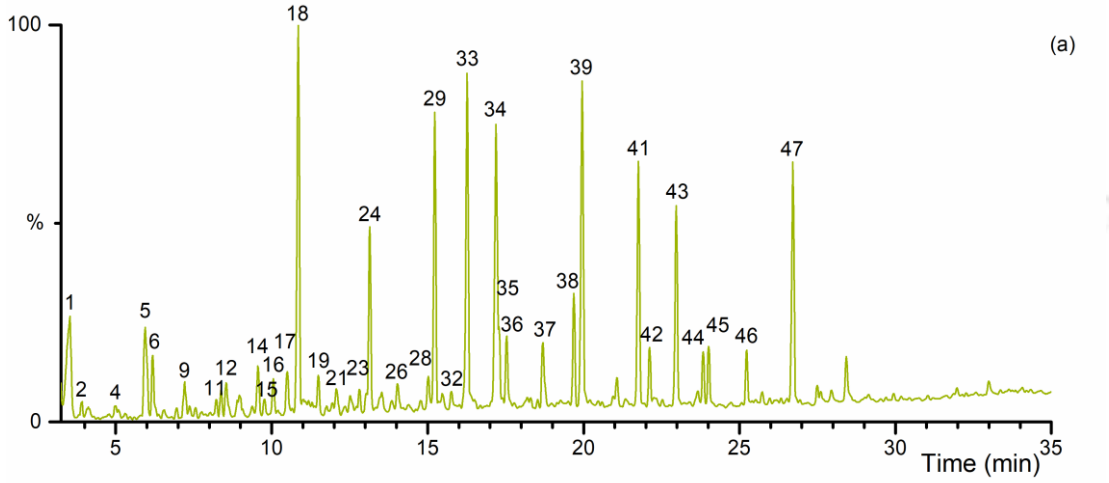

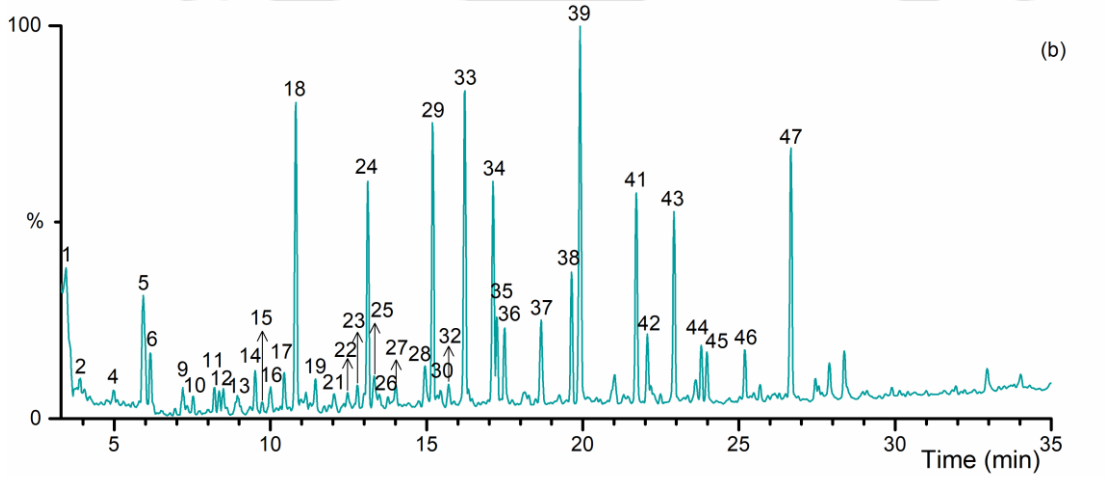

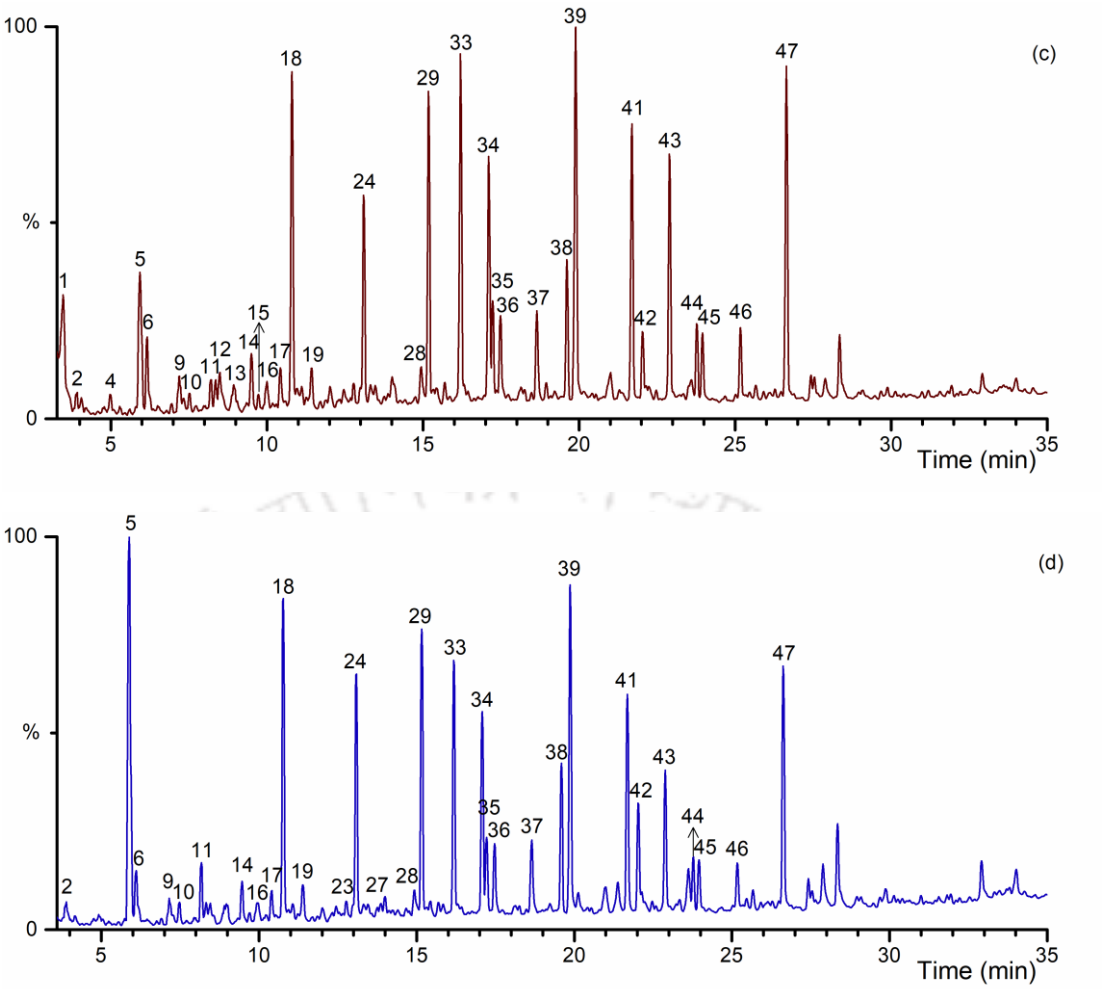

Figure C.9: GC Spectra of bio-oil from pyrolysis of *P. juliflora* doped with (a) 2% CH_3COOK, (b) 2% KCl (c) 2% MgO and (d) 2% $MgCl_2$

Annexure D

Table D.1: Identified chemicals from pyrolysis of treated *A. donax*

Compound name	Yield (% v/v)					
	1% H_2SO_4	3% H_2SO_4	1% H_3PO_4	3% H_3PO_4	1% NaOH	5% NaOH
Carboxylic acids						
acetic acid	4.31	1.95	-	3.03	2.51	-
	4.31	**1.95**	-	**3.03**	**2.51**	-
Ketones						
3-penten-2-one	1.23	1.00	-	0.23	1.66	-
2-methyl-2-cyclopenten-1-one	0.83	0.68	0.46	0.69	1.63	1.81
1-cyclohexanone	0.93	1.14	0.48	0.97	1.51	1.09
2-hydroxy-3-methyl-2-cyclopenten-1-one	1.50	1.39	0.76	1.05	2.54	2.11
2,3-dimethyl-2-cyclopenten-1-one	0.22	0.19	0.16	0.12	0.70	1.63
3-ethyl-2-hydroxy-2-cyclopenten-1-one	0.91	0.50	0.45	1.11	1.46	3.22
	5.63	**4.90**	**2.31**	**4.18**	**9.50**	**9.86**
Others						
2,2-diethyl-3-methyl-oxazolidine	1.07	0.53	0.76	1.87	0.81	2.45
	1.07	**0.53**	**0.76**	**1.87**	**0.81**	**2.45**
Furans						
2,5-dimethylfuran	-	0.70	5.54	0.24	1.28	-
furfural	16.32	15.12	16.66	21.20	7.92	10.46
2-furanmethanol	1.13	1.19	0.34	0.32	3.41	-
5-methyl-2-furaldehyde	2.38	3.34	1.73	2.57	1.50	5.85
5-acetoxymethyl-2-furaldehyde	0.36	0.27	0.44	0.78	0.51	-
	20.18	**20.62**	**24.70**	**25.10**	**14.62**	**16.31**
Phenols						
phenol	1.69	1.94	0.71	1.66	1.37	1.11
2-methylphenol (o-cresol)	0.66	1.07	0.55	0.62	2.20	1.17
4-methylphenol (p-cresol)	1.71	1.96	1.11	1.26	2.26	1.37
3,5-dimethylphenol	-	0.22	0.55	0.22	0.74	0.94
2-ethylphenol	4.93	4.70	4.81	3.53	2.30	1.36
1-(2-hydroxy-5-methylphenyl)ethanone	7.28	7.35	7.41	8.26	4.72	3.67
1-(2,5-dihydroxyphenyl)propan-1-one	0.61	1.01	0.46	0.47	0.19	1.16
	16.88	**18.25**	**15.58**	**16.02**	**13.77**	**10.76**

Benzenediols						
resorcinol	-	-	0.43	-	-	-
catechol	0.09	-	-	-	-	-
3-methoxybenzene-1,2-diol	-	-	-	1.26	-	-
1-(2,6-dihydroxyphenyl)ethanone	-	-	0.16	0.19	0.89	-
	0.09	-	**0.59**	**1.45**	**0.89**	-
Methoxyphenol derivatives						
guaiacol	2.77	3.60	1.87	2.25	4.40	3.83
creosol	4.22	6.28	3.51	3.88	3.64	5.65
4-ethyl-2-methoxyphenol	4.29	4.87	3.46	3.10	5.28	4.49
syringol	1.90	2.71	1.07	1.33	1.85	1.63
eugenol	0.78	1.11	0.60	0.59	0.77	0.73
2-allyl-6-methoxyphenol	0.83	0.95	0.34	0.36	0.19	0.46
trans-isoeugenol	3.52	4.62	2.52	2.67	3.11	3.13
4-propylguaiacol	-	-	0.13	0.61	-	0.48
1-(4-hydroxy-3-methoxyphenyl)propan-2-one	0.61	0.79	0.26	0.50	0.45	0.60
1-(3,4-dimethoxyphenyl)ethanone	1.08	-	0.63	0.90	1.49	0.55
4-allylsyringol	3.90	4.86	3.18	3.75	2.85	2.21
	23.89	**29.79**	**17.56**	**19.95**	**24.03**	**23.74**
Aromatic non-oxygenates						
toluene	0.29	0.56	1.70	0.39	0.32	-
1,3-xylene	0.18	0.09	0.21	0.11	-	-
styrene	-	-	0.23	0.21	0.32	-
1-methyl-2,3-dihydro-1*H*-indene	-	-	0.14	0.13	-	-
1-phenylpropylbenzene	0.34	0.41	0.26	0.54	0.49	0.51
1-ethyl-4-phenylbenzene	4.42	1.60	0.90	7.15	2.42	1.35
	5.24	**2.66**	**3.43**	**8.52**	**3.56**	**1.86**
Aromatic oxygenates						
2,3-dihydro-1-benzofuran	10.27	9.90	11.91	12.07	3.44	4.21
2,3-dihydroinden-1-one	-	-	0.05	-	-	-
1,2,4-trimethoxybenzene	2.09	2.95	1.33	1.61	1.32	1.23
	12.35	**12.85**	**13.29**	**13.68**	**4.76**	**5.44**

Table D.2: Identified chemicals from pyrolysis of treated *P. juliflora*

Compound name	Yield (% v/v)				
	1% H_2SO_4	3% H_2SO_4	1% H_3PO_4	3% H_3PO_4	1% NaOH
Ketones					
2-methyl-2-cyclopenten-1-one	0.79	0.83	0.88	2.10	1.39
1-cyclohexanone	0.49	0.34	0.44	0.65	0.27
2-hydroxy-3-methyl-2-cyclopenten-1-one	0.66	0.79	0.73	0.99	0.85
3-ethyl-2-hydroxy-2-cyclopenten-1-one	0.64	0.62	0.66	3.23	0.31
	2.57	**2.58**	**2.71**	**6.96**	**2.83**
Others					
2,2-diethyl-3-methyl-oxazolidine	0.58	0.26	1.08	1.68	1.42
	0.58	**0.26**	**1.08**	**1.68**	**1.42**
Furans					
5-methyl-2-furaldehyde	2.90	2.96	3.26	4.25	0.22
	2.90	**2.96**	**3.26**	**4.25**	**0.22**
Phenols					
phenol	1.40	1.57	1.36	1.82	2.52
2-methylphenol (o-cresol)	0.48	0.88	0.59	0.70	0.96
4-methylphenol (p-cresol)	1.05	1.37	1.12	1.29	1.61
3,5-dimethylphenol	0.61	0.93	0.74	0.51	1.06
2-ethylphenol	0.64	0.80	0.89	0.46	1.28
1-(2-hydroxy-5-methylphenyl)ethanone	4.47	3.59	4.24	2.94	7.09
1-(2,5-dihydroxyphenyl)propan-1-one	2.45	2.61	1.89	0.95	2.30
	11.1	**11.75**	**10.82**	**8.68**	**16.81**
Methoxyphenol derivatives					
guaiacol	6.19	6.79	6.31	6.93	10.11
creosol	12.91	11.45	13.86	9.62	6.97
4-ethyl-2-methoxyphenol	9.23	10.65	7.62	5.16	7.82
syringol	3.41	3.78	3.31	2.36	6.09
eugenol	0.75	1.15	0.59	0.41	-
2-allyl-6-methoxyphenol	1.02	0.83	0.99	0.59	1.78
trans-isoeugenol	6.62	5.42	6.62	4.04	6.84
4-propylguaiacol	1.38	1.61	1.74	6.59	-
1-(4-hydroxy-3-methoxyphenyl)propan-2-one	3.47	3.98	3.76	6.53	4.13
1-(3,4-dimethoxyphenyl)ethanone	1.49	1.20	1.49	1.05	3.69
4-allylsyringol	4.99	3.66	5.03	3.76	5.92
	51.46	**50.51**	**51.31**	**47.04**	**53.36**
Aromatic non-oxygenates					
1-phenylpropylbenzene	1.40	1.40	1.17	0.52	1.20

1-ethyl-4-phenylbenzene	3.92	4.72	4.59	2.07	3.80
	5.31	**6.11**	**5.76**	**2.59**	**5.00**
Aromatic oxygenates					
2,3-dihydro-1-benzofuran	0.41	0.41	0.35	1.81	0.19
1,2,4-trimethoxybenzene	5.29	5.15	4.87	3.94	1.93
	5.70	**5.56**	**5.22**	**5.74**	**2.13**

Table D.3: Identified chemicals from pyrolysis of AAEM infused *P. juliflora* and *A. donax* biomass samples

Compound name	Yield (% v/v)							
	PJ - KAc	PJ - KCl	PJ - MgO	PJ-MgCl	AD-KAc	AD-KCl	AD-MgO	AD-MgCl
Carboxylic acids								
acetic acid	5.30	7.27	2.48	3.10	6.64	1.77	2.14	-
	5.30	**7.27**	**2.48**	**3.10**	**6.64**	**1.77**	**2.14**	**-**
Ketones								
pent-3-en-2-one	0.30	0.24	0.83	0.59	0.97	0.14	1.07	1.24
2-methyl-2-cyclopenten-1-one	0.85	0.54	1.08	0.80	1.17	1.13	1.18	1.13
1-cyclohexanone	-	0.38	0.87	0.79	0.68	0.72	-	0.74
2-hydroxy-3-methyl-2-cyclopenten-1-one	1.22	0.93	1.28	0.97	1.21	1.11	0.79	1.22
2,3-dimethyl-2-cyclopenten-1-one	0.38	0.22	0.30	-	0.39	0.35	0.50	0.24
3-ethyl-2-hydroxy-2-cyclopenten-1-one	0.75	0.70	0.88	0.88	1.43	0.77	0.33	0.78
	3.50	**3.00**	**5.24**	**4.02**	**5.84**	**4.21**	**3.86**	**5.36**
Furans								
furfural	3.02	3.42	4.34	11.53	12.32	10.63	21.40	23.01
2-furanmethanol	1.55	1.41	1.89	1.51	2.54	2.25	1.81	2.64
5-methyl-2-furaldehyde	0.38	0.48	0.68	1.29	-	0.40	-	0.89
5-acetoxymethyl-2-furaldehyde	0.41	0.53	-	-	-	-	-	-
	5.35	**5.84**	**6.92**	**14.33**	**14.86**	**13.27**	**23.20**	**26.53**
Others								
2,2-diethyl-3-methyl-oxazolidine	-	0.16	0.27	-	1.10	0.94	1.07	1.10
	-	**0.16**	**0.27**	**-**	**1.10**	**0.94**	**1.07**	**1.10**
L-H Units								

phenol	1.01	0.74	1.43	0.31	2.18	2.82	2.48	2.21
2-methylphenol (o-cresol)	0.99	0.70	0.82	0.70	0.87	0.90	1.47	0.61
4-methylphenol (p-cresol)	1.08	0.89	0.90	0.66	1.40	1.38	1.18	1.48
3,5-dimethylphenol	0.64	0.45	-	-	-	0.61	-	-
2-ethylphenol	-	0.38	-	-	5.36	5.33	4.07	5.34
1-(2-hydroxy-5-methylphenyl)ethanone	8.62	7.60	7.60	5.53	9.28	10.85	8.40	9.24
1-(2,5-dihydroxyphenyl)propan-1-one	1.93	1.82	2.19	1.80	0.68	0.87	0.82	0.70
	14.27	**12.58**	**12.93**	**9.00**	**19.77**	**22.76**	**18.40**	**19.58**
L-G Units								
guaiacol	9.41	6.68	7.61	7.16	7.67	5.90	9.03	5.79
creosol	4.71	5.15	4.36	5.21	2.27	2.03	1.34	2.37
4-ethyl-2-methoxyphenol	6.71	6.47	6.72	6.29	5.04	5.04	4.94	4.96
eugenol	1.32	1.77	2.16	1.83	1.00	0.97	-	1.00
2-allyl-6-methoxyphenol	1.95	2.05	2.32	2.02	0.76	1.32	0.39	0.77
trans-isoeugenol	8.51	8.85	9.52	7.81	3.56	4.38	2.96	3.32
1-(4-hydroxy-3-methoxyphenyl)propan-2-one	1.25	1.51	1.30	2.14	0.46	0.86	-	0.98
	33.88	**32.48**	**34.00**	**32.47**	**20.77**	**20.50**	**18.67**	**19.19**
L-S Units								
syringol	7.98	4.93	5.70	4.71	4.01	4.40	4.15	3.69
4-allylsyringol	8.41	7.94	11.03	7.92	4.53	5.79	3.40	4.41
1,2,4-trimethoxybenzene	2.61	2.77	3.14	3.43	1.29	1.46	1.07	1.43
	19.00	**15.64**	**19.86**	**16.06**	**9.83**	**11.64**	**8.62**	**9.53**
Other Aromatics								
catechol	-	0.71	-	-	-	-	-	-
3-methoxycatechol	0.80	1.23	1.00	0.76	-	-	-	-
4-ethylresorcinol	0.44	0.40	-	0.34	-	-	-	-

2-acetyl-resorcinol	-	0.44	-	-	-	0.86	-	0.56
1-(3,4-dimethoxyphenyl)ethanone	4.99	4.29	5.85	3.28	1.98	2.42	1.84	1.77
toluene	0.50	0.47	0.58	-	0.54	0.44	1.07	0.39
1-phenylpropylbenzene	1.44	1.21	1.54	1.34	0.54	0.63	0.73	0.48
1-ethyl-4-phenylbenzene	6.22	4.77	6.51	5.13	2.29	2.50	2.65	1.98
2,3-dihydro-1-benzofuran	0.75	0.26	-	-	13.92	16.04	9.85	12.23
3,4-Dimethoxytoluene	-	0.67	-	0.34	-	-	-	-
	15.14	**14.45**	**15.48**	**11.19**	**19.28**	**22.90**	**16.15**	**17.42**

RESEARCH OUTPUTS

RESEARCH PAPERS PUBLISHED

OUT OF THESIS

1. **Philip Bernstein Saynik** and Vijayanand S. Moholkar. (2020). "Insight into chemical pretreatment of hardwood (*Arundo donax*) for improvement of pyrolysis." *Bioresource Technology Reports*, *11*, 100545.
2. **Philip Bernstein Saynik** and Vijayanand S. Moholkar. (2021). "Investigations in influence of different pretreatments on *A. donax* pyrolysis: Trends in product yield, distribution and chemical composition." *Journal of Analytical and Applied Pyrolysis*, 158, 105276.
3. **Philip Bernstein Saynik** and Vijayanand S. Moholkar. "Influence of different salts of alkali and and alkaline earth metals on the pyrolysis of hardwood (*Prosopis juliflora*)." (Under Review)

OTHER PUBLICATIONS

1. Mriganka Saha[†], **Philip Bernstein Saynik**[†], Arupjyoti Borah, Ritesh S. Malani, Prachi Arya, Shivangi, Vijayanand S. Moholkar. (2019). "Dioxane-based extraction process for production of high quality lignin." *Bioresource Technology Reports*, 5, 206-211. ([†] Co-first authors)
2. Sumitha Banu Jamaldheen, **Philip Bernstein Saynik**, Vijayanand S. Moholkar, Arun Goyal. (2021). "Fermentation and pyrolysis of Finger millet straw: Significance of hydrolysate composition for ethanol production and characterization of bio-oil." *Bioresource Technology Reports*, 13, 100630.

CONFERENCE PRESENTATIONS

1. **Oral Presentation:** "A comparative study of the pyrolytic products of pre-treated samples of *Arundo donax* and *Prosopis juliflora*". 3rd International Conference on Sustainable Energy and Environmental Challenges (SEEC). 18th-21st Dec 2018; IIT Roorkee, Roorkee, INDIA. **(Best Oral Presentation Award)**
2. **Oral Presentation:** "Enhancement of the chemical properties of bio-oil as a sustainable energy replacement for petroleum based fuels". International Conference on Engaging India and Canada: Challenges of Sustainable Development Goals. 8th-9th July 2018; India International Centre, New Delhi, INDIA.
3. **Poster Presentation:** "Exploring pre-treatment of hard wood for bio-oil production". Research Conclave. 14th-17th Mar 2019; IIT Guwahati, Guwahati, INDIA.
4. **Poster Presentation:** "Pyrolysis of invasive weed *Arundo donax*: improvement of products through pre-treatment". International Conference on Biotechnological Research and Innovation for Sustainable Development (BioSD). 22nd-25th Nov 2018; CSIR-IICT, Hyderabad, INDIA.
5. **Poster Presentation:** "A comparative study on the chemical storage characteristics of bio-oil obtained by the pyrolysis of invasive weeds *Prosopis juliflora* and *Arundo donax*". 2nd International Conference on Waste Management (RECYCLE). 22nd-24th Feb 2018; IIT Guwahati, Guwahati, INDIA. **(Best Poster Presentation Award)**
6. **Poster Presentation:** "Influence of chemical pre-treatment techniques on the physical properties of *Prosopis juliflora* biomass for bio-oil production". Recent Trends in Bioprocessing for Healthcare, Energy and Environment; 9th-11th Dec 2017; IIT Guwahati, Guwahati, INDIA.
7. Attended 10th World Renewable Energy Technology Congress (WRETC) as a delegate. 21st-23rd Aug 2019; NDCC Convention Centre, New Delhi, INDIA.